UNIVERSITAT DE BARCELONA

Population genomics, phylogeographic history, and evolutionary patterns in Antartic shallow-water benthic invertebrates

Carlos Leiva Martinez

UNIVERSITAT DE BARCELONA
FACULTAT DE BIOLOGIA

Programa de Doctorat de Genètica
Departament de Genètica, Microbiologia i Estadística

Tesi realitzada entre la Universitat de Barcelona i
The Natural History Museum of London, UK

Population genomics, phylogeographic history, and evolutionary patterns in Antarctic shallow-water benthic invertebrates

Memòria presentada per en Carlos Leiva Martínez per
optar al grau de doctor per la Universitat de Barcelona

Director: Dr. Sergi Taboada Moreno

Directora: Dra. Ana Riesgo Gil

Tutora: Dra. Marta Pascual Berniola

Doctorand: Carlos Leiva Martínez

Barcelona, 2019

Agraïments

El ‘long-distance dispersal’ ha acabat sent un dels temes centrals d’aquesta tesi, i com no havia de ser així? Certament, una de les principals característiques de la meva vida durant aquests últims anys ha estat aquesta ‘long-distance dispersal’, sempre amb un vol a la vista. Ara, veient-ho amb perspectiva, estic més que agraït a que hagi estat així, per tota la gent fantàstica que m'he trobat pel camí i que m’ha acollit allà on he estat. Començant amb els meus directors, Ana y Sergi, brillantes científicos y maravillosas personas. Mil gracias por todo lo que me habéis enseñado. Desde la primera PCR habéis estado ahí, codo con codo en el lab, analizando y discutiendo resultados, siempre con *el software* de Ana listo para evitar mis paranoias mentales. Trabajar con vosotros es una gozada, sois mis padres científicos! Y, por si fuera poco, me habéis acogido en vuestra casa innumerables veces, donde me he sentido parte de vuestra familia. Many thanks to the fabulous Riesgo Lab members, I have enjoyed many moments with you all during the last few years: Vassia, Nadia, Nathan, Bruna, Cristina, Eleonora, Alex Mitchell, Olivia, Emilio, and Fernanda. I also want to thank the indispensable support from Thibaut Jombart during our first steps of data analysis. Vull agrair a la meva tutora, Marta Pascual, per acollir-me al programa de doctorat de Genètica quan més necessitava aquest canvi, moltes gràcies.

També tinc molt a agrair a un altre científic brillant, Gonzalo Giribet. Moltíssimes gràcies per rebre’m al teu lab. Ets un referent per mi de com es pot ser un gran investigador i alhora tocar de peus a terra i ser una gran persona. Y dentro del Giribet Lab, tengo mucho que agradecerle a David Combosch, tu ayuda fue imprescindible en mis primeros pasos en el complejo mundo del RADseq.

Y aunque después no es lo más visible, a veces durante las campañas nos enfrentamos a situaciones difíciles, agravadas por el duro trabajo que realizamos casi sin descanso, y la distancia a la que quedan familia y amistades. Muchísimas gracias a aquellas personas que en estas circunstancias pasaron de ser compañeros de campaña a ser familia: Cristobo, Patri, Juan Moles, Juan Junoy, Uri y Gonzalo.

Y como no, estoy extremadamente agradecido a todas esas personas que, aunque no directamente, han hecho posible esta tesis: mi familia, tanto la que me ha tocado como la que he elegido. A mis padres por su apoyo incondicional (y tapers incondicionales también!). A ellos, a mi hermana, Deivid, tíos, primos, yaya, por cada celebración de la vida que nos hemos dado. Muchas gracias Rosa y Ligia por las birras del Queen’s Head y las happy hours! Cristina por las patinadas con LondonSkate. Many thanks to Jess, Layla, and Tommy, I felt like at home with you. I moltíssimes gràcies a totes aquelles persones que

m’han tret de la cova en algun moment durant aquests anys i m’han recordat que la vida va més enllà dels meus ‘cuquets’: Gelen, Amaia, Cande, Dos, Stan, Sara, Borja, Mario, Nurieta, Montse, Clàudia, Juanan, sou molt grans! I finalment vull agrair a dues persones que han estat molt a prop meu tots aquests anys i especialment pel que han fet durant aquestes últimes setmanes llegint-se, revisant i dissenyant la tesi amb mi: Auri i Euge, sense vosaltres això no hauria estat possible.

"Life did not take over the world by combat,
but by networking."

Lynn Margulis

"We wish to discuss a structure for the salt of deoxyribose
nucleic acid (D.N.A.). This structure has novel features
which are of considerable biologic interest."

Rosalind Franklin

Abstract

Benthic organisms inhabiting the shallow waters of the Southern Ocean are considered excellent models to study evolutionary processes, population connectivity patterns, and adaptation. They have evolved in an extreme environment, with expanding and retreating periods following glacial cycles, in an alternation pattern. Repeated rounds of population fragmentation in glacial refugia during glacial cycles followed by expansions and secondary contacts during interglacials were the main evolutionary force that brought Antarctic shallow-water ecosystems to their current state. In my PhD dissertation I have investigated in detail these singular evolutionary histories left in the genomes of our target species. Besides the past geological events, currently, threats from global warming arrive to the isolated southernmost continent. Indeed, coastal waters off West Antarctica are some of the most affected oceanic regions of the planet by global warming, with rather pessimistic projections for the near future. Considering this and the increasing local threats to which shallow-water ecosystems are exposed, it is fundamental to develop a well-connected network of Marine Protected Areas (MPAs) throughout the Southern Ocean. Despite genetic connectivity is not usually considered in MPA planning, population genetic studies can provide extremely valuable information to design connected MPA networks. In my dissertation I have also disentangled gene-flow patterns of Antarctic shallow-water benthic invertebrates, aiming to help to improve the current status of Southern Ocean MPAs.

In order to achieve my goals, I combined information coming from 'traditional' genetic markers, single nucleotide polymorphisms (SNPs) derived from restriction-site associated DNA sequencing (ddRADseq), transcriptomes, and draft-level genomes. A wide range of species presenting different reproductive modes was selected in order to test whether this factor plays a role on connectivity and evolutionary patterns in the explained scenario of glacial alternations: the brooding congeneric nemerteans *Antarctonemertes valida*, *A. riesgoae*, and *A. unilineata*; the demosponges *Dendrilla antarctica* and *Mycale acerata*, which present lecithotrophic larvae; and the annelids *Pterocirrus giribeti* (new species described in the Chapter 1 of my PhD dissertation) and *Neanthes kerguelensis*, that presumably presents planktotrophic larvae.

Our results regarding the evolutionary history of our target species revealed different glacial-refugium strategies independent of their reproductive mode, and generalised signals of bottleneck events. Moreover, blurred species boundaries were detected for the *Antarctonemertes* lineages, with a central role of glacial cycles in their introgressive evolutionary history. Additionally, we identified adaptive genes for particular glacial-refugium strategies and for the rise of prezygotic barriers during speciation and reinforcement events. Our connectivity results confirmed that genetic connectivity in the Southern Ocean is not determined by *a priori* dispersal abilities resulting from different reproductive strategies. We revealed an overall high gene flow along the Western Antarctic Peninsula (WAP), which is particularly exceptional for sponges and brooding species. Interestingly, loci under divergent selection were identified for *D. antarctica* despite admixture, broadly differentiating between the populations of Northern and Southern WAP. We suggest that ongoing natural selection is governed by differences in sea-ice extent and duration, exhibiting the vulnerability of the WAP benthic ecosystems due to the decline in the sea ice predicted for the near future. Finally, we demonstrated that long-distance connectivity did not surpass the regional WAP scale, supporting the

implementation of an MPA covering the WAP and the coastal waters off the South Orkneys.

Overall, the studies presented in my PhD dissertation represent a step forward in understanding global forces and processes affecting the evolutionary history of Antarctic marine organisms. We illustrated the adaptability of shallow-water benthic invertebrates to the natural changes of the Southern Ocean, while manifesting their vulnerability to future global warming. Remarkably, we highlight the importance of using population genetic data of various benthic invertebrate species to implement MPA networks in one of the most threatened areas of the planet by global warming. The results of my thesis will be fundamental to address the suitability and effectiveness of an MPA network comprising the already implemented MPA at South Georgia and South Sandwich Islands and the proposed MPA covering the WAP and the South Orkney Islands, essential for the survival of Antarctic marine ecosystems.

TABLE OF CONTENTS

General Introduction & Objectives

1- General aspects of Antarctica and the Southern Ocean

Despite ancient Greeks were already convinced of the existence of a southern continent balancing the northern land masses of Europe, Asia and North Africa (Clancy, Manning, & Brolsma, 2013), Antarctica remained pristine until 1820, when a Russian expedition beheld the austral continent for the first time. With more than 14M km², Antarctica is larger than continental Europe and nearly twice the size of Australia. Lying almost completely south of the Antarctic Circle, 98% of its continental surface is covered by an ice sheet 2 km thick in average (Fretwell et al., 2013), containing approximately 90% of the world's ice and 70% of the world's fresh water. Legally, Antarctica remains as the only land in the world that does not belong to any country, but it is internationally regulated following the Antarctic Treaty System. The agreements in the Antarctic Treaty, originally signed in 1959 and subsequently amplified until the Environmental Protocol adopted in 1991, arrived after a century of intense and locally devastating whaling and sealing activities, and designated Antarctica as "a natural reserve, devoted to peace and science". The international scientific cooperation enabled by the Antarctic Treaty has been essential for Antarctic scientists to overcome the adversities of working in the driest, coldest, and windiest continent on Earth, surrounded by the rough waters of the Southern Ocean. Indeed, several oceanic fronts, strong winds, and the largest marine current on Earth (the Antarctic Circumpolar Current, ACC) isolate Antarctica and the Southern Ocean from the Pacific, Atlantic and Indian Oceans, giving to Antarctica its characteristic inaccessibility (see BOX 1 for the different definitions of Antarctica and the Southern Ocean; Figure 1).

Apart from delaying the human discovery of the austral continent, the isolation of Antarctica and its inaccessibility have had a great influence on the unique biota that we find there. Both terrestrial and marine habitats exhibit a high degree of endemism, ranging from 35 to 90% for marine groups (Arntz et al., 1997) and even reaching 100% of the species for some terrestrial taxa (Andrássy, 1998). Focusing on the Antarctic marine fauna, one of its most distinguishing peculiarities is its unique species composition regarding certain taxa, which differs from the distribution of species found elsewhere in the world. Specifically, generally abundant groups in warmer seas, such as brachyuran crabs, balanomorph barnacles, and sharks are completely missing from Antarctic waters (Barnes et al., 2006). Moreover, fishes and molluscs, which account for a great percentage of species in other latitudes, are poorly represented in the Southern Ocean (Clarke & Johnston, 2003). On the other hand, pycnogonids and peracarid crustaceans are exceptionally diverse (Clarke & Johnston, 2003). This singular biota found in Antarctic waters is the result of geological events (see Section 2) that have impeded the survival of some taxa, while promoted the diversification and dominance of other groups that have adapted to the severe conditions of the Southern Ocean.

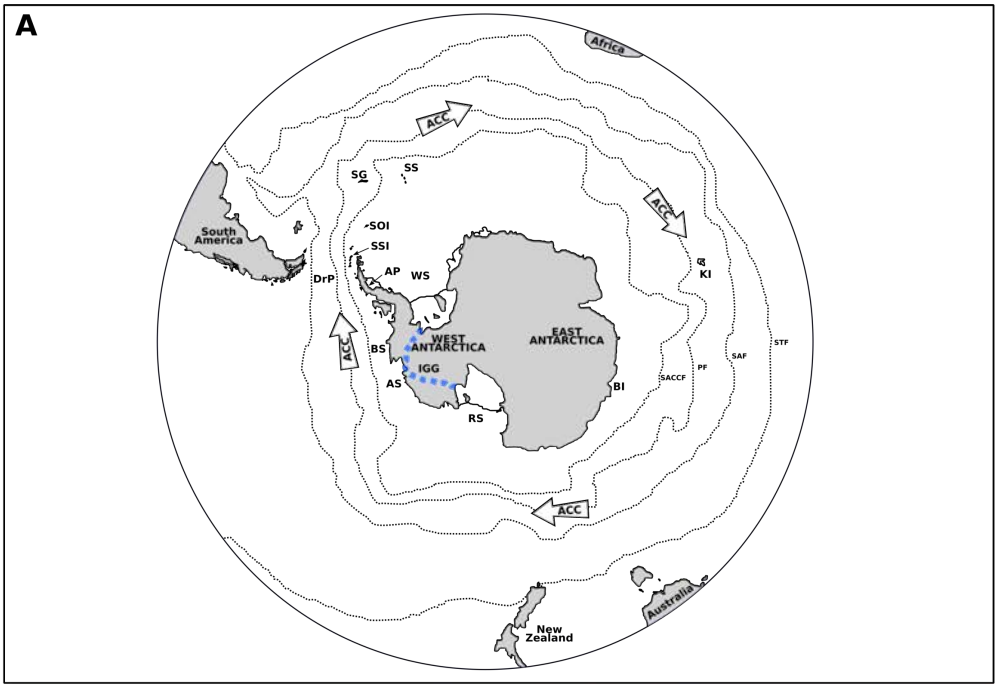
A
Africa
ACC
SG
SS
South America
SOI
SSI
DrP
AP
WS
KI
WEST ANTARCTICA
EAST ANTARCTICA
BS
IGG
AS
BI
RS
SACCF
PF
SAF
STF
New Zealand
Australia

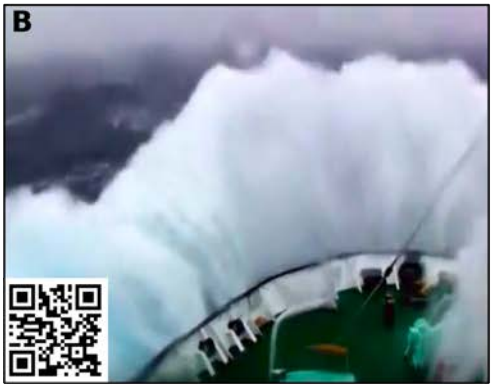
B


C


D


E

Unfortunately, despite its remoteness, Antarctica does not escape from the effects of global warming and climate change. In fact, some areas of West Antarctica are currently undergoing one of the most rapid warmings documented on the planet (Vaughan et al., 2003; Schmidtko et al., 2014). For instance, surface water summer temperature off the Western Antarctic Peninsula (WAP) increased by more than 1°C during the second half of the 20th century (Meredith & King, 2005; Mulvaney et al., 2012). This West Antarctic ocean warming has severe consequences for ice sheets and glaciers in the Antarctic Peninsula and the Bellingshausen and Amundsen Seas (Cook et al., 2005; Mouginot et al., 2014; Rignot et al., 2014), with serious repercussions on projected sea-level rise. Also, a recent study on Antarctic sea-ice coverage (Parkinson, 2019) showed a huge loss of sea ice in the Southern Ocean during the 2014-2017 period after three decades of overall increase, far exceeding the rates of sea-ice loss in the Arctic Ocean. After a modest uptick in 2017-2018, sea ice extent has fallen again in 2019 (Vaughan, 2019). Although these unprecedented losses cannot be exclusively linked to climate change, the 40-year negative trend in the WAP and the Bellingshausen-Amundsen area (Parkinson, 2019) could indeed be mostly caused by global warming. A matter of concern is that Southern Ocean warming especially threatens Antarctic shallow-water organisms, which are less resilient to temperature increases than species elsewhere (Peck & Conway, 2000), with their essential biological functions being extremely sensitive to temperature fluctuations (Peck et al., 2004). This “sensitivity” is originated by their adaptation to almost constant gelid water temperatures all over the year and throughout millions of years of their evolutionary histories.

Apart from global threats, fishing and the growing tourism industries locally threaten Antarctic biodiversity. Although regulated by the Commission for the

Figure 1. (A) Map of Antarctica and the Southern Ocean. Oceanic Fronts are represented by dashed lines: SACCF, Southern Antarctic Circumpolar Current Front; PF, Polar Front; SAF, Subantarctic Front; STF, Subtropical Front. The Antarctic Circumpolar Current (ACC) flows clockwise from west to east between the SACCF and the SAF, and it is represented by four ACC arrows. The different areas mentioned throughout this PhD dissertation are shown in the map: WS, Weddell Sea; RS, Ross Sea; AS, Amundsen Sea; BS, Bellingshausen Sea; IGG, Interglacial gateway; DrP, Drake Passage; AP, Antarctic Peninsula; SSI, South Shetland Islands; SOI, South Orkney Islands; SG, South Georgia Island; SS, South Sandwich Islands; BI, Beall Island; KI, Kerguelen Islands. **(B)** Image showing a storm during a Drake Passage crossing, from South America to Antarctica. Read the QR Code to access the video from which the screenshot was taken (https://youtu.be/AoIiIvmRohM). **(C)** Image of the PhD candidate sampling by SCUBA diving at Whalers Bay, Deception Island (South Shetland Islands). Read the QR Code to access the video from which the screenshot was taken (https://youtu.be/Z1Okrx8caUk). **(D)** Image of the intertidal sampling at Cierva Cove (West Antarctic Peninsula). **(E)** Image of the PhD candidate sampling the intertidal area next to King Edward Point, South Georgia Island.

Conservation of Antarctic Marine Living Resources (CCAMLR) since 1982, the fishing industry presents potential problems such as overfishing target species, causing cascading effects on other species that depend on the target species, killing other species accidentally caught alongside the target species, and the destruction of habitat by fishing gear. Likewise, Antarctic tourism is regulated by the International Association of Antarctic Tour Operators (IAATO) since 1991, applying strict guidelines limiting the size of the ships and the number of tourists that can land at each landing site. However, although Antarctic tourism has been claimed to increase the environmental awareness of tourists, there is no evidence for this hypothesis (Eijgelaar et al., 2010) and, moreover, Antarctic tourism creates up to eight times more greenhouse gas emissions than the average international tourism trips (Eijgelaar et al., 2010). Furthermore, tourism landing sites and research stations are a significant focus of local human pressure for the environment, mainly placed close to breeding sites (ice-free areas) with a high affluence during the breeding season (austral summer). Thus, disappearing of breeding areas and behavioural changes of gentoo, chinstrap, and Adélie penguins, southern giant petrels, Weddell seals, and southern elephant seals have been related to human activity near research stations and visited areas (Culik & Wilson, 1991; Martín et al., 2004; Chwedorzewska & Korczak, 2010),

BOX 1: Different definitions of Antarctica and the Southern Ocean

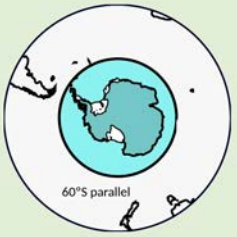

Politically, Antarctica is defined by the Antarctic Treaty System as all land masses and ice shelves south of the 60°S parallel. Similarly, the Southern Ocean is considered by the International Hydrographic Organization as the ocean south of the 60° parallel.

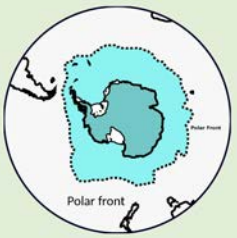

However, for **scientists**, especially for oceanographers and marine biologists, the most commonly accepted definition for the Southern Ocean is all the waters south of the Polar Front.

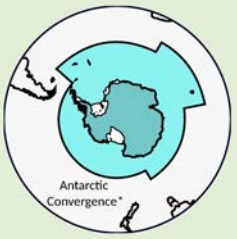

Regarding the **management** of its living resources, the Commission for the Conservation of Antarctic Marine Living Resources (CCAMLR) defines the Antarctic Convergence* as the line represented in the illustration and the Antarctic Marine Ecosystem as all living resources and their physical environment south of the Antarctic Convergence*.

*In oceanography, the Polar Front is also sometimes referred as the Antarctic Convergence.

highlighting the need for local protection to specific areas.

In order to protect specific areas from such local pressures, 75 Antarctic Specifically Protected Areas (ASPAs) and seven Antarctic Specifically Managed Areas (ASMAs) were adopted in 1991 by the Environmental Protocol. ASPAs and ASMAs were not designated just to protect areas with environmental importance, but also areas with a scientific, historic, aesthetic or wilderness value. Among them, ten ASPAs and three ASMAs protect marine or partially marine environments. A part from these ASPAs and ASMAs, CCAMLR delimited two Marine Protected Areas (MPAs) southern to the 60°S parallel: South Orkney Islands Southern Shelf MPA and Ross Sea Region MPA, the latter being the world's largest MPA (Figure 2A). Northern to the 60°S parallel but including waters south of the Antarctic Convergence *sensu* CCAMLR (see BOX 1), there are six protected regions designated by sovereign countries: South Georgia and the South Sandwich Islands MPA (UK), Bouvet Island Marine Reserve (Norway), Prince Edward Islands MPA (South Africa), Crozet Islands MPA (France), Kerguelen Islands MPA (France), and Heard Island and McDonald Islands Marine Reserve (Australia) (Figure 2A). Three additional MPAs southern to the 60°S parallel have been proposed or are under discussion, but still not adopted by the CCAMLR: Domain 1 MPA (covering areas of the WAP and the South Scotia Arc region), Weddell Sea MPA, and East Antarctica Representative System of MPAs (Figure 2A). Moreover, although nowadays there are almost no local human pressures in the Amundsen and Bellingshausen Seas, they are in need of protection due to the drastic changes undergoing in the area concerning ocean warming (Mouginot et al., 2014; Rignot et al., 2014; Parkinson, 2019). The adoption of all these MPAs is paramount to create a

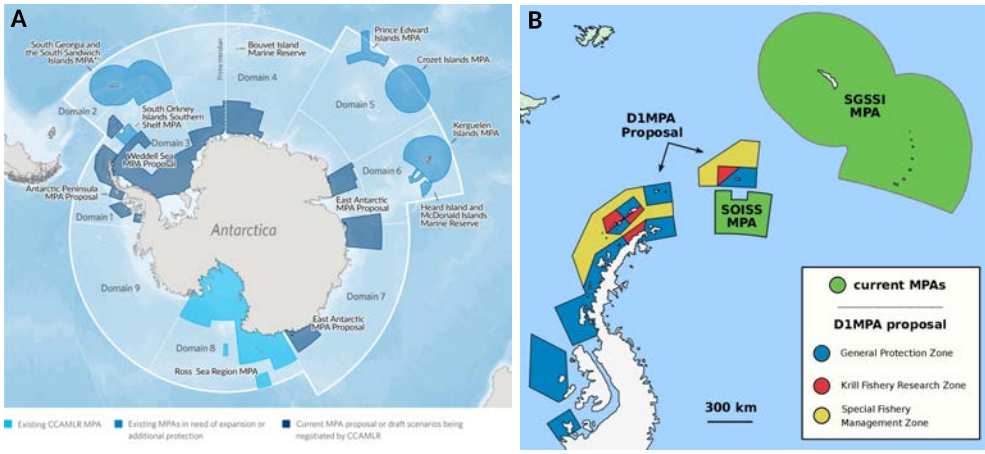

Figure 2. (A) Map showing MPAs and MPA proposals within the CCAMLR area (from the Pew Charitable Trust). **(B)** Map of the current MPAs (SOISS and SGSSI MPAs) and the proposed Domain 1 MPA (D1MPA) in our study area. Differently protected regions are marked for D1MPA proposal, following Friedlaender et al. (2018).

network of connected MPAs all around Antarctica, which is an objective of CCAMLR since 2002 in order to preserve Antarctic biodiversity and conduct a rational management of its living resources.

Key features that should be taken into account for MPA design are larval dispersal and population connectivity (Palumbi, 2003; Krueck et al., 2017), which leave a genetic track that is now easily traced with sequencing techniques. Thus, understanding gene flow patterns of Antarctic marine organisms is crucial to protect Southern Ocean biodiversity. However, this information is still scarce (see Section 3), as many Antarctic marine taxa are just beginning to be studied from a population genetics perspective (Riesgo et al., 2015). Although current gene flow levels have a fundamental role on the spatial patterns of genetic diversity, it is important to understand first the geological processes that took the Antarctic biota to its present state (see Section 2), which modelled their historical demography leaving behind conspicuous genetic signals in their genomes. The discipline studying such genetic signals, both within species boundaries and between species, in combination with the environmental and geological events driving such process is called Phylogeography.

2- Antarctica and the Southern Ocean in a geological time scale

Although Antarctic organisms are descendants of Gondwanan species, the most relevant events affecting their current biogeographic patterns began after the breakup of Gondwanaland (Halanych & Mahon, 2018). By 42 Mya, the separation of Antarctica from South America started with the formation of the Drake Passage and the subsequent isolation of the Antarctic continent. The Antarctic isolation was followed by a global cooling event starting at ca. 34 Mya, at the Eocene-Oligocene boundary (see Figure 3), with a rapid temperature decrease that led to a marine mass extinction (Ivany et al., 2000). Different hypotheses have been risen to explain whether Antarctic ice sheet formation was a consequence of the thermal isolation due to the marine gateways opened around Antarctica (Tasmanian Seaway and Drake Passage) (Kennett, 1977), or a consequence of the CO_2 drawdown occurred globally during the Eocene-Oligocene boundary (DeConto & Pollard, 2003). Recent studies seem to rather indicate to a combination of both hypotheses, with the widening of Southern Ocean gateways increasing upwellings, productivity, and diatom proliferation (Zachos et al., 1996; Diester-Haass & Zahn, 2001; Egan et al., 2013), which affected the biogeochemical carbon cycle (Fyke et al., 2015), causing the atmospheric CO_2 decline that induced the Antarctic ice sheet formation (Lear & Lunt, 2016).

The Antarctic glaciation marked the beginning of the ongoing ice age, the Late Cenozoic Ice Age, and affected global climate by increasing Earth's albedo and changing oceanic currents (Goldner et al., 2014), which favoured further global cooling (Figure 3).

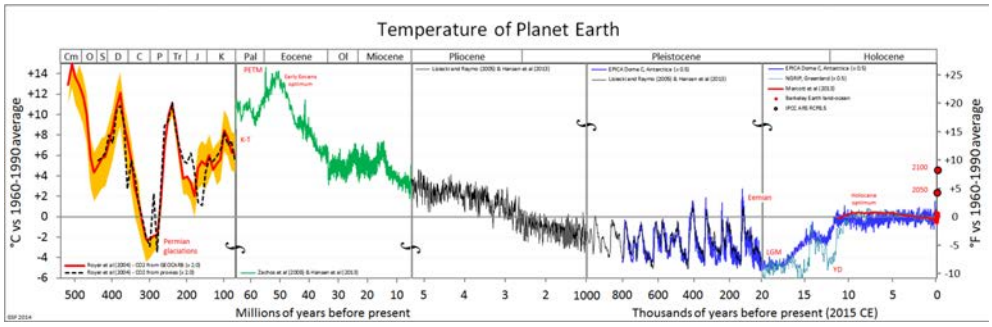

Figure 3. Global averaged temperature estimates for the last 540 Mya (Author: Glen Fergus, downloaded from Wikimedia commons in August 2019: https://commons.wikimedia.org/wiki/File:All_palaeotemps.png).

At about 32–28 Mya, the Antarctic Circumpolar Current (ACC), the Antarctic Polar Front (APF), and the Subantarctic Front (SAF) were already formed and close to their current positions (Lawver & Gahagan, 2003; Halanych & Mahon, 2018). These oceanographic phenomenona are generally considered the forces allowing for the passive organismal dispersal around Antarctica (ACC) and impeding the connectivity between Antarctic and temperate waters (APF and SAF).

The Late Cenozoic Ice Age is well known by its repeated glacial cycles, consisting in the alternation of glacial and interglacial periods (Figures 3–4). Periodical variations on Earth's orbital precession, obliquity, and eccentricity (Milankovitch cycles) are the dominant factors governing glacial cycles, which are reinforced by feedback mechanisms such as atmospheric CO_2 concentration and Earth's albedo (Spiegel et al., 2010). Although Antarctic ice sheets were not yet expanding all over the continent at first, repeated glacial cycles already occurred during the Oligocene (ca. 34–23 Mya) and into the Miocene (ca. 23–5 Mya) (Crame, 1999; Liebrand et al., 2017), associated with substantial faunal extinctions (Prothero, 1994). A major ice expansion occurred 14–17 Mya, with the development of the West Antarctic ice shelf at 5–6 Mya (Halanych & Mahon, 2018). Later on, glacial cycles continued during the Pliocene (ca. 5–2.5 Mya) and Pleistocene (from ca. 2.5 Mya to 11.7 Kya) epochs, with at least 38 glacial cycles during the last five million years (Naish et al., 2009).

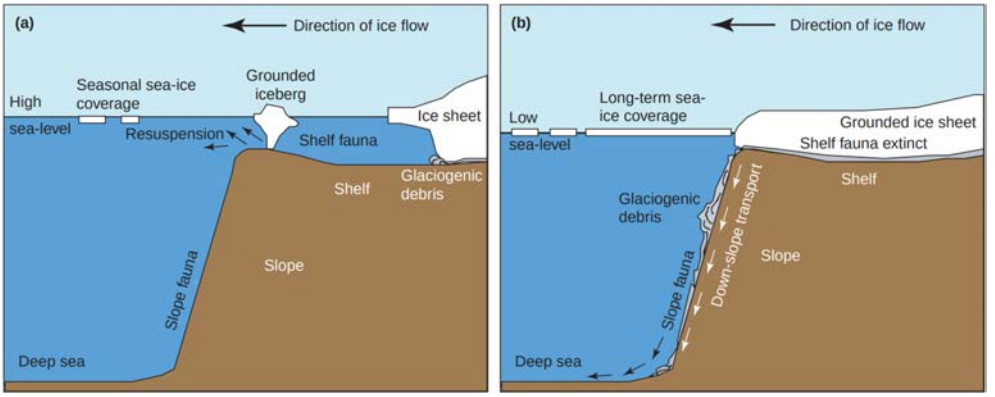

Figure 4. Environmental conditions on the Antarctic continental margin during interglacial **(A)** and glacial **(B)** periods. (Figure from Thatje et al., 2005).

Pliocene–Pleistocene glacial cycles are considered to be the major factors shaping the current biodiversity and biogeography of the Southern Ocean (Thatje et al., 2005). During glacial periods, Antarctic continental shelf was largely occupied by grounded ice sheets, destroying most of the habitat for shallow-water organisms (Thatje et al., 2005; see Figure 4). However, even during glacial maxima, there were some ice-free areas in the continental shelf available for shallow-water organisms. For instance, coastal polynyas caused by katabatic winds were widespread along the Antarctic continental margin during the Last Glacial Maximum (LGM) (Smith et al., 2010). Moreover, the non-simultaneity on the advances and retreats of East and West Antarctic Ice Sheets allowed the presence of continental shelf ice-free areas throughout glacial periods (Anderson et al., 2002). Also, geothermal active regions were capable of maintaining ice-free areas during glacial periods even during intervals of volcanic inactivity (Fraser et al., 2014). Afterwards, during interglacial periods, ice retreat allowed the continental shelf recolonization by organisms expanding from glacial refugia (see Figure 4). Interestingly, there are evidences supporting that during some especially warm interglacials, such as MIS 31 (ca. 1 Mya), MIS 11c (ca. 400 Kya), and the Last Interglacial Period (MIS 5e, 127–116 Kya), the West Antarctica Ice Sheet collapsed, opening ocean gateways between the Weddell, Amundsen, and Ross Seas (Pollard & DeConto, 2009; Raymo & Mitrovica, 2012; O'Leary et al., 2013; Sutter et al., 2016), and thus, allowing migration between these areas and providing potential routes of recolonization.

3- Evolutionary history, connectivity, and phylogeography of Antarctic shallow-water organisms

3.1 Effects of glacial cycles on Antarctic fauna

As expounded above, glacial cycles are considered the most influential events affecting the demographic history of Antarctic shallow-water organisms. During glacial periods, grounded ice sheets expanding over the continental shelf caused major extinctions, with profound consequences for the surviving organisms. Three different refugium hypotheses have been proposed for the glacial survival of shallow-water species: (i) migration to the slope and abyssal deeper waters (e.g. *Astrotoma agassizii*, see Hunter & Halanych (2008)), (ii) migration to Subantarctic areas (e.g. *Nacella concinna*, see González-Wevar et al. (2013)), and (iii) *in situ* survival in ice-free areas (e.g. *Sterechinus neumayeri*, see Díaz et al. (2011, 2018)). These three different strategies left behind characteristic genomic signatures and contrasting spatial patterns of genetic diversity, allowing us to unveil glacial evolutionary histories of Antarctic organisms through the study of genetic markers (see Figure 5), in most of the cases, using the cytochrome c oxidase I (*COI*) mitochondrial marker. However, High-Throughput Sequencing methodologies can relatively easily obtain hundreds-thousands of genome-wide markers for non-model organisms (see BOX 2). Although the implementation of genome-wide techniques is nowadays a common practice in the population genetics field, they have been seldom used to resolve phylogeographic patterns of Antarctic marine invertebrates (see BOX 2).

Regardless of the refugium strategy, glacial cycles are intrinsically related to many characteristic features of Antarctic shallow-water organisms. During glacial periods, ice expansions caused generalised population decimations producing bottleneck events, which are easily detected by genetic diversity analyses (Rogers, 2007; Allcock & Strugnell, 2012). A recent and severe bottleneck event typically leaves behind extremely low genetic diversities accompanied by signals of demographic expansion (Figure 5A and 5C for the populations of *Nacella concinna* from South Orkneys, South Shetlands and the Antarctic Peninsula). Moreover, habitat fragmentation and population isolation in different refugia are considered determinant factors explaining the prevalence of cryptic species in Antarctica (Allcock & Strugnell, 2012), which have been pervasively found across a wide variety of taxa such as amphipods (Baird et al., 2011), sea spiders (Krabbe et al., 2010), sea slugs (Wilson et al., 2009), octopods (Allcock et al., 2011), brittle stars (Hunter & Halanych, 2008), crinoids (Wilson et al., 2007), annelids (Schueller, 2011), and nemerteans (Thornhill et al., 2008). Similarly, allopatric speciation events occurring during glacial periods can produce adaptive radiations, a phenomenon referred as the Antarctic Biodiversity Pump (Clarke & Johnston, 1996; Rogers, 2007). This event increases Southern Ocean biodiversity balancing glacial-related extinctions. Afterwards, during interglacial periods, population

expansions may induce secondary contacts between species and lineages that recently diverged and evolved in different refugia, allowing for a potential high hybridisation scenario between these young lineages that may still be able to interbreed. However, to the best of our knowledge, this scenario still remains unexplored for Antarctic organisms.

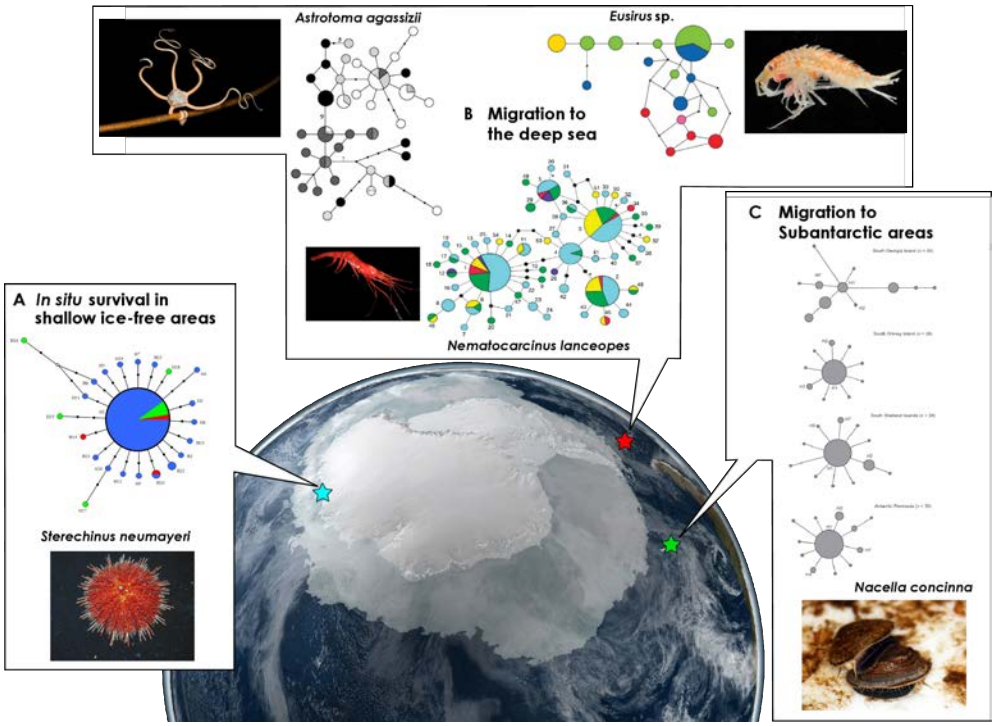

Figure 5. Representation of Antarctica and the Southern Ocean during a glacial period, showing the different glacial refugia strategies proposed for shallow-water benthic invertebrates and the resulting haplotype networks after interglacial expansion. Image from the NASA Scientific Visualisation Studio. Haplotype networks of a (A) *in situ* survival refugium in the Antarctic continental shelf from Díaz et al. (2018) (*Sterechinus neumayeri*), (B) deep-sea refugia from Hunter & Halanych (2008) (*Astrotoma agassizii*), Allcock & Strugnell (2012) (*Eusirus* sp. and *Nematocarcinus lanceopes*), and (C) Subantarctic refugium from González-Wevar et al. (2013) (*Nacella concinna*).

BOX 2: High-Throughput Sequencing (HTS) and Antarctic non-model organisms

During the last decade we lived the great expansion of HTS methodologies, enabling the low-cost discovery and genotyping of genome-wide markers for phylogenetic, phylogeographic, and population genomic studies of non-model organisms. However, traditional genetic markers are still useful to resolve questions at specific evolutionary scales.

Within HTS approaches, whole genome sequencing is not cost-effective yet for its use in non-model species. On the other hand, reduced-representation sequencing techniques, such as restriction site-associated DNA sequencing approaches (RADseq) and transcriptomics, have become the most widely used methodologies in evolutionary, adaptation, and population genomic studies of non-model species. Their main strength is that these methods do not require any prior genomic information for the taxa being studied (Andrews et al., 2016; Catchen et al., 2017). Although these techniques are currently widely used, there is still a taxonomic bias, with a higher number of studies focusing on vertebrates, followed by arthropods (e.g. Gompert et al., 2012; Lack et al., 2012; Li et al., 2016; Ottenburghs et al., 2016; Bernal et al., 2017; Corrigan et al., 2017; Irisarri et al., 2018; Perry et al., 2018).

With only four studies to date, genome-wide markers obtained from HTS methodologies have just reached Antarctic marine invertebrates. RADseq approaches were used to assess population genetic structure of the Antarctic krill *Euphausia superba* (Deagle et al., 2015), the brittle stars *Ophionotus victoriae* (Galaska et al., 2017a) and *Astrotoma agassizii* (Galaska et al., 2017b), and the sea spider *Nymphon australe* (Collins et al., 2018).

3.2 Circumpolarity and euribathy challenged by molecular evidence

Classical assumptions on the genetic connectivity patterns of Antarctic marine organisms included circumpolar connectivity and eurybathy (the ability of organisms thriving at a wide range of depths). Circumpolar connectivity was understood as a consequence of the ACC and its role on the long-distance transportation of larvae and propagules. Secondly, glacial cycles may have promoted eurybathy, following the deep-sea glacial refugium hypothesis. However, these hypotheses were mainly based on morphological studies and theoretical presumptions, and hence they have been challenged with the advent and spread of the use of molecular techniques to assess population connectivity (see BOX 2). For some species, circumpolarity and/or eurybathy were indeed confirmed, such as the eurybathy for the amphipod *Abyssorchomene* sp. (Havermans, 2011) and the sea spider *Nymphon australe* (Arango et al., 2011), and the circumpolarity for the octopus *Pareledone aequipapillae* (Allcock et al., 2011). Similarly, the analysis of RADseq data of the Antarctic krill *Euphasia superba* indicated apparent circumpolar panmixia and ongoing gene flow (Deagle et al., 2015). However, population structure and parochial haplotype networks were present in some other circumpolar species (e.g. Arango et al., 2011; Havermans,

2011), possibly denoting lack of current connectivity. Other species showed clear population structure, lack of population connectivity, and cryptic speciation events refuting circumpolarity and eurybathy. For instance, in the annelid *Glycera kerguelensis*, extreme eurybathy was proved false in favour of the recognition of numerous cryptic species occupying restricted depth ranges (Schueller, 2011). Likewise, geographic structure was found in the brittle star *Ophionotus victoriae*, revealed from mitochondrial markers and RADseq data (Galaska et al., 2017a), suggesting no current migration between the different sampled areas. Interestingly, Hemery et al., (2012) reported the presence of cryptic mitochondrial lineages in the crinoid *Promachocrinus kerguelensis*, but instead of presenting geographic structure, they constituted a complex of sympatric, eurybathic and circumpolar cryptic lineages.

The rejection of a generalised circumpolarity and eurybathy by the description of cryptic species complexes presents taxonomic implications that usually remain out of the scope of molecular studies (e.g. Wilson et al., 2007; Krabbe et al., 2010; Schuller 2011; Hemery et al., 2012). However, it is crucial to describe key features of the taxa under study, such as the putative species distributions and bathymetry, morphological characters, and reproductive strategy, which will allow a proper design of population genetic and phylogeographic studies. The recognition of cryptic speciation events adds difficulties to the taxonomy of Antarctic organisms, which already presented inherent challenges associated to Antarctic inaccessibility, such as the huge cost that sampling in the Southern Ocean entails. Furthermore, because circumpolarity was commonly assumed, morphologically similar and closely related species from distant areas were identified as belonging to the same species, thus underestimating the true biodiversity of the Southern Ocean (Allcock & Strugnell, 2012). Hence, species that are relatively abundant and common in Antarctic waters are still described or re–described (e.g. Allcock et al., 2007; Taboada et al., 2013; Vecchi et al., 2016; Moles et al., 2016). In addition, this underestimation has been muddied by the numerous poor original descriptions from the 19th and early 20th centuries (e.g. Kinberg, 1866; McIntosh, 1876, 1885; Ehlers, 1897) in most of the cases lacking diagnostic characters, the loss of type material, and an absence of exhaustive and deep taxonomical reviews of many Southern Ocean faunal groups.

3.3 Influence of the reproductive mode on the connectivity of benthic invertebrates

Larval dispersal and life history traits involved in reproduction are generally considered crucial aspects for population connectivity of marine organisms (e.g. Cowen & Sponaugle, 2009; Selkoe & Toonen, 2011; Baco et al., 2016; O'Donnell et al., 2017; Pascual et al., 2017). Particularly for benthic invertebrates, which mainly present sessile adults or adults with limited motility, their reproductive strategy and larval dispersal are key factors for understanding population connectivity patterns (e.g. Mokhtar-Jamaï et al., 2011; Haye et al., 2014; Riesgo et al., 2016; Riesgo et al., 2019).

To understand the effects of reproductive strategies on population connectivity, we should distinguish between prezygotic and postzygotic features. First, fertilization can occur inside the female body (internal fertilization) or in the water column after spawning (external fertilization). The release into the water column of eggs and sperm by broadcast spawning species may confer them a prezygotic opportunity to disperse, and hence higher population connectivity levels. After fertilization, eggs can be brooded by progenitors, directly developing into adult-like juveniles or, otherwise, females release planktonic larval stages, which present obvious higher dispersal capabilities. Among species with planktonic larval stages, some present feeding planktotrophic larvae and others non-feeding lecithotrophic larvae (exclusively relying on their yolk), with the former conferring *a priori* higher dispersal abilities.

Although it is considered to be a universal correlation, the intimate relationship between reproductive strategy and population connectivity is not always identified. For instance, brooding species and species with direct development sometimes present high genetic connectivity (e.g. Richards et al., 2007; Hunter & Halanych, 2008), while broadcast spawning species and species with planktotrophic larvae occasionally display the opposite pattern, i.e. high population differentiation (e.g. Piggott et al., 2008; Ayre et al., 2009; Nagel et al., 2015). Whether such differences are driven by environmental or oceanographic processes more than potential dispersal capabilities still remains to be solved. In this sense, comparing the genetic connectivity patterns of co-existing species subjected to similar oceanographic features but with divergent reproductive strategies can broaden our understanding on the relationship between population connectivity and dispersal capabilities.

3.4 Implications of molecular connectivity studies on conservation

There is a wealth of studies with a continental approach in Antarctica (see section 2.2), and in contrast, very few research has focused on the gene flow and population structure at regional and local scales. Most of the population genetics and phylogeographic studies cited above considered large areas, such as the WAP and its surrounding islands, as a single location. However, the WAP is a complex area presenting different water masses, strong currents, oceanographic fronts, and eddies systems (Gordon & Nowlin, 1978; Zhou et al., 2002; Sangrà et al., 2011). These oceanic features undoubtedly affect the genetic structure and gene flow of species that rely on planktonic stages of their life cycle to connect their populations. Hence, taking into account the fundamental role of connectivity for maintaining metapopulation persistence (Palumbi, 2003; Krueck et al., 2017), there is a deficiency of an essential information required for properly designing networks of protected areas in Antarctica. For instance, focusing on the WAP, there is still scarce data about how different areas within the WAP are connected and whether there is current gene flow between the WAP region and the MPAs located further north (South Orkney

Islands Southern Shelf MPA and South Georgia and South Sandwich Islands MPA). This is especially noteworthy because the region including the WAP and both MPAs cited above is the main fishing area for the Antarctic krill fishery (data from CCAMLR website: www.ccamlr.org/en/fisheries/krill), the largest fishery by tonnage in the Southern Ocean (Nicol et al, 2011). Fishing interests in the Southern Ocean have been interfering with conservation objectives in the past (Brooks, 2013; Cordonnery & Kriwoken, 2015), such as in the adoption of the South Orkney Islands Southern Shelf MPA. Although it protects a large continental shelf area, this MPA fails to protect the regions adjacent to the Islands, which are biologically rich areas with high values for conservation objectives, but are also prime krill fishing grounds (Brooks, 2013). Moreover, the Domain 1 MPA proposal discussed in the 37th CCAMLR Meeting in 2018 (see Figure 2B) comprised General Protection Zones combined with Krill Fishery Research Zones and Special Fishery Management Zones (Friedlaender et al., 2018). This spatially patchy distribution of zones requires a deep understanding of the connectivity between the differently protected areas, and we are very far from it yet. For instance, results from González-Wevar et al. (2013) suggested population homogeneity for the Antarctic limpet *Nacella concinna* along the WAP and the South Orkney Islands, and differentiation between this homogeneous group and the organisms collected from South Georgia Island, indicating no current gene flow between these two distinct populations. However, within the WAP, Galaska et al. (2017a) found signals of population differentiation in the brittle star *Ophionotus victoriae* between the central and the northern WAP regions, the latter presenting higher genetic diversity and grouping with Weddell Sea populations. Other studies seem to agree with the northern WAP region being an area of high genetic diversity (e.g. Wilson et al., 2007, 2013; Mahon et al., 2008), which could be explained by the mixing of waters that take place in the Bransfield Strait. In summary, such shallow understanding of gene flow in one of the most threatened areas of the planet by global warming, calls for a stronger effort in disentangling the evolutionary forces driving the past and present distributions of the organisms living there.

Objectives

Overall, my PhD dissertation aims to understand the evolutionary history, phylogeographic and connectivity patterns of seven Antarctic shallow-water benthic invertebrates, with the goal of shedding light on the limited knowledge that we have about these subjects at regional scales. Moreover, the studied species were selected from different phyla, presenting different reproductive strategies and hence different dispersal capabilities (see BOX 3). We used three congeneric brooding nemerteans, namely *Antarctonemertes valida*, *Antarctonemertes riesgoae*, and *Antarctonemertes unilineata*; the demosponges *Dendrilla antarctica* and *Mycale acerata*, with lecithotrophic larvae; the annelids *Pterocirrus giribeti*, which presents planktotrophic larvae, and *Neanthes kerguelensis*, also having planktotrophic larvae but displaying epitoky in addition. This selection allowed us to assess whether the reproductive strategy plays a role on the connectivity as it does in other oceans (e.g. Selkoe & Toonen, 2011; Pascual et al., 2017), or contrarily, population connectivity in the Southern Ocean is independent of the reproductive strategy as suggested by Halanych & Mahon (2018). Specific objectives for each chapter are summarised below.

BOX 3: Reproductive strategies and dispersal abilities of the selected species

Reproductive strategy plays an important role in the dispersal capabilities of all marine organisms, but it is even more important when studying benthic invertebrates (see Introduction section 2.3). In my PhD dissertation, seven species from three different phyla have been studied, representing a wide variety of reproductive strategies:

***Antarctonemertes* spp.** The three species selected (*A. valida*, *A. riesgoae*, and *A. unilineata*) are brooders. Females build cocoons where they lay the eggs that are subsequently fertilized by males. Since they do have a well-documented direct development and adults are not known to actively disperse, these species depend on passive transportation of adults by drifting algae for population connectivity (and cocoons in the case of *A. valida*, see illustration above).

***Dendrilla antarctica* and *Mycale acerata*.** These two demosponges present sessile adults, with their dispersal abilities totally relying upon their non-feeding lecithotrophic larvae. Their larvae have been found to present a remarkable content of proteinaceous yolk (Koutsouveli et al., 2018), which could potentially confer them with a longer planktonic larval duration than expected.

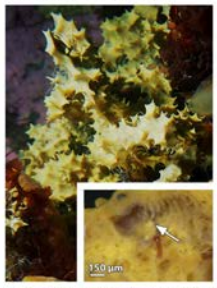

Image from Koutsouveli et al. (2018). White arrow points out *D. antarctica* embrios.

***Neanthes kerguelensis*.** This species presents epitoky, a bizarre life cycle characterised by the presence of two adult forms: a benthic and sexually immature 'atoke' and a pelagic and sexually mature 'epitoke'. During sexual maturation, drastic changes in behaviour, morphology and physiology occur. Epitokes are generally non-feeding and specialised for swimming and reproducing, with elongated parapodia and paddle-like chaetae. For their population connectivity, *N. kerguelensis* may rely on pelagic epitokes drifted by the currents as well as on the passive transportation of atokes by drifting algae. Besides, planktotrophic larvae (never described for *N. kerguelensis* but assumed as in many other epitoke nereids) may also increase dispersal abilities of the species.

***Pterocirrus giribeti*.** Despite not being described yet, *P. giribeti* may present planktotrophic (feeding) larvae as other phyllodocid annelids. This kind of larva may confer the species high dispersal abilities, as they may last for weeks in the water column. Moreover, adults can be drifted away on the algae they inhabit.

Chapter 1: "Population structure and phylogenetic relationships of a new shallow-water Antarctic phyllodocid annelid"

In this chapter we present the formal taxonomic description and phylogenetic positioning (using two nuclear and two mitochondrial markers) of a new phyllodocid annelid of the genus *Pterocirrus*. In the past, this new species was erroneously identified as *Eulalia subulifera*, which still requires a deep taxonomic review. We also investigated the genetic diversity, demographic patterns and gene flow of the new species across the Western Antarctic Peninsula and the South Shetland Islands, using two mitochondrial markers (*16S rRNA* and *COI*).

Chapter 2: "Population substructure and signals of divergent adaptive selection despite admixture in the sponge *Dendrilla antarctica* from shallow waters surrounding the Antarctic Peninsula"

Here, we aim to assess the genetic diversity, connectivity, and demographic history of *Dendrilla antarctica* at a regional scale in the Western Antarctic Peninsula and associated islands using ddRADseq-derived single nucleotide polymorphisms (SNPs). We also evaluated the suitability of the full mitochondrial genome in *D. antarctica* to assess genetic diversity and connectivity. Finally, we tested for genetic signatures of divergent selection using SNPs identified as under positive selection. Through the annotation of these outlier SNPs using our *de novo* transcriptomes we suggest which are the main selective pressures currently acting on *D. antarctica* populations.

Chapter 3: "Phylogeographic history of the Antarctic *Antarctonemertes* (Hoplonemertea): reticulate evolution, introgression, and hybridisation"

In this chapter, we aim to unravel the phylogeographic and evolutionary history of the Antarctic species of the genus Antarctonemertes, with a special focus on the hybridisation potential between them both at the present and in the past. We used a combined approach of morphological, mitochondrial (*COI*), and nuclear (ddRADseq-derived SNPs) markers in order to develop robust phylogeographic hypotheses. Our ddRADseq approach also allowed us to study the genomics of adaptation to specific evolutionary histories.

Chapter 4: "Towards a network of connected Marine Protected Areas in Antarctica: insights from genetic connectivity of benthic invertebrates"

The main aim of this chapter is to assess the genetic connectivity between the Marine Protected Areas (MPAs) already present at the Scotia Sea (South Georgia and South Sandwich Islands MPA and South Orkney Islands Southern Shelf MPA) and the MPA proposal that covers the Western Antarctic Peninsula and the South Scotia Sea (Domain 1 MPA). We used sequences of the mitochondrial marker *COI* from five benthic invertebrates representing a wide variety of dispersal abilities, and also ddRADseq-derived SNPs for two of them. We also investigated whether the patchy Domain 1 MPA proposal effectively protects the genetic diversity and is consistent with the migration patterns of the area.

Impact and authorship report of the publications

Supervisors: Dr. Ana Riesgo and Dr. Sergi Taboada

Two out of the four articles that conform this thesis dissertation (Chapter 1–4) have already been published in two high impact journals covering the fields of Zoology, Evolutionary Biology, Molecular Biology, and Ecology. These two papers published in *Zoologica Scripta* and *Molecular Ecology* have been indexed in bibliographic databases (PubMed, ISI). The other two papers are currently in preparation for *Molecular Ecology* (Chapter 3) and *Conservation Biology* (Chapter 4).

Carlos Leiva has been the first author in the four papers, which include international collaborators from Harvard University (USA), the University of Guam (USA), the Scripps Institution of Oceanography (USA), and the Natural History Museum of London (UK).

The specific contributions of Carlos Leiva to each publication are indicated below, together with the yearly impact factor and ranking of each journal, following the ISI ranking.

Chapter 1

Carlos Leiva, Ana Riesgo, Conxita Avila, Greg W. Rouse, Sergi Taboada (2018) Population structure and phylogenetic relationships of a new shallow-water Antarctic phyllodocid annelid. ***Zoologica Scripta*** 47(6): 714-726.
Impact Factor (2018): 2.609
Journal ranking: Zoology Q1 (14/170); Evolutionary Biology Q2 (24/50)
Authorship: CL, AR and ST conceived and designed the study; CL and ST conducted fieldwork, collected samples and conducted lab work; CL, AR and ST wrote the manuscript, and all authors edited various versions of the manuscript.

Chapter 2

Carlos Leiva, Sergi Taboada, Nathan J. Kenny, David Combosch, Gonzalo Giribet, Thibaut Jombart, Ana Riesgo (2019) Population substructure and signals of divergent adaptive selection despite admixture in the sponge *Dendrilla antarctica* from shallow waters surrounding the Antarctic Peninsula. ***Molecular Ecology*** 28: 3151–3170.
Impact Factor (2018): 5.855
Journal ranking: Evolutionary Biology Q1 (8/50); Ecology Q1 (13/164); Biochemistry & Molecular Biology Q1 (40/298)
Authorship: CL, ST, GG and AR conceived and designed the study; CL and GG conducted fieldwork and collected samples; CL, ST, DC and NJK conducted laboratory work; CL, ST, TJ, NJK and AR performed statistical analyses and interpreted the results; CL, ST and AR wrote the manuscript, and all authors edited various versions of the manuscript.

Chapter 3

Carlos Leiva, Sergi Taboada, Ana Riesgo (in preparation for ***Molecular Ecology***) Glacial phylogeographic history of the Antarctic *Antarctonemertes* (Nemertea, Hoplonemertea): reticulate evolution, introgression, and hybridisation.
Impact Factor (2018): 5.855
Journal ranking: Evolutionary Biology Q1 (8/50); Ecology Q1 (13/164); Biochemistry & Molecular Biology Q1 (40/298)
Authorship: CL, ST, and AR conceived and designed the study; CL, ST, and AR conducted fieldwork and collected samples; CL, ST, and AR conducted laboratory work; CL, ST, and AR performed statistical analyses and interpreted the results; CL, ST and AR wrote the manuscript.

Chapter 4

Carlos Leiva, David Combosch, Gonzalo Giribet, Rachel Downey, Ana Riesgo, Sergi Taboada (in preparation for ***Conservation Biology***) Towards a network of Marine Protected Areas in Antarctica: insights from genetic connectivity of benthic invertebrates.

Impact Factor (2018): 6.194
Journal ranking: Biodiversity Conservation Q1 (3/58); Ecology Q1 (11/164); Environmental Sciences Q1 (19/250)
Authorship: CL, ST, and AR conceived and designed the study; CL, ST, GG, RD and AR conducted fieldwork and collected samples; CL, ST, DC and AR conducted laboratory work; CL, ST, and AR performed statistical analyses and interpreted the results; CL, ST and AR wrote the manuscript, and all authors edited various versions of the manuscript.

Dr. Ana Riesgo

Dr. Sergi Taboada

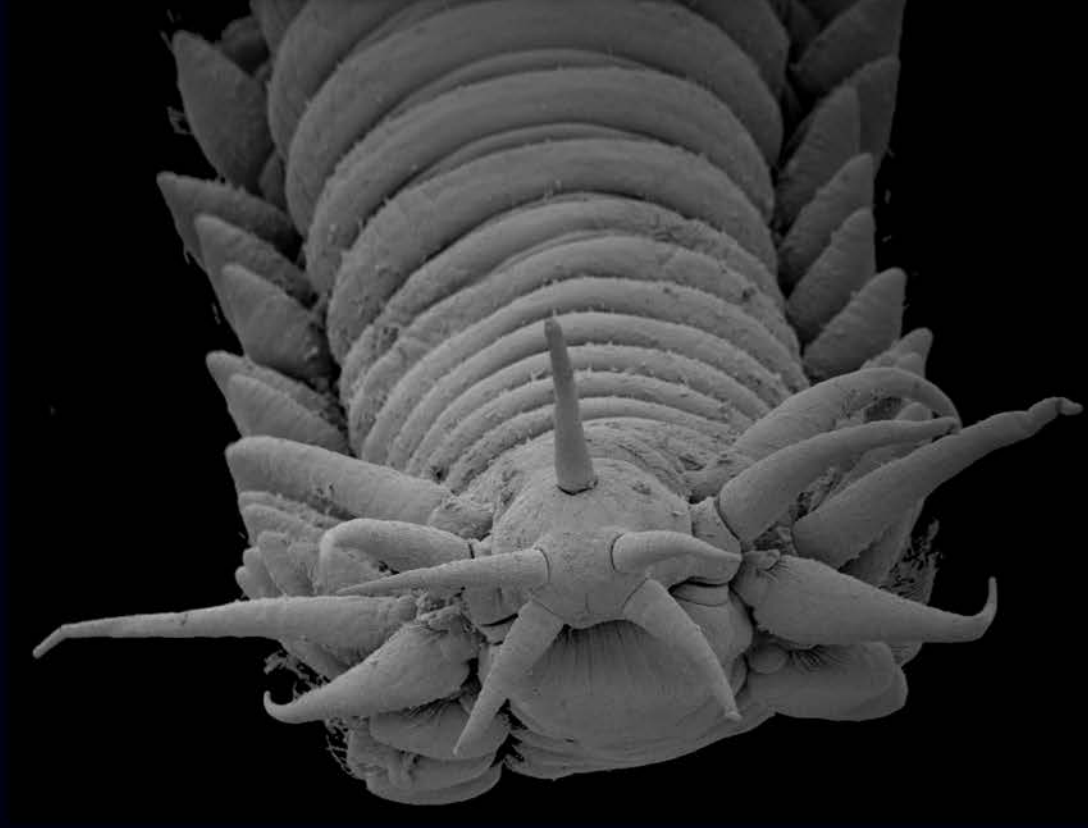

CHAPTER 1

Population structure and phylogenetic relationships of a new shallow-water Antarctic phyllodocid annelid

Received: 18 February 2018 | Revised: 20 July 2018 | Accepted: 21 July 2018

DOI: 10.1111/zsc.12313

ORIGINAL ARTICLE

WILEY Zoologica Scripta

Population structure and phylogenetic relationships of a new shallow-water Antarctic phyllodocid annelid

Carlos Leiva[1,2] | **Ana Riesgo**[2] | **Conxita Avila**[3] | **Greg W. Rouse**[4] | **Sergi Taboada**[2]

[1]Department of Genetics, Microbiology and Statistics, Facultat de Biologia, Universitat de Barcelona, Barcelona, Spain

[2]Department of Life Sciences, Natural History Museum of London, London, UK

[3]Department of Evolutionary Biology, Ecology, and Environmental Sciences, Facultat de Biologia, Universitat de Barcelona, Barcelona, Spain

[4]MBRD, Scripps Institution of Oceanography, La Jolla, California

Correspondence
Carlos Leiva, Department of Genetics, Microbiology and Statistics, Faculty of Biology, University of Barcelona, Av. Diagonal 643, 08028 Barcelona, Spain
Email: cleivama@gmail.com

Funding information
Spanish Ministry of Economy and Competitiveness, Grant/Award Number: CGL2007-65453/ANT, CTM2010-17415/ANT and CTM2013-42667/ANT; Natural History Museum, Grant/Award Number: SDF14032

Abstract

Shallow-water polychaetes are abundant and diverse components of the Southern Ocean benthic communities, and although they have been widely studied, new species that are relatively common are still discovered. Here, we report the discovery of *Pterocirrus giribeti* sp. n., a new and abundant intertidal and upper-subtidal Antarctic phyllodocid. To establish the phylogenetic relationships of the new species, we sequenced two nuclear (*18S* and *28S*) and two mitochondrial (*COI* and *16S*) markers. Although the phylogenetic relationships obtained for the family Phyllodocidae were not fully resolved, we assigned our new phyllodocid to the genus *Pterocirrus* based on both its phylogenetic position and its morphological characters. Using *COI* and *16S* sequences of 126 and 118 individuals, respectively, from eight populations across the South Shetland Islands and the Antarctic Peninsula, we also investigated the genetic diversity and gene flow patterns of this new species. Our results suggested that all populations were panmictic, likely due to the presence of planktotrophic larvae allowing long-distance dispersal. Interestingly, some genetic substructure was detected despite panmixis, and we identified a semipermeable barrier coinciding with an oceanic front produced by the intrusion into the Bransfield Strait of a tongue of water from the Weddell Sea. This front produced signatures of differentiation on populations at the tip of the West Antarctic Peninsula. Moreover, our results indicated a recent demographic expansion throughout the sampled area, in agreement with the "glacial refugium" hypothesis stated for other Antarctic shallow-water invertebrates.

1 | INTRODUCTION

The Southern Ocean is probably one of the most interesting scenarios in which to study how marine life copes with drastic environmental shifts and geological events at an evolutionary time scale. A unique combination of tectonic, oceanographic and climatic shifts has affected Southern Ocean marine organisms over time, with the repeated Pliocene–Pleistocene glacial cycles being the major factors shaping its current diversity and distribution (Thatje, Hillenbrand, & Larter, 2005). Over the past 5 million years, at least 38 glacial cycles have occurred (Naish et al., 2009), consisting in the alternation of glacial and interglacial periods. During glacial periods, most of the Antarctic continental shelf is occupied by grounded ice sheets, which afterwards retreat during interglacial periods. The alternation of these periods might have specially affected shallow-water benthic invertebrates, destroying most of the available habitats during glacial maxima (Allcock & Strugnell, 2012; Thatje et al., 2005). However, ice-free areas of continental shelves might have existed even at glacial maxima due to the nonsimultaneous East and West Antarctic ice sheets (Anderson, Shipp, Lowe, Wellner, & Mosola, 2002),

and to the presence of polynyas along the continental margin caused by katabatic winds (Smith, Hillenbrand, Pudsey, Allen, & Graham, 2010). Hence, three different refugium hypotheses have been proposed for the survival of the shelf species during glacial periods (Allcock & Strugnell, 2012; Thatje et al., 2005): (a) migration to slope and abyssal deeper waters, (b) migration to Subantarctic areas and (c) in situ survival in ice-free areas.

Regardless of the refugium strategy adopted by the organisms, glacial periods in the Southern Ocean are inherently responsible for population isolation and fragmentation, loss of genetic diversity and bottleneck events (Allcock & Strugnell, 2012; Rogers, 2007). Many studies have used molecular approaches (using one or several markers for population genetics) as a way to discover signatures of evolutionary history (Riesgo, Taboada, & Avila, 2015). Thus, using molecular techniques, recent demographic expansions (e.g., González-Wevar, David, & Poulin, 2011), highly structured populations (e.g., Krabbe, Leese, Mayer, Tollrian, & Held, 2010), cryptic or pseudocryptic species complexes (e.g., Baird, Miller, & Stark, 2011), genetic homogeneous areas (e.g., Janosik, Mahon, & Halanych, 2011) or extinction-recolonization events (e.g., González-Wevar, Saucède, Morley, Chown, & Poulin, 2013) have been reported and linked to different glacial-survival strategies, with a crucial influence being exerted by the reproductive and dispersal abilities of the organisms (Thatje, 2012). Surprisingly, there is still scant information about genetic variation in the organisms inhabiting the shallowest waters and the intertidal zone in the Southern Ocean (Griffiths, 2010; Riesgo et al., 2015), because sampling in Antarctica has traditionally involved trawling and dredging in moderate (10–100's m) depths (Griffiths, 2010). Moreover, many of these studies have a continental approach (e.g., Arango, Soler-Membrives, & Miller, 2011; Hemery et al., 2012; Baird et al., 2011), considering vast and oceanographically complex areas, like the West Antarctic Peninsula and the South Shetland Islands, as a single location (Gordon & Nowlin, 1978; Sangrà et al., 2011; Zhou, Niiler, & Hu, 2002), instead of delving into the investigation of local gene flow and connectivity within these regions.

Besides depth and scale tendencies, there is also a taxonomic bias in the Southern Ocean, with many phyla understudied using molecular approaches, regardless of their abundance and distribution patterns (Riesgo et al., 2015). The phylum Annelida is a perfect example of this, since, although Annelida is the second phylum in terms of described species in the Southern Ocean (Clarke & Johnston, 2003), the phylogeography and connectivity patterns of only two species have been studied so far: the glycerid *Glycera kerguelensis* McIntosh, 1885 (Schüller, 2011) and the polynoid *Austrolaenilla antarctica* Bergström, 1916 (Neal, Wiklund, Muir, Linse, & Glover, 2014). Remarkably, both deep-sea species showed cryptic genetic lineages bathymetrically segregated, most likely resulting from glacial cycle disturbances (Neal et al., 2014; Schüller, 2011).

Interestingly, despite the fact that annelids are a large component of the Antarctic shallow-water benthic ecosystems (e.g., Siciński et al., 2011; Angulo-Preckler, Leiva, Avila, & Taboada, 2017), still new species, which are often common, are discovered (e.g., Taboada et al., 2013; Taboada, Bas, & Avila, 2015). This lack of knowledge of the true biodiversity of the Southern Ocean annelid fauna is accentuated by the numerous poor descriptions lacking diagnostic characters from the 19th and early 20th centuries (e.g., Kinberg, 1866; McIntosh, 1885; Ehlers, 1897, 1900; Ehlers & Vanhöffen, 1913; Gravier, 1907). Moreover, an underestimation of the diversity generally occurs because of the assumption of circumpolar, wide-bathymetric and trans-Antarctic-Circumpolar-Current distributions for morphologically similar species (e.g., Hartmann, 1964). Therefore, for several annelid families (if not for all), there is a clear need for a deep taxonomical review, including reinvestigation of type material and resampling of type localities for phylogenetic purposes, aiming to shed light on the real annelid biodiversity that the Southern Ocean harbours.

Here, we present the formal taxonomic description and phylogenetic positioning (using two nuclear and two mitochondrial datasets) of a new species of phyllodocid, a highly diverse and abundant family of annelids in the Southern Ocean (Clarke & Johnston, 2003). The new phyllodocid from the genus *Pterocirrus* Claparède, 1868, is a relatively common species from intertidal and shallow subtidal areas of the Antarctic Peninsula and South Shetland Islands. We also investigated the genetic diversity, demographic patterns and molecular connectivity of the new *Pterocirrus* across the West Antarctic Peninsula and the South Shetlands, using two mitochondrial markers (*16S rRNA* –*16S*– and cytochrome *c* oxidase subunit I –*COI*–), in order to identify the effects that the past climatic events and current oceanographic features of the region might have had on their genetic diversity and population structure.

2 | MATERIALS AND METHODS

2.1 | Sample collection and preservation

A total of 143 specimens of *Pterocirrus* sp. n. were collected in the intertidal and subtidal zones, under rocks and among algae during the ACTIQUIM-2 (2009–2010), ACTIQUIM-4 (2012–2013) and DISTANTCOM-1 (2015–2016) campaigns. Only one organism was collected in 2009–2010, from Deception Island (DEC). The sampling stations surveyed in 2012–2013 included Livingston Island (LIV), Half Moon Island (HM), and King George Island (KG) in the South Shetland Islands, and Cierva Cove (CIE) on the Antarctic Peninsula (Figure 1; Table

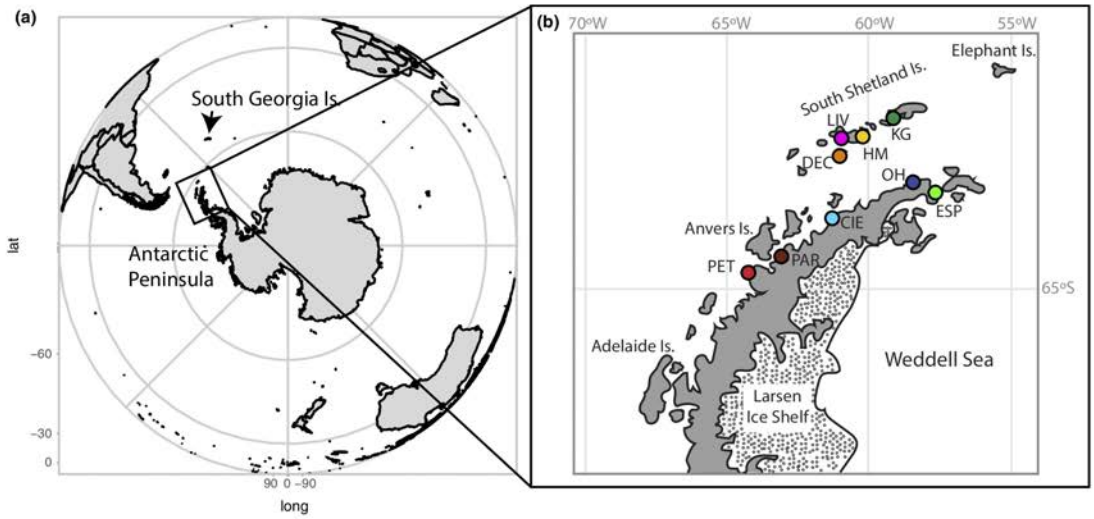

FIGURE 1 (a) Map of Antarctica showing the Subantarctic South Georgia Island and the studied area in the Antarctic Peninsula. (b) Detailed map of the Antarctic Peninsula and the South Shetland Islands showing the sampling stations—PET: Petermann Island; PAR: Paradise Bay; CIE: Cierva Cove; OH: O'Higgins Bay; ESP: Esperanza Bay; DEC: Deception Island; LIV: Livingston Island; HM: Half Moon Island; KG: King George Island

TABLE 1 Collection details for all sampling sites included in the study. *N* = number of specimens of *Pterocirrus giribeti* sp. n. collected

Station	Code	Coordinates	*N*	Depth	Date of collection
Deception Is.	DEC	62°59'25"S 60°37'31"W	1	Intertidal	13/01/2010
Livingston Is.	LIV	62°39'05"S 60°35'50"W	15	Intertidal	28/12/2012
Half Moon Is.	HM	62°35'41"S 59°54'07"W	32	Intertidal	02/01/2013
King George Is.	KG	62°11'55"S 58°56'59"W	21	Intertidal	30/12/2012
Cierva Cove	CIE	64°09'20"S 60°57'12"W	36	Intertidal	05/01/2013
Petermann Is.	PET	65°10'24"S 64°08'36"W	22	Intertidal	14/02/2016
Paradise Bay	PAR	64°49'24"S 62°51'24"W	2	8 m	16/02/2016
O'Higgins Bay	OH	63°18'52"S 57°54'27"W	13	Intertidal	19/02/2016
Esperanza Bay	ESP	63°23'45"S 56°59'45"W	1	Intertidal	22/02/2016
Total			143		

1). The sites sampled in 2015–2016 were Petermann Island (PET), Paradise Bay (PAR), O'Higgins Bay (OH) and Esperanza Bay (ESP), all of them in the Antarctic Peninsula (Figure 1; Table 1). Prior to preservation, organisms were anaesthetized in a 7% solution of $MgCl_2$ in fresh water, observed in vivo and photographed using a stereo microscope. The specimen from DEC was preserved in 10% buffered formalin in seawater and later transferred to 70% ethanol for morphological analysis, and the remaining 142 specimens from the eight other populations (LIV, HM, KG, CIE, PET, PAR, OH and ESP) were preserved in 95% EtOH, replaced three times and stored at −20°C for both molecular purposes and morphological analysis.

2.2 | Morphological analysis

The general morphology of all specimens of *Pterocirrus* sp. n. was examined under a dissecting stereo microscope. For *SEM* observations, three specimens were dehydrated in an ascending ethanol series, critical-point-dried, mounted on pins and coated with gold and imaged with a Zeiss DSM 940A scanning electron microscope in the *Centres Científics i Tecnològics de la Universitat de Barcelona* (CCiT-UB). All specimens examined for morphological analysis were deposited in the Natural History Museum of London (NHM) (see vouchers in Appendix S3).

In addition, material of Antarctic phyllodocids, including the type specimen of *Eulalia subulifera* Ehlers, 1897, deposited at the Hamburg Zoological Museum (V4717) and a specimen of *E. subulifera* from the NHM (NHMUK1930.10.8.1002-1003) were examined under a dissecting stereo microscope and using *SEM*. For *SEM*, these specimens were dehydrated in an ascending ethanol series, critical-point-dried and imaged using low vacuum conditions in a FEI/Philips XL-30 FEG ESEM at the NHM Imaging and Analytical Centre (IAC).

2.3 | DNA extraction and amplification

Between 3 and 5 dorsal cirri, depending on the size of the individual, of 142 specimens of *Pterocirrus* sp. n. were used to extract genomic DNA using the Speedtools Tissue DNA Extraction Kit (Biotools) following the manufacturer's protocol. For the phylogenetic analyses, fragments of the nuclear genes *18S rRNA* (*18S*: 1,748 bp) and *28S rRNA* region D1-D5 (*28S*: 681 bp) and the mitochondrial cytochrome *c* oxidase subunit I (*COI*: 600 bp) and *16S rRNA* (*16S*: 528 bp) were amplified from the *Pterocirrus* sp. n. holotype specimen (see voucher in Appendix S3), and also from one specimen of *Pterocirrus* sp. (SIO-BIC-A4755), *Pterocirrus burtoni* Pleijel, Aguado & Rouse, 2012 (SIO-BIC-A2624), *Pterocirrus nidarosiensis* Pleijel, 1987 (SIO-BIC-A6056), and a specimen of *Pterocirrus montereyensis* (Hartman, 1936) (SIO-BIC-A2631), all of them deposited in the Scripps Institution of Oceanography Benthic Invertebrate Collection (SIO-BIC). Information about the primers used and the temperature profile for the amplification of the different genes is shown in Appendix S1. For the population genetics analyses, *COI* was successfully amplified for 126 *Pterocirrus* sp. n. individuals and *16S* for 118 using the primers and PCR programs shown in Appendix S1.

Amplification products for all the genetic markers mentioned above were purified and sequenced in both directions at the CCiT-UB, in the Sequencing Facilities of the NHM, or by the Rouse Lab. Sequences were edited in Geneious 8.1.8 (Kearse et al., 2012), primers were removed, and overlapping fragments merged into consensus sequences.

2.4 | Phylogenetics analyses

To assess the phylogenetic position of *Pterocirrus* sp. n., the newly generated sequences of *COI, 16S, 18S* and *28S* for a single individual of this species and for the four *Pterocirrus* mentioned above were aligned by marker with other sequences of 42 phyllodocids and four out-group species available in NCBI (Appendix S2) using the Q-INS-I option of MAFFT v7 (Katoh & Standley, 2013). A total of 21 of these 46 sequences (Appendix S2) were originally used to construct the phylogenetic hypothesis for Phyllodocidae given in Eklöf, Pleijel, and Sundberg (2007). Furthermore, 19 of the remaining sequences were originally used by Rousset, Pleijel, Rouse, Erséus, and Siddall (2007), Struck et al. (2007), Carr, Hardy, Brown, Macdonald, and Hebert (2011), Hardy et al. (2011), Norlinder, Nygren, Wiklund and Pleijel (2012), Lobo et al. (2016), Richter, Schwarz, Hering, Böggemann and Bleidorn (2015), Schimmenti et al. (2016) and Seixas, Zanol, Magalhaes and Paiva (2017) for a variety of studies, and finally six sequences were available in NCBI from unpublished studies (Appendix S2). To test the validity, *that is,* monophyly, of the type species of the genus *Eulalia*, *Eulalia viridis* (Linnaeus, 1767), we used all sequences for this species (16 of the 42 phyllodocid sequences) available in NCBI, although none of the specimens were collected at the type locality. The resulting concatenated alignment contained 3,728 bp: 519 bp for *16S*, 1,802 bp for *18S,* 808 bp for *28S* and 599 bp for *COI*. The most appropriate evolutionary model for each gene was estimated with the software packages JMODELTEST v2.1.7 (Darriba, Taboada, Doallo, & Posada, 2012) and PARTITIONFINDER2 v2.1 (Lanfear, Frandsen, Wright, Senfeld, & Calcott, 2016) using the Akaike information criterion (AIC): GTR+I + G for *16S*, for *28S* and for the first codon position of *COI*; K80+I + G for *18S* and for the second codon position of *COI*; and HKY+I + G for the third codon position of *COI*.

The alignments of the four markers were concatenated and partitioned as described above (using codon-specific models for the *COI* partition) for phylogenetic analyses. The maximum-likelihood (ML) analysis was performed with randomized accelerated maximum likelihood (RAXML) v8.1.22 (Stamatakis, 2014) using the GTR+G evolutionary model following the recommendations in the RAXML manual. The ML tree search was conducted by performing 50 runs, with 1,000 thorough bootstrap replicates conducted to evaluate nodal support. Bayesian inference (BI) analysis was conducted with MRBAYES v3.1.2 (Ronquist & Huelsenbeck, 2003) using the evolutionary models inferred for the different genes as stated above. Analyses were run twice, starting from random trees and running for 5,000,000 generations with four chains running simultaneously (two cold and two heated). Chains were sampled every 1,000 generations with 25% of the generations discarded as burn-in. Convergence was checked using TRACER v1.6.0 (Rambaut, Suchard, Xie, & Drummond, 2014), and trees were visualized in FIGTREE v 1.4.2 (Rambaut, 2006).

2.5 | Population genetics analyses

The *COI* ($n = 126$) and *16S* ($n = 118$) data sets were used to calculate the genetic diversity of the eight populations of *Pterocirrus* sp. n. The software DNASP 5.10.01 (Librado & Rozas, 2009) was used to calculate the number of haplotypes

(H), the haplotype diversity (Hd) and the nucleotide diversity (π). Both *COI* and *16S* genetic data sets of *Pterocirrus* sp. n. were used to construct un-rooted haplotype networks with the program POPART 1.7 (www.popart.otago.ac.nz) using the median-joining network option (Bandelt, Forster, & Röhl, 1999).

We also assessed the historical population demography in *Pterocirrus* sp. n. using both the *COI* and the *16S* data sets and different methodologies. Given that the sample sizes for PAR and ESP were less than three individuals, we removed them from the analysis described below. To test whether the populations of *Pterocirrus* sp. n. had been affected by bottlenecks, recent population expansions, selective sweeps or balancing selection, we used the program ARLEQUIN 3.5.1.3 to calculate Tajima's D (Tajima, 1989) and Fu's F test (Fu, 1997). Fu's F test was selected as it is supposed to be the best neutrality test for our dataset, because (a) tests that rely on haplotype frequencies are the most powerful for detecting expansions on nonrecombining genomic regions as the mitochondrial markers used herein (Ramírez-Soriano, 2008), and (b) Fu's F test is the best-performing statistic for large sample sizes (>100 individuals in total; Ramos-Onsins & Rozas, 2002). The significance levels for the tests were assessed with 10,000 permutations. In addition, past demographic expansions and/or bottlenecks were also inferred comparing the sum of squared deviations between the observed mismatch distribution of the DNA substitution pairwise differences and the expected mismatch distribution under a model of sudden population expansion (Rogers & Harpending, 1992). These analyses were carried out using ARLEQUIN, and the significance was assessed with 10,000 bootstrap replicates.

Furthermore, fixation indices (ϕ_{ST}) were estimated to measure the differentiation between pairs of stations for both markers, as implemented in ARLEQUIN. The significance of the ϕ_{ST} values was assessed by a permutation test with 10,000 replicates.

The overall population gene flow estimation (Nm) was performed using DNAsp, calculated by substituting Nst for ϕ_{ST} in Wright's equation (Wright, 1951). This was only calculated for the *COI* data set (Hudson, Slatkin, & Maddison, 1992): $\phi_{ST} = 1/(1 + 2\,Nm)$.

The software BARRIER v. 2.2 (Manni, Guerard, & Heyer, 2004) was used to identify and represent the most robust barriers in the *COI* data set genetic landscape. This software uses an improved Monmonier's Algorithm to detect genetic barriers from a matrix of genetic distances (ϕ_{ST}) linked to a matrix of geographic distances. In addition, a hierarchical analysis of molecular variance (AMOVA) was performed in ARLEQUIN to test whether the genetic differentiation between sampling localities was explained by the groups inferred by the Barrier analysis (grouping the populations on each side of the "strongest" barrier): Group 1 including OH, HM, KG, and Group 2 including LIV, CIE, PET.

Finally, a Mantel test was performed in R version 3.2.2 for the *COI* data set using the mantel.randtest function in the ade4 package (Dray & Dufour, 2007). The Mantel test is widely used in population genetics studies to test the isolation-by-distance model, examining the correlation between the geographic and the genetic distances matrices.

3 | RESULTS

3.1 | Taxonomy

The taxonomical description, in vivo photographs and *SEM* micrographs of the newly described species *Pterocirrus giribeti* sp. n. and the type material of *Eulalia subulifera* Ehlers, 1897 are included in Appendices S3, S4 and S5.

3.2 | Phylogenetic analysis

Both ML and BI analyses recovered similar tree topologies (Figure 2), and therefore, we selected the tree obtained from the ML analysis of the concatenated alignment for the graphical visualization and included the support recovered from the BI analysis on the nodes. Phyllodocidae was recovered with robust support for both ML and BI and contained two main clades, Clade A and Clade B, the latter robustly supported for BI (Figure 2). Within Clade A, only the subclade A3 was recovered with high support, containing the sequenced species from the genera *Sige*, *Eumida*, *Torrea*, *Alciopina* and *Rynchonereella* (Figure 2). Subclade A1 contained all sequenced species of *Pterocirrus*, including the type species *P. macroceros*, being resolved as a monophyletic genus, although with no support (Figure 2). Within subclade A1, *Pterocirrus giribeti* sp. n. appeared more closely related to *P. nidarosiensis* in a clade recovered with moderate support (Figure 2). The subclade A2 contained species of *Eulalia* [*Eulalia mustela* Pleijel, 1987, *Eulalia expusilla* Pleijel, 1987 and *Eulalia bilineata* (Johnston, 1840)], *Protomystides* and *Pseudomystides*, although their relationships were only supported in the BI analysis for the group formed by *Pseudomystides limbata* (Saint-Joseph, 1888), *E. expusilla* and *E. bilineata* (Figure 2). Finally, subclade A4 contained only *Eulalia* species, including the type species *E. Viridis*, although all specimens identified as *Eulalia viridis* were not grouped together (Figure 2). Only two subclades were identified within Clade B, one containing the genus *Phyllodoce* (subclade B1, recovered as monophyletic with full support) and subclade B2, which comprised species of the genera *Chaetoparia*, *Notophyllum*, *Mystides*, *Nereiphylla*, *Paranaitis* (not monophyletic) and *Eteone* (Figure 2).

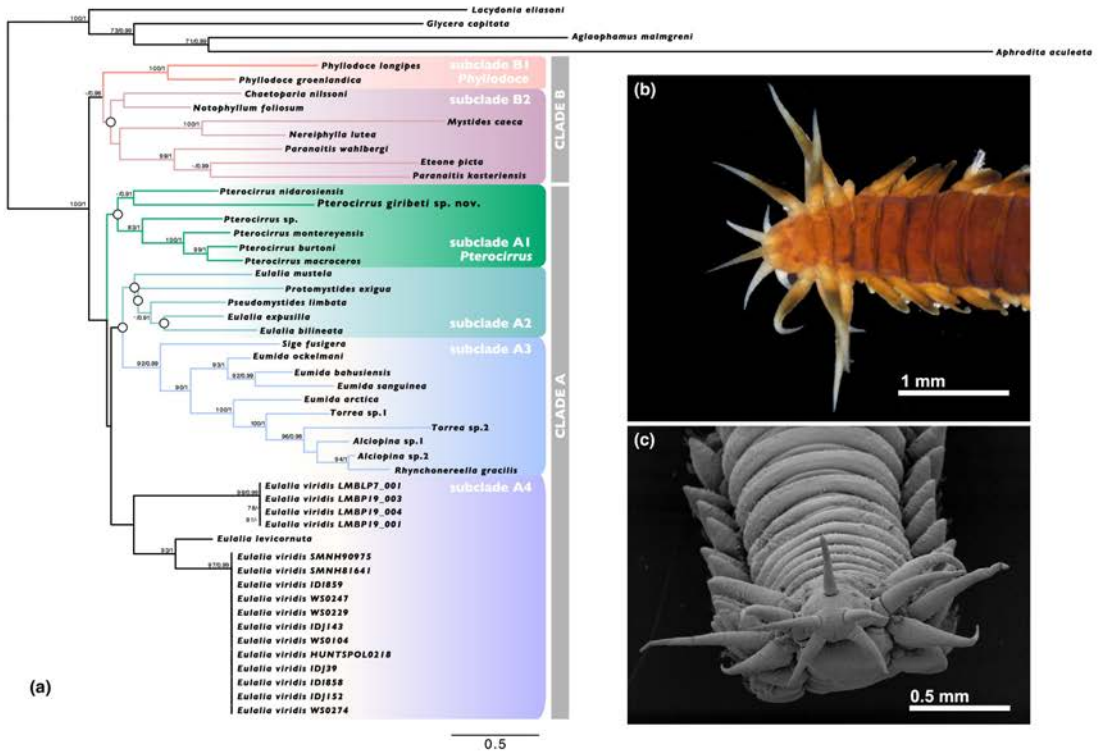

FIGURE 2 (a) Phylogenetic tree from the concatenated and partitioned maximum-likelihood (ML) analysis for all genetic data (*COI*, *16S*, *18S* and *28S*), showing the phylogenetic relationships between members of the family Phyllodocidae. Branch supports shown as bootstrap value (ML)—left—and posterior probability (Bayesian inference, BI)—righ. Only bootstrap values >70 and posterior probabilities >0.90 are shown. White circles show clades recovered by both ML and BI analyses but under the indicated threshold. (b) Live specimen of *Pterocirrus giribeti* sp. n., anterior part, dorsal view. (c) Scanning electron micrograph of *P. giribeti* sp. n., anterior part, front view

3.3 | Population genetics analyses

The COI data set for the population genetics analyses contained 565 bp for 126 individuals, while the 16S data set contained 528 bp for 118 specimens.

3.3.1 | Genetic diversity

A total of 31 haplotypes were recovered for the *COI* data set, with the three most frequent haplotypes accounting for 45.8% of the total number of individuals and with most of the localities present in all of these haplotypes (Figure 3a; Table 2). A total of 18 of these 31 haplotypes were private, which were present in all localities except OH and PAR (Figure 3a). A total of 35 segregating sites (*S*) were recovered (6.2%), 26 were parsimony informative, ranging from zero in PAR to 26 in HM (Table 2). The haplotype diversity (Hd) ranged from zero in PAR to 0.949 ± 0.051 in KG, with a mean value of 0.926 ± 0.013 across all locations (Table 2). The nucleotide diversity (π) across all locations was 0.009 ± 0.001, ranging from zero in PAR to 0.011 ± 0.001 in PET (Table 2). The low values of genetic diversity in PAR were due to the presence of a single haplotype, probably related to the small sampling size ($n = 2$). After PAR, OH showed the next lowest values of segregating sites ($S = 9$), with a haplotype diversity of Hd = 0.583 ± 0.183, and a nucleotide diversity of $\pi = 0.004 \pm 0.002$ (Table 2).

In contrast to the high genetic diversity found in the *COI* data set, the *16S* data set was characterized by low values of genetic diversity (Table 2). A total of five haplotypes were found with one of them accounting for 91.5% of the total number of individuals and being present at all the sampling stations; three of these haplotypes were private and present in CIE and HM (Figure 3b). The number of segregating sites (*S*) ranged from zero in KG, LIV, ESP and PAR, to three in CIE, with a total value of five when pooling all populations (Table 2). Haplotype diversity (Hd)

across all populations was 0.161 ± 0.045, ranging from zero, at the stations with null *S* values, to 0.363 ± 0.131 in CIE (Table 2). The nucleotide diversity (π) across all locations was 0.0003 ± 0.00009, ranging from zero, again at the stations with null *S* values, to 0.0008 ± 0.0003 in CIE (Table 2).

3.3.2 | Demographic history analyses

The results of the demographic history analyses for the *COI* data set are shown in Table 3. All sampling stations treated separately and the whole set of samples together fitted the demographic expansion model, given that the observed mismatch distributions did not departure from the mismatch distributions expected under the expansion model (i.e., SSD values not significant). Tajima's D values were all negative, which could be indicating an excess of rare polymorphic sites, although *p*-values showed no significant deviation from the neutrality (Table 3). Fu's *F* test values were negative for all stations (except for OH), indicating a general presence of rare haplotypes in contrast to what would be expected under neutrality. In addition, significant *p*-values

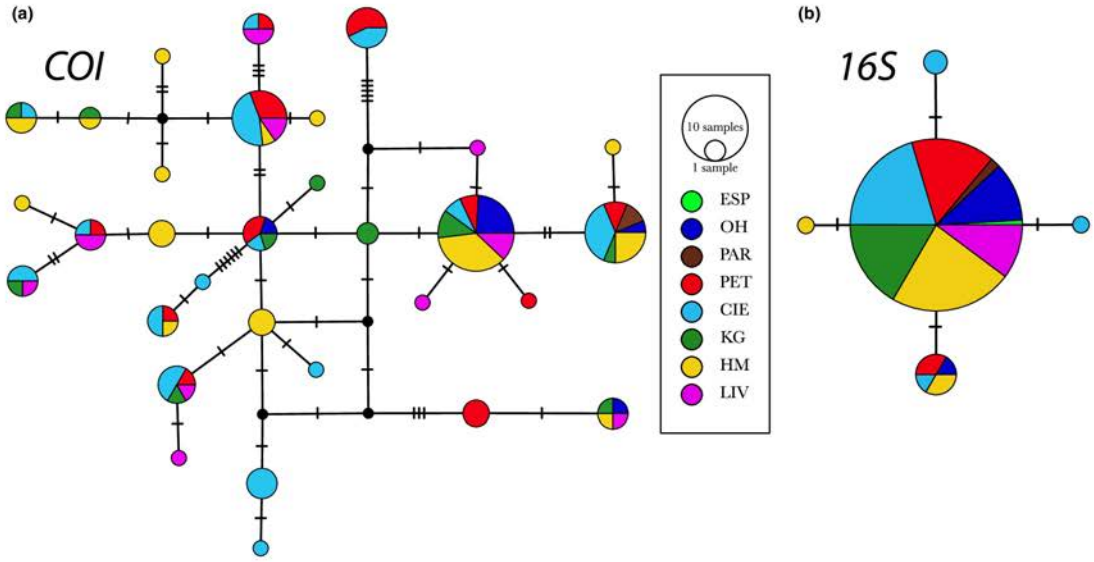

FIGURE 3 Median-joining haplotype networks based on the *COI* (a) and the *16S* (b) mitochondrial markers. Circles are proportional to the number of individuals for each haplotype, number of mutations between haplotypes are indicated with crossed lines, and colour coding is indicated for every sampling locality. Nonsampled or extinct inferred haplotypes are in black

TABLE 2 Genetic diversity estimators for the studied populations of *Pterocirrus giribeti* sp. n. for *COI* and *16S*

		COI					*16S*				
Location	**Code**	***n***	***h***	***S***	**Hd**	π	***n***	***h***	***S***	**Hd**	π
King George Is.	KG	13	10	18	0.949 ± 0.051	0.008 ± 0.001	18	1	0	0	0
Half Moon Is.	HM	30	14	26	0.887 ± 0.042	0.008 ± 0.001	28	3	2	0.204 ± 0.098	0.0004 ± 0.0002
Livingston Is.	LIV	15	10	19	0.943 ± 0.040	0.009 ± 0.001	11	1	0	0	0
Esperanza Bay	ESP	—	—	—	—	—	1	1	0	0	0
O'Higgins Bay	OH	9	4	9	0.583 ± 0.183	0.004 ± 0.002	13	2	1	0.154 ± 0.126	0.0003 ± 0.0002
Paradise Bay	PAR	2	1	0	0	0	2	1	0	0	0
Petermann Is.	PET	22	11	25	0.922 ± 0.031	0.011 ± 0.001	19	2	1	0.199 ± 0.112	0.0004 ± 0.0002
Cierva Cove	CIE	35	15	25	0.924 ± 0.134	0.010 ± 0.002	26	4	3	0.286 ± 0.112	0.0006 ± 0.0002
Total		126	31	35	0.924 ± 0.013	0.009 ± 0.001	118	5	4	0.161 ± 0.045	0.0003 ± 0.00009

Note. *n*: number of individuals; *h*: number of haplotypes; *S*: number of segregating sites; Hd: haplotype diversity; π: nucleotide diversity.

		COI			*16S*		
Location	**Code**	***D***	***Fs***	***SSD***	***D***	***Fs***	***SSD***
O'Higgins Bay	OH	−1.359	0.724	0.145	−1.149	**−0.537**	0.028
Petermann Is.	PET	−0.419	−0.613	0.026	−0.562	−0.055	0.332
Cierva Cove	CIE	−0.084	−1.743	0.016	−1.513	**−2.499**	0.006
King George Is.	KG	−0.998	**−3.458**	0.015	—	—	—
Half Moon Is.	HM	−1.067	−2.887	0.015	−1.241	**−1.586**	0.002
Livingston Is.	LIV	−0.675	−2.213	0.025	—	—	—
Total		−0.619	**−8.823**	0.005	**−1.504**	**−4.713**	0.0007

Note. *D*: Tajima's D test; *Fs*: Fu's test; *SSD*: sum of square deviation. Significant values are shown in bold.

TABLE 3 Summary statistics for demographic tests for all populations of *Pterocirrus giribeti* sp. n. using *COI* and *16S* data sets

for Fu's *F* values were found in KG and when considering all populations together, which indicated a significant population expansion in the sampling area (Table 3).

As with *COI*, results for *16S* when considering all sampling stations separately and when pooling all populations together fitted the population expansion model, showing low and not significant SSD values (Table 3). Tajima's *D* values were all negative, showing a significant *p*-value (<0.05) when all samples were analysed together (Table 3). Negative and significant Fu's Fs test values were obtained for OH, CIE, HM and for all samples pooled, indicating again that populations of *P. giribeti* sp. n. were in demographic expansion (Table 3).

3.3.3 | Population differentiation

Due to the extremely low genetic diversity in the *16S*, population differentiation was not analysed for this data set. Pairwise ϕ_{ST} values for *COI* were significant between OH vs. PET, OH vs. CIE, OH vs. LIV, HM vs. PET and HM vs. CIE (Table 4). For the *P. giribeti* sp. n. *COI*, ϕ_{ST} values lied within the moderate (0.05–0.15) and the high (0.15–0.25) intervals of genetic differentiation (following Wright, 1978; Hartl & Clark, 1997) for the three pairwise significant comparisons for OH, and within the small (0–0.05) and the moderate intervals of differentiation for the significant pairwise comparisons for HM (Table 4).

Population gene flow (*Nm*) estimates were 18.06 for *COI*, indicating a high genetic connectivity in the study area (*Nm* value > 1) shown by this marker. Moreover, the Mantel test showed a nonsignificant value of 0.19 (*p*-value = 0.2), refuting the isolation-by-distance hypothesis. Results of the Barrier analysis using the *COI* data set are shown in Figure 4. The main barrier or genetic discontinuity divided the sampling stations into two areas: the north-eastern area (including KG, HM and OH) and the south-western area (including LIV, CIE and PET) (Figure 4). The second most important barrier separated OH from the rest of the sampling stations, coinciding with the Peninsula Front, PF (Figure 4). However, the AMOVA analysis showed no significant differences between the two areas (inferred by the main barrier: north-eastern vs. south-western), and significant differences were only found within populations (Table 5).

TABLE 4 Pairwise ϕ_{ST} values for the *COI* data set (below diagonal) and their *p*-values (over diagonal) among the populations of *Pterocirrus giribeti* sp. n. with more than three individuals

	OH	**PET**	**CIE**	**KG**	**HM**	**LIV**
OH	—	0	0	0.026	0	0
PET	**0.158**	—	0	0.051	0	0.015
CIE	**0.166**	−0.003	—	0.046	0	0.015
KG	0.056	0.028	0.023	—	0.025	0
HM	0.04	**0.051**	**0.047**	−0.007	—	0
LIV	**0.098**	0.011	0.016	−0.008	0.021	—

Note. Significant values are shown in bold.

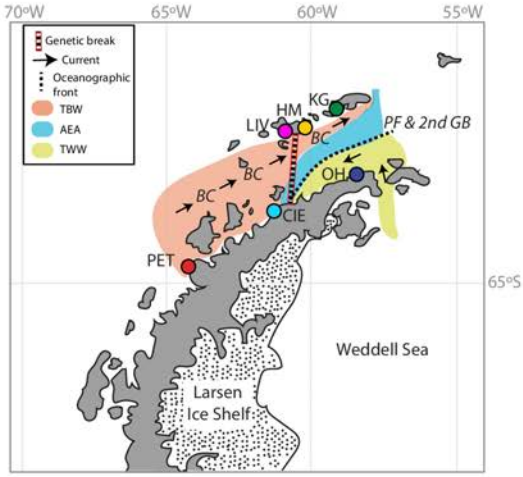

FIGURE 4 Map of the study area showing the two main genetic (semipermeable) barriers inferred with the program BARRIER for *P. giribeti* sp. n. Bransfield Strait currents and water masses (Sangrà et al., 2011) are also shown. AEA: Anticyclonic Eddies Area; BC: Bransfield Current; PF & 2nd GB: Peninsula Front coinciding with the second-genetic break; TBW: Transitional Zonal Water with Bellingshausen Sea influence; TWW: Transitional Zonal Water with Weddell Sea influence

TABLE 5 Hierarchical AMOVA results. Evaluation of spatial population genetic structure within and among the groups inferred by the Barrier analysis and within populations

Source of variation	*df*	Sum of squares	Variance components	% of variation	*p*-Value
Among groups	1	1.883	0.022	4.61	0.0993
Among populations within groups	4	2.148	0.005	1	0.162
Within populations	118	52.888	0	94.4	**0.0004**

Note. Significant value is shown in bold.

4 | DISCUSSION

4.1 | Taxonomy and phylogeny

Our initial morphological observations pointed to similarities between *Pterocirrus giribeti* sp. n. and *Eulalia subulifera*. The revision of the type material of *E. subulifera* collected in the Magellan Strait was key to clarify the status of the new species described here. Our in-depth morphological analysis using environmental *SEM* techniques of the type material of *E. subulifera* indicated that although the similarities between the new species and the original description of *E. subulifera*, the type material does not possess all the characters specified in its original description (see Remarks in the taxonomic description, Appendix S3). Consequently, we suggest it needs a thorough review to clarify its status as a species of *Eulalia* or to transfer it to another genus. Interestingly, although the type locality of *E. subulifera* was the Magellan strait, its original description also described its occurrence in South Georgia Island and contained material examined from the South Georgia Islands. Indeed, the drawings and description by Ehlers (1897) showed a mix of characters of both *P. giribeti* sp. n. and the type material of *E. subulifera* (see Remarks in the taxonomic description, Appendix S3). We thus believe that Ehlers collected the two species from both areas and assigned them to a single species, *E. subulifera*, subsequently including in its original description a mixture of characters of both the type material of *E. subulifera* and *P. giribeti* sp. n. Since then, phyllodocids collected in the Southern Ocean similar to the description provided by Ehlers have been identified as *E. subulifera*. However, according to our results, these identifications should be challenged in order to clarify whether they belong to *P. giribeti* sp. n. or to another species. Also importantly, our taxonomical revision of material collected in South Georgia Island by Monro (1930) concluded that these specimens also correspond to *P. giribeti* sp. n., thus expanding the distribution of the new species from the Western Antarctic Peninsula and the South Shetlands to Subantarctic areas. *Pterocirrus giribeti* sp. n. is the first species of the genus described in Antarctic waters and, although the new species lacks the foliose ventral tentacular cirri distinctive of the genus (Pleijel, 1991), it shares other morphological characteristics with its congeneric species (see the taxonomical description in the Appendix S3).

Our phylogenetic analyses identified two clades (A and B) within the family Phyllodocidae, being one of them (B) recovered here for the first time to the best of our knowledge (Figure 2). Eklöf et al. (2007) already recovered Clade A, comprising species from the genera *Eulalia*, *Protomystides*, *Pseudomystides*, *Pterocirrus*, *Eumida* and *Sige*, which is now expanded with the newly sequenced *Pterocirrus* species (i.e., *P. giribeti* sp. n., *P. burtoni*, *P. nidarosiensis*, *P. montereyensis* and *Pterocirrus* sp.) and other genera we included in our analyses (i.e., *Torrea*, *Alciopina* and *Rhynchonereella*). The type species of the genus *Eulalia*, *E. viridis*, was not recovered as a monophyletic group. This is most likely because of a misidentification of the four individuals from Portugal waters, which should be re-examined and properly identified, because *E. viridis* does not occur in Europe south of the English Channel (Bonse, Schmidt, Eibye-Jacobsen, & Westheide, 1996). The pervasive paraphyletic and polyphyletic nature of most genera within phyllodocids require further phylogenetic analyses and taxonomical revisions to unequivocally clarify the phylogeny of the family and the taxonomical status of the different genera. The low support values for most of the internal nodes within both clades evidenced the need of using a higher number of markers and/or to use a more extensive taxon sampling (including the type species of the different genera), to be able to undertake any taxonomical action regarding the validity of the genera. Moreover, comparison with previous strictly morphologically based cladograms for Phyllodocidae (Eibye-Jacobsen, 1993; Orrhage & Eibye-Jacobsen, 1998; Pleijel, 1991) indicated the disagreement between the morphological- and the molecular-based phylogenies for Phyllodocidae, revealing the need of a fully resolved phylogeny for the family.

4.2 | Population genetics and evolutionary history

Our population genetics analyses revealed the traces left by both past climatic events and contemporary oceanic currents on the genetic landscape of *P. giribeti* sp. n. As in other studies addressing the connectivity and phylogeography for Antarctic benthic invertebrates, *COI* was highly variable

while *16S* showed very low genetic variability (e.g., Raupach et al., 2010; Sands, O'Hara, Barnes, & Martín-Ledo, 2015; Galaska, Sands, Santos, Mahon, & Halanych, 2017). For this reason, the following discussion about population connectivity just focuses on the results we obtained for *COI,* while the discussion about the demographic history uses the information from both markers.

The high genetic variability observed in the *COI* data set of *P. giribeti* sp. n. showed the effects of the relatively recent and contemporary geological and environmental events on its populations, a similar scenario also having been reported in the ophiuroid *Ophiura (Ophiuroglypha) carinifera* (Koehler, 1901) in the same area (Sands et al., 2015). We found a remarkably high connectivity for *P. giribeti* sp. n. throughout the sampled area, supported by the high *Nm* migration values and also by the lack of geographic structure in the haplotype networks, with haplotypes shared between organisms from distant locations spanning ca. 500 km (Figure 3a). This high connectivity we observed within the study area might be explained by the fact that phyllodocids have planktotrophic larvae (Giangrande, 1997), which may confer the species with high dispersal abilities, as has been suggested for other Antarctic marine invertebrates with planktotrophic larvae also displaying high gene flow among their populations (e.g., Raupach et al., 2010, González-Wevar et al., 2011; Janosik et al., 2011). In addition to the type of larva, the high gene flow detected in *P. giribeti* sp. n. could also be due to the passive transportation of adults with drifting algae, as already suggested in the past for a few marine invertebrates, allowing them to disperse for 100's of km along the Subantarctic islands (Fraser, Kay, Plessis, & Ryan, 2017; Helmuth, Veit, & Holberton, 1994; Nikula, Fraser, Spencer, & Waters, 2010; Smith, 2002).

Although we did not detect a clear and robust structure in our *COI* data set, we detected a weak genetic substructure, suggested by the moderate-to-high ϕ_{ST} values for some pairwise comparisons among populations (Table 4), which allowed us to identify various genetic breaks or barriers (Figure 4). Interestingly, these barriers coincided with an oceanic front produced by the intrusion in the Bransfield Strait of a tongue of water from the Weddell Sea (Sangrà et al., 2011), isolating the tip of the West Antarctic Peninsula (where OH is located) from the rest of the sampled area with a semipermeable barrier. The results from the AMOVA analysis, showing no significant differences between the two areas inferred by the main barrier (Table 5), agree with the idea of having a substructure determined by a relatively recently created semipermeable barrier, allowing certain levels of gene flow and migration within the study area. Interestingly, a similar break has also been reported recently for a study using single nucleotide polymorphisms—SNPs—in the brittle star *Ophionotus victoriae* Bell, 1902, separating populations in the Western Antarctic Peninsula (including samples genetically similar to samples from the Ross Sea) to those in the Western Weddell Sea, although with moderate gene flow among them (Galaska et al., 2017).

Despite the relatively high variability of *COI* (i.e., high mutation levels), we detected indications of a significant demographic expansion for *P. giribeti* sp. n. Taking into account the high *Nm* migration values and the results of the AMOVA, the most relevant demographic tests are those considering all the samples together. The overall significant negative Tajima's D and Fu's F indices we found for both genetic markers (Table 3) are evidence of excess of low-frequency haplotypes relative to neutral mutation-drift equilibrium. All these results, both from the *COI* and the *16S* analyses, strongly support the existence of a recent and rapid demographic expansion for *P. giribeti* sp. n. in the study area, probably following a bottleneck event, most likely caused after a recent glacial maximum. In other shallow-water Antarctic benthic invertebrates, this has been suggested to be the signal left in the genome by the last glacial-interglacial transition, after the last glacial maximum (LGM; ~20,000 years ago) (Allcock & Strugnell, 2012). Interestingly, other studies on shallow-water Antarctic invertebrates have also found genetic evidence of recent demographic expansions in the same geographic area (Díaz, Féral, David, Saucède, & Poulin, 2011; Gonzalez-Wevar et al., 2011; Thornhill, Mahon, Norenburg, & Halanych, 2008), suggesting that due to their narrow bathymetric range, the glacial periods must have had a dramatic effect on the Antarctic populations of the strictly shallow-water species. Under this scenario, species with narrow shallow bathymetric ranges and high dispersal capabilities *(i.e.,* planktonic larvae) are more likely to have migrated northwards to the Subantarctic islands during glacial periods and returned to the Antarctic shelf during interglacial periods, as has already been suggested for the Antarctic limpet *Nacella concinna* (Strebel, 1908) (González-Wevar et al., 2013). Hence, more individuals of *P. giribeti* sp. n. from Subantarctic locations are necessary to test the hypothesis of the glacial-survival history of the species in these locations, and to test whether the expansion–contraction model is verified for this new phyllodocid.

ACKNOWLEDGEMENTS

We are indebted to Patricia Álvarez-Campos, Gonzalo Giribet, Juan Junoy, Javier Cristobo, Juan Moles, Carlos Angulo-Preckler, Laura Núñez-Pons, Maria Bas and Blanca Figuerola for their help during fieldwork in Antarctica. Two anonymous reviewers greatly improved an early version of the manuscript. Antarctic material was collected under appropriate collection permits (CPE-EIA-2011-7 and CPE-EIA-2015-7 from the Spanish Ministry of Economy and Competitiveness) and within approved ethics guidelines. This work was supported by grants of the Spanish Ministry of Economy and Competitiveness (ACTIQUIM I: CGL2007-65453/ANT,

and II: CTM2010-17415/ANT, and DISTANTCOM: CTM2013-42667/ANT) to CA, and a DIF grant of the Natural History Museum of London (SDF14032) to AR.

ORCID

Carlos Leiva http://orcid.org/0000-0003-4398-329X
Ana Riesgo http://orcid.org/0000-0002-7993-1523
Conxita Avila http://orcid.org/0000-0002-5489-8376
Greg W. Rouse http://orcid.org/0000-0001-9036-9263
Sergi Taboada http://orcid.org/0000-0003-1669-115

REFERENCES

Allcock, A. L., & Strugnell, J. M. (2012). Southern Ocean diversity: New paradigms from molecular ecology. *Trends in Ecology & Evolution*, *27*(9), 520–528. https://doi.org/10.1016/j.tree.2012.05.009.

Anderson, J. B., Shipp, S. S., Lowe, A. L., Wellner, J. S., & Mosola, A. B. (2002). The Antarctic Ice Sheet during the Last Glacial Maximum and its subsequent retreat history: A review. *Quaternary Science Reviews*, *21*(1), 49–70. https://doi.org/10.1016/S0277-3791(01)00083-X.

Angulo-Preckler, C., Leiva, C., Avila, C., & Taboada, S. (2017). Macroinvertebrate communities from the shallow soft-bottoms of Deception Island (Southern Ocean): A paradise for opportunists. *Marine Environmental Research*, *127*, 62–74. https://doi.org/10.1016/j.marenvres.2017.03.008.

Arango, C. P., Soler-Membrives, A., & Miller, K. J. (2011). Genetic differentiation in the circum—Antarctic sea spider *Nymphon australe* (Pycnogonida; Nymphonidae). *Deep Sea Research Part II: Topical Studies in Oceanography*, *58*(1), 212–219. https://doi.org/10.1016/j.dsr2.2010.05.019.

Baird, H. P., Miller, K. J., & Stark, J. S. (2011). Evidence of hidden biodiversity, ongoing speciation and diverse patterns of genetic structure in giant Antarctic amphipods. *Molecular Ecology*, *20*(16), 3439–3454. https://doi.org/10.1111/j.1365-294X.2011.05173.x.

Bandelt, H. J., Forster, P., & Röhl, A. (1999). Median-joining networks for inferring intraspecific phylogenies. *Molecular Biology and Evolution*, *16*(1), 37–48. https://doi.org/10.1093/oxfordjournals.molbev.a026036.

Bergström, E. (1914). *Zur Systematik der Polychaetenfamilie der Phyllodociden*. Stockholm: Almqvist & Wiksells boktryckeri AB.

Bonse, S., Schmidt, H., Eibye-Jacobsen, D., & Westheide, W. (1996). *Eulalia viridis* (Polychaeta: Phyllodocidae) is a complex of two species in northern Europe: Results from biochemical and morphological analyses. *Cahiers De La Biologie Marine*, *37*, 33–48.

Carr, C. M., Hardy, S. M., Brown, T. M., Macdonald, T. A., & Hebert, P. D. (2011). A tri-oceanic perspective: DNA barcoding reveals geographic structure and cryptic diversity in Canadian polychaetes. *PLoS One*, *6*(7), e22232. https://doi.org/10.1371/journal.pone.0022232.

Claparède, É. (1868). Les annélides chétopodes du Golfe de Naples. *Mémoires De La Société De Physique Et D'histoire Naturelle De Genève*, *19*(2), 313–584.

Clarke, A., & Johnston, N. M. (2003). Antarctic marine benthic diversity. *Oceanography and Marine Biology*, *41*, 47–114.

Darriba, D., Taboada, G. L., Doallo, R., & Posada, D. (2012). jModelTest 2: More models, new heuristics and parallel computing. *Nature Methods*, *9*(8), 772–772. https://doi.org/10.1038/nmeth.2109.

Díaz, A., Féral, J. P., David, B., Saucède, T., & Poulin, E. (2011). Evolutionary pathways among shallow and deep-sea echinoids of the genus *Sterechinus* in the Southern Ocean. *Deep Sea Research Part II: Topical Studies in Oceanography*, *58*(1), 205–211. https://doi.org/10.1016/j.dsr2.2010.10.012.

Dray, S., & Dufour, A. B. (2007). The ade4 package: Implementing the duality diagram for ecologists. *Journal of Statistical Software*, *22*(4), 1–20.

Ehlers, E. H. (1897). *Polychaeten: Hamburger Magalhaensische Sammelreise*. Hamburg: Friederichsen.

Ehlers, E. (1900). Magellanische Anneliden gesammelt während der schwedischen Expedition nach den Magellansländer. *Nachrichten Von Der Gesellschaft Der Wissenschaften Zu Göttingen, Mathematisch-Physikalische Klasse*, *1900*, 206–223.

Ehlers, E. H., & Vanhöffen, E. (1913). *Die Polychaeten-Sammlungen der deutschen Südpolar-Expedition 1901–1903*. Berlin: G. Reimer.

Eibye-Jacobsen, D. (1991). Observations on setal morphology in the Phyllodocidae (Polychaeta: Annelida), with some taxonomic considerations. *Bulletin of Marine Science*, *48*(2), 530–543.

Eibye-Jacobsen, D. (1993). On the phylogeny of the Phyllodocidae (Polychaeta Annelida): An alternative. *Journal of Zoological Systematics and Evolutionary Research*, *31*(3), 174–197. https://doi.org/10.1111/j.1439-0469.1993.tb00188.x.

Eklöf, J., Pleijel, F., & Sundberg, P. (2007). Phylogeny of benthic Phyllodocidae (Polychaeta) based on morphological and molecular data. *Molecular Phylogenetics and Evolution*, *45*(1), 261–271. https://doi.org/10.1016/j.ympev.2007.04.015.

Fraser, C. I., Kay, G. M., Plessis, M. D., & Ryan, P. G. (2017). Breaking down the barrier: Dispersal across the Antarctic Polar Front. *Ecography*, *40*(1), 235–237. https://doi.org/10.1111/ecog.02449.

Fu, Y. X. (1997). Statistical tests of neutrality of mutations against population growth, hitchhiking and background selection. *Genetics*, *147*(2), 915–925.

Galaska, M. P., Sands, C. J., Santos, S. R., Mahon, A. R., & Halanych, K. M. (2017). Geographic structure in the Southern Ocean circumpolar brittle star *Ophionotus victoriae* (Ophiuridae) revealed from mtDNA and single-nucleotide polymorphism data. *Ecology and Evolution*, *7*(2), 475–485. https://doi.org/10.1002/ece3.2617.

Giangrande, A. (1997). Polychaete reproductive patterns, life cycles and life histories: An overview. *Oceanography and Marine Biology*, *35*, 323–386.

González-Wevar, C. A., David, B., & Poulin, E. (2011). Phylogeography and demographic inference in *Nacella* (Patinigera) concinna (Strebel, 1908) in the western Antarctic Peninsula. *Deep Sea Research Part II: Topical Studies in Oceanography*, *58*(1), 220–229. https://doi.org/10.1016/j.dsr2.2010.05.026.

González-Wevar, C. A., Saucède, T., Morley, S. A., Chown, S. L., & Poulin, E. (2013). Extinction and recolonization of maritime Antarctica in the limpet *Nacella concinna* (Strebel, 1908) during the last glacial cycle: toward a model of Quaternary biogeography in shallow Antarctic invertebrates. *Molecular Ecology*, *22*(20), 5221–5236. https://doi.org/ 10.1111/mec.12465.

Gordon, A. L., & Nowlin, W. D. Jr (1978). The basin waters of the Bransfield Strait. *Journal of Physical Oceanography*, *8*(2), 258–264. https://doi.org/10.1175/1520-0485(1978)008aabbb0258:TBWOTBaaabb2.0.CO;2

Gravier, C. (1896). Recherches sur les Phyllodociens. Doctoral dissertation.

Gravier, C. (1907). Sur les Annélides polychètes recueillies par l'expédition antarctique française (Terebelliens, Serpuliens). *Bulletin Du Muséum D'histoire Naturelle, Paris*, *13*, 46–52.

Griffiths, H. J. (2010). Antarctic marine biodiversity–what do we know about the distribution of life in the Southern Ocean? *PLoS One*, *5*(8), e11683. https://doi.org/10.1371/journal.pone.0011683.

Grube, A. E. (1860). Beschreibung neuer oder wenig bekannter Anneliden. *Archiv Für Naturgeschichte*, *26*(1), 71–118.

Hardy, S. M., Carr, C. M., Hardman, M., Steinke, D., Corstorphine, E., & Mah, C. (2011). Biodiversity and phylogeography of Arctic marine fauna: Insights from molecular tools. *Marine Biodiversity*, *41*(1), 195–210. https://doi.org/10.1007/s12526-010-0056-x.

Hartl, D. L., & Clark, A. G. (1997). *Principles of population genetics*, Vol. *116*. Sunderland, MA: Sinauer Associates.

Hartmann, O. (1964). Polychaeta Errantia of Antarctica. *Antarctic Research Series*, *3*, 1–131.

Hartmann-Schroder, G. (1971). *Die Tierwelt Deutschlands, Vol 58: Annelida, Borstenwiirmer, Polychaeta*. Jena: Gustav Fischer.

Helmuth, B., Veit, R. R., & Holberton, R. (1994). Long-distance dispersal of a subantarctic brooding bivalve (*Gaimardia trapesina*) by kelp-rafting. *Marine Biology*, *120*(3), 421–426. https://doi.org/10.1007/BF00680216

Hemery, L. G., Eléaume, M., Roussel, V., Améziane, N., Gallut, C., Steinke, D. … Wilson, N. G. (2012). Comprehensive sampling reveals circumpolarity and sympatry in seven mitochondrial lineages of the Southern Ocean crinoid species Promachocrinus kerguelensis (Echinodermata). *Molecular Ecology*, *21*(10), 2502–2518. https://doi.org/ 10.1111/j.1365-294X.2012.05512.x.

Hudson, R. R., Slatkin, M., & Maddison, W. P. (1992). Estimation of levels of gene flow from DNA sequence data. *Genetics*, *132*(2), 583–589.

Janosik, A. M., Mahon, A. R., & Halanych, K. M. (2011). Evolutionary history of Southern Ocean *Odontaster* sea star species (Odontasteridae; Asteroidea). *Polar Biology*, *34*(4), 575–586. https://doi.org/10.1007/s00300-010-0916-7.

Katoh, K., & Standley, D. M. (2013). MAFFT multiple sequence alignment software version 7: Improvements in performance and usability. *Molecular Biology and Evolution*, *30*(4), 772–780. https://doi.org/10.1093/molbev/mst010.

Kearse, M., Moir, R., Wilson, A., Stones-Havas, S., Cheung, M., Sturrock, S., … Drummond, A. (2012). Geneious basic: An integrated and extendable desktop software platform for the organization and analysis of sequence data. *Bioinformatics*, *28*(12), 1647–1649. https://doi.org/10.1093/bioinformatics/bts199.

Kinberg, J. G. H. (1866). Annulata nova. *Öfversigt Af Kongliga Vetenskaps-akademiens Förhandlingar*, *22*, 167–179.

Krabbe, K., Leese, F., Mayer, C., Tollrian, R., & Held, C. (2010). Cryptic mitochondrial lineages in the widespread pycnogonid *Colossendeis megalonyx* Hoek, 1881 from Antarctic and Subantarctic waters. *Polar Biology*, *33*(3), 281–292. https://doi.org/10.1007/s00300-009-0703-5.

Lanfear, R., Frandsen, P. B., Wright, A. M., Senfeld, T., & Calcott, B. (2016). PartitionFinder 2: New methods for selecting partitioned models of evolution for molecular and morphological phylogenetic analyses. *Molecular Biology and Evolution*, msw260. 10.1093/molbev/msw260.

Levinsen, G. M. R. (1883). Systematisk-geografisk oversigt over den nordiske Annulata, Gephyrea, Chætognathi og Balanoglossi. B. Copenhagen: Lunos Kgl. Hof-bogtrykkeri.

Librado, P., & Rozas, J. (2009). DnaSP v5: A software for comprehensive analysis of DNA polymorphism data. *Bioinformatics*, *25*(11), 1451–1452. https://doi.org/10.1093/bioinformatics/btp187.

Lobo, J., Teixeira, M. A., Borges, L., Ferreira, M. S., Hollatz, C., Gomes, P. T., … Costa, F. O. (2016). Starting a DNA barcode reference library for shallow water polychaetes from the southern European Atlantic coast. *Molecular Ecology Resources*, *16*(1), 298–313. https://doi.org/10.1111/1755-0998.12441.

Malmgren, A. J. (1865). *Nordiska hafs-annulater*. Stockholm: P.A. Norstedt & Söner.

Manni, F., Guerard, E., & Heyer, E. (2004). Geographic patterns of (genetic, morphologic, linguistic) variation: how barriers can be detected by using Monmonier's algorithm. *Human Biology*, *76*(2), 173–190. https://doi.org/ 10.1353/hub.2004.0034.

McIntosh, W. C. (1885). Report on the Annelida Polychaeta Collected by HMS Challenger. Challenger Reports. *Zoology*, *12*, 1–554.

Monro, C. C. A. (1930). *Polychaete worms*, Vol. *2*. Cambridge, UK: Cambridge University Press.

Naish, T., Powell, R., Levy, R., Wilson, G., Scherer, R., Talarico, F., … Carter, L. (2009). Obliquity-paced Pliocene West Antarctic ice sheet oscillations. *Nature*, *458*(7236), 322–328. https://doi.org/ 10.1038/nature07867.

Neal, L., Wiklund, H., Muir, A. I., Linse, K., & Glover, A. G. (2014). The identity of juvenile Polynoidae (Annelida) in the Southern Ocean revealed by DNA taxonomy, with notes on the status of *Herdmanella gracilis* Ehlers sensu Augener. *Memoirs of Museum Victoria*, *71*, 203–216. https://doi.org/10.24199/j.mmv.2014.71.16

Nikula, R., Fraser, C. I., Spencer, H. G., & Waters, J. M. (2010). Circumpolar dispersal by rafting in two subantarctic kelp-dwelling crustaceans. *Marine Ecology Progress Series*, *405*, 221–230. https://doi.org/10.3354/meps08523.

Norlinder, E., Nygren, A., Wiklund, H., & Pleijel, F. (2012). Phylogeny of scale-worms (Aphroditiformia, Annelida), assessed from 18SrRNA, 28SrRNA, 16SrRNA, mitochondrial cytochrome c oxidase subunit I (COI), and morphology. *Molecular Phylogenetics and Evolution*, *65*(2), 490–500. https://doi.org/10.1016/j.ympev.2012.07.002.

Orrhage, L., & Eibye-Jacobsen, D. (1998). On the anatomy of the central nervous system of Phyllodocidae (Polychaeta) and the phylogeny of phyllodocid genera: A new alternative. *Acta Zoologica*, *79*(3), 215–234. https://doi.org/10.1111/j.1463-6395.1998.tb01160.x

Perkins, T. H. (1984). New species of Phyllodocidae and Hesionidae (Polychaeta), principally from Florida. *Proceedings of the Biological Society of Washington*, *97*(3), 555–582.

Pleijel, F. (1990). A revision of the genus *Sige* Malmgren (Polychaeta: Phyllodocidae). *Zoological Journal of the Linnean Society*, *98*(2), 161–184. https://doi.org/10.1111/j.1096-3642.1990.tb01214.x

Pleijel, F. (1991). Phylogeny and classification of the Phyllodocidae (Polychaeta). *Zoologica Scripta*, *20*(3), 225–261. https://doi.org/10.1111/j.1463-6409.1991.tb00289.x

Rambaut, A., Suchard, M. A., Xie, D., & Drummond, A. J. (2014) *Tracer v1.6*. Retrieved from https://beast.bio.ed.ac.uk/Tracer.

Rambaut, A. (2006). FigTree v1.3.1. [Computer software and manual]. Retrieved from https://tree.bio.ed.ac.uk/software/figtree.

Ramírez-Soriano, A. (2008). *Selection and linkage desequilibrium tests under complex demographies and ascertainment bias*. Barcelona: Universitat Pompeu Fabra. Doctoral dissertation.

Ramos-Onsins, S. E., & Rozas, J. (2002). Statistical properties of new neutrality tests against population growth. *Molecular Biology and*

Evolution, *19*(12), 2092–2100. https://doi.org/10.1093/oxfordjournals.molbev.a004034.

Raupach, M. J., Thatje, S., Dambach, J., Rehm, P., Misof, B., & Leese, F. (2010). Genetic homogeneity and circum-Antarctic distribution of two benthic shrimp species of the Southern Ocean, *Chorismus antarcticus* and *Nematocarcinus lanceopes*. *Marine Biology*, *157*(8), 1783–1797. https://doi.org/10.1007/s00227-010-1451-3.

Richter, S., Schwarz, F., Hering, L., Böggemann, M., & Bleidorn, C. (2015). The utility of genome skimming for phylogenomic analyses as demonstrated for glycerid relationships (Annelida, Glyceridae). *Genome Biology and Evolution*, *7*(12), 3443–3462. https://doi.org/10.1093/gbe/evv224

Riesgo, A., Taboada, S., & Avila, C. (2015). Evolutionary patterns in Antarctic marine invertebrates: An update on molecular studies. *Marine Genomics*, *23*, 1–13. https://doi.org/10.1016/j.margen.2015.07.005.

Rogers, A. D. (2007). Evolution and biodiversity of Antarctic organisms: A molecular perspective. *Philosophical Transactions of the Royal Society of London B: Biological Sciences*, *362*(1488), 2191–2214. https://doi.org/10.1098/rstb.2006.1948.

Rogers, A. R., & Harpending, H. (1992). Population growth makes waves in the distribution of pairwise genetic differences. *Molecular Biology and Evolution*, *9*(3), 552–569.

Ronquist, F., & Huelsenbeck, J. P. (2003). MrBayes 3: Bayesian phylogenetic inference under mixed models. *Bioinformatics*, *19*(12), 1572–1574. https://doi.org/10.1093/bioinformatics/btg180.

Rousset, V., Pleijel, F., Rouse, G. W., Erséus, C., & Siddall, M. E. (2007). A molecular phylogeny of annelids. *Cladistics*, *23*(1), 41–63. https://doi.org/10.1111/j.1096-0031.2006.00128.x.

Sands, C. J., O'Hara, T., Barnes, D. K., & Martín-Ledo, R. (2015). Against the flow: Evidence of multiple recent invasions of warmer continental shelf waters by a Southern Ocean brittle star. *Frontiers in Ecology and Evolution*, *3*, 63. https://doi.org/10.3389/fevo.2015.00063.

Sangrà, P., Gordo, C., Hernández-Arencibia, M., Marrero-Díaz, A., Rodríguez-Santana, A., Stegner, A., … Pichon, T. (2011). The Bransfield current system. *Deep Sea Research Part I: Oceanographic Research Papers*, *58*(4), 390–402. https://doi.org/10.1016/j.dsr.2011.01.011.

Savigny, J. D. (1818). Les Annelides. *Lamarck JB, Histoire Naturelle Des Animaux sans Vertèbres*, *5*, 302–374.

Schimmenti, E., Musco, L., Lo Brutto, S., Mikac, B., Nygren, A., & Badalamenti, F. (2016). Mediterranean record of *Eulalia ornata* (Annelida: Phyllodocidae) corroborating its fidelity link with the *Sabellaria alveolata* reef habitat. *Mediterranean Marine Science*, *17*(2), 359–370. https://doi.org/10.12681/mms.1485.

Schüller, M. (2011). Evidence for a role of bathymetry and emergence in speciation in the genus *Glycera* (Glyceridae, Polychaeta) from the deep Eastern Weddell Sea. *Polar Biology*, *34*(4), 549–564. https://doi.org/10.1007/s00300-010-0913-x.

Seixas, V. C., Zanol, J., Magalhães, W. F., & Paiva, P. C. (2017). Genetic diversity of *Timarete punctata* (Annelida: Cirratulidae): Detection of pseudo-cryptic species and a potential biological invader. *Estuarine, Coastal and Shelf Science*, *197*, 214–220. https://doi.org/10.1016/j.ecss.2017.08.039.

Siciński, J., Jażdżewski, K., De Broyer, C., Presler, P., Ligowski, R., Nonato, E. F., … Campos, L. S. (2011). Admiralty Bay Benthos Diversity—A census of a complex polar ecosystem. *Deep Sea Research Part II: Topical Studies in Oceanography*, *58*(1), 30–48. https://doi.org/10.1016/j.dsr2.2010.09.005.

Smith, S. D. (2002). Kelp rafts in the Southern Ocean. *Global Ecology and Biogeography*, *11*(1), 67–69. https://doi.org/10.1046/j.1466-822X.2001.00259.x.

Smith, J. A., Hillenbrand, C. D., Pudsey, C. J., Allen, C. S., & Graham, A. G. (2010). The presence of polynyas in the Weddell Sea during the Last Glacial Period with implications for the reconstruction of sea-ice limits and ice sheet history. *Earth and Planetary Science Letters*, *296*(3), 287–298. https://doi.org/10.1016/j.epsl.2010.05.008.

Stamatakis, A. (2014). RAxML version 8: A tool for phylogenetic analysis and post-analysis of large phylogenies. *Bioinformatics*, *30*(9), 1312–1313. https://doi.org/10.1093/bioinformatics/btu033.

Struck, T. H., Schult, N., Kusen, T., Hickman, E., Bleidorn, C., McHugh, D., & Halanych, K. M. (2007). Annelid phylogeny and the status of Sipuncula and Echiura. *BMC Evolutionary Biology*, *7*(1), 57. https://doi.org/10.1186/1471-2148-7-57.

Taboada, S., Bas, M., & Avila, C. (2015). A new *Parougia* species (Annelida, Dorvilleidae) associated with eutrophic marine habitats in Antarctica. *Polar Biology*, *38*(4), 517–527. https://doi.org/10.1007/s00300-014-1614-7.

Taboada, S., Wiklund, H., Glover, A. G., Dahlgren, T. G., Cristobo, J., & Avila, C. (2013). Two new Antarctic *Ophryotrocha* (Annelida: Dorvilleidae) described from shallow-water whale bones. *Polar Biology*, *36*(7), 1031–1045. https://doi.org/10.1007/s00300-013-1326-4.

Tajima, F. (1989). Statistical method for testing the neutral mutation hypothesis by DNA polymorphism. *Genetics*, *123*(3), 585–595.

Thatje, S. (2012). Effects of capability for dispersal on the evolution of diversity in Antarctic benthos. *Integrative and Comparative Biology*, *52*(4), 470–482. https://doi.org/10.1093/icb/ics105.

Thatje, S., Hillenbrand, C. D., & Larter, R. (2005). On the origin of Antarctic marine benthic community structure. *Trends in Ecology & Evolution*, *20*(10), 534–540. https://doi.org/10.1016/j.tree.2005.07.010.

Thornhill, D. J., Mahon, A. R., Norenburg, J. L., & Halanych, K. M. (2008). Open-ocean barriers to dispersal: A test case with the Antarctic Polar Front and the ribbon worm *Parborlasia corrugatus* (Nemertea: Lineidae). *Molecular Ecology*, *17*(23), 5104–5117. https://doi.org/10.1111/j.1365-294X.2008.03970.x.

Wright, S. (1951). The genetical structure of populations. *Annals of Eugenics*, *15*, 323–354.

Wright, S. (1978). Variability within and among natural populations. *Evolution and the Genetics of Populations: A Treatise in Four Volumes*, Vol. *4*. Chicago, IL: University of Chicago Press.

Zhou, M., Niiler, P. P., & Hu, J. H. (2002). Surface currents in the Bransfield and Gerlache Straits, Antarctica. *Deep Sea Research Part I: Oceanographic Research Papers*, *49*(2), 267–280. https://doi.org/10.1016/S0967-0637(01)00062-0.

SUPPORTING INFORMATION

Additional supporting information may be found online in the Supporting Information section at the end of the article.

How to cite this article: Leiva C, Riesgo A, Avila C, Rouse GW, Taboada S. Population structure and phylogenetic relationships of a new shallow-water Antarctic phyllodocid annelid. *Zool Scr*. 2018;00:1–13. https://doi.org/10.1111/zsc.12313

CHAPTER 2

Population substructure and signals of divergent adaptive selection despite admixture in the sponge *Dendrilla antarctica* from shallow waters surrounding the Antarctic Peninsula

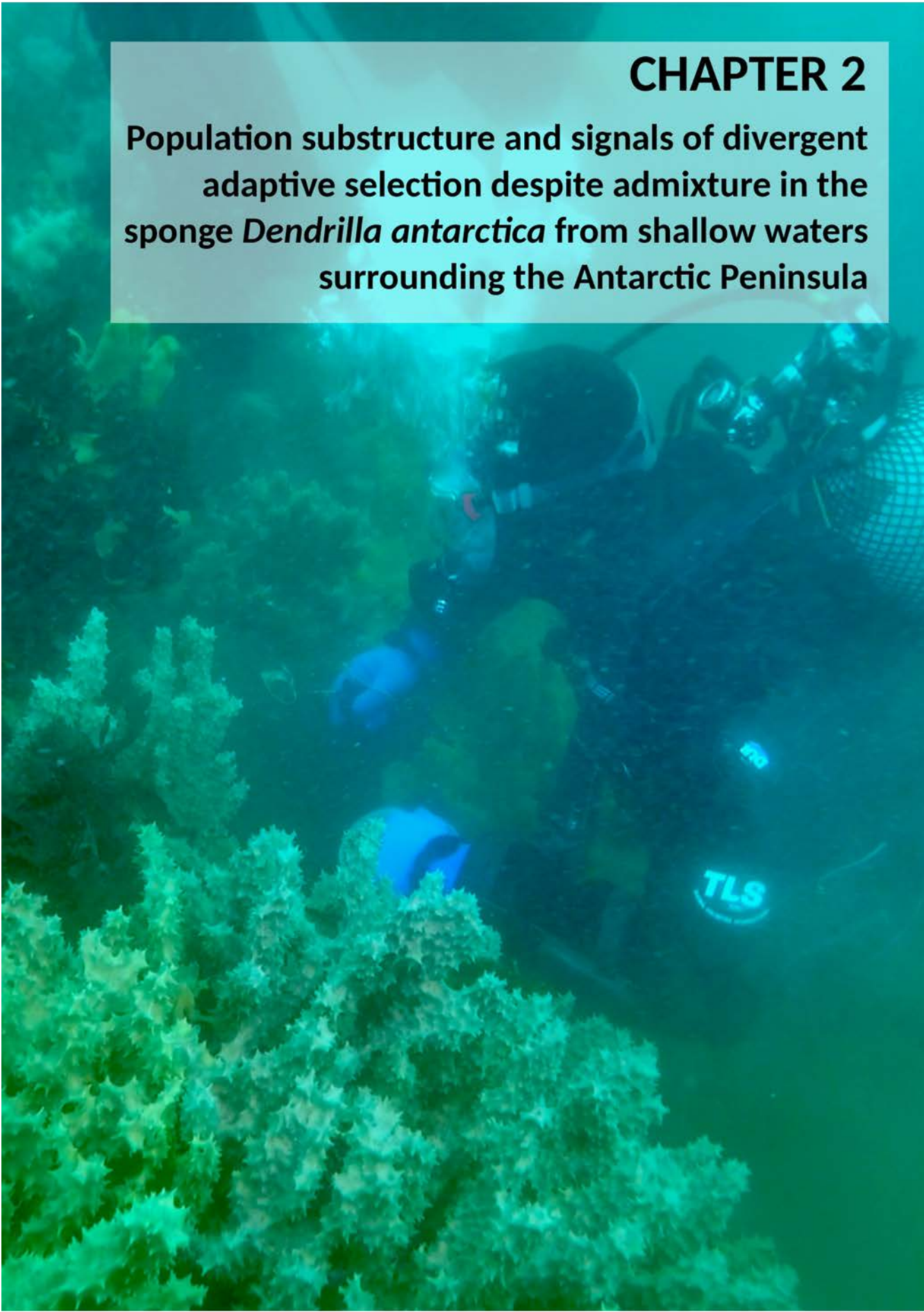

Received: 29 January 2019 | Revised: 29 April 2019 | Accepted: 13 May 2019

DOI: 10.1111/mec.15135

ORIGINAL ARTICLE

MOLECULAR ECOLOGY WILEY

Population substructure and signals of divergent adaptive selection despite admixture in the sponge *Dendrilla antarctica* from shallow waters surrounding the Antarctic Peninsula

Carlos Leiva[1,2] | Sergi Taboada[1,3] | Nathan J. Kenny[1] | David Combosch[4] | Gonzalo Giribet[5] | Thibaut Jombart[6] | Ana Riesgo[1]

[1]Department of Life Sciences, The Natural History Museum of London, London, UK

[2]Department of Genetics, Microbiology and Statistics, Faculty of Biology, University of Barcelona, Barcelona, Spain

[3]Department of Biology, Faculty of Science, Autonomous University of Madrid, Madrid, Spain

[4]Marine Laboratory, University of Guam, Mangilao, Guam

[5]Deparment of Organismic and Evolutionary Biology, Harvard University, Cambridge, Massachusetts

[6]Department of Infectious Disease Epidemiology, London School of Hygiene and Tropical Medicine, London, UK

Correspondence
Carlos Leiva, Department of Life Sciences, The Natural History Museum of London, London, UK.
Email: cleivama@gmail.com

Funding information
European Commission, Grant/Award Number: IF750937; Ministerio de Economía y Competitividad, Grant/Award Number: CTM2013-42667/ANT; Natural History Museum, Grant/Award Number: SDF14032 and SDR17012

Abstract

Antarctic shallow-water invertebrates are exceptional candidates to study population genetics and evolution, because of their peculiar evolutionary history and adaptation to extreme habitats that expand and retreat with the ice sheets. Among them, sponges are one of the major components, yet population connectivity of none of their many Antarctic species has been studied. To investigate gene flow, local adaptation and resilience to near-future changes caused by global warming, we sequenced 62 individuals of the sponge *Dendrilla antarctica* along the Western Antarctic Peninsula (WAP) and the South Shetlands (spanning ~900 km). We obtained information from 577 double digest restriction site-associated DNA sequencing (ddRAD-seq)-derived single nucleotide polymorphism (SNP), using RADseq techniques for the first time with shallow-water sponges. In contrast to other studies in sponges, our 389 neutral SNPs data set showed high levels of gene flow, with a subtle substructure driven by the circulation system of the studied area. However, the 140 outlier SNPs under positive selection showed signals of population differentiation, separating the central–southern WAP from the Bransfield Strait area, indicating a divergent selection process in the study area despite panmixia. Fourteen of these outliers were annotated, being mostly involved in immune and stress responses. We suggest that the main selective pressure on *D. antarctica* might be the difference in the planktonic communities present in the central–southern WAP compared to the Bransfield Strait area, ultimately depending on sea-ice control of phytoplankton blooms. Our study unveils an unexpectedly long-distance larval dispersal exceptional in Porifera, broadening the use of genome-wide markers within nonmodel Antarctic organisms.

KEYWORDS
adaptation, ddRADseq, mitochondrial genome, RNA-seq, SNPs, South Shetland Islands

1 | INTRODUCTION

The gene flow and phylogeographical patterns of Southern Ocean shallow-water marine invertebrates in general, and sponges in particular, are interesting for a number of reasons. From an evolutionary history perspective, the Southern Ocean provides a unique scenario for studying the impact of drastic environmental shifts on the population dynamics of marine species, with repeated

Pliocene–Pleistocene glacial cycles being the major factor in shaping the current diversity and distribution of the Antarctic fauna (Thatje, Hillenbrand, & Larter, 2005). The alternation of glacial and interglacial periods might have especially affected shallow-water benthic invertebrates, eliminating most of the available habitat during glacial maxima (Allcock & Strugnell, 2012; Rogers, 2007; Thatje et al., 2005). These dramatic environmental events left characteristic signatures throughout the genome of these shallow-water invertebrates, most of which have only been assessed using traditional mitochondrial (a fragment of the *cytochrome c oxidase subunit I* gene [*COI*]) and nuclear (18S and 28S rRNA genes) markers (e.g., González-Wevar, David, & Poulin, 2011; González-Wevar, Saucède, Saucède, Morley, Chown, & Poulin, 2013; Janosik, Mahon, & Halanych, 2011; Krabbe, Leese, Leese, Mayer, Tollrian, & Held, 2010). Although shallow-water sponges form massive reefs dominating an important fraction of the available hard substrate in Antarctica (Dayton, 1989), no study has yet addressed the population genetics and connectivity of any of the 397 described sponges from this continent (Downey, Griffiths, Linse, & Janussen, 2012; Riesgo, Taboada, & Avila, 2015). To our knowledge, the only study incorporating analyses of the genetic diversity of an Antarctic sponge was conducted on the deep-sea species *Stylocordyla chupachups* using microsatellites (Carella, Agell, & Uriz, 2019), but we did not consider it as a population genetics and connectivity study because the authors only focused on the sponge clonal reproduction at a very small scale (<2 km).

The Antarctic Peninsula is currently one of the most rapidly warming regions of the planet (Vaughan et al., 2003). The mean atmospheric temperature rose nearly 3°C during the second half of the 20th century (King, 1994; King & Harangozo, 1998; Turner et al., 2005), with profound consequences for ice sheets and glaciers (Cook, Fox, Vaughan, & Ferrigno, 2005). Moreover, the summer temperature of the surface waters adjacent to the Western Antarctic Peninsula (WAP) increased by more than 1°C during the same period (Meredith & King, 2005), threatening shallow-water Antarctic species, which are less resilient to temperature increases than species elsewhere (Peck & Conway, 2000), and whose essential biological functions are extremely sensitive to temperature fluctuations (Peck, Webb, & Bailey, 2004). This aspect is especially concerning for sponges, as all are sessile organisms known to have lecithotrophic larvae (Maldonado, 2006), which would imply limited dispersal abilities and therefore higher vulnerability (Pascual, Rives, Schunter, & Macpherson, 2017). However, although in the Southern Ocean the reproductive life history stages appear to have little influence in structuring genetic patterns (Halanych & Mahon, 2018), sponge larvae from other latitudes are not usually able to disperse over large distances (Pérez-Portela & Riesgo, 2018), with some exceptions (see Maldonado, 2006). These limited dispersal capabilities generally result in highly structured and isolated populations (Pérez-Portela & Riesgo, 2018), with high levels of inbreeding and a consequently reduced resilience (Botsford et al., 2009). Hence, to assess the degree of resilience that Antarctic sponges will have under future predicted habitat shifts (IPCC 2013th Assessment Report, 2013), it is urgent to investigate their connectivity patterns and gene flow.

Population genetics, which delves into the distribution of genetic diversity within and between populations, depends essentially on the presence of genetic variability to work with. The mitochondrial genome (mitogenome, mtDNA) has been widely used for population genetic and phylogenetic analyses in Metazoa (Avise et al., 1987) due to its high substitution rates (Brown, George, & Wilson, 1979) and its maternal inheritance and haploidy (see Ernster & Schatz, 1981). However, in some early-splitting animal lineages, such as the members of the phylum Porifera, mtDNA variation within and between species is extremely low, due to its slow-evolving nature (Huang, Meier, Todd, & Chou, 2008). With some notable exceptions (DeBiasse, Richards, & Shivji, 2010; Duran & Rützler, 2006; López-Legentil & Pawlik, 2009; Xavier et al., 2010), intraspecific relationships in sponges have therefore only been recently addressed using microsatellites (e.g., Blanquer & Uriz, 2010; Calderón et al., 2007; Giles, Saenz-Agudelo, Saenz-Agudelo, Hussey, Ravasi, & Berumen, 2015; Riesgo et al., 2016; Taboada et al., 2018). Within the past few years, new promising approaches for population genetics based on reduced representation genomic libraries combined with high-throughput sequencing techniques, such as restriction-associated DNA sequencing (RADseq) and genotyping by sequencing (GBS), have become routinely implemented in marine invertebrates but hardly on early-splitting lineages (reviewed in Pérez-Portela & Riesgo, 2018). These methods are revolutionizing the ecological, evolutionary and conservation genetic fields because of their power to recover hundreds to thousands of neutral single nucleotide polymorphisms (SNPs) for fine-scale population analyses (Andrews, Good, Good, Miller, Luikart, & Hohenlohe, 2016). However, only one study to date has recovered SNPs in sponges, which used amplicon sequencing to obtain 67 SNPs and detect the small-scale genetic structure of *Aphrocallistes vastus* (Brown, Davis, & Leys, 2017), the main reef-building glass sponge of the British Columbia continental shelf.

To date, the analysis of RADseq-derived SNPs has just reached Antarctic marine invertebrates with only four studies addressing the population genetic structure of the Antarctic krill *Euphausia superba* (Deagle, Faux, Faux, Kawaguchi, Meyer, & Jarman, 2015), the brittle stars *Ophionotus victoriae* (Galaska, Sands, Sands, Santos, Mahon, & Halanych, 2017a) and *Astrotoma agassizii* (Galaska, Sands, Sands, Santos, Mahon, & Halanych, 2017b), and the sea spider *Nymphon australe* (Collins, Galaska, Halanych, & Mahon, 2018). Although RADseq data can potentially be used for discovering genomic regions under selective pressure (Catchen et al., 2017; McKinney, Larson, Seeb, & Seeb, 2017), none of the above-mentioned studies has used this approach to delve into the footprints that natural selection and local adaptation left in the genome of the three Antarctic species listed above. In contrast, in other latitudes, RADseq has been successfully used to detectloci under selection, providing the grounds to understand processes of adaptive ecological divergence in a range of nonmodel marine organisms (e.g., Araneda, Larraín, Hecht, & Narum, 2016; Combosch, Lemer, Lemer, Ward, Landman, & Giribet, 2017; Ferchaud & Hansen, 2016; Gleason & Burton, 2016).

The dendroceratid *Dendrilla antarctica* Topsent, 1905 is one of the dominant sponges inhabiting West Antarctic shallow waters

(Sarà, Balduzzi, Balduzzi, Barbieri, Bavestrello, & Burlando, 1992), playing a key role by providing shelter and food for many other marine invertebrates (e.g., Moles et al., 2017). Its distribution spans along the Antarctic Peninsula and its associated islands, to the South Orkney Archipelago as the northernmost point of its range (data from World Porifera Database: www.marinespecies.org/porifera/porifera.php?p=taxdetails&id=164875). *D. antarctica* is a brooding sponge, with yolky lecithotrophic larvae that are released during the Antarctic summer (Koutsouveli et al., 2018). In the present study, we aim to assess the genetic diversity, demographic history, and genetic connectivity of *D. antarctica* at a regional scale in the WAP and South Shetland Islands using double digest (dd)RADseq-derived SNPs. We also evaluate the suitability of the full mitochondrial genome in *D. antarctica* to assess genetic diversity and connectivity. Finally, we test for genetic signatures of divergent selection using SNPs identified in an F_{ST} outlier test, and measure the expression levels of the genes identified under selection in three transcriptome samples spanning the whole latitudinal range of our sampling area.

2 | MATERIALS AND METHODS

2.1 | Sample collection, preservation and DNA extraction

For the population genomics study with ddRADseq, we collected ~1 cm^3 of tissue from 67 specimens of *Dendrilla antarctica* during the 2015–2016 austral summer in seven locations across the WAP and the South Shetland Islands (Figure 1; Table 1). Sampling was performed by SCUBA diving at 5–25 m depth. Sponge fragments were preserved in 96% ethanol, with the ethanol being replaced three times, and stored at −20°C until further processing. We extracted DNA from all samples using the DNeasy Blood & Tissue kit (Qiagen) following the manufacturer's protocol, with minor modifications in the cell lysis time (which was conducted with an overnight incubation) and the final DNA elution step (performed twice using 50 µl of elution buffer each time). DNA quantity was assessed with a Qubit dsDNA HS assay (Life Technologies).

For mitogenome reconstruction, we collected a fragment (~1 cm^3) of a specimen in 96% ethanol from Deception Island to perform draft-level genomic sequencing, with genomic DNA (gDNA) extracted as described above. Furthermore, we subsampled tissue fragments (~1 cm^3) of three individuals for additional mitogenome reconstruction and transcriptomic analysis, from three different sampling stations (O'Higgins Bay, n = 1; Deception Island, n = 1; and Adelaide Island, n = 1), covering the whole latitudinal range of the sponge in our study. We preserved the subsampled tissue fragments in RNA*later* (Life Technologies) immediately after collection, stored them for 24 hr at 4°C, replaced the RNA*later* once, and then stored samples at −80°C until further processing.

2.2 | Transcriptomic and genomic library preparation and sequencing

For transcriptomics, total RNA was extracted using a standard trizol-based method using TRI Reagent (Life Sciences) following the manufacturer's instructions. Subsequent mRNA purification was

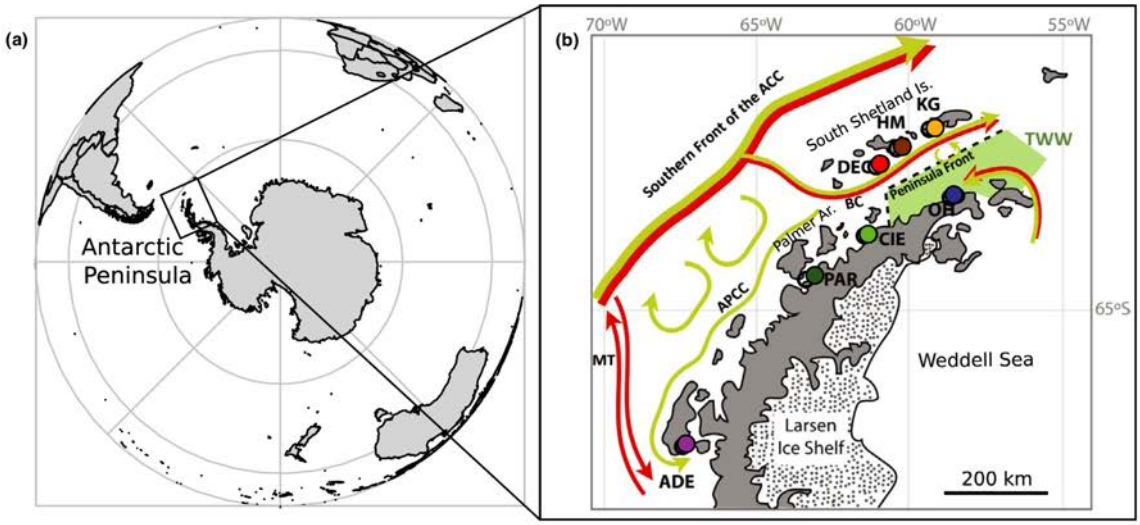

FIGURE 1 (a) Map of Antarctica showing the study area. (b) Detailed map of the Antarctic Peninsula, South Shetland archipelago and adjacent islands, showing sampling sites: ADE, Adelaide Island; CIE, Cierva Cove; DEC, Deception Island; HM, Half Moon Island; KG, King George Island; OH, O'Higgins Bay; PAR, Paradise Bay. Oceanic currents and water masses of the study area are outlined. Yellow and red arrows represent surface and deep currents, respectively; green shadowed area on the tip of the Western Antarctic Peninsula correspond to the Transitional Water with Weddell Sea Influence (TWW), delimited by the Peninsula Front represented by a black dashed line. APCC, Antarctic Peninsula Coastal Current; BC, Bransfield Current; MT, Marguerite Trough CDW Intrusion

TABLE 1 Collection details for all sampling sites, including abbreviations, coordinates, number of individuals used in the analyses, and date of collection

Station	Abbreviation	Coordinates	Number of individuals	Date of collection
Deception Island	DEC	62°59′25″S 60°37′31″W	9	13/1/2016
Half Moon Island	HM	62°35′41″S 59°54′07″W	9	24/2/2016
King George Island	KG	62°11′55″S 58°56′59″W	16	21/2/2016
O'Higgins Bay	OH	63°18′52″S 57°54′27″W	5	19/2/2016
Cierva Cove	CIE	64°09′20″S 60°57′12″W	9	17/2/2016
Paradise Bay	PAR	64°49′24″S 62°51′24″W	3	15/2/2016
Adelaide Island	ADE	67°34′04″S 68°08′55″W	11	12/2/2016
Total			62	

performed with a Dynabeads mRNA Purification Kit (Invitrogen) also following the manufacturer's protocol. Three cDNA libraries were constructed with the SCRIPTSEQ version 2 kit (Illumina), using adapters 9, 10 and 11, and sequenced alongside other samples in a single flowcell of an Illumina NextSeq 500, at 150 bp paired-end read length at the sequencing unit of the Natural History Museum, London (NHM).

Our genomic library for mitogenome recovery was prepared using a TruSeq DNA PCR-free library kit (Illumina) and sequenced on an Illumina MiSeq at 150 bp nominal paired read length at the sequencing unit of the Natural History Museum, London (NHM).

2.3 | Transcriptome and mitochondrial assembly, and mitogenome screening

A total of 123,782,845 paired reads (Den_ROT_3 = 29,840,417 reads, Den_OH_2 = 39,434,819 reads, and Den_DEC_19 = 54,507,609 reads) were obtained in our transcriptomic run. A total of 9,644,983 paired raw reads were obtained in our gDNA run, 8,484,436 paired reads after trimming and filtering. Both transcriptomic and gDNA reads were cleaned using TRIMMOMATIC 0.33 (Bolger, Lohse, & Usadel, 2014) with the following settings: ILLUMINACLIP:../Adapters.fa:2:30:10 LEADING:3 TRAILING:3 SLIDINGWINDOW:4:20 MINLEN:30 where the Adapters.fa file was substituted for the appropriate adapters for each library. Sequence quality was assessed before and after trimming using FASTQC (Andrews, 2010) to ensure complete removal of adapter and low-quality sequence data. The final cleaned read files for transcriptomic analyses contained 26,523,504 reads for the sample Den_ROT_3, 30,645,339 reads for the sample Den_OH_2, and 49,611,670 reads for the sample Den_DEC_19.

gDNA reads from the sample from Deception Island were assembled using VELVET 1.2.10 (Zerbino & Birney, 2008) at *k*-mer sizes of 71 and 91, which were the best *k*-mers after optimization trials. A local BLAST database was made from these gDNA assemblies using the makeblastdb command (Altschul et al., 1997). The complete mitochondrial protein-coding sequence for the gDNA sample was obtained by blasting (TBLASTN) the complete mitochondrial genome of *Igernella notablis* (NC_010216) to these assemblies and extracting the best-hit contigs. Reciprocal BLASTX of the translated nucleotide sequences to the nonredundant database confirmed the homology of these assemblies to Porifera, Dendroceratida.

The three individual transcriptomes were assembled into a de novo reference transcriptome using TRINITY version 2013_08_14 (Grabherr et al., 2011) with standard settings except for a minimum contig length of 200 bp and in silico read normalization. This de novo reference transcriptome contained 74,762 transcripts with an N_{50} of 658 and a total of 38.8 Mb with GC content of 44.9%. Similarly, the three samples were assembled separately using the same Trinity pipeline as above. In addition to the complete mitochondrial genome recovered from the gDNA sample, three more mitochondrial genomes were obtained from the transcriptomic reads or the assembled transcriptomes using the pipeline Trimitomics (Plese et al., 2018). Subsequently, all four mitochondrial genomes (one coming from the gDNA sample and three from the transcriptomes) were aligned in GENEIOUS 8.1.8 (Kearse et al., 2012) using the Q-INS-I algorithm of MAFFT version 7 (Katoh & Standley, 2013), which is used as the default algorithm for rRNA alignments because it considers secondary structure information, as a form of base-pairing probability (Katoh & Toh, 2008). The software DNASP 5.10.01 (Librado & Rozas, 2009) was used to calculate the number of segregating sites (*S*), haplotype number (*H*), haplotype diversity (*Hd*) and nucleotide diversity (π).

2.4 | ddRADseq library preparation and sequencing

Library preparation was conducted following Peterson, Weber, Weber, Kay, Fisher, and Hoekstra (2012) with the following modifications (as in Combosch et al., 2017). gDNA (100–1,000 ng) was digested using the high-fidelity restriction enzymes *Sbf*1 and *Eco*R1 (New England Biolabs). Resulting digested fragments were cleaned with an Apollo 324 (IntegenX) using Agencourt AMPure beads (1.5 × volume ratio; Beckham Coulter), and were subsequently quantified with a Qubit dsDNA HS assay (Life Technologies). Resulting fragments were ligated to custom-made P1 and P2 adapters containing sample-specific barcodes and primer annealing sites. Individually

barcoded samples were pooled into libraries, cleaned by manual pipetting using AMPure beads (1.5 × volume ratio), and size-selected (270–600 bp) using a Pippin Prep (Sage Science). Each library was then PCR-amplified using Phusion polymerase with 14–20 PCR cycles (98°C for 10 s, 65°C for 30 s and 72°C for 90 s, with an initial denaturation step at 98°C for 30 s and a final extension step at 72°C for 5 min). Resulting libraries were cleaned with an Apollo 324 to remove remaining adapters and primers using AMPure beads (0.8 × volume ratio). Each library was quantified using a qPCR Kapa library quantification kit (Kapa Biosystems) and quality-checked on an Agilent BioAnalyzer 2100 (Agilent Technologies). Libraries were pooled normalizing their concentration, subsequently pooled with RNA-seq libraries in the same flowcell, and paired-end sequenced (150 bp) on an Illumina HiSeq 2500 (Illumina) at the Center for Systems Biology, Harvard University (Cambridge, MA, USA).

2.5 | ddRADseq locus assembly and outlier detection

Quality filtering and locus assembly was conducted with the STACKS pipeline, version 1.44 (Catchen, Hohenlohe, Hohenlohe, Bassham, Amores, & Cresko, 2013). RAD-tags (DNA fragments with the two appropriate restriction enzyme cut sites that were selected, amplified and sequenced) were processed using *process_radtags*, where raw reads were quality-trimmed to remove low-quality reads, reads with uncalled bases, and reads without a complete barcode or restriction cut site. The *process_radtags* rescue feature (-r) was used to recover minimally diverged barcodes and RAD-tags (--barcode_dist 3; --adapter_mm 2). The *process_radtags* trimming feature (-t) was used to trim remaining reads to 120 bp, in order to increase confidence in SNP calling. After performing these filtering steps in *process_radtags*, we retained a total of 161,847,986 reads from the initial 220,380,548 raw reads, with an average of 2,247,889 reads per sample. Preliminary tests were carried out following Jeffries et al. (2016) to identify optimal STACKS parameters. Final parameter values were as follows: *ustacks*: M = 2, m = 3, allowing for gaps (--gapped; --max_gaps 3; --min_aln_len 0.80), using the removal (-r) and deleveraging (-d) algorithms; *cstacks*: *n* = 4, allowing for gaps (--gapped; --max_gaps 3; --min_aln_len 0.80); *sstacks*: allowing for gaps (--gapped). Mean locus coverage among all samples was 47.435, ranging from 23.359 to 199.138.

The STACKS *populations* module was used to conduct a first filtering of the data, retaining those SNPs present in at least 20% of the individuals (*r* = 0.2). To prevent the analysis of physically linked loci, and hence meet the assumptions of subsequent analyses, we used the "--write_single_SNP" option to retain only the first SNP from each RAD-tag. A subsequent more accurate filtering was performed using the *adegenet* R package (Jombart, 2008; Jombart & Ahmed, 2011; R Core Team, 2014), assessing SNP distributions across individual samples and sampling stations, and testing different filtering thresholds in order to maximize the number of retained SNPs and minimize missing data. This approach provides significant help in defining final thresholds in comparison with the STACKS *populations* module. Thus, we finally retained loci present in at least 40% of the individuals, and filtered out individuals with less than 30% of the final loci, resulting in a data set containing 577 SNPs and 62 individuals.

In order to differentiate neutral SNPs from putative SNPs under positive selection, the database containing 577 SNPs was analysed using default parameters in LOSITAN (Antao, Lopes, Lopes, Lopes, Beja-Pereira, & Luikart, 2008). We used LOSITAN because it implements the FDIST2 approach of Beaumont and Nichols (1996), which provides a robust method when populations deviate from the island model of migration (Tigano, Shultz, Shultz, Edwards, Robertson, & Friesen, 2017). Also, it incorporates heterozygosity and simulates a distribution for neutrally distributed markers (De Mita et al., 2013; Narum & Hess, 2011). We considered that these features were more appropriate for our model species studied herein, *D. antarctica*, than the characteristics of other F_{ST}-outlier methods. Moreover, we also run BAYESCAN (Foll & Gaggiotti, 2008) with default parameters, which only detected one locus under selection already detected by LOSITAN. We discuss LOSITAN results given the reasons stated above.

2.6 | Population genetic analyses

The neutral SNP data set (389 SNPs, 62 organisms, vcf file in Appendix S1) was used for the population genetic analyses. Genetic diversity and demographic statistics were calculated using the *ape* (Paradis, Claude, & Strimmer, 2004), *pegas* (Paradis, 2010) and *adegenet* R packages. Expected (H_E) and observed (H_O) heterozygosities per SNP were extracted and subsequently averaged across samples within sampling stations from the *adegenet* "*genind*" objects, and then the *hw.test* function in *pegas* was used to test for deviations from Hardy–Weinberg equilibrium per SNP. To test whether *D. antarctica* populations were in expansion we used the *tajima.test* function in *pegas* to obtain the Tajima's *D* statistic for each sampling site and for the whole set of samples together. To assess inbreeding within sampling stations and differentiation among them, we used F_{IS} and F_{ST} *F*-statistics respectively, both obtained with the *fstat* function in the R package *hierfstat* (Goudet, 2005).

Population structure was assessed using the function *snapclust* in the R package *adegenet* (Beugin, Gayet, Gayet, Pontier, Devillard, & Jombart, 2018), the discriminant analysis of principal components (DAPC) as implemented in the *adegenet* R package (Jombart, Devillard, & Balloux, 2010), and STRUCTURE version 2.3 (Pritchard, Stephens, & Donnelly, 2000). STRUCTURE and *snapclust* may produce similar individual membership probability plots, but they have totally different approaches to the genetic clustering problem: while STRUCTURE uses a Bayesian approach with Markov chain Monte Carlo (MCMC) method to estimate allele frequencies in each cluster and population memberships for every individual, *snapclust* is a fast likelihood optimization method combining both model-based and geometric clustering approaches, which uses the Expectation-Maximization (EM) algorithm to assign genotypes to populations and detect admixture patterns. Initial group memberships for *snapclust* were chosen using the k-means algorithm (pop.ini = "kmeans"), allowing a maximum *K* (number of clusters) of 10 (max = 10), and a

maximum number of iterations of 100 (max.iter = 100). The analysis successfully converged at the second iteration. The DAPC analysis was performed by grouping samples by sampling stations, and the number of retained principal components analysis (PCA) axes was chosen using the cross-validation *xvalDapc* function in the *adegenet* R package. STRUCTURE was run twice, using two distinct data sets: (a) all neutral SNPs (389 SNPs, 62 individuals) and (b) just the neutral SNPs in Hardy–Weinberg equilibrium (210 SNPs, 62 individuals). Both analyses were run for 200,000 MCMC iterations using the admixture model, with a burn-in of 100,000 iterations, setting the putative *K* (number of clusters) from 1 to 10 with 20 replicates for each run. STRUCTURE HARVESTER (Earl & vonHoldt, 2012) and CLUMPP version 1.1.2 (Jakobsson & Rosenberg, 2007) were used to determine the most likely number of clusters and to average each individual's membership coefficient across the *K* value replicates, respectively.

Pairwise F_{ST} values were estimated to measure the differentiation between pairs of sampling stations using the *pairwise.fst* function in the *hierfstat* R package. Their significance was tested with 1,000 permutations using the *ade4* R package (Dray & Dufour, 2007). The software BARRIER version 2.2 (Manni, Guerard, & Heyer, 2004) was then used to identify and position genetic breaks in the sampling area. This software uses an improved Monmonier's algorithm to detect genetic barriers from a matrix of genetic distances (pairwise F_{ST} table) linked to a matrix of geographical distances. A Mantel test was performed to test the isolation by distance model, examining the correlation between geographical (accounting for coastlines) and genetic distances, using the *mantel.randtest* function in the *ade4* R package.

To test whether the DAPC grouping or the Barrier's genetic break explained a significant part of the total genetic variation, two hierarchical analyses of molecular variance (AMOVAs) were performed using the *poppr.amova* function in the *poppr* R package.

Finally, to identify gene flow patterns in our study area, Nei's G_{ST} method was used to estimate the relative contemporary migration between sampling stations, using the *divMigrate* function of the *diveRsity* R package (Keenan, McGinnity, McGinnity, Cross, Crozier, & Prodöhl, 2013).

2.7 | Annotation, expression values and structure of putative loci under selection

To improve the annotation step, all RAD-loci containing an outlier SNP under positive selection were mapped back to our de novo reference transcriptome using CLC Genomics Workbench 5.1 local BLAST (Altschul et al., 1997) to obtain the contig for each RAD-locus. All contigs with uniquely mapped loci were then subjected to a BLASTX and BLASTN search against *nr* (default parameters, Altschul et al., 1997), and this annotation was retained for the mapped RAD-locus. A functional annotation analysis was then performed using DAVID 6.8 (Huang Sherman, & Lempicki, 2008a, 2008b). Expression values for putative contigs under selection in each of the three RNA-seq data sets were determined by mapping reads from individual samples to the de novo reference transcriptome using the RSEM package (Li & Dewey, 2011; --aln_method bowtie2) in Trinity (Grabherr et al., 2011). The abundance_estimates_to_matrix.pl script was used to determine comparable values of expression (cross-sample normalization: trimmed mean of M-values, TMM), and the obtained TMM values were subsequently normalized to TPM values (transcripts per kilobase million).

To detect signals of geographically divergent adaptive selection, we used the same structuring analyses used for the neutral SNP data set. Hence, STRUCTURE, *snapclust* and DAPC were run for the data set containing the SNPs under positive selection (140 SNPs, 62 individuals, vcf file in Appendix S2) using the same parameters mentioned above for the neutral data set. Moreover, global F_{ST} statistic and pairwise F_{ST} values were estimated using the *hierfstat* and *ade4* R packages as specified for the neutral data set. The software BARRIER was also used on the loci under positive selection and, subsequently, two AMOVAs were also performed in the *poppr* R package to test whether the DAPC grouping or the BARRIER's genetic break explained a significant part of the genetic variation.

3 | RESULTS

3.1 | Mitogenome diversity

The total length of the mitochondrial genome obtained from our gDNA reads from Deception Island was 19,498 bp, of which 10,949 bp comprised protein-encoding sequences. From our de novo transcriptomes, we were able to recover 10,859 bp for the sample from Adelaide Island, 10,682 bp for the sample from Deception Island and 10,893 bp for the sample from O'Higgins Bay. The alignment of the four sequences encompassed 9,433 bp, with four different haplotypes (*H*) but only three segregating sites (representing 0.032% of the total) (alignments of the 15 mitochondrial genes in Appendix S3). Specifically, we found one mutation in the gene ATP8 (site 141, T → A) in the transcriptomic sample from Deception Island, one nucleotide varied in the sample from Adelaide Island in NAD4 (site 620, A → C), and finally one nucleotide varied in the gDNA sample from Deception Island in the *cytochrome c oxidase I* (*COI*) gene (site 902, T → C). Nucleotide diversity (π) was 0.00016 ± 0.00004 and, because each of the four samples analysed accounted for a different haplotype, haplotype diversity (*Hd*) was 1.

3.2 | Population genetics analyses using neutral SNPs

Population genetics statistics are shown in Table 2. Tajima's *D* values were all negative, showing significant *p*-values ($p < 0.05$) in all stations separately and for the whole data set (Table 2). Average expected heterozygosity (H_E) ranged from 0.054 in Paradise Bay to 0.142 in King George Island, with a value of 0.162 when all samples were analysed together (Table 2). Average observed heterozygosity (H_O) ranged from 0.052 in Paradise Bay to 0.079 in Half Moon Island, with a value of 0.067 for the whole data set (Table 2). The number

TABLE 2 Population genetic statistics and demographic estimators from the 389 neutral SNPs data set

	D	Av H_E	Av H_O	$H_E - H_O$	H-W	F_{IS}
Cierva Cove	**−4.180**	0.126	0.075	0.051	5/385	0.405
Deception Is.	**−4.182**	0.131	0.076	0.055	4/388	0.420
Half Moon Is.	**−4.227**	0.133	0.079	0.054	7/389	0.406
King George Is.	**−3.830**	0.142	0.062	0.080	27/388	0.563
O'Higgins Bay	**−3.881**	0.121	0.062	0.059	1/387	0.488
Paradise Bay	**−3.634**	0.054	0.052	0.002	0/319	0.037
Adelaide Is.	**−4.069**	0.138	0.053	0.085	22/389	0.616
Total	**−3.321**	0.162	0.067	0.095	178/389	0.586

Note: *D*, Tajima's *D* values, bold numbers showing significant deviation from 0; Av H_E, averaged expected heterozygosity; Av H_O, averaged observed heterozygosity; $H_E - H_O$, difference between averaged expected and averaged observed heterozygosities; H-W, number of SNPs not in Hardy–Weinberg equilibrium compared to the total SNPs obtained for each station; F_{IS}, inbreeding coefficient estimated from averaged observed and averaged expected heterozygosities.

of loci not found in Hardy–Weinberg equilibrium ranged from 0 in Paradise Bay to 27 in King George Island, and a total of 178 loci when all samples were treated together (Table 2). Inbreeding coefficient (F_{IS}) estimated from heterozygosity ($F_{IS} = 1 - (H_O/H_E)$) ranged from 0.037 in Paradise Bay to 0.616 in Adelaide Island, with a value of 0.586 for the entire data set (Table 2). *F*-statistics estimated in the *hierfstat* R package for all the samples together were $F_{IS} = 0.595$ and $F_{ST} = 0.011$.

The results of the STRUCTURE analysis for all neutral loci (389 SNPs) are shown in Figure 2a. Although the most likely number of clusters was $K = 4$—inferred from delta *K* (Evanno, Regnaut, & Goudet, 2005), shown in Appendix S4a—and many of the samples were assigned to one of the four clusters with a high confidence, there is no clear pattern of geographical structure from these results. In fact, STRUCTURE results may be interpreted as an indication of panmixia or high gene flow among sampled stations. Similarly, *snapclust* results (Figure 2b) revealed a lack of geographical structure, although the most likely number of clusters for this analysis inferred from Akaike's information criterion (AIC) was $K = 2$ (see Appendix S4b). STRUCTURE results for the data set just containing the 210 SNPs in Hardy–Weinberg equilibrium are shown in Appendix S5. Due to the lack of geographical structure in the results from both data sets, we retained information for all 389 SNPs in Figure 2a.

The two-dimensional representation of the DAPC results taking the first and second DAPC axes showed differentiation of some of the sampling sites (Figure 2c), with O'Higgins Bay and Adelaide Island appearing as the two most divergent stations (see Appendix S6a for the first-third DAPC axes representation, showing a similar population structuring). Adelaide Island is the southernmost site in our sampling area, while O'Higgins Bay represents the northernmost sampled area in the Antarctic Peninsula, which is in fact oceanographically isolated by the Peninsula Front (see Figure 1b).

Pairwise F_{ST} comparisons showed low to moderate F_{ST} values ranging from 0 to 0.124 (Table 3, above diagonal). Although all F_{ST} values were nonsignificant, they allowed us to identify genetic barriers in *Dendrilla antarctica*'s genetic landscape using the BARRIER software. The strongest genetic break separated O'Higgins Bay and King George Island stations from the rest of the sampling localities (Figure 2d). The Mantel test indicated no correlation between the geographical distance matrix and the genetic distance matrix ($p = 0.687$), refuting the isolation by distance hypothesis and thus indicating that other factors (e.g., oceanographic features) might be explaining the geographical distribution of *D. antarctica*'s genetic diversity.

The full migration G_{ST} table is shown in Appendix S7. The highest migration values (>0.8) are represented in the migration network (Figure 3), indicating an isolation of the Central Antarctic Peninsula (Cierva Cove and Paradise Bay), and high contemporary migration between Adelaide Island and the South Shetlands, and within the South Shetlands. High contemporary migration was also detected from O'Higgins Bay to King George Island (Figure 3).

The AMOVA results for the neutral SNP data set are shown in Table 4a. Both the DAPC and the BARRIER groupings appeared to be nonsignificant portions of the genetic variance ($p = 0.468$ and 0.248, respectively), the two of them representing less than 1% of the total variation (Table 4a).

3.3 | Putative loci under selection

A total of 188 F_{ST} outlier SNPs were detected by LOSITAN, 48 of them identified as under balancing selection and 140 as under positive selection. These 140 SNPs represented 24.3% of the complete SNPs data set.

From the 140 RAD-tags with outlier SNPs under positive selection, 31 matched contigs in our de novo assembled reference transcriptome of *D. antarctica* and for 16 of them we retrieved a BLAST hit against the *nr* NCBI database with e-value 1e−05 or lower (Table 5). One of them corresponded to an uncharacterized protein, and another one matched a bacterial aminotransferase (Table 5). This low ratio of only one RAD-tag matching a bacterial gene out of the 140 under positive selection (0.7%) is in agreement with previous knowledge on the microbiome of *D. antarctica*, a sponge that is considered to have low microbial abundance (Koutsouveli et al., 2018). For the 14 remaining annotated loci, gene characterization and DAVID

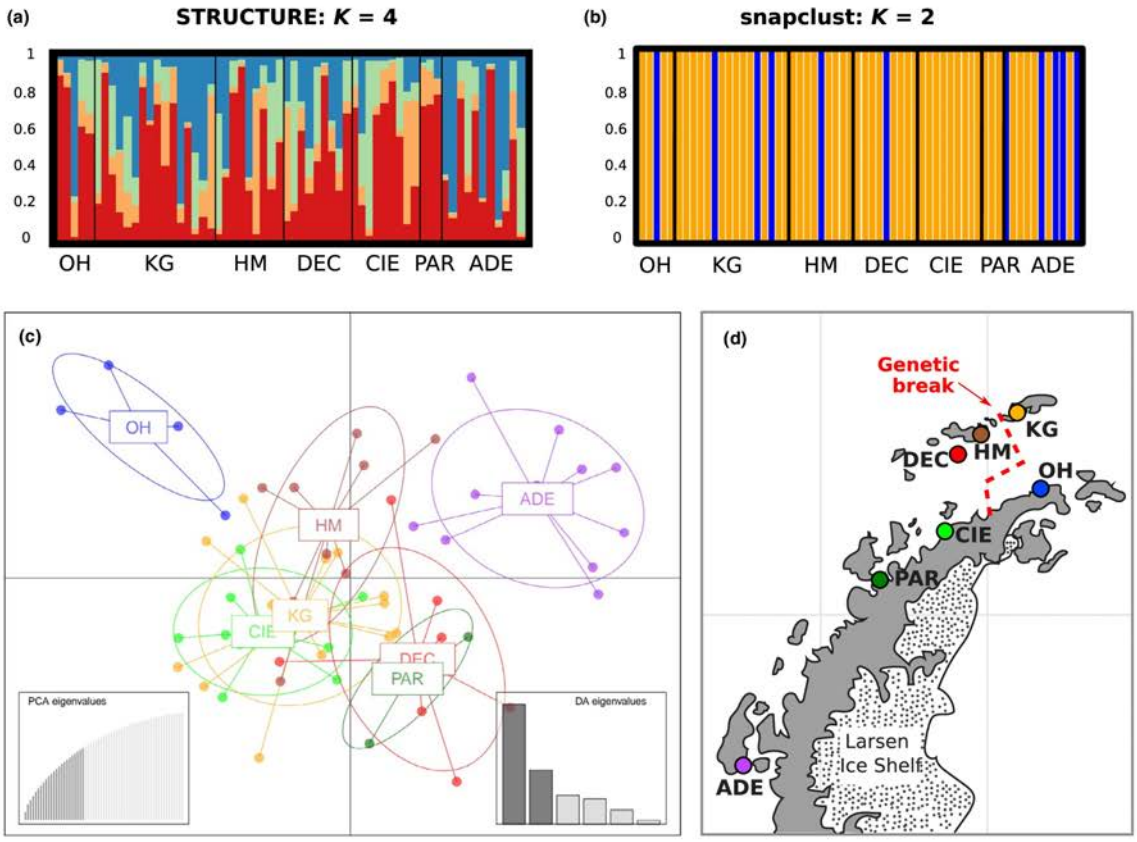

FIGURE 2 Population structure and differentiation analyses based on the 389 neutral SNPs data set. (a) STRUCTURE results with $K = 4$ (see delta K plot in Appendix S4), (b) *snapclust* results with $K = 2$ (see AIC plot in Appendix S4), and (c) DAPC results: two-dimensional representation of the first (horizontal axis) and second (vertical axis) PCA eigenvalues. (d) Map of the study area with the genetic break from the BARRIER analysis shown as a red dashed line. See abbreviations in Figure 1

functional annotation analysis assigned them to six cellular functions (Figure 4): (a) cytoskeleton reorganization, cell morphology and motility; (b) ubiquitination; (c) apoptosis; (d) response to environmental stressors; (e) biological detoxification and (f) RNA post-transcriptional modifications. The expression levels of these genes were relatively similar across two of the sampling sites, Adelaide Island and O'Higgins Bay (Table 5), with almost all values within each gene in the same order of magnitude, and nearly all genes overexpressed in the individual from Deception Island (Table 5; Figure 4). Only one gene appeared overexpressed in the individual from O'Higgins Bay (*DNAH3*) and three genes overexpressed (*IPP*, *PLGR1* and *PAE1850*) in the individual from Adelaide Island (Table 5; Figure 4).

TABLE 3 Pairwise F_{ST} values for the neutral SNP data set (above diagonal) and the data set composed of putative SNPs under positive selection (below diagonal)

	Cierva Cove	Deception Is.	King George Is.	Half Moon Is.	O'Higgins Bay	Paradise Bay	Adelaide Is.
Cierva Cove		0.102	0.077	0.114	0.119	0	0.121
Deception Is.	**0.302**		0.073	0.102	0.123	0	0.106
King George Is.	**0.210**	0.141		0.084	0.073	0	0.094
Half Moon Is.	**0.208**	**0.238**	0.121		0.124	0	0.094
O'Higgins Bay	**0.421**	**0.280**	**0.150**	**0.167**		0	0.102
Paradise Bay	**0.204**	0.063	0.099	0.167	0.017		0
Adelaide Is.	**0.323**	**0.301**	**0.220**	**0.231**	**0.250**	0.120	

Note: Significant F_{ST} values ($p < 0.05$) are shown in bold.

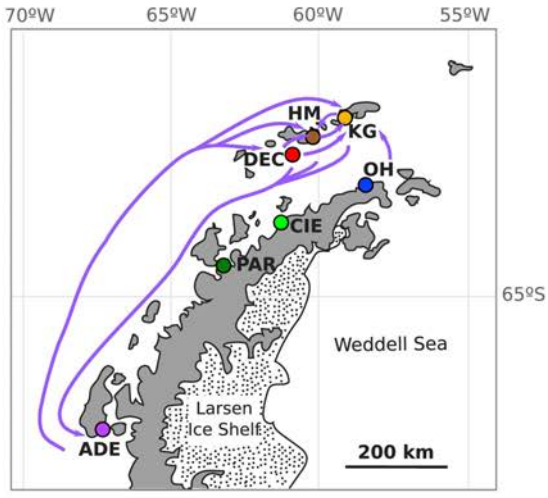

FIGURE 3 Contemporary migration network inferred from *divMigrate*. Map of the study area with purple arrows representing the migration values higher than 0.8 in the migration table (see Appendix S7)

The results of the STRUCTURE analysis for the 140 SNPs under positive selection are shown in Figure 5a. The most likely number of clusters was $K = 2$, with $K = 5$ as the second most likely number of clusters (inferred from delta K, shown in Appendix S4c). These results indicate a lack of geographical structure in the data set under positive selection, which may be the result of the high migration and gene flow detected in the neutral data set. Similarly, *snapclust* (Figure 5b) did not retrieve any clear geographical structure for the five clusters inferred from AIC (see Appendix S4d).

The representation of the DAPC results based on the 140 SNPs under positive selection taking the first and second DAPC axes is shown in Figure 5c (see Appendix S6b for the first to third DAPC axes representation). Samples from the Bransfield Strait stations (i.e., South Shetland Islands, O'Higgins Bay and Cierva Cove) were grouped together, while Paradise Bay and Adelaide Island appeared as the most divergent sites (Figure 5c), the latter being the most differentiated sampling station based on the first eigenvalue.

The F_{ST} statistic for the 140 SNPs under positive selection was estimated at 0.205 in the *hierfstat* R package. Pairwise F_{ST} comparisons showed high and mostly significant F_{ST} values, ranging from 0.017 to 0.421 (Table 3, below diagonal). The most robust genetic break

TABLE 4 Hierarchical AMOVA results: evaluation of genetic differentiation within and among sampling stations, and within and among the groups inferred from the DAPC and Barrier results for the 389 neutral SNPs data set (a) and the 140 under positive selection SNPs data set (b)

	df	Sum Sq	Mean Sq	Percentage of variation	*p*-value
(a) Neutral data set					
DAPC: ADE/OH/Rest					
Between DAPC clusters	2	296.97	148.48	−0.15	0.468
Between populations	4	610.61	152.65	0.78	0.283
Between samples	55	7,731.82	140.58	59.21	**0.001**
Within samples	62	2,207.68	35.61	40.17	**0.001**
BARRIER: KG + OH/Rest					
Between BARRIER clusters	1	178.45	178.45	0.61	0.248
Between populations	5	729.13	145.83	0.37	0.373
Between samples	55	7,731.82	140.58	59	**0.001**
Within samples	62	2,207.68	35.61	40.02	**0.001**
(b) Positive selection data set					
DAPC: ADE/PAR/Rest					
Between DAPC clusters	2	291.76	145.88	6.72	**0.043**
Between populations	4	370.48	92.62	4.03	**0.002**
Between samples	55	3,482.35	63.32	72.38	**0.001**
Within samples	62	409.65	6.61	16.87	**0.001**
BARRIER: CIE/Rest					
Between BARRIER clusters	1	128.11	128.11	1.45	0.124
Between populations	5	534.13	106.83	6.77	**0.001**
Between samples	55	3,482.35	63.32	74.43	**0.001**
Within samples	62	409.45	6.61	17.35	**0.001**

TABLE 5 Genes (and their corresponding RAD-tags) under positive selection in *Dendrilla antarctica*, alongside BLAST annotations and expression values in the three transcriptome samples

RAD-tag	Contig in reference transcriptome	Annotation	Abbreviation	E-value	Expression (TMM-corrected TPM)		
					ADE	OH	DEC
3332	TRINITY_DN40585_c0_g1_i1	Dimethylaniline monooxygenase [N-oxide-forming] 5	FMO5	1.87E−20	0	0	1.313
7288	TRINITY_DN35887_c1_g1_i1	Actin-binding protein IPP-like	IPP	6.05E−42	12.231	7.113	4.738
9345	TRINITY_DN29758_c0_g1_i1	arf-GAP with GTPase, ANK repeat and PH domain-containing protein 1-like	AGAP1	7.54E−23	0.837	0.557	0.948
11872	TRINITY_DN30313_c0_g1_i1	Cilia and flagella associated protein 54	CFAP54	5.13E−64	0.749	0.807	1.202
9419	TRINITY_DN36218_c2_g3_i4	Death-inducer obliterator 1-like	DIDO1	1.29E−27	1.927	3.813	4.41
390	TRINITY_DN46058_c0_g1_i1	Dynein heavy chain 3	DNAH3	6.37E−08	0.506	0.865	0.266
14033	TRINITY_DN17138_c0_g1_i1	E3 ubiquitin-protein ligase UBR5	UBR5	4.64E−12	0	0	0.242
9205	TRINITY_DN31666_c0_g1_i3	Glycylpeptide N-tetradecanoyltransferase 1	NMT1	5.13E−64	0	0	0.446
1845	TRINITY_DN36199_c4_g2_i2	kelch domain-containing protein 8A	KLHDC8A	1.12E−52	2.059	0.411	6.931
2166	TRINITY_DN36199_c4_g2_i4	Kelch domain-containing protein 8A	KLHDC8A	6.46E−45	3.743	1.892	9.235
7585	TRINITY_DN42392_c0_g1_i1	Pleiotropic regulator 1-like	PLRG1	2.27E−29	1.343	0	0
2069	TRINITY_DN17268_c1_g1_i1	Putative scavenger receptor cysteine-rich protein type 12 isoform X1	CD163L1	2.35E−38	0.275	0.411	0.502
2347	TRINITY_DN27486_c0_g1_i1	RING finger protein 157	RNF157	5.13E−64	1.706	1.76	4.602
3110	TRINITY_DN27486_c0_g1_i1	RING finger protein 157	RNF157	2.01E−63	1.706	1.76	4.602
6870	TRINITY_DN36204_c5_g4_i24	rRNA intron-encoded homing endonuclease	PAE1850	1.92E−60	12,432.867	11,436.449	4,836.602
4535	TRINITY_DN34338_c2_g1_i2	SH3 domain-containing kinase-binding protein 1-like isoform X2	SH3KBP1	2.71E−13	0	0	9.65
2011	TRINITY_DN46934_c0_g1_i1	Uncharacterized protein	–	1.25E−61	0.363	0	0.074
9873	TRINITY_DN25724_c0_g1_i1	Aminotransferase BACTERIA	–	5.13E−64	–	–	–

Abbreviations: TMM, trimmed mean of M-values; TPM, transcripts per kilobase million.

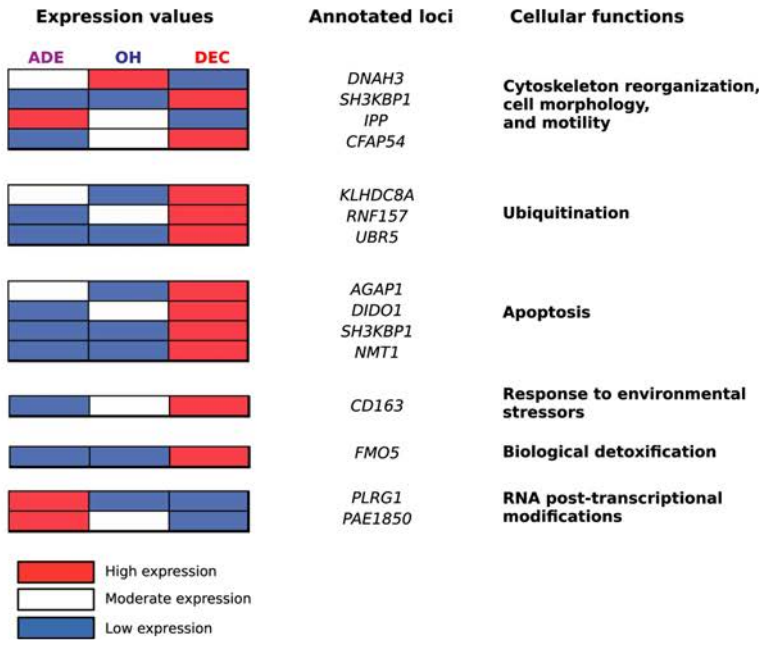

FIGURE 4 Functional annotation analysis showing the 14 annotated loci under selection, their cellular function, and relative expression levels presented in heatmaps (actual values can be seen in Table 5). Red indicates higher expression, white moderate expression and blue low expression, based on the values reported in Table 5

determined by the BARRIER software using these pairwise F_{ST} values separated Cierva Cove from the rest of the stations (Figure 5d).

AMOVA results for the "under positive selection" data set are shown in Table 4b. The BARRIER grouping isolating Cierva Cove (Figure 5d) represented a nonsignificant 1.45% of the total variation (p = 0.124). On the other hand, the DAPC clustering separating Adelaide Island, Paradise Bay and the Bransfield Strait stations (Figure 5c) reached a significant 6.72% of the total genetic variance (p = 0.043).

4 | DISCUSSION

4.1 | Mitogenome diversity

Our study unveiled an extremely low mitochondrial diversity in *Dendrilla antarctica*, with only four individual SNPs across 9,433 bp of protein-coding mitochondrial sequence data. Although mitogenome sequences were only obtained from four individuals, the low nucleotide diversity we observed in organisms spanning the whole latitudinal range of our sampling area (~900 km, which is almost the entire species distribution) indicates that protein-coding mitochondrial markers provide almost no resolution for population genetic studies for *D. antarctica*. This extremely low variability in mitochondrial markers is not uncommon in sponges because *COI* has traditionally showed relatively low genetic variation at both intra- and interspecific levels (e.g., Dailianis, Tsigenopoulos, Dounas, & Voultsiadou, 2011; León-Pech, Cruz-Barraza, Cruz-Barraza, Carballo, Calderon-Aguilera, & Rocha-Olivares, 2015; Riesgo et al., 2016; Setiawan et al., 2016; Taboada et al., 2018) with just a few exceptions (DeBiasse et al., 2010; Duran & Rützler, 2006; López-Legentil & Pawlik, 2009; Xavier et al., 2010), probably due to slower rates of mitochondrial genome evolution and/or the presence of active mitochondrial repair mechanisms (Huang, Meier, et al., 2008).

4.2 | Population genomic analyses using neutral SNPs

In contrast with the low variability of the mitochondrial genome in *D. antarctica*, our study revealed a high resolution power of ddRAD-seq-derived SNPs for population genetic studies. The analyses of our 389 neutral SNPs showed the characteristic signatures of a complex evolutionary history, probably the result of consecutive demographic shifts due to glacial cycles. For instance, significantly negative Tajima's *D* values were found in all sampling stations and in the whole data set (Table 2), indicating a deviation in the haplotype frequencies from the neutrality model (Tajima, 1989). These results support the existence of a recent and rapid demographic expansion of *D. antarctica* in the WAP and the South Shetlands, which could have started after the last glacial–interglacial alternation (~20,000–10,000 years ago) when the last Antarctic shelf recolonization took place (see Allcock & Strugnell, 2012). This hypothesis has been suggested for other shallow-water Antarctic invertebrates (Díaz, Féral, Féral, David, Saucède, & Poulin, 2011; González-Wevar et al., 2011; Leiva, Riesgo, Riesgo, Avila, Rouse, & Taboada, 2018; Thornhill, Mahon, Norenburg, & Halanych, 2008), which could have migrated northwards to sub-Antarctic islands during glacial periods and recolonized the Antarctic shelf during interglacial periods. This expansion–contraction model has already been tested for the Antarctic limpet *Nacella concinna* (Strebel, 1908), demonstrating its glacial survival in the sub-Antarctic South Georgia Island, followed

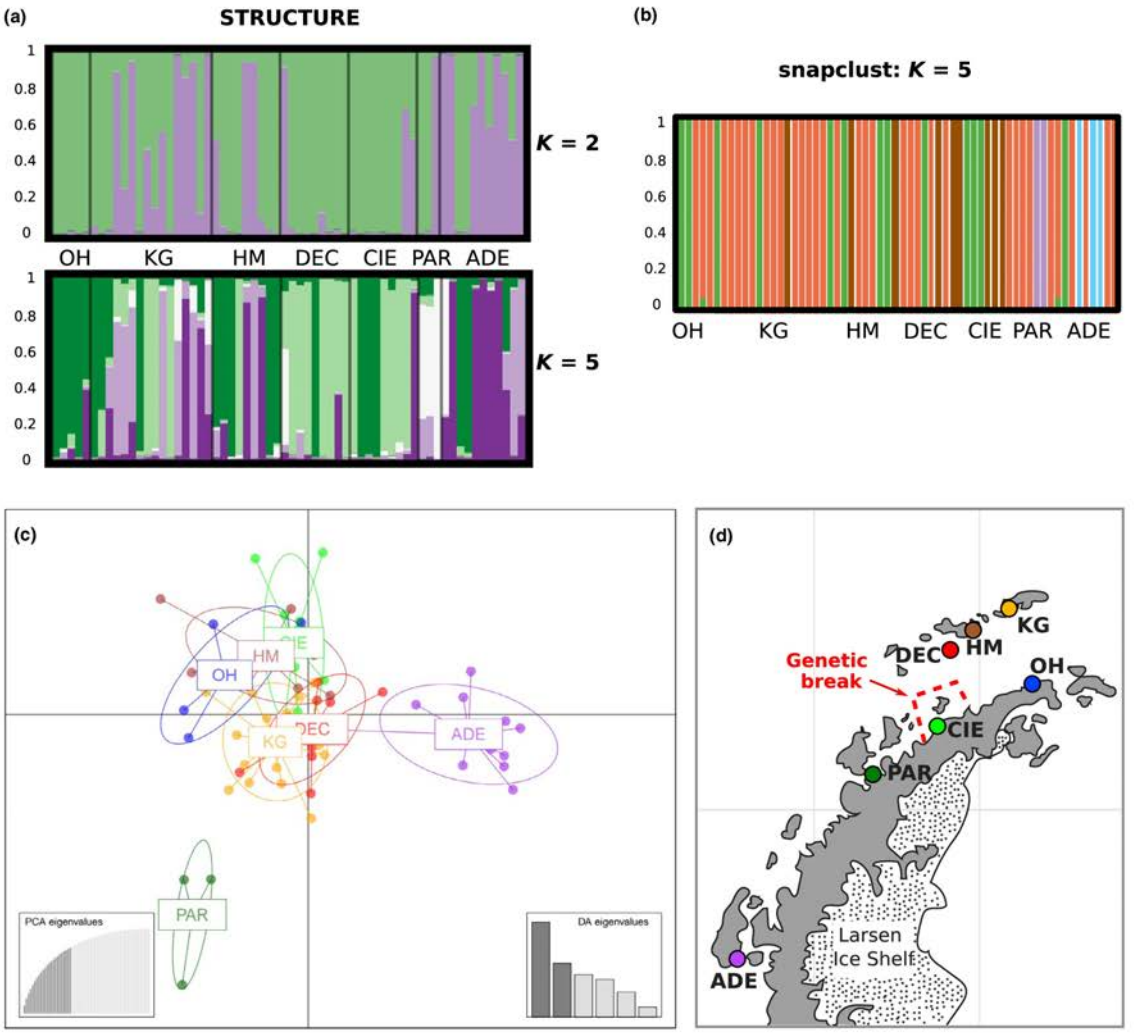

FIGURE 5 Genetic structure results based on the 140 outlier SNPs under positive selection. (a) STRUCTURE results with $K = 2$ and $K = 5$, the first and second most probable number of clusters, respectively (see delta K plot in Appendix S4), (b) *snapclust* results with $K = 5$ (see AIC plot in Appendix S4), and (c) DAPC results: two-dimensional representation of the first (horizontal axis) and second (vertical axis) PCA eigenvalues. (d) Map of the study area with the genetic break from the BARRIER analysis shown as a red dashed line. See abbreviations in Figure 1

by post-glacial recolonization of the Antarctic Peninsula shelf (González-Wevar et al., 2013).

Taking expected heterozygosity (H_E) as a measure of genetic diversity, as originally defined (Nei, 1973), we found significantly lower genetic diversity values for *D. antarctica* (Table 2: $H_E = 0.162$ ranging from 0.054 to 0.142) than those reported for similar population genetic studies on sponges using microsatellite markers (average H_E ranging from 0.4 to 0.8; see Pérez-Portela & Riesgo, 2018), and lower than the H_E values (from 0.24 to 0.323) reported in the only previously published study using SNPs in sponges (Brown et al., 2017). In other examples using SNPs in different animal phyla, H_E ranged from 0.298 to 0.312 in the salmon louse *Lepeophtheirus salmonis* (Jacobs et al., 2018), from 0.211 to 0.214 in the Galapagos shark *Carcharhinus galapagensis* (Pazmiño, Maes, Maes, Simpfendorfer, Salinas-de-León, & Herwerden, 2017), or from 0.128 to 0.276 in the sea anemone *Nematostella vectensis* (Reitzel, Herrera, Herrera, Layden, Martindale, & Shank, 2013), thus corroborating our low values for *D. antarctica*. The extremely low genetic diversity of *D. antarctica* could be related to the particular evolutionary history of the shallow-water Antarctic benthic fauna, a consequence of the bottleneck events affecting benthic species during glacial periods. These demographic events dramatically reduce genetic diversity after

population decimations, as has already been reported for other shallow-water Antarctic fauna (see Allcock & Strugnell, 2012).

Our results revealed high admixture and lack of population differentiation, supported by the low global F_{ST} of 0.011 and the nonsignificant pairwise F_{ST} values (Table 3), suggesting high connectivity and dispersal capability of *D. antarctica* throughout the sampling area, which covered most of the species distribution. We propose that this could be due to the relatively long planktonic life of *D. antarctica* larvae as a result of the great amount of proteinaceous yolk that they contain (Koutsouveli et al., 2018) in comparison with sponge larvae from congeneric species from lower latitudes (e.g., Ereskovsky & Tokina, 2004). Furthermore, the strong oceanic currents in the study area (Moffat, Beardsley, Owens, & Van Lipzig, 2008; Zhou, Niiler, & Hu, 2002; see Figure 1b) may increase the dispersal ability of *D. antarctica* larvae. Remarkably, our results differ from most previous population genetic studies on sponges, which generally report highly structured and differentiated populations, even at local and regional scales (e.g., Brown et al., 2017; DeBiasse et al., 2010; Pérez-Portela, Noyer, & Becerro, 2015; Riesgo et al., 2016). Even compared to some oviparous sponges such as *Cliona delitrix* which appears to disperse along the ~315 km of the Florida reef track (Chaves-Fonnegra, Feldheim, Secord, & Lopez, 2015), our results suggested an unprecedent ~900 km contemporary migration. However, although this long-distance connectivity is unusual in sponges, it is common in other Antarctic marine invertebrates. Examples of high gene flow are shown in many Antarctic species, such as the brittle stars *A. agassizii* (Galaska et al., 2017a) and *Ophionotus victoriae* (Galaska et al., 2017b), the Antarctic limpet *N. concinna* (González-Wevar et al., 2013), the nemertean *Parborlasia corrugatus* (Thornhill et al., 2008) and the annelid *Pterocirrus giribeti* (Leiva et al., 2018).

In agreement with STRUCTURE and *snapclust* results, relatively high gene flow was detected in our contemporary migration network between the South Shetlands and Adelaide Island (Figure 3). We propose that these high migration values are a consequence of the Antarctic Peninsula Coastal Current (APCC) running southwards off the WAP (Moffat et al., 2008; Figure 1b) and the ACC running northwards, connecting stations ~900 km apart. Other high migration values were found within the South Shetlands Archipelago, and from O'Higgins Bay to King George Island (Figure 3). This result could be explained by different factors that may be occasionally weakening the Peninsula Front, an oceanic front produced by the intrusion of a tongue of water from the Weddell Sea in the Bransfield Strait (Sangrà et al., 2011; Figure 1b). For instance, its seasonality is not completely understood yet, due to the sampling season solely extending during austral summer (Huneke, Huhn, & Schröeder, 2016; Sangrà et al., 2011; Zhou, Niiler, Zhu, & Dorland, 2006). Also, the interfrontal anticyclonic eddy system found between the Peninsula Front and the Bransfield Current (Sangrà et al., 2011) could be potentially interfering with the impermeability of the Peninsula Front. Moreover, the Southern Annular Mode (SAM) and El Niño Southern Oscillation (ENSO) have been found to play a role in the water masses distribution of the Bransfield Strait (Dotto, Kerr, Mata, & Garcia, 2016; Barlett, Tosonotto, Tosonotto, Piola, Sierra, & Mata, 2018, respectively), which may cause interannual variation of the Peninsula Front. Interestingly, our contemporary migration network also showed that the most disconnected region in our study area was the centre of the WAP, where both Cierva Cove and Paradise Bay sampling sites are located (Figure 3). The oceanic features of our study area could also be behind the isolation of this region, which is disconnected from other areas by the Peninsula Front in the north and by the APCC in the west, running through the western side of the Palmer Archipelago (Moffat et al., 2008; Figure 1b).

Despite the lack of strong population structure, DAPC detected slight patterns of population differentiation between O'Higgins Bay, Adelaide Island and the remaining sampling stations. This differentiation could be driven by the contemporary oceanographic features in the study area, with Adelaide Island as the southernmost sampling site and O'Higgins Bay representing the area at the tip of the WAP isolated by the Peninsula Front. Accordingly, the main genetic break we detected partially coincided with the Peninsula Front, but grouping King George Island together with O'Higgins Bay (Figure 2d), which is in agreement with the high migration flow from O'Higgins Bay to King George Island discussed above. A similar genetic break coincident with the Peninsula Front has already been identified for the brittle star *O. victoriae* using SNPs (Galaska et al., 2017a), and also for the intertidal phyllodocid *P. giribeti* using a fragment of the mitochondrial *COI* marker (Leiva et al., 2018). In addition, different reproductive timing due to, for instance, the effects of north–south differences in sea-ice retreat (Stammerjohn, Martinson, Smith, & Iannuzzi, 2008) could also play a role in population substructure with distinct breeding groups (Sugg, Chesser, Dobson, & Hoogland, 1996).

However, both DAPC and BARRIER groupings appeared as a nonsignificant part of the total genetic variation in the AMOVAs (Table 4a). This may be due to the high admixture and migration detected in the neutral data set (Figures 2a,b and 3), and hence we suggest that both groupings should be understood as permeable barriers.

4.3 | Signals of divergent adaptive selection

In our SNP data set we identified 140 outlier SNPs as candidates for positive selection. Based on this data set, we recovered a high F_{ST}-statistic value of 0.205, along with high and significant pairwise F_{ST} values (Table 3, below diagonal), revealing geographically divergent adaptive selection. In species with high levels of population connectivity, such as *D. antarctica* here, local adaptation requires high levels of divergent selection. This has already been reported for other marine invertebrates with planktonic larvae, such as the marine snail *Chlorostoma funebralis* (Gleason & Burton, 2016) and the red abalone *Haliotis rufescens* (De Wit & Palumbi, 2013), both from the Pacific coast of California in the USA. Other examples from fish with a similar pattern are the Atlantic cod *Gadus morhua* (Barth et al., 2017) and the Atlantic herring *Clupea harengus* (Limborg et al., 2012). These results are particularly relevant for the Southern Ocean, as they challenge the classic consideration of Antarctic organisms as stable and homogeneous along their distributions.

The STRUCTURE and *snapclust* results from the 140 SNPs under positive selection also showed the effects of the admixture and high migration discussed above in the neutral data set (Figure 5a,b). However, we observed two unique genetic clusters at the central and southern WAP (Paradise Bay and Adelaide Island), one of them appearing at both stations (purple individuals in Figure 5b) and the other one exclusively present at Adelaide Island (blue individuals in Figure 5b). In agreement, the DAPC analysis clustered together all the stations from the Bransfield Strait area, separating Adelaide Island (as the most divergent sampling station) and Paradise Bay (Figure 5c). The significant 6.72% of the variance explained by this DAPC grouping (Table 4b) suggests different selective pressures in the central–southern WAP (Adelaide Island and Paradise Bay) and in the Bransfield Strait area (remaining sampling stations).

In this scenario with divergent selective pressures promoting local adaptation, we identified the function of the genes with signatures of selection, with some of them related to the organization of the cytoskeleton (Figure 4). Two of these genes, *dynein heavy chain 3* (*DNAH3*) and *cilia and flagella associated protein 54* (*CFAP54*), are involved in the assembly, function, motility and power stroke of flagella and cilia (Asai & Koonce, 2001; Carter, 2013; McKenzie et al., 2015). As with most other sponges, *D. antarctica* is a filter-feeding sponge that relies on flagellar beating to modulate the inflow current for particle feeding, and therefore we suggest that the selection signatures in the previously mentioned genes might be related to divergent filtering abilities between the Bransfield Strait area and the central and southern WAP. Furthermore, in general terms, cytoskeletal elements are involved in the regulation of many cellular functions related to immune response, such as cell migration, antigen recognition and phagocytosis (Vicente-Manzanares & Sánchez-Madrid, 2004). The gene *actin-binding protein IPP-like* (*IPP*) plays a role in organizing the actin cytoskeleton (Ciobanasu, Faivre, & Le Clainche, 2013), which is essential for immune responses (Wickramarachchi, Theofilopoulos, & Kono, 2010). In addition, heavy chain dyneins such as *DNAH3* have also been reported to aid in the formation of stress granules (SGs) (Kwon, Zhang, & Matthias, 2007; Loschi, Leishman, Berardone, & Boccaccio, 2009). SGs are cytosolic aggregations consisting of RNAs and RNA-binding proteins which appear in response to different stressors, with important function in preserving mRNA and regulating its translation during stress responses (Kedersha & Anderson, 2002). In addition, SGs also prevent apoptosis (e.g., Buchan & Parker, 2009), contain antioxidant machinery (Takahashi et al., 2013), and are involved in cellular recovery after stress exposure (Kedersha et al., 2002). Gleason and Burton (2016) found a *heavy chain dynein* under positive selection in the marine snail *C. funebralis*, relating the selective pressure in this locus to the formation of SGs and their function during thermal stress.

Furthermore, four other genes with functions related to apoptosis appeared under positive selection throughout our sampling area (Figure 4). Apoptosis is a conserved mechanism that occurs during antibacterial responses in sponges (Wiens et al., 2006). Da Fonseca, Kosiol, Kosiol, Vinař, Siepel, and Nielsen (2010) reviewed previous studies on selective pressure in apoptosis-related genes, concluding that positive selection in apoptotic genes is caused by their immune function. Indeed, some of the other genes under positive selection in our data set were related to ubiquitination (Figure 4), a function also related to the immune system, as it regulates the pattern-recognition receptor signalling that mediates immune responses (Hu & Sun, 2016). Moreover, ubiquitination has been related to local adaptation in corals, where it responds to different environmental factors that cause stress (Bay & Palumbi, 2014; Jin et al., 2016; van Oppen et al., 2018). This is due to its role in removing macromolecular debris such as reactive oxygen species (ROS) generated by cellular stress (Kültz, 2003). Interestingly, *dimethylaniline monooxigenase 5* (*FMO5*), the enzyme resulting from one of the genes under positive selection retrieved here for *D. antarctica*, catalyses the oxygenation of *N*,*N*-dimethylanilines, a reaction present in the ROS biological detoxification pathway (Jakoby, Bend, & Caldwell, 2012). Furthermore, *CD163*, which also appeared to be under positive selection here, is associated with the immune system and the response to environmental stressors as well (Figure 4; Burkard et al., 2017; Fabriek et al., 2009). Finally, two RNA post-transcriptional modification genes were identified as under positive selection (Figure 4). This mechanism aids gene regulation under various cellular stress situations (e.g., Anderson & Kedersha, 2009; Chinnusamy, Zhu, & Zhu, 2007; Filipowicz, Bhattacharyya, & Sonenberg, 2008; Floris, Mahgoub, Mahgoub, Lanet, Robaglia, & Menand, 2009).

The signatures of selection in stress and immune responses that we detected are mostly related to the molecular toolkit that sponges, which are generally filter-feeders, use to discriminate between, and react to, food, pathogens and symbionts in the seawater that they filter and that runs through their bodies (Pita, Hoeppner, Ribes, & Hentschel, 2018). Hence, different microbiome complements in the seawater in different areas would elicit divergent adaptive strategies in sponges in the particular genes that we detected here as under positive selection. Interestingly, differences in sea-ice duration in the Antarctic Peninsula's shallow waters usually translate into highly divergent seawater microbiota, both in composition and in abundance (Ducklow et al., 2013; Vernet et al., 2008). While total sea-ice duration in the vicinity of Adelaide Island is around 250 days a year, with a summer sea-ice retreat, total sea-ice duration is below 150 days in the other sampling stations, generally with spring retreats (Stammerjohn et al., 2008). This difference in sea-ice duration is key to maintaining vastly different planktonic communities between the southern WAP and the Bransfield Strait area, because the presence and magnitude of phytoplankton blooms in the Southern Ocean are regulated by the timing of sea-ice retreat (Ducklow et al., 2013; Luria, Ducklow, & Amaral-Zettler, 2014; Vernet et al., 2008). Generally, the later the sea-ice retreats, the higher the phytoplankton productivity, as a consequence of sea-ice inhibition of the formation of a spring deep mixed layer, which in turn inhibits phytoplankton (Ducklow et al., 2013). Furthermore, phytoplankton–bacteria trophic coupling has been demonstrated in the Antarctic Peninsula by the direct bacterial assimilation of recent photosynthetic products (Morán & Estrada, 2002; Morán, Gasol, Pedrós-Alió,

& Estrada, 2001) and by the bacterial dependence on dissolved organic matter, which in turn depends on phytoplankton (Ducklow et al., 2013). Apart from the effects on the planktonic communities, a later sea-ice retreat produces fresher and colder summer surface waters in the southern WAP, due to more recent or ongoing seasonal ice melting (Ducklow et al., 2013).

Thus, due to the ice–plankton interaction outlined above, phytoplankton and bacterial communities, as well as summer surface water temperature, differ widely between the southern WAP, and the Bransfield Strait area. Because sponges are able to feed on both diatoms and bacteria, the different composition of these communities across our study area could potentially drive local adaptation of *D. antarctica* populations, not only because of their relevant role in food availability, but also as potential agents of diseases and other stresses. Further studies will be directed to test whether this local adaptation hypothesis we suggest for *D. antarctica* is a general pattern also present in other benthic filter-feeding invertebrates sampled in the same studied area, or even whether microplankton composition generally drives the adaptation of sponges.

A comparison of normalized expression values for the 14 annotated genes under positive selection showed that most of the variation occurred between the sample from Deception Island and the other two samples (Table 5; Figure 4). This contrasts with the DAPC results of the neutral and under positive selection data sets (Figures 2c and 5c), and it is probably because of the physicochemical particularities of the waters of Deception Island, which is an active volcano with a submerged caldera (Port Foster) where our samples were collected. The waters of Port Foster are characterized by the presence of suspended volcaniclastic particles (Baldwin & Smith, 2003) and chemicals from local geothermal activity (Deheyn, Gendreau, Baldwin, & Latz, 2005; Elderfield, 1972). Moreover, the fumarolic emissions and geothermal springs spotting the sedimentary seafloor confer upon Port Foster unusually high bottom-water temperatures of 2–3°C (Ortiz et al., 1992). These features undoubtedly affect and stress benthic filter feeders such as *D. antarctica*, and may have contributed to the upregulation of genes related to different stresses. Proper differential gene expression analyses will be conducted to test whether particular physicochemical water features at Deception Island are determinant in shaping gene expression in a wide array of shallow-water invertebrates, thus testing their adaptation potential at the transcriptome level.

5 | CONCLUSIONS

Overall, the current gene flow scenario for *Dendrilla antarctica* is characterized by high migration and low population differentiation, with a subtle population substructure driven by the oceanic features of the region. Remarkably, despite this background of population admixture, we identified divergent selective pressures along the studied region that could be explained by the sea-ice–benthos coupling via planktonic communities. Local adaptation was long assumed to be erased when high population connectivity was present in marine organisms. However, recent investigations indicate that even though few larvae might suffice to maintain genetic homogeneity between populations, that is hardly possible for loci under selection (Sanford & Kelly, 2011). The implications of our results are therefore vast. Our relatively slight patterns of local adaptation are indicative of the potential for plastic physiological responses to environmental shifts. In addition, and in contrast to previous studies of shallow-water sponges, we report a well-connected network of populations across ~1,000 km. Our study therefore corroborates that populations that appear homogeneous for neutral loci may also exhibit local adaptation. In this sense, our study suggests a finely tuned physiological response to current conditions but high resilience to future changes for *D. antarctica* in the Antarctic Peninsula. However, due to larval reliance on oceanic currents to maintain high dispersal abilities, this exceptional gene flow might be threatened by changes that increasing sea temperature could create in Southern Ocean oceanographic circulation patterns, which are not completely understood yet (Meijers, 2014). Moreover, a general reduction of planktonic larval duration is expected for all larvae in the near future, because their metabolic, developmental and growth rates are determined by water temperature (O'Connor et al., 2007). Thus, a shorter larval stage could imply a reduction of the dispersal capabilities of *D. antarctica*, with implications for its gene flow and resilience, due to a putatively higher proportion of larvae dying before reaching a suitable settlement site, as has been proposed for fish larvae (Kendall, Poti, Poti, Wynne, Kinlan, & Bauer, 2013; O'Connor et al., 2007). Therefore, our results can be used as a baseline for future assessments of the effects of a changing Southern Ocean on the population connectivity and resilience of *D. antarctica*.

ACKNOWLEDGEMENTS

We are indebted to Patricia Álvarez-Campos, Oriol Sacristán, Javier Cristobo, Juan Junoy, Juan Moles, Carlos Angulo-Preckler, Blanca Figuerola and Conxita Avila for their help during sampling collection, and the Spanish Base 'Gabriel de Castilla' and 'BIO/Hésperides' crew for their logistical support. We also thank the Giribet Lab for all the help and support provided during library construction in the laboratory. Special thanks are given to Eugènia Almacellas for her support during manuscript writing and for her brilliant suggestions and ideas. We also thank four anonymous reviewers and the Editor for their valuable comments and suggestions. This work was supported by two DIF grants of The Natural History Museum, London (SDF14032 and SDR17012) to A.R., a Marie Sklodowska Curie grant (IF750937) to N.J.K., and a grant of the Spanish Ministry of Economy and Competitiveness in which A.R., S.T., G.G. and C. L. have been involved (DISTANTCOM: CTM2013-42667/ANT).

AUTHOR CONTRIBUTIONS

C.L., S.T., G.G. and A.R. conceived and designed the study; C.L. and G.G. conducted fieldwork and collected samples; C.L., S.T., D.C. and

N.J.K. conducted laboratory work; C.L., S.T., T.J., N.J.K. and A.R. performed statistical analyses and interpreted the results; C.L., S.T. and A.R. wrote the manuscript, and all authors edited various versions of the manuscript.

DATA ACCESSIBILITY

RAD-seq data for each individual sample are deposited in the NCBI SRA database, BioProject PRJNA531366, Biosamples SAMN11350306–SAMN11350367 (Leiva et al., 2019). Data of the three transcriptomes are deposited in the same BioProject under accession numbers SRR8886798, SRR8886808 and SRR8886813. Alignments of the 15 mitochondrial genes and vcf files of both the neutral data set and the SNPs under positive selection are found in Appendices S1–S3.

ORCID

Carlos Leiva https://orcid.org/0000-0003-4398-329X
Sergi Taboada https://orcid.org/0000-0003-1669-1152
David Combosch https://orcid.org/0000-0001-7004-7435
Thibaut Jombart https://orcid.org/0000-0003-2226-8692
Ana Riesgo https://orcid.org/0000-0002-7993-1523

REFERENCES

Allcock, A. L., & Strugnell, J. M. (2012). Southern Ocean diversity: New paradigms from molecular ecology. *Trends in Ecology and Evolution*, *27*, 520–528. https://doi.org/10.1016/j.tree.2012.05.009

Altschul, S. F., Madden, T. L., Schäffer, A. A., Zhang, J., Zhang, Z., Miller, W., & Lipman, D. J. (1997). Gapped BLAST and PSI-BLAST: A new generation of protein database search programs. *Nucleic Acids Research*, *25*, 3389–3402. https://doi.org/10.1093/nar/25.17.3389

Anderson, P., & Kedersha, N. (2009). RNA granules: Post-transcriptional and epigenetic modulators of gene expression. *Nature Reviews Molecular Cell Biology*, *10*, 430–436. https://doi.org/10.1038/nrm2694

Andrews, K. R., Good, J. M., Miller, M. R., Luikart, G., & Hohenlohe, P. A. (2016). Harnessing the power of RADseq for ecological and evolutionary genomics. *Nature Reviews Genetics*, *17*, 81. https://doi.org/10.1038/nrg.2015.28

Andrews, S. (2010). *FastQC: A quality control tool for high throughput sequence data*. Retrieved from http://www.bioinformatics.babraham.ac.uk/projects/fastqc

Antao, T., Lopes, A., Lopes, R. J., Beja-Pereira, A., & Luikart, G. (2008). LOSITAN: A workbench to detect molecular adaptation based on a F_{ST}-outlier method. *BMC Bioinformatics*, *9*, 323.

Araneda, C., Larraín, M. A., Hecht, B., & Narum, S. (2016). Adaptive genetic variation distinguishes Chilean blue mussels (*Mytilus chilensis*) from different marine environments. *Ecology and Evolution*, *6*, 3632–3644.

Asai, D. J., & Koonce, M. P. (2001). The dynein heavy chain: Structure, mechanics and evolution. *Trends in Cell Biology*, *11*, 196–202. https://doi.org/10.1016/S0962-8924(01)01970-5

Avise, J. C., Arnold, J., Ball, R. M., Bermingham, E., Lamb, T., Neigel, J. E., … Saunders, N. C. (1987). Intraspecific phylogeography: The mitochondrial DNA bridge between population genetics and systematics. *Annual Review of Ecology and Systematics*, *18*, 489–522. https://doi.org/10.1146/annurev.es.18.110187.002421

Baldwin, R. J., & Smith, K. L. Jr (2003). Temporal dynamics of particulate matter fluxes and sediment community response in Port Foster, Deception Island, Antarctica. *Deep Sea Research Part II: Topical Studies in Oceanography*, *50*, 1707–1725. https://doi.org/10.1016/S0967-0645(03)00089-4

Barlett, E. M. R., Tosonotto, G. V., Piola, A. R., Sierra, M. E., & Mata, M. M. (2018). On the temporal variability of intermediate and deep waters in the Western Basin of the Bransfield Strait. *Deep Sea Research Part II: Topical Studies in Oceanography*, *149*, 31–46. https://doi.org/10.1016/j.dsr2.2017.12.010

Barth, J. M. I., Berg, P. R., Jonsson, P. R., Bonanomi, S., Corell, H., Hemmer-Hansen, J., … André, C. (2017). Genome architecture enables local adaptation of Atlantic cod despite high connectivity. *Molecular Ecology*, *26*, 4452–4466. https://doi.org/10.1111/mec.14207

Bay, R. A., & Palumbi, S. R. (2014). Multilocus adaptation associated with heat resistance in reef-building corals. *Current Biology*, *24*, 2952–2956. https://doi.org/10.1016/j.cub.2014.10.044

Beaumont, M. A., & Nichols, R. A. (1996). Evaluating loci for use in the genetic analysis of population structure. *Proceedings of the Royal Society London B: Biological Sciences*, *263*, 1619–1626.

Beugin, M. P., Gayet, T., Pontier, D., Devillard, S., & Jombart, T. (2018). A fast likelihood solution to the genetic clustering problem. *Methods in Ecology and Evolution*, *9*, 1006–1016. https://doi.org/10.1111/2041-210X.12968

Blanquer, A., & Uriz, M. J. (2010). Population genetics at three spatial scales of a rare sponge living in fragmented habitats. *BMC Evolutionary Biology*, *10*, 13. https://doi.org/10.1186/1471-2148-10-13

Bolger, A. M., Lohse, M., & Usadel, B. (2014). Trimmomatic: A flexible trimmer for Illumina sequence data. *Bioinformatics*, *30*, 2114–2120. https://doi.org/10.1093/bioinformatics/btu170

Botsford, L. W., White, J. W., Coffroth, M.-A., Paris, C. B., Planes, S., Shearer, T. L., … Jones, G. P. (2009). Connectivity and resilience of coral reef metapopulations in marine protected areas: Matching empirical efforts to predictive needs. *Coral Reefs*, *28*, 327–337. https://doi.org/10.1007/s00338-009-0466-z

Brown, R. R., Davis, C. S., & Leys, S. P. (2017). Clones or clans: The genetic structure of a deep-sea sponge, *Aphrocallistes vastus*, in unique sponge reefs of British Columbia, Canada. *Molecular Ecology*, *26*, 1045–1059.

Brown, W. M., George, M., & Wilson, A. C. (1979). Rapid evolution of animal mitochondrial DNA. *Proceedings of the National Academy of Sciences of the United States of America*, *76*, 1967–1971. https://doi.org/10.1073/pnas.76.4.1967

Buchan, J. R., & Parker, R. (2009). Eukaryotic stress granules: The ins and outs of translation. *Molecular Cell*, *36*, 932–941. https://doi.org/10.1016/j.molcel.2009.11.020

Burkard, C., Lillico, S. G., Reid, E., Jackson, B., Mileham, A. J., Ait-Ali, T., … Archibald, A. L. (2017). Precision engineering for PRRSV resistance in pigs: Macrophages from genome edited pigs lacking CD163 SRCR23 domain are fully resistant to both PRRSV genotypes while maintaining biological function. *PLoS Path*, *13*, e1006206. https://doi.org/10.1371/journal.ppat.1006206

Calderón, I., Ortega, N., Duran, S., Becerro, M., Pascual, M., & Turon, X. (2007). Finding the relevant scale: Clonality and genetic structure in a marine invertebrate (*Crambe crambe*, Porifera). *Molecular Ecology*, *16*, 1799–1810. https://doi.org/10.1111/j.1365-294X.2007.03276.x

Carella, M., Agell, G., & Uriz, M. J. (2019). Asexual reproduction and heterozygote selection in an Antarctic demosponge (*Stylocordyla chupachus*, Suberitida). *Polar Biology*, *42*(3), 475–483.

Carter, A. P. (2013). Crystal clear insights into how the dynein motor moves. *Journal of Cell Science*, *126*(3), 705–713. https://doi.org/10.1242/jcs.120725

Catchen, J. M., Hohenlohe, P. A., Bassham, S., Amores, A., & Cresko, W. A. (2013). Stacks: An analysis tool set for population genomics. *Molecular Ecology*, *22*, 3124–3140. https://doi.org/10.1111/mec.12354

Catchen, J. M., Hohenlohe, P. A., Bernatchez, L., Funk, W. C., Andrews, K. R., & Allendorf, F. W. (2017). Unbroken: RADseq remains a powerful tool for understanding the genetics of adaptation in natural populations. *Molecular Ecology Resources*, *17*, 362–365. https://doi.org/10.1111/1755-0998.12669

Chaves-Fonnegra, A., Feldheim, K. A., Secord, J., & Lopez, J. V. (2015). Population structure and dispersal of the coral-excavating sponge *Cliona delitrix*. *Molecular Ecology*, *24*, 1447–1466.

Chinnusamy, V., Zhu, J., & Zhu, J. K. (2007). Cold stress regulation of gene expression in plants. *Trends in Plant Science*, *12*, 444–451. https://doi.org/10.1016/j.tplants.2007.07.002

Ciobanasu, C., Faivre, B., & Le Clainche, C. (2013). Integrating actin dynamics, mechanotransduction and integrin activation: The multiple functions of actin binding proteins in focal adhesions. *European Journal of Cell Biology*, *92*, 339–348. https://doi.org/10.1016/j.ejcb.2013.10.009

Collins, E. E., Galaska, M. P., Halanych, K. M., & Mahon, A. R. (2018). Population genomics of *Nymphon australe* Hodgson, 1902 (Pycnogonida, Nymphonidae) in the Western Antarctic. *The Biological Bulletin*, *234*, 190–191.

Combosch, D. J., Lemer, S., Ward, P. D., Landman, N. H., & Giribet, G. (2017). Genomic signatures of evolution in Nautilus—An endangered living fossil. *Molecular Ecology*, *26*, 5923–5938.

Cook, A. J., Fox, A. J., Vaughan, D. G., & Ferrigno, J. G. (2005). Retreating glacier fronts on the Antarctic Peninsula over the past half-century. *Science*, *308*, 541–544. https://doi.org/10.1126/science.1104235

Da Fonseca, R. R., Kosiol, C., Vinař, T., Siepel, A., & Nielsen, R. (2010). Positive selection on apoptosis related genes. *FEBS Letters*, *584*, 469–476. https://doi.org/10.1016/j.febslet.2009.12.022

Dailianis, T., Tsigenopoulos, C. S., Dounas, C., & Voultsiadou, E. (2011). Genetic diversity of the imperilled bath sponge *Spongia officinalis* Linnaeus, 1759 across the Mediterranean Sea: Patterns of population differentiation and implications for taxonomy and conservation. *Molecular Ecology*, *20*, 3757–3772. https://doi.org/10.1111/j.1365-294X.2011.05222.x

Dayton, P. K. (1989). Interdecadal variation in an Antarctic sponge and its predators from oceanographic climate shifts. *Science*, *245*, 1484–1486. https://doi.org/10.1126/science.245.4925.1484

De Mita, S., Thuillet, A. C., Gay, L., Ahmadi, N., Manel, S., Ronfort, J., & Vigouroux, Y. (2013). Detecting selection along environmental gradients: Analysis of eight methods and their effectiveness for outbreeding and selfing populations. *Molecular Ecology*, *22*, 1383–1399. https://doi.org/10.1111/mec.12182

De Wit, P., & Palumbi, S. R. (2013). Transcriptome-wide polymorphisms of red abalone (*Haliotis rufescens*) reveal patterns of gene flow and local adaptation. *Molecular Ecology*, *22*, 2884–2897.

Deagle, B. E., Faux, C., Kawaguchi, S., Meyer, B., & Jarman, S. N. (2015). Antarctic krill population genomics: Apparent panmixia, but genome complexity and large population size muddy the water. *Molecular Ecology*, *24*, 4943–4959. https://doi.org/10.1111/mec.13370

DeBiasse, M. B., Richards, V. P., & Shivji, M. S. (2010). Genetic assessment of connectivity in the common reef sponge, *Callyspongia vaginalis* (Demospongiae: Haplosclerida) reveals high population structure along the Florida reef tract. *Coral Reefs*, *29*, 47–55. https://doi.org/10.1007/s00338-009-0554-0

Deheyn, D. D., Gendreau, P., Baldwin, R. J., & Latz, M. I. (2005). Evidence for enhanced bioavailability of trace elements in the marine ecosystem of Deception Island, a volcano in Antarctica. *Marine Environmental Research*, *60*, 1–33. https://doi.org/10.1016/j.marenvres.2004.08.001

Díaz, A., Féral, J. P., David, B., Saucède, T., & Poulin, E. (2011). Evolutionary pathways among shallow and deep-sea echinoids of the genus *Sterechinus* in the Southern Ocean. *Deep Sea Research Part II: Topical Studies in Oceanography*, *58*, 205–211. https://doi.org/10.1016/j.dsr2.2010.10.012

Dotto, T. S., Kerr, R., Mata, M. M., & Garcia, C. A. (2016). Multidecadal freshening and lightening in the deep waters of the Bransfield Strait, Antarctica. *Journal of Geophysical Research: Oceans*, *121*, 3741–3756. https://doi.org/10.1002/2015JC011228

Downey, R. V., Griffiths, H. J., Linse, K., & Janussen, D. (2012). Diversity and distribution patterns in high southern latitude sponges. *PLoS ONE*, *7*, e41672. https://doi.org/10.1371/journal.pone.0041672

Dray, S., & Dufour, A. B. (2007). The ade4 package: Implementing the duality diagram for ecologists. *Journal of Statistical Software*, *22*, 1–20.

Ducklow, H., Fraser, W., Meredith, M., Stammerjohn, S., Doney, S., Martinson, D., … Amsler, C. (2013). West Antarctic Peninsula: An ice-dependent coastal marine ecosystem in transition. *Oceanography*, *26*, 190–203. https://doi.org/10.5670/oceanog.2013.62

Duran, S., & Rützler, K. (2006). Ecological speciation in a Caribbean marine sponge. *Molecular Phylogenetics and Evolution*, *40*, 292–297. https://doi.org/10.1016/j.ympev.2006.02.018

Earl, D. A., & vonHoldt, B. M. (2012). STRUCTURE HARVESTER: A website and program for visualizing STRUCTURE output and implementing the Evanno method. *Conservation Genetics Resources*, *4*, 359–361. https://doi.org/10.1007/s12686-011-9548-7

Elderfield, H. (1972). Effects of volcanism on water chemistry, Deception Island, Antarctica. *Marine Geology*, *13*, M1–M6. https://doi.org/10.1016/0025-3227(72)90066-7

Ereskovsky, A. V., & Tokina, D. B. (2004). Morphology and fine structure of the swimming larvae of *Ircinia oros* (Porifera, Demospongiae, Dictyoceratida). *Invertebrate Reproduction and Development*, *45*, 137–150.

Ernster, L., & Schatz, G. (1981). Mitochondria: A historical review. *Journal of Cell Biology*, *91*, 227s–255s. https://doi.org/10.1083/jcb.91.3.227s

Evanno, G., Regnaut, S., & Goudet, J. (2005). Detecting the number of clusters of individuals using the software STRUCTURE: A simulation study. *Molecular Ecology*, *14*, 2611–2620. https://doi.org/10.1111/j.1365-294X.2005.02553.x

Fabriek, B. O., van Bruggen, R., Deng, D. M., Ligtenberg, A. J. M., Nazmi, K., Schornagel, K., … van den Berg, T. K. (2009). The macrophage scavenger receptor CD163 functions as an innate immune sensor for bacteria. *Blood*, *113*, 887–892. https://doi.org/10.1182/blood-2008-07-167064

Ferchaud, A. L., & Hansen, M. M. (2016). The impact of selection, gene flow and demographic history on heterogeneous genomic divergence: Three-spine sticklebacks in divergent environments. *Molecular Ecology*, *25*, 238–259. https://doi.org/10.1111/mec.13399

Filipowicz, W., Bhattacharyya, S. N., & Sonenberg, N. (2008). Mechanisms of post-transcriptional regulation by microRNAs: Are the answers in sight? *Nature Reviews Genetics*, *9*, 102. https://doi.org/10.1038/nrg2290

Floris, M., Mahgoub, H., Lanet, E., Robaglia, C., & Menand, B. (2009). Post-transcriptional regulation of gene expression in plants during abiotic stress. *International Journal of Molecular Sciences*, *10*, 3168–3185. https://doi.org/10.3390/ijms10073168

Foll, M., & Gaggiotti, O. (2008). A genome-scan method to identify selected loci appropriate for both dominant and codominant markers: A Bayesian perspective. *Genetics*, *180*, 977–993. https://doi.org/10.1534/genetics.108.092221

Galaska, M. P., Sands, C. J., Santos, S. R., Mahon, A. R., & Halanych, K. M. (2017a). Geographic structure in the Southern Ocean circumpolar brittle star *Ophionotus victoriae* (Ophiuridae) revealed from mtDNA and single-nucleotide polymorphism data. *Ecology and Evolution*, *7*, 475–485.

Galaska, M. P., Sands, C. J., Santos, S. R., Mahon, A. R., & Halanych, K. M. (2017b). Crossing the divide: Admixture across the Antarctic polar front revealed by the brittle star *Astrotoma agassizii*. *The Biological Bulletin*, *232*, 198–211.

Giles, E. C., Saenz-Agudelo, P., Hussey, N. E., Ravasi, T., & Berumen, M. L. (2015). Exploring seascape genetics and kinship in the reef sponge *Stylissa carteri* in the Red Sea. *Ecology and Evolution*, *5*, 2487–2502.

Gleason, L. U., & Burton, R. S. (2016). Genomic evidence for ecological divergence against a background of population homogeneity in the marine snail *Chlorostoma funebralis*. *Molecular Ecology*, *25*, 3557–3573.

González-Wevar, C. A., David, B., & Poulin, E. (2011). Phylogeography and demographic inference in *Nacella* (Patinigera) concinna (Strebel, 1908) in the western Antarctic Peninsula. *Deep Sea Research Part II: Topical Studies in Oceanography*, *58*, 220–229. https://doi.org/10.1016/j.dsr2.2010.05.026

González-Wevar, C. A., Saucède, T., Morley, S. A., Chown, S. L., & Poulin, E. (2013). Extinction and recolonization of maritime Antarctica in the limpet *Nacella concinna* (Strebel, 1908) during the last glacial cycle: Toward a model of Quaternary biogeography in shallow Antarctic invertebrates. *Molecular Ecology*, *22*, 5221–5236.

Goudet, J. (2005). hierfstat, a package for R to compute and test hierarchical F-statistics. *Molecular Ecology Notes*, *5*, 184–186. https://doi.org/10.1111/j.1471-8286.2004.00828.x

Grabherr, M. G., Haas, B. J., Yassour, M., Levin, J. Z., Thompson, D. A., Amit, I., … Regev, A. (2011). Full-length transcriptome assembly from RNA-Seq data without a reference genome. *Nature Biotechnology*, *29*, 644. https://doi.org/10.1038/nbt.1883

Halanych, K. M., & Mahon, A. R. (2018). Challenging dogma concerning biogeographic patterns of Antarctica and the Southern Ocean. *Annual Review of Ecology, Evolution, and Systematics*, *49*, 355–378. https://doi.org/10.1146/annurev-ecolsys-121415-032139

Hu, H., & Sun, S. C. (2016). Ubiquitin signaling in immune responses. *Cell Research*, *26*, 457. https://doi.org/10.1038/cr.2016.40

Huang, D., Meier, R., Todd, P. A., & Chou, L. M. (2008). Slow mitochondrial COI sequence evolution at the base of the metazoan tree and its implications for DNA barcoding. *Journal of Molecular Evolution*, *66*, 167–174. https://doi.org/10.1007/s00239-008-9069-5

Huang, D. W., Sherman, B. T., & Lempicki, R. A. (2008a). Systematic and integrative analysis of large gene lists using DAVID bioinformatics resources. *Nature Protocols*, *4*, 44. https://doi.org/10.1038/nprot.2008.211

Huang, D. W., Sherman, B. T., & Lempicki, R. A. (2008b). Bioinformatics enrichment tools: Paths toward the comprehensive functional analysis of large gene lists. *Nucleic Acids Research*, *37*, 1–13. https://doi.org/10.1093/nar/gkn923

Huneke, W. G. C., Huhn, O., & Schröeder, M. (2016). Water masses in the Bransfield Strait and adjacent seas, austral summer 2013. *Polar Biology*, *39*, 789–798. https://doi.org/10.1007/s00300-016-1936-8

Intergovernmental Panel on Climate Change (IPCC) (2013). *Climate change 2013: The physical science basis. Working group I contribution to the IPCC 5th assessment report—Changes to the underlying scientific/technical assessment*. Geneva, Switzerland: IPCC.

Jacobs, A., De Noia, M., Praebel, K., Kanstad-Hanssen, Ø., Paterno, M., Jackson, D., … Llewellyn, M. S. (2018). Genetic fingerprinting of salmon louse (*Lepeophtheirus salmonis*) populations in the North-East Atlantic using a random forest classification approach. *Scientific Reports*, *8*, 1203. https://doi.org/10.1038/s41598-018-19323-z

Jakobsson, M., & Rosenberg, N. A. (2007). CLUMPP: A cluster matching and permutation program for dealing with label switching and multimodality in analysis of population structure. *Bioinformatics*, *23*, 1801–1806. https://doi.org/10.1093/bioinformatics/btm233

Jakoby, W. B., Bend, J. R., & Caldwell, J. (2012). *Metabolic basis of detoxification: Metabolism of functional groups*. New York, NY: Academic Press.

Janosik, A. M., Mahon, A. R., & Halanych, K. M. (2011). Evolutionary history of Southern Ocean *Odontaster* sea star species (Odontasteridae; Asteroidea). *Polar Biology*, *34*, 575–586. https://doi.org/10.1007/s00300-010-0916-7

Jeffries, D. L., Copp, G. H., Lawson Handley, L., Olsén, K. H., Sayer, C. D., & Hänfling, B. (2016). Comparing RAD seq and microsatellites to infer complex phylogeographic patterns, an empirical perspective in the Crucian carp, *Carassius carassius*, L. *Molecular Ecology*, *25*, 2997–3018.

Jin, Y. K., Lundgren, P., Lutz, A., Raina, J.-B., Howells, E. J., Paley, A. S., … van Oppen, M. J. H. (2016). Genetic markers for antioxidant capacity in a reef-building coral. *Science Advances*, *2*, e1500842. https://doi.org/10.1126/sciadv.1500842

Jombart, T. (2008). adegenet: A R package for the multivariate analysis of genetic markers. *Bioinformatics*, *24*, 1403–1405. https://doi.org/10.1093/bioinformatics/btn129

Jombart, T., & Ahmed, I. (2011). adegenet 1.3-1: New tools for the analysis of genome-wide SNP data. *Bioinformatics*, *27*, 3070–3071. https://doi.org/10.1093/bioinformatics/btr521

Jombart, T., Devillard, S., & Balloux, F. (2010). Discriminant analysis of principal components: A new method for the analysis of genetically structured populations. *BMC Genetics*, *11*, 94. https://doi.org/10.1186/1471-2156-11-94

Katoh, K., & Standley, D. M. (2013). MAFFT multiple sequence alignment software version 7: Improvements in performance and usability. *Molecular Biology and Evolution*, *30*, 772–780. https://doi.org/10.1093/molbev/mst010

Katoh, K., & Toh, H. (2008). Recent developments in the MAFFT multiple sequence alignment program. *Briefings in Bioinformatics*, *9*, 286–298. https://doi.org/10.1093/bib/bbn013

Kearse, M., Moir, R., Wilson, A., Stones-Havas, S., Cheung, M., Sturrock, S., … Drummond, A. (2012). Geneious Basic: An integrated and extendable desktop software platform for the organization and analysis of sequence data. *Bioinformatics*, *28*, 1647–1649. https://doi.org/10.1093/bioinformatics/bts199

Kedersha, N., & Anderson, P. (2002). Stress granules: Sites of mRNA triage that regulate mRNA stability and translatability. *Biochemical Society Transactions*, *30*, 963–969. https://doi.org/10.1042/bst0300963

Kedersha, N., Chen, S., Gilks, N., Li, W., Miller, I. J., Stahl, J., & Anderson, P. (2002). Evidence that ternary complex (eIF2-GTP-tRNAi Met)–deficient preinitiation complexes are core constituents of mammalian stress granules. *Molecular Biology of the Cell*, *13*, 195–210.

Keenan, K., McGinnity, P., Cross, T. F., Crozier, W. W., & Prodöhl, P. A. (2013). diveRsity: An R package for the estimation and exploration of population genetics parameters and their associated errors. *Methods in Ecology and Evolution*, *4*, 782–788.

Kendall, M. S., Poti, M., Wynne, T. T., Kinlan, B. P., & Bauer, L. B. (2013). Consequences of the life history traits of pelagic larvae on interisland connectivity during a changing climate. *Marine Ecology Progress Series*, *489*, 43–59. https://doi.org/10.3354/meps10432

King, J. C. (1994). Recent climate variability in the vicinity of the Antarctic Peninsula. *International Journal of Climatology*, *14*, 357–369. https://doi.org/10.1002/joc.3370140402

King, J. C., & Harangozo, S. A. (1998). Climate change in the western Antarctic Peninsula since 1945: Observations and possible causes. *Annals of Glaciology*, *27*, 571–575.

Koutsouveli, V., Taboada, S., Moles, J., Cristobo, J., Ríos, P., Bertran, A., … Riesgo, A. (2018). Insights into the reproduction of some Antarctic dendroceratid, poecilosclerid, and haplosclerid demosponges. *PLoS ONE*, *13*, e0192267. https://doi.org/10.1371/journal.pone.0192267

Krabbe, K., Leese, F., Mayer, C., Tollrian, R., & Held, C. (2010). Cryptic mitochondrial lineages in the widespread pycnogonid *Colossendeis megalonyx* Hoek, 1881 from Antarctic and Subantarctic waters. *Polar Biology*, *33*, 281–292. https://doi.org/10.1007/s00300-009-0703-5

Kültz, D. (2003). Evolution of the cellular stress proteome: From monophyletic origin to ubiquitous function. *Journal of Experimental Biology*, *206*, 3119–3124. https://doi.org/10.1242/jeb.00549

Kwon, S., Zhang, Y., & Matthias, P. (2007). The deacetylase HDAC6 is a novel critical component of stress granules involved in the stress

response. *Genes and Development*, *21*, 3381–3394. https://doi.org/10.1101/gad.461107

Leiva, C., Riesgo, A., Avila, C., Rouse, G. W., & Taboada, S. (2018). Population structure and phylogenetic relationships of a new shallow-water Antarctic phyllodocid annelid. *Zoologica Scripta*, *47*, 714–726. https://doi.org/10.1111/zsc.12313

Leiva, C., Taboada, S., Kenny, N. J., Combosch, D., Giribet, G., Jombart, T., & Riesgo, A. (2019). *Dendrilla antarctica* raw sequence reads. *NCBI SRA Database*, *PRJNA531366*.

León-Pech, M. G., Cruz-Barraza, J. A., Carballo, J. L., Calderon-Aguilera, L. E., & Rocha-Olivares, A. (2015). Pervasive genetic structure at different geographic scales in the coral-excavating sponge *Cliona vermifera* (Hancock, 1867) in the Mexican Pacific. *Coral Reefs*, *34*, 887–897. https://doi.org/10.1007/s00338-015-1316-9

Li, B., & Dewey, C. N. (2011). RSEM: Accurate transcript quantification from RNA-Seq data with or without a reference genome. *BMC Bioinformatics*, *12*, 323. https://doi.org/10.1186/1471-2105-12-323

Librado, P., & Rozas, J. (2009). DnaSP v5: A software for comprehensive analysis of DNA polymorphism data. *Bioinformatics*, *25*, 1451–1452. https://doi.org/10.1093/bioinformatics/btp187

Limborg, M. T., Helyar, S. J., De Bruyn, M., Taylor, M. I., Nielsen, E. E., Ogden, R. O. B., … Bekkevold, D. (2012). Environmental selection on transcriptome-derived SNPs in a high gene flow marine fish, the Atlantic herring (*Clupea harengus*). *Molecular Ecology*, *21*, 3686–3703.

López-Legentil, S., & Pawlik, J. R. (2009). Genetic structure of the Caribbean giant barrel sponge *Xestospongia muta* using the I3–M11 partition of COI. *Coral Reefs*, *28*, 157–165. https://doi.org/10.1007/s00338-008-0430-3

Loschi, M., Leishman, C. C., Berardone, N., & Boccaccio, G. L. (2009). Dynein and kinesin regulate stress-granule and P-body dynamics. *Journal of Cell Science*, *122*, 3973–3982. https://doi.org/10.1242/jcs.051383

Luria, C. M., Ducklow, H. W., & Amaral-Zettler, L. A. (2014). Marine bacterial, archaeal and eukaryotic diversity and community structure on the continental shelf of the western Antarctic Peninsula. *Aquatic Microbial Ecology*, *73*, 107–121. https://doi.org/10.3354/ame01703

Maldonado, M. (2006). The ecology of the sponge larva. *Canadian Journal of Zoology*, *84*, 175–194. https://doi.org/10.1139/z05-177

Manni, F., Guerard, E., & Heyer, E. (2004). Geographic patterns of (genetic, morphologic, linguistic) variation: How barriers can be detected by using Monmonier's algorithm. *Human Biology*, *76*, 173–190. https://doi.org/10.1353/hub.2004.0034

McKenzie, C. W., Craige, B., Kroeger, T. V., Finn, R., Wyatt, T. A., Sisson, J. H., … Lee, L. (2015). CFAP54 is required for proper ciliary motility and assembly of the central pair apparatus in mice. *Molecular Biology of the Cell*, *26*, 3140–3149. https://doi.org/10.1091/mbc.e15-02-0121

McKinney, G. J., Larson, W. A., Seeb, L. W., & Seeb, J. E. (2017). RAD seq provides unprecedented insights into molecular ecology and evolutionary genetics: Comment on Breaking RAD by Lowry et al. (2016). *Molecular Ecology Resources*, *17*, 356–361.

Meijers, A. J. S. (2014). The Southern Ocean in the coupled model intercomparison project phase 5. *Philosophical Transactions of the Royal Society A: Mathematical, Physical and Engineering Sciences*, *372*, 20130296.

Meredith, M. P., & King, J. C. (2005). Rapid climate change in the ocean west of the Antarctic Peninsula during the second half of the 20th century. *Geophysical Research Letters*, *32*, L19604. https://doi.org/10.1029/2005GL024042

Moffat, C., Beardsley, R. C., Owens, B., & Van Lipzig, N. (2008). A first description of the Antarctic Peninsula Coastal Current. *Deep Sea Research Part II: Topical Studies in Oceanography*, *55*, 277–293. https://doi.org/10.1016/j.dsr2.2007.10.003

Moles, J., Wägele, H., Cutignano, A., Fontana, A., Ballesteros, M., & Avila, C. (2017). Giant embryos and hatchlings of Antarctic nudibranchs (Mollusca: Gastropoda: Heterobranchia). *Marine Biology*, *164*, 114. https://doi.org/10.1007/s00227-017-3143-8

Morán, X. A. G., & Estrada, M. (2002). Phytoplanktonic DOC and POC production in the Bransfield and Gerlache Straits as derived from kinetic experiments of 14C incorporation. *Deep Sea Research Part II: Topical Studies in Oceanography*, *49*, 769–786. https://doi.org/10.1016/S0967-0645(01)00123-0

Morán, X. A. G., Gasol, J. M., Pedrós-Alió, C., & Estrada, M. (2001). Dissolved and particulate primary production and bacterial production in offshore Antarctic waters during austral summer: Coupled or uncoupled? *Marine Ecology Progress Series*, *222*, 25–39. https://doi.org/10.3354/meps222025

Narum, S. R., & Hess, J. E. (2011). Comparison of F_{ST} outlier tests for SNP loci under selection. *Molecular Ecology Resources*, *11*, 184–194.

Nei, M. (1973). Analysis of gene diversity in subdivided populations. *Proceedings of the National Academy of Sciences*, *70*(12), 3321–3323. https://doi.org/10.1073/pnas.70.12.3321

O'Connor, M. I., Bruno, J. F., Gaines, S. D., Halpern, B. S., Lester, S. E., Kinlan, B. P., & Weiss, J. M. (2007). Temperature control of larval dispersal and the implications for marine ecology, evolution, and conservation. *Proceedings of the National Academy of Sciences of the United States of America*, *104*, 1266–1271. https://doi.org/10.1073/pnas.0603422104

Ortiz, R., Vila, J., García, A., Camacho, A. G., Diez, J. L., Aparicio, A., & Petrinovic, I. (1992). Geophysical features of Deception Island. In Y. Yoshida et al. (Eds.), *Recent Progress in Antarctic Earth Science* (443–448). Tokio, Japan: Terra Sci.

Paradis, E. (2010). pegas: An R package for population genetics with an integrated–modular approach. *Bioinformatics*, *26*, 419–420. https://doi.org/10.1093/bioinformatics/btp696

Paradis, E., Claude, J., & Strimmer, K. (2004). APE: Analyses of phylogenetics and evolution in R language. *Bioinformatics*, *20*, 289–290. https://doi.org/10.1093/bioinformatics/btg412

Pascual, M., Rives, B., Schunter, C., & Macpherson, E. (2017). Impact of life history traits on gene flow: A multispecies systematic review across oceanographic barriers in the Mediterranean Sea. *PLoS ONE*, *12*, e0176419. https://doi.org/10.1371/journal.pone.0176419

Pazmiño, D. A., Maes, G. E., Simpfendorfer, C. A., Salinas-de-León, P., & van Herwerden, L. (2017). Genome-wide SNPs reveal low effective population size within confined management units of the highly vagile Galapagos shark (*Carcharhinus galapagensis*). *Conservation Genetics*, *18*, 1151–1163. https://doi.org/10.1007/s10592-017-0967-1

Peck, L. S., & Conway, L. Z. (2000). The myth of metabolic cold adaptation: Oxygen consumption in stenothermal Antarctic bivalves. *Geological Society, London, Special Publications*, *177*, 441–450. https://doi.org/10.1144/GSL.SP.2000.177.01.29

Peck, L. S., Webb, K. E., & Bailey, D. M. (2004). Extreme sensitivity of biological function to temperature in Antarctic marine species. *Functional Ecology*, *18*, 625–630. https://doi.org/10.1111/j.0269-8463.2004.00903.x

Pérez-Portela, R., Noyer, C., & Becerro, M. A. (2015). Genetic structure and diversity of the endangered bath sponge *Spongia lamella*. *Aquatic Conservation: Marine and Freshwater Ecosystems*, *25*, 365–379.

Pérez-Portela, R., & Riesgo, A. (2018). Population genomics of early-splitting lineages of metazoans. In Om P. Rajora (Ed.), *Population genomics* (pp. 1–35). Cham, Switzerland: Springer.

Peterson, B. K., Weber, J. N., Kay, E. H., Fisher, H. S., & Hoekstra, H. E. (2012). Double digest RADseq: An inexpensive method for de novo SNP discovery and genotyping in model and non-model species. *PLoS ONE*, *7*, e37135. https://doi.org/10.1371/journal.pone.0037135

Pita, L., Hoeppner, M. P., Ribes, M., & Hentschel, U. (2018). Differential expression of immune receptors in two marine sponges upon exposure to microbial-associated molecular patterns. *Scientific Reports*, *8*, 16081. https://doi.org/10.1038/s41598-018-34330-w

Plese, B., Rossi, M. E., Kenny, N., Taboada, S., Koutsouveli, V., & Riesgo, A. (2018). Trimitomics: An efficient pipeline for mitochondrial assembly from transcriptomic reads in non-model species. *bioRxiv*, *413138*.

Pritchard, J. K., Stephens, M., & Donnelly, P. (2000). Inference of population structure using multilocus genotype data. *Genetics*, *155*, 945–959.

R Core Team (2014). *A language and environment for statistical computing*. Vienna, Austria: R Foundation for Statistical Computing. Retrieved from http://www.R-project.org

Reitzel, A. M., Herrera, S., Layden, M. J., Martindale, M. Q., & Shank, T. M. (2013). Going where traditional markers have not gone before: Utility of and promise for RAD sequencing in marine invertebrate phylogeography and population genomics. *Molecular Ecology*, *22*, 2953–2970. https://doi.org/10.1111/mec.12228

Riesgo, A., Pérez-Portela, R., Pita, L., Blasco, G., Erwin, P. M., & López-Legentil, S. (2016). Population structure and connectivity in the Mediterranean sponge *Ircinia fasciculata* are affected by mass mortalities and hybridization. *Heredity*, *117*, 427. https://doi.org/10.1038/hdy.2016.41

Riesgo, A., Taboada, S., & Avila, C. (2015). Evolutionary patterns in Antarctic marine invertebrates: An update on molecular studies. *Marine Genomics*, *23*, 1–13. https://doi.org/10.1016/j.margen.2015.07.005

Rogers, A. D. (2007). Evolution and biodiversity of Antarctic organisms: A molecular perspective. *Philosophical Transactions of the Royal Society of London B: Biological Sciences*, *362*, 2191–2214.

Sanford, E., & Kelly, M. W. (2011). Local adaptation in marine invertebrates. *Annual Review of Marine Science*, *3*, 509–535. https://doi.org/10.1146/annurev-marine-120709-142756

Sangrà, P., Gordo, C., Hernández-Arencibia, M., Marrero-Díaz, A., Rodríguez-Santana, A., Stegner, A., … Pichon, T. (2011). The Bransfield current system. *Deep Sea Research Part I: Oceanographic Research Papers*, *58*, 390–402. https://doi.org/10.1016/j.dsr.2011.01.011

Sarà, M., Balduzzi, A., Barbieri, M., Bavestrello, G., & Burlando, B. (1992). Biogeographic traits and checklist of Antarctic demosponges. *Polar Biology*, *12*, 559–585. https://doi.org/10.1007/BF00236980

Setiawan, E., de Voogd, N. J., Swierts, T., Hooper, J. N., Wörheide, G., & Erpenbeck, D. (2016). MtDNA diversity of the Indonesian giant barrel sponge *Xestospongia testudinaria* (Porifera: Haplosclerida)–implications from partial cytochrome oxidase 1 sequences. *Journal of the Marine Biological Association of the United Kingdom*, *96*, 323–332.

Stammerjohn, S. E., Martinson, D. G., Smith, R. C., & Iannuzzi, R. A. (2008). Sea ice in the western Antarctic Peninsula region: Spatio-temporal variability from ecological and climate change perspectives. *Deep Sea Research Part II: Topical Studies in Oceanography*, *55*, 2041–2058.

Sugg, D. W., Chesser, R. K., Dobson, F. S., & Hoogland, J. L. (1996). Population genetics meets behavioral ecology. *Trends in Ecology and Evolution*, *11*, 338–342. https://doi.org/10.1016/0169-5347(96)20050-3

Taboada, S., Riesgo, A., Wiklund, H., Paterson, G. L. J., Koutsouveli, V., Santodomingo, N., … Glover, A. G. (2018). Implications of population connectivity studies for the design of marine protected areas in the deep sea: An example of a demosponge from the Clarion-Clipperton Zone. *Molecular Ecology*, *27*, 4657–4679. https://doi.org/10.1111/mec.14888

Tajima, F. (1989). Statistical method for testing the neutral mutation hypothesis by DNA polymorphism. *Genetics*, *123*, 585–595.

Takahashi, M., Higuchi, M., Matsuki, H., Yoshita, M., Ohsawa, T., Oie, M., & Fujii, M. (2013). Stress granules inhibit apoptosis by reducing reactive oxygen species production. *Molecular and Cellular Biology*, *33*, 815–829. https://doi.org/10.1128/MCB.00763-12

Thatje, S., Hillenbrand, C. D., & Larter, R. (2005). On the origin of Antarctic marine benthic community structure. *Trends in Ecology and Evolution*, *20*, 534–540. https://doi.org/10.1016/j.tree.2005.07.010

Thornhill, D. J., Mahon, A. R., Norenburg, J. L., & Halanych, K. M. (2008). Open-ocean barriers to dispersal: A test case with the Antarctic Polar Front and the ribbon worm *Parborlasia corrugatus* (Nemertea: Lineidae). *Molecular Ecology*, *17*, 5104–5117.

Tigano, A., Shultz, A. J., Edwards, S. V., Robertson, G. J., & Friesen, V. L. (2017). Outlier analyses to test for local adaptation to breeding grounds in a migratory arctic seabird. *Ecology and Evolution*, *7*, 2370–2381. https://doi.org/10.1002/ece3.2819

Turner, J., Colwell, S. R., Marshall, G. J., Lachlan-Cope, T. A., Carleton, A. M., Jones, P. D., … Iagovkina, S. (2005). Antarctic climate change during the last 50 years. *International Journal of Climatology*, *25*, 279–294. https://doi.org/10.1002/joc.1130

van Oppen, M. J., Bongaerts, P., Frade, P., Peplow, L. M., Boyd, S. E., Nim, H. T., & Bay, L. K. (2018). Adaptation to reef habitats through selection on the coral animal and its associated microbiome. *Molecular Ecology*, *27*, 2956–2971. https://doi.org/10.1111/mec.14763

Vaughan, D. G., Marshall, G. J., Connolley, W. M., Parkinson, C., Mulvaney, R., Hodgson, D. A., … Turner, J. (2003). Recent rapid regional climate warming on the Antarctic Peninsula. *Climatic Change*, *60*, 243–274.

Vernet, M., Martinson, D., Iannuzzi, R., Stammerjohn, S., Kozlowski, W., Sines, K., … Garibotti, I. (2008). Primary production within the sea-ice zone west of the Antarctic Peninsula: I—Sea ice, summer mixed layer, and irradiance. *Deep Sea Research Part II: Topical Studies in Oceanography*, *55*, 2068–2085.

Vicente-Manzanares, M., & Sánchez-Madrid, F. (2004). Role of the cytoskeleton during leukocyte responses. *Nature Reviews Immunology*, *4*, 110. https://doi.org/10.1038/nri1268

Wickramarachchi, D. C., Theofilopoulos, A. N., & Kono, D. H. (2010). Immune pathology associated with altered actin cytoskeleton regulation. *Autoimmunity*, *43*, 64–75. https://doi.org/10.3109/08916930903374634

Wiens, M., Korzhev, M., Perović-Ottstadt, S., Luthringer, B., Brandt, D., Klein, S., & Müller, W. E. (2006). Toll-like receptors are part of the innate immune defense system of sponges (Demospongiae: Porifera). *Molecular Biology and Evolution*, *24*, 792–804. https://doi.org/10.1093/molbev/msl208

Xavier, J. R., Rachello-Dolmen, P. G., Parra-Velandia, F., Schönberg, C. H. L., Breeuwer, J. A. J., & Van Soest, R. W. M. (2010). Molecular evidence of cryptic speciation in the "cosmopolitan" excavating sponge *Cliona celata* (Porifera, Clionaidae). *Molecular Phylogenetics and Evolution*, *56*, 13–20. https://doi.org/10.1016/j.ympev.2010.03.030

Zerbino, D., & Birney, E. (2008). Velvet: Algorithms for de novo short read assembly using de Bruijn graphs. *Genome Research*, *18*(5), 821–829. https://doi.org/10.1101/gr.074492.107

Zhou, M., Niiler, P. P., & Hu, J. H. (2002). Surface currents in the Bransfield and Gerlache straits, Antarctica. *Deep Sea Research Part I: Oceanographic Research Papers*, *49*, 267–280. https://doi.org/10.1016/S0967-0637(01)00062-0

Zhou, M., Niiler, P. P., Zhu, Y., & Dorland, R. D. (2006). The western boundary current in the Bransfield Strait, Antarctica. *Deep Sea Research Part I: Oceanographic Research Papers*, *53*, 1244–1252. https://doi.org/10.1016/j.dsr.2006.04.003

SUPPORTING INFORMATION

Additional supporting information may be found online in the Supporting Information section at the end of the article.

How to cite this article: Leiva C, Taboada S, Kenny NJ, et al. Population substructure and signals of divergent adaptive selection despite admixture in the sponge *Dendrilla antarctica* from shallow waters surrounding the Antarctic Peninsula. *Mol Ecol*. 2019;00:1–20. https://doi.org/10.1111/mec.15135

CHAPTER 3

Glacial phylogeographic history of the Antarctic *Antarctonemertes* (Nemertea, Hoplonemertea): reticulate evolution, introgression, and hybridisation

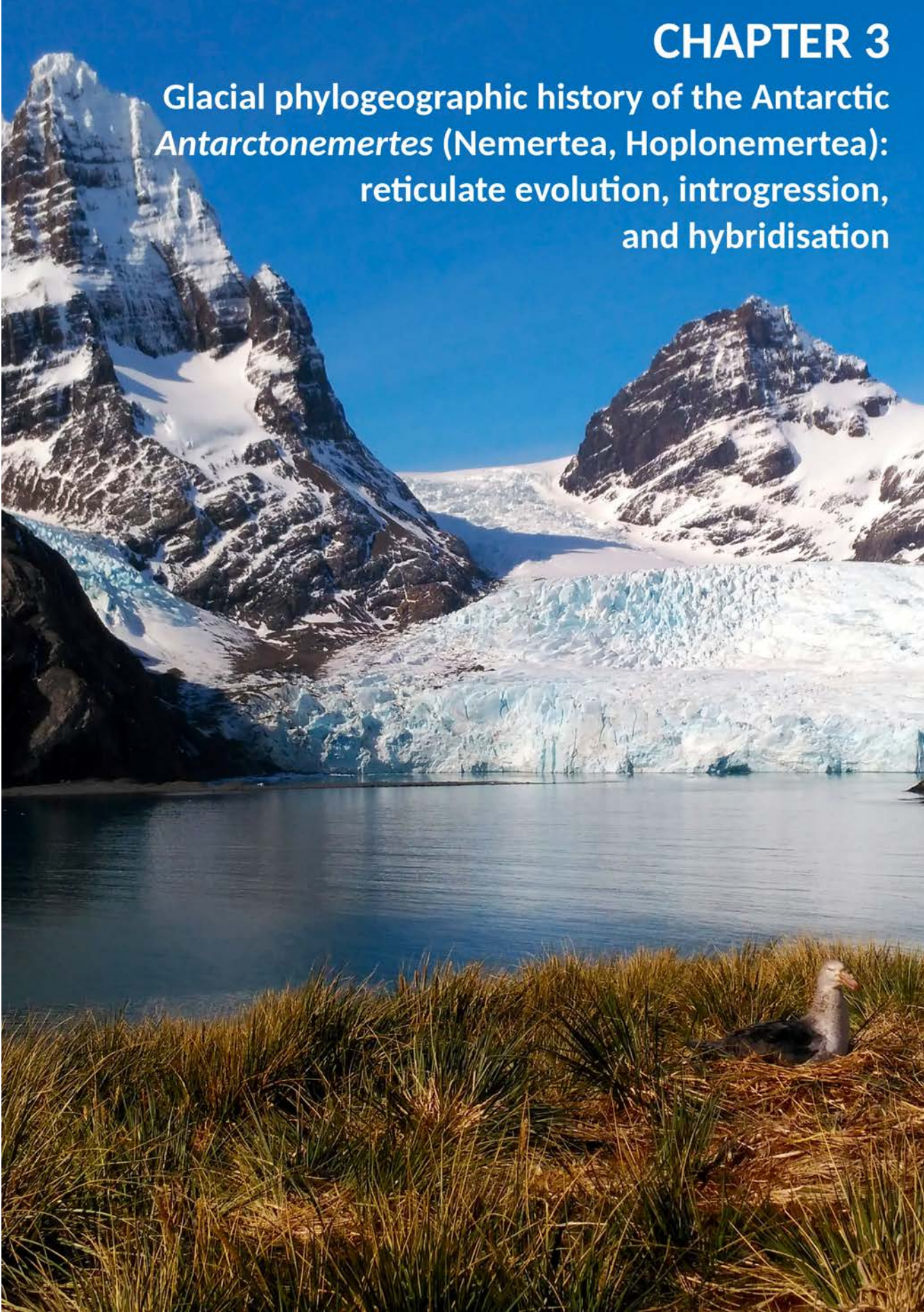

[1]Department of Life Sciences, The Natural History Museum of London, London, UK

[2]Department of Genetics, Microbiology and Statistics, Faculty of Biology, University of Barcelona, Barcelona, Spain

[3]Department of Biology (Zoology), Faculty of Science, Autonomous University of Madrid, Madrid, Spain

Glacial phylogeographic history of the Antarctic *Antarctonemertes* (Nemertea, Hoplonemertea): reticulate evolution, introgression, and hybridisation

Authors:

Carlos Leiva[1,2], Ana Riesgo[1], Sergi Taboada[1,3]

Abstract

Species boundaries and speciation events have intrigued biologists for centuries. Antarctic shallow waters are an exceptional scenario to study these processes, since its organisms present singular evolutionary histories characterised by cycles of contraction and fragmentation during glacial periods, followed by expansions and secondary contacts during interglacials. The hoplonemertean genus *Antarctonemertes* is an exemplary case to study speciation in Antarctica: it includes three common shallow-water Antarctic species, two of them occur in sympatry in West Antarctica (*A. valida* and *A. riesgoae*), and the third species (*A. unilineata*) is mainly present in East Antarctica. Here, we used a dataset of 542 organisms belonging to the three species, collected in the Western Antarctic Peninsula (WAP), the Subantarctic South Georgia Island (SG), and East Antarctica, to understand speciation patterns in the Southern Ocean. Using the *COI* mitochondrial marker (494 specimens), ddRADseq-derived SNPs (212 specimens), and *de novo* transcriptomes (9 specimens) we reconstructed the phylogeographic history of these three *Antarctonemertes* species and detected two past introgression events that left mito-nuclear discordances. Moreover, we discovered hybrids between *A. valida* and *A. riesgoae* at SG, indicating ongoing hybridisation between these two species, occurring exclusively in this Subantarctic island. Our results pointed to *A. valida* from WAP as the only lineage surviving the last glacial maximum in Antarctic shallow waters, undergoing adaptations in many genes with diverse functions, such as eye development and immune and stress responses. We also identified diverging loci involved in reproduction, suggesting the presence of prezygotic barriers to hybridisation, a signal of reinforcement events in agreement with the introgression detected. Overall, our study illustrates how the combination of sequencing techniques can resolve complex phylogeographic histories and unveil the molecular mechanisms behind adaptation and speciation.

Keywords: ddRADseq, mito-nuclear discordances, *COI*, transcriptomics, ABBA-BABA, demographic history

1 | Introduction

Natural hybridisation in animals, once considered rare and without any major evolutionary role (Mayr, 1963), is nowadays recognised as an ubiquitous phenomenon with notorious implications in speciation (Feder, Egan, & Nosil, 2012; Seehausen et al., 2014), invasion biology (Lack et al., 2012), and in the emergence of evolutionary innovations (Arnold & Kunte, 2017). During the last decade, the decrease in the price of high-throughput sequencing methodologies allowed the proliferation of genome-wide studies in non-model organisms, which revealed the extent and prevalence of hybridisation in nature (Taylor & Larson, 2019). However, still today there is a pronounced taxonomic bias across such studies, with most of them addressing hybridisation and introgression events in vertebrates, followed by arthropods (e.g. Bernal, Gaither, Simison, & Rocha, 2017; Gompert et al., 2012; Lack et al., 2012; Li, Davis, Eizirik, & Murphy, 2016; Nadeau et al., 2012; Perry et al., 2018). To a lesser extent, marine invertebrates have also been found to show hybridisation, for instance, in sponges (e.g. Riesgo, Pérez-Portela, et al., 2016), tunicates (e.g. Bouchemousse, Liautard-Haag, Bierne, & Viard, 2016), echinoderms (e.g. Harper, Addison, & Hart, 2007; Weber, Stöhr, & Chenuil, 2019), and corals (e.g. Banguera-Hinestroza et al., 2018; Combosch & Vollmer, 2015; Hatta, et al., 1999; Mcfadden & Hutchunson, 2004; Van Oppen, Willis, Van Rheede, & Miller, 2002).

Many of the studies cited above used the information from both mitochondrial and nuclear genetic markers, generating robust phylogenetic hypothesis and some of them detecting mito-nuclear discordances (i.e. conflicting patterns between mitochondrial and nuclear phylogenies). These discrepant mitochondrial and nuclear phylogeographic histories have been mostly attributed to two contrasting scenarios: incomplete lineage sorting or introgressive hybridisation (Toews & Brelsford, 2012). Patterson's *D* statistic, also known as four-taxon ABBA-BABA test, is a simple and computationally efficient method used on nuclear genome-wide markers that is gaining in popularity to test introgression against the null hypothesis of incomplete lineage sorting (Durand et al., 2011; Martin, Davey, & Jiggins, 2014; Reich et al., 2010). Hence, signals of past introgression events detected in the nuclear genome by ABBA-BABA tests have been taken as an evidence for the introgressive nature of particular mito-nuclear discordances (e.g. Ivanov, Lee, & Mutanen, 2018; Li et al., 2016). However, some introgression events can lead to mito-nuclear discordances without any sign left on the nuclear genome, such as the phenomenon known as 'mitochondrial capture', in which there is a replacement of the full mitochondrial genome of one of the hybridising species with the mitogenome of the

other. Selective backcrosses with one of the parental hybridising species, selection on the mitochondrial genome, and sex-biased dispersal play essential roles on mitochondrial capture events (Toews & Brelsford, 2012; Wielstra & Arntzen, 2012). Furthermore, mitochondrial capture is common in events involving range expansions, such as biological invasions (Currat, Ruedi, Petit, & Excoffier, 2008) and species displacements (Wielstra & Arntzen, 2012), interacting with other effects related to range expansions, e.g. gene surfing (Excoffier, Foll, & Petit, 2009; Wielstra & Arntzen, 2012).

Besides shedding light on the phylogeny and phylogeography of all branches along the tree of life, the expansion of high throughput sequencing methodologies has enabled the low-cost discovery and genotyping of genome-wide markers on natural populations of non-model organisms, i.e. at the intraspecific level (Andrews et al., 2016; Catchen et al., 2017). Among all reduced-representation sequencing techniques, restriction site-associated DNA sequencing approaches (RADseq) have become the most widely used methodologies for single nucleotide polymorphism (SNP) genotyping. These are widely used in evolutionary, adaptation, and population genomics studies of non-model species, mostly because they do not require any prior genomic information for the taxa being studied (Andrews et al., 2016; Catchen, et al., 2017). Generally, RADseq-derived SNPs provide higher resolution for the detection of genetic structure compared to mitochondrial markers or microsatellites (Blanco-Bercial & Bucklin, 2016; Toews & Brelsford, 2012), which is useful for fine- and medium-scale population genetics studies. However, although the implementation of RADseq techniques is nowadays a common practice in the population genetics field, it has still been very scarcely used to resolve speciation, phylogeography, gene flow, and structure of Antarctic fauna. Indeed, only five studies have used RADseq-derived SNPs to address population genetic structure in Antarctic marine invertebrates: in the Antarctic krill *Euphausia superba* (Deagle et al., 2015), in the brittle stars *Ophionotus victoriae* (Galaska et al., 2017a) and *Astrotoma agassizii* (Galaska et al., 2017b), in the sea spider *Nymphon australe* (Collins, Galaska, Halanych, & Mahon, 2018), and in the sponge *Dendrilla antarctica* (Leiva et al., 2019).

Generally, Antarctic marine invertebrates possess low genetic variability, which has been correlated with their evolutionary histories characterised by bottleneck events and demographic expansions associated to the Pliocene–Pleistocene glacial cycles (Allcock & Strugnell, 2012; Rogers, 2007). Glacial cycles are alternated glacial and interglacial periods, with grounded ice sheets occupying most of the Antarctic continental shelf during glacial periods, followed by ice-sheet retreats during interglacial periods (Thatje, Hillenbrand, & Larter, 2005). Such alternations are proposed to be what is called the

Antarctic Biodiversity Pump, leading to a high rate of cryptic species complexes (e.g. Held & Wägele, 2005; Krabbe et al., 2010; Wilson, Hunter, Lockhart, & Halanych, 2007) and therefore to adaptive radiation increasing Southern Ocean biodiversity (Clarke & Johnston, 1996; Rogers, 2007). Such recent allopatric speciation events are suggested to be frequent during glacial periods due to fragmentation and isolation of populations in refugia. Interestingly, three different refugium hypotheses have been proposed for their glacial survival (Allcock & Strugnell, 2012; Thatje et al., 2005): (i) migration to slope and abyssal deeper waters, (ii) migration to Subantarctic areas, and (iii) *in situ* survival in coastal polynyas, i.e. ice-free continental shelf areas produced by katabatic winds. Each of these glacial-refugium strategies leave characteristic genetic signatures, since they create geographically different genetic diversity patterns (Allcock & Strugnell, 2012). For Antarctic marine invertebrates, glacial refugia in the deep-sea (e.g. Baird, Miller, & Stark, 2011), in Subantarctic areas (e.g. González-Wevar et al., 2013), and in the Antarctic continental shelf (e.g. Díaz, et al., 2011) have been identified using molecular markers.

In Antarctica, nemerteans are an important component of the marine benthic fauna, with 42–45 benthic and two pelagic species reported to date (Mahon, Thornhill, Norenburg, & Halanych, 2010). Among the most abundant nemerteans of Antarctic shallow waters are the members of the genus *Antarctonemertes*, a group of small-sized hoplonemerteans, with four species described to date in the Southern Ocean (see Taboada et al., 2018): *Antarctonemertes valida* (Bürger, 1893), *Antarctonemertes riesgoae* Taboada et al., 2013, *Antarctonemertes unilineata* (Joubin, 1910), and *Antarctonemertes belgica* (Bürger, 1904). *Antarctonemertes valida*, *A. riesgoae* and *A. unilineata* form a strongly supported phylogenetic clade, with the two former appearing as sister species and being commonly present in West Antarctica and in the Subantarctic South Georgia Island (Taboada et al., 2018), and with *A. unilineata* mainly found in East Antarctica (including continental East Antarctica and the Subantarctic Crozet and Kerguelen Islands; Taboada et al., 2018), although occasionally present in the Western Antarctic Peninsula (de la Uz, 2005). Interestingly, morphologically hybrid individuals between *A. valida* and *A. riesgoae* have been recently found in the South Shetland Islands (authors' personal observations), sparking our interest in clarifying the species boundaries between the species of the genus. Here, we aim to unravel the phylogeographic and evolutionary history of the members of the genus *Antarctonemertes* in the Southern Ocean, with a special focus on the hybridisation potential between the species both at the present and in the past. Furthermore, we dig into the genomics of adaptation of *A. valida* from the Western Antarctic Peninsula to its peculiar evolutionary history.

2 | Material and Methods

2.1 | Sample collection and preservation

A total of 542 individuals of the genus *Antarctonemertes* were used in this study. During two campaigns along the Western Antarctic Peninsula and its surrounding islands (WAP) in 2012–2013 and 2015–2016, we collected 187 specimens of *A. riesgoae*, 204 of *A. valida*, and 12 *Antarctonemertes* with 'hybrid morphology' (Figure 1; Table 1). This 'hybrid morphology' consisted on adults possessing the two cephalic white patches characteristic of *A. valida*, with a very faded V-shaped pattern characteristic of *A. riesgoae* (see Figure 3B). In 2017, during a campaign in South Georgia Island, we collected 48 individuals of *A. riesgoae* and 40 of *A. valida* (Figure 1; Table 1). In addition, we used 42 specimens of *A. unilineata* collected in 2013–2014 by Taboada et al. (2018) at Beall Island (BI) near Casey research station, East Antarctica, and also 26 individuals of *A. valida* and 24 of *A. riesgoae* collected in 2013 by Taboada et al. (2018) at Deception Island (Table 1). In all cases, sampling was performed in the intertidal or by SCUBA-diving at a maximum depth of 25 m, collecting the organisms attached to rocks and algae. Specimens were preserved in 96% ethanol that was replaced three times, and later stored at -20 °C until further processing. Permits to collect samples were issued by the Spanish Ministry of Economy and Competitivity (CPE-EIA-2011-7 and CPE-EIA-2015-7).

For transcriptome assembly, we collected three individuals of *A. riesgoae* and six organisms of *A. valida*, all of them from WAP (Table 1). We preserved the specimens in RNA*later* (Life Technologies) immediately after collection, stored for 24h at 4 °C, replaced the RNA*later* once, and then stored at -80 °C until further processing.

2.2 | DNA extraction, mitochondrial marker amplification and sequencing

We extracted DNA from a small portion of midbody tissue (ca. 2–3 mm3) of all 441 samples preserved in 96% ethanol using the DNeasy Blood & Tissue kit (Qiagen) following the manufacturer's protocol. For 402 individuals (198 individuals of *A. riesgoae*, 197 individuals of *A. valida*, and 7 of *A.* 'hybrid morphology'; Supplementary Material 1), we amplified a fragment of ca. 600 bp of the mitochondrial marker *COI* using specific primers (ANT_COI-F/ANT_COI-R) and amplification protocols detailed in Taboada et al. (2018). PCR products were purified and sequenced in both directions using the primers mentioned above at the Centres Científics i Tecnològics de la Universitat de Barcelona (CCiT-UB) and the Sequencing Facilities of the Natural History Museum of London (NHM). Overlapping sequence fragments were cleaned and assembled into consensus sequences using the

software Geneious v.10.2.6 (https://www.geneious.com, Kearse et al., 2012) and then checked for contamination using BLAST (Altschul et al., 1990). We added the 92 sequences from Taboada et al. (2018) to these newly sequenced *COI* sequences to obtain the *COI* dataset used in subsequent analyses: a total of 494 sequences belonging to 222 A. riesgoae, 223 A. valida, 7 A. 'hybrid morphology', and 42 A. unilineata (Table 1).

2.3 | *Phylogeny, population genetics, and demographic history analyses using* COI

All sequences from *A. valida*, *A. riesgoae*, *A.* 'hybrid morphology', and *A. unilineata* individuals were aligned with the inbuilt MAFFT v.7.309 (Katoh et al. 2002) in Geneious v.10.2.6, using the Q-INS-I option, resulting in an alignment of 456 bp for a total of 494 individuals (Table 1).

The most appropriate evolutionary model (GTR+I+G) was obtained by running the alignment in jModelTest (Posada, 2008) via the Akaike Information Criterion (AIC), and subsequently used in all model-based phylogenetic analyses. A Maximum Likelihood (ML)

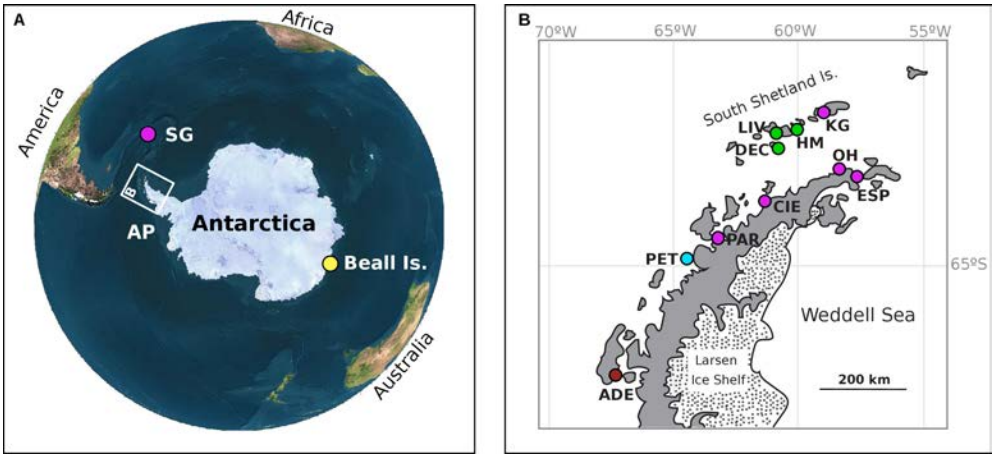

FIGURE 1 **(A)** Map of the Southern Ocean showing the study areas. **(B)** Sampling sites off the Antarctic Peninsula. Each sampling station is represented by a circle, whose colour indicates which *Antarctonemertes* species were collected at each location: yellow, only *A. unilineata*; blue, only *A. valida*; brown, only *A. riesgoae*; pink, *A. valida* and *A. riesgoae*; green, *A. valida*, *A. riesgoae*, and *Antarctonemertes* 'hybrid morphology'. Abbreviations: SG, South Georgia Island; WAP, Antarctic Peninsula and surrounding islands; KG, King George Island; HM, Half Moon Island; LIV, Livingston Island; DEC, Deception Island; OH, O'Higgins Bay; ESP, Esperanza Bay; CIE, Cierva Cove; PAR, Paradise Bay; PET, Petermann Island; ADE, Adelaide Island.

Sampling Areas	Sampling Stations	Coordinates	A. validus	A. riegeae	A. 'hybrid morphology'	A. unifasciata
East Antarctica	Beall Is. (Taboada et al., 2018)	66°17'47"S 110°29'38"E				42
Antarctic Peninsula	King George Is.	62°11'15"S 58°56'59"W	15	26		
	Half Moon Is.	62°35'41"S 59°54'07"W	22	25	2	
	Livingston Is.	62°39'07"S 60°36'28"W	24	9	5	
	Deception Is.	62°59'25"S 60°35'31"W	4 (+26 from Taboada et al., 2018) (+1 RNAlater)	24 from Taboada et al. (2018) (+1 RNAlater)	5	
	O'Higgins Bay	63°18'52"S 57°54'10"W	25	29		
	Esperanza Bay	63°23'47"S 56°59'47"W	26 (+1 RNAlater)	17 (+1 RNAlater)		
	Cierva Cove	64°09'28"S 60°57'22"W	26	30		
	Paradise Bay	64°49'24"S 62°51'24"W	34	1		
	Petermann Is.	65°10'24"S 64°08'36"W	22			
	Adelaide Is.	67°34'04"S 68°08'55"W		26 (+1 RNAlater)		
South Georgia Is.	Cape Demidov	54°08'23"S 37°43'21"W	6	18		
	Mouse Cove	54°14'26"S 37°19'51"W	9			
	Right Whale Bay	54°00'44"S 37°41'37"W	6	12		
	Iris Bay	54°44'10"S 35°52'49"W	13	12		
	Wirik Bay	54°45'10"S 35°50'48"W	6	6		

TABLE 1 Collection details for all sampling stations included in the study.

analysis was conducted using RaxML version 8.2.12 (Stamatakis, 2014) and a Bayesian inference (BI) analysis was performed using in MrBayes 2.1.2 (Ronquist & Huelsenbeck, 2003). The ML tree search was conducted by performing 50 runs, with 1,000 thorough bootstrap replicates to evaluate nodal support. BI analyses were run twice, starting from random trees and running for 5,000,000 generations with four chains running simultaneously (two cold and two heated). Chains were sampled every 1,000 generations with 25% of the generations discarded as burn-in. Convergence was checked using Tracer v1.7 (Rambaut et al., 2018).

We also assessed the demographic history of each *Antarctonemertes* species from WAP and SG using the *COI* dataset. To test whether their populations are in demographic expansion we used the *tajima.test* function to obtain the Tajima's *D* statistic (Tajima, 1989) in the *pegas* R package (Paradis, Claude, & Strimmer, 2004; R Core Team, 2014). The *COI* alignment was used to construct un-rooted haplotype networks using the median-joining network option (Bandelt, Forster, & Röhl, 1999) with the program POPART 1.7 (www.popart.otago.ac.nz). In order to estimate population dynamics through time for all species, we used Extended Bayesian Skyline Plots (EBSP) as implemented in BEAST 2.3.2 (Bouckaert et al., 2014). We conducted a Bayesian MCMC run for each dataset using the GTR+G+I model previously estimated by jModelTest, with a chain length of 250 x 10^6 steps sampling every 1000 iterations and discarding 10% of the trees as burn-in. Due to the lack of an evolutionary rate for nemerteans, we chose the tenfold evolutionary rate for nacellids (10% per million years, González-Wevar et al., 2013), which is, to our knowledge, one of the closest available. The convergence of runs was confirmed again using Tracer 1.7, checking the Effective Sample Size (ESS) of each statistic. We used the script *plotEBSP.R* included in BEAST 2 to generate the different EBSPs in an R environment.

2.4 | ddRADseq library preparation and sequencing

Library preparation was conducted as described in Leiva et al. (2019), at both the Museum of Comparative Zoology Labs, Harvard University, and the NHM. Libraries were paired-end sequenced (150bp) on two lanes of an Illumina HiSeq 2500 (Illumina): one at the Center for Systems Biology, Harvard University (Cambridge, MA, USA) and another in Macrogen Europe (Macrogen).

2.5 | ddRADseq locus assembly

ddRADseq locus assembly was conducted using the Stacks pipeline, version 2.2 (Catchen et al., 2013). RAD-tags were processed and demultiplexed using *process_radtags*, where low quality reads, reads with uncalled bases, and reads without a complete barcode or restriction cut site were removed. After these filtering steps, the original 195,499,088 raw reads were filtered to 181,318,113 reads, with an average of 784,926.896 reads per sample. After preliminary tests to optimise Stacks parameters according to Jeffries et al. (2016), and following the recommendations of Paris, Stevens, and Catchen (2017) when different species are present in a dataset, optimal final parameter values were set to M = 4, m = 5, and n = 4.

In order to optimise the number and SNPs representation for each different analysis, the Stacks *populations* module was run three times on three different sets of individuals: (i) including all the samples, to perform phylogenetic analyses (dataset called 'ALL' hereafter); (ii) considering only samples from WAP and SG (for both *A. riesgoae* and *A. valida* and the hybrids), in order to perform admixture and structure analyses (dataset 'WAP–SG'); and (iii) just using the samples from SG of both *A. valida* and *A. riesgoae*, to investigate their current hybridisation in SG (dataset 'SG').

For the 'ALL' dataset, containing samples from all species and areas, the Stacks *populations* module was used to conduct an initial filtering of the data, retaining those SNPs present in at least 40% of all the individuals (r = 0.4), and filtered out individuals with less than 20% of the loci using the *adegenet* R package (Jombart, 2008; Jombart & Ahmed, 2011). The resulting dataset contained 3,938 SNPs and 198 individuals, with 43.04% of average missing data, consisting of nine *A. unilineata*, five *A.* 'hybrid morphology', 34 *A. riesgoae* collected from the WAP, 18 *A. riesgoae* from SG, 123 individuals of *A. valida* from the WAP, and nine *A. valida* organisms collected at SG.

For the second subset ('WAP-SG'), including organisms from WAP and SG, we ran *populations* retaining those SNPs present in at least 40% of the individuals within groups (r = 0.4) and present in at least two of the five groups (p = 2; groups considered here were: *A. valida* from WAP, *A. valida* from SG, *A. riesgoae* from WAP, *A. riesgoae* from SG, and the *Antarctonemertes* 'hybrid morphology'). Then we used *adegenet* to retain SNPs present in at least 25% of the individuals and filtered out individuals with less than 15% of the loci, resulting in a dataset containing 3,374 SNPs and 197 individuals, with 49.55% of average missing data. The 'WAP-SG' dataset contained five *A.* 'hybrid morphology', 64 *A. riesgoae* organisms (43 from the WAP and 16 from SG), and 133 *A. valida* individuals (124 from the WAP and nine from SG).

For the third subset ('SG'), only including *A. valida* and *A. riesgoae* from SG, the Stacks *populations* module was run with a subset of the 25 individuals from SG with the lowest missing data values, retaining those SNPs present in at least 40% of the individuals (r = 0.4). The resulting dataset contained 9,396 SNPs and 25 individuals (nine *A. valida* and 16 *A. riesgoae*), with 40.04% of average missing data.

2.6 | Phylogenetic, introgression, and hybridisation analyses using ddRADseq-derived SNPs

We used the TreeMix software (Pickrell & Pritchard, 2012) in order to infer a ML tree taking into account historical migration events, which builds ML trees and tests allowing for the presence of gene flow between diverged lineages. Using the 'ALL' dataset including individuals from all species and locations (198 individuals and 3,938 SNPs), we estimated a ML tree rooted using an individual of *A. unilineata* and set the migration events to 0 (no admixture). Migration events were sequentially added until no significant improvement in the fit of the model was found. In order to verify the migration events suggested by TreeMix, we estimated Patterson's *D* statistic as implemented in the *CalcD* function of the *evobiR* R package (Blackmon & Adams, 2015). *CalcD* was run resolving biallelic ambiguities (ambig = "R") and significance was assessed with 1,000 bootstrap replicates (sig.test = "B", replicate = 1000). In addition, we ran the *CalcD* function 1,000 times for each test, thus testing the robustness of the results when dealing with the stochasticity produced by resolving biallelic ambiguities. In order to infer the mixing proportions of the introgression events detected by Patterson's *D* statistics, we estimated the f_4-ratio following Patterson, et al., (2012), estimating each f_4 with the *fourpop* function in TreeMix.

Admixture and population structure for the dataset 'WAP–SG' were explored using the *snapclust.choose.k* and *snapclust* functions (Beugin, et al., 2018) in the *adegenet* R package, and the STRUCTURE software version 2.3 (Pritchard, Stephens, & Donnelly, 2000). We used the Akaike Information Criterion (IC = AIC) to identify the optimal number of clusters in *snapclust.choose.k*, and then initial memberships for *snapclust* were chosen using the k-means algorithm (pop.ini = "kmeans"), allowing a maximum *K* (number of clusters) of 10 (max = 10), and a maximum number of iterations of 100 (max.iter = 100). STRUCTURE was run for 200,000 MCMC iterations using the admixture model, with a burn-in of 100,000 iterations, setting the putative *K* from 1 to 10 with 10 replicates for each run. STRUCTURE HARVESTER (Earl, 2012) and CLUMPP v.1.1.2 (Jakobsson & Rosenberg, 2007) were used to determine the most likely number of clusters and to average each individual's membership coefficient across the *K* value replicates, respectively.

Due to the high mixing proportion values found between *A. valida* and *A. riesgoae* from SG, we performed a hybridisation analysis on the dataset 'SG' to test whether hybridising signatures could be detected between both species. We used the *snapclust.choose.k* and *snapclust* functions as described above to identify the optimal number of clusters and to assign individual membership probabilities, respectively. Then, we performed a discriminant analysis of principal components (DAPC; Jombart, Devillard, & Balloux, 2010) as implemented in the *adegenet* R package to investigate the structure between the clusters. The number of retained PCA axes was chosen using the cross-validation *xvalDapc* function in *adegenet*, and the *dapc* function was run grouping samples by their cluster assignment returned by *snapclust*. Afterwards, we used the function *hybridise* in *adegenet* to simulate a population of 20 hybrid individuals between the two most distant clusters, and subsequently analysed the structure of both real and simulated individuals together using the same pipeline described above (*snapclust.choose.k*, *snapclust*, *xvalDapc*, and *dapc* functions). Alternatively, we used the fineRADstructure pipeline (Malinsky et al., 2018) to assess the shared ancestry in the SG dataset, which uses ddRAD-haplotype linkage information and gets high-resolution co-ancestry data. The pipeline (*RADpainter* and *finestructure*) was run with the default values following the indications at the fineRADstructure online tutorial (http://cichlid.gurdon.cam.ac.uk/fineRADstructure.html): -x 100,000, -y 100,000, -z 1,000 to assign individuals to populations, and -x 10,000 for the tree building. Graphic interpretation of the results was performed using Finestructure R Library and *fineRADstructurePlot.R* script, both included within the fineRADstructure package.

2.7 | RNA extraction and transcriptome library preparation, sequencing, and assembly

Total RNA was extracted using a standard Trizol-based method using TRI Reagent (Life Sciences) following the manufacturer's instructions. Subsequent mRNA purification was performed with Dynabeads mRNA Purification Kit (Invitrogen) also following the manufacturer's protocol. cDNA libraries were constructed with the ScriptSeq v2 kit (Illumina) and sequenced in a NextSeq 500, at 150bp paired end read length at the Sequencing Facilities of the NHM.

A total of 407,473,408 pared reads were obtained for sex individuals in our transcriptomic run for *A. valida*, and 71,535,679 for *A. riesgoae*. Transcriptomic raw reads were cleaned using Trimmomatic 0.33 (Bolger, Lohse, & Usadel, 2014) with the following settings: ILLUMINACLIP:./Adapters.fa:2:30:10 LEADING:3 TRAILING:3

SLIDINGWINDOW:4:20 MINLEN:30 where the Adapters.fa file was substituted for the appropriate adapters for each library, resulting in a total of 292,333,312 paired raw reads for *A. valida* and 51,832,072 for *A. riesgoae*. In order to ensure complete removal of adapter and low-quality sequence data, sequence quality was assessed using FastQC (Andrews, 2010) before and after trimming. A *de novo* reference transcriptome was assembled for each species (for *A. valida* using 6 RNAseq libraries and for *A. riesgoae* using 3 RNAseq libraries) with the Trinity version 2.4.4 (Grabherr et al., 2011) with standard settings except for a minimum contig length of 200 bp and *in silico* read normalisation. The assembly of *A. valida* contained 78 Mb and 132,662 transcripts with an N50 of 1015 after filtering out the bacteria. The assembly of *A. riesgoae* comprissed a total of 131 Mb, 222,700 transcripts, and an N50 of 861 after filtering out the bacteria.

2.8 | Adaptive ddRAD-loci identification and annotation

Given that (i) the *A. valida* lineage from the WAP was the only presenting clear evidences of an *in situ* glacial refugium in Antarctic shallow waters (see Results section 3.1) and (ii) it appeared as highly differentiated from the rest of the species in the admixture and structure results (see Results section 3.2), we aimed to identify the ddRAD-loci that contributed most to this divergence. Our hypothesis is that these loci may have had a putative role in the adaptation of the *A. valida* lineage from the WAP to the glacial survival in Antarctic shallow waters. Also, the detection of adaptive loci will allow us to identify loci with key roles on speciation processes. To achieve it, we followed two different approaches: an F_{ST}-outlier method and a DAPC-based procedure.

We used BayeScan v2.1 (Foll & Gaggiotti, 2008) to detect candidate loci under selection through specific F_{ST} coefficients. We first used default parameters to obtain the F_{ST} coefficients for all SNPs. Then, we ran BayeScan using default parameters of the MCMC chain, but decreasing the prior odds for the neutral model to 1, since we were running the algorithm with different species instead of different populations within the same species. We used the R package *ggplot2* (Wickham, 2016) to plot the F_{ST} coefficient from the first BayeScan run, and the function *plot_bayescan* from the *plot_R* script in order to plot BayeScan results from the second run, with a False Discovery Rate of 0.10 (FDR = 0.1). For the DAPC-based approach, we first ran a DAPC separating the *A. valida* individuals collected in the WAP from the rest of organisms. Then, following Jombart and Collins (2015), we extracted the information of the SNPs that most contributed to the segregation

of the samples through the Discriminant function 1, using the *loadingplot* function of the *adegenet* R package, with a 0.01 threshold (thres = 0.01).

In order to annotate ddRAD-loci with a putative role in the adaptation of *A. valida* from WAP, all the ddRAD-loci containing SNPs detected as under positive selection by BayeScan and the ddRAD-loci including highly informative SNPs detected by the DAPC-based approach were mapped back to our *de novo* reference transcriptome using Geneious 10.2.6 local blast (Altschul et al., 1997) to obtain the contig ID matching to each ddRAD-locus. Any contig that a ddRAD-locus uniquely mapped to or with a top hit with an *e*-value two orders of magnitude lower than the next closest hit, was then subjected to a BLASTX search against *nr* (default parameters, Altschul et al., 1997), and this annotation was retained for the mapped ddRAD-locus.

3 | Results

3.1 | *Mitochondrial* COI *phylogeny, population genetics, and demography*

Given that both ML and BI analyses recovered highly similar topologies, we selected the tree from the ML analysis for the graphical visualization and included the branch supports from both ML and BI analyses on the nodes (Figure 2A). All *A. riesgoae* organisms (WAP + SG) and *A. valida* individuals from SG appeared in a robustly supported clade, while *A. valida* organisms collected in the WAP clustered together with the *Antarctonemertes* 'hybrid morphology' individuals as sister to the rest of *A. riesgoae* and *A. valida* individuals in a highly supported clade (Figure 2A). Haplotype networks (Figure 2B) of *A. valida* from WAP + *Antarctonemertes* 'hybrid morphology' and *A. valida* from SG were connected by 28 mutational steps, the former displaying a remarkable star-like topology with a dominant haplotype accounting for the 88.54 % of the sequences. *Antarctonemertes valida* from SG also presented a star-like topology, but less pronounced than that of *A. valida* from WAP, with a central haplotype accounting for the 56.41 % of the sequences. A total of 19 mutational steps were found between the haplotype networks of *A. valida* from SG and *A. riesgoae* from SG (Figure 2B). Networks of *A. riesgoae* from WAP and *A. riesgoae* from SG were connected by only 3 mutational steps (Figure 2B), and therefore all *A. riesgoae* were treated as a single species in subsequent analyses with *COI*. The *A. riesgoae* lineage presented a parochial haplotype network with three main haplotypes in WAP and three haplotypes in SG, displaying a clear geographic genetic structure (Figure 2B). Nineteen mutational steps were found between the haplotype networks of *A. valida* from SG and *A. riesgoae* from SG (Figure 2B).

Tajima's *D* presented values of 0.18 for *A. riesgoae*, -1.19 for *A. valida* from SG and -2.26 for *A. valida* from WAP + *Antarctonemertes* 'hybrid morphology', being the latter value significantly different from zero (p-value < 0.05). EBSPs (Figure 2C) are represented using the same time scale to ease the comparison between them. EBSP for *A. valida* from WAP + *Antarctonemertes* 'hybrid morphology' showed the most recent expansion, starting between 10,000 – 15,000 years ago (Figure 2C).

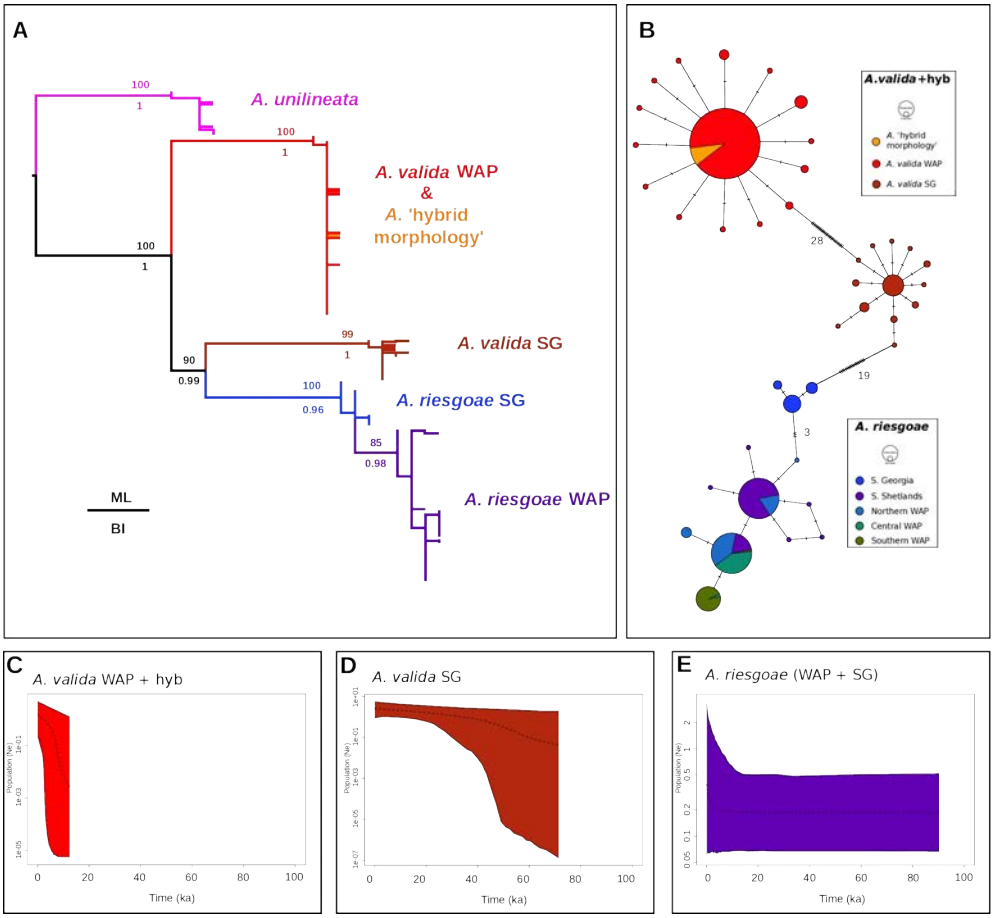

FIGURE 2 Phylogeographic and demographic results from the *COI* mitochondrial marker (494 individuals, 456 bp). **(A)** Maximum Likelihood tree showing the phylogenetic relationships between the Antarctic *Antarctonemertes*. Branch support shown as bootstrap value (ML) over the tree branch and posterior probability (BI) under the tree branch. **(B)** Median-joining haplotype network based on the *COI* of *Antarctonemertes* sampled in WAP and SG (*A. valida*, *A. riesgoae*, and *Antarctonemertes* 'hybrid morphology'). Circle size is proportional to the number of individuals for each haplotype and number of mutations between haplotypes are indicated with crossed lines or with numbers between lineages. **(C-E)** Historical demographic trends of the effective population size (Ne) constructed using the Extended Bayesian Skyline Plot approach. Median estimates are shown as black dashed lines, with 95% highest probability density limits shown in colours.

3.2 | *Phylogeography, structure, and ancient introgressions from ddRADseq-derived SNPs*

The ML tree resulting from TreeMix analysis is shown in Figure 3A, which also summarises ABBA-BABA tests results and f_4-ratio estimations. In contrast to the ML tree obtained with mitochondrial *COI* sequences, here *A. valida* from WAP and *A. valida* from SG clustered together, with *Antarctonemertes* 'hybrid morphology' appearing as sister group to the *A. riesgoae* lineage (Figure 3A). Two introgressive events were detected by TreeMix and corroborated by ABBA-BABA tests: one between *A. valida* from SG and *A. riesgoae* from SG (F_4-ratio estimations resulting in a 40.11% of admixture for this introgression), and another one between *A. valida* from SG and *A. riesgoae* from WAP (with a 14.79% of admixture) (Figure 3A). Instead of two independent introgressive events, a model with just one introgression would be more parsimonious and feasible, and would also explain our results: an introgressive event between *A. valida* from SG and *A. riesgoae* occurring previously to the differentiation of the two *A. riesgoae* populations. Hence, we ran an additional ABBA-BABA test for this admixture event, which resulted significant (Figure 3B).

Admixture and structuring results for the *Antarctonemertes* species from WAP and SG are shown in Figure 3C. AIC of the *snapclust* analysis suggested four optimal

FIGURE 3 Phylogeographic, introgression, and structuring results from the ddRADseq-derived SNPs. **(A)** TreeMix ML tree from the 'ALL' dataset (198 individuals, 3,938 SNPs), showing two introgression events: between *A. valida* from SG and both *A. riesgoae* populations. Red insert shows Patterson's *D* statistic and F_4-ratio results for the introgression between *A. valida* from SG and *A. riesgoae* from SG, while green insert shows the results for the introgression between *A. valida* from SG and *A. riesgoae* from WAP. Inserts show the frequency distribution of the Patterson's *D* value across 1000 runs. **(B)** Phylogeographic hypothesis for the Antarctic *Antarctonemertes* from TreeMix analysis and Patterson's *D* statistics using the 'ALL' dataset. Nuclear (blue) and the mitochondrial (orange) genealogies are shown within the species tree, including two introgression events (horizontal branches) and the inferred extinction of mitochondrial lineages marked with red crosses. The introgression event that left signals in the nuclear genome (horizontal blue dashed line) is supported by a significantly negative Patterson's *D* statistic, shown in the insert framed with a blue dashed line. Picture of the living *A. unilineata* correspond to a specimen collected from Beall Island; pictures of living *A. valida* (WAP) and *A. valida* (SG) correspond to a specimen of *A. valida* from Deception Island; pictures of living *A. riesgoae* (WAP) and *A. riesgoae* (SG) correspond to a specimen of *A. riesgoae* from Deception Island; picture of the living specimen of *Antarctonemertes* 'hybrid morphology' correspond to a specimen from Livingson Island. **(C)** *snapclust* and STRUCTURE results for the 'WAP-SG' dataset (197 individuals, 3,374 SNPs). Due to the optimal number of clusters varied between 2 and 4 (see Supplementary Material 2A-B), we show the results for *K*=2, *K*=3, and *K*=4 for both analyses.

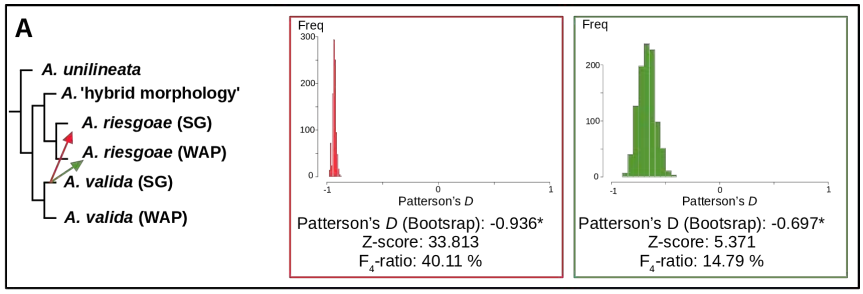
A
A. unilineata
A. 'hybrid morphology'
A. riesgoae (SG)
A. riesgoae (WAP)
A. valida (SG)
A. valida (WAP)
Freq
Patterson's D
Patterson's D (Bootsrap): -0.936*
Z-score: 33.813
F4-ratio: 40.11 %
Freq
Patterson's D
Patterson's D (Bootsrap): -0.697*
Z-score: 5.371
F4-ratio: 14.79 %

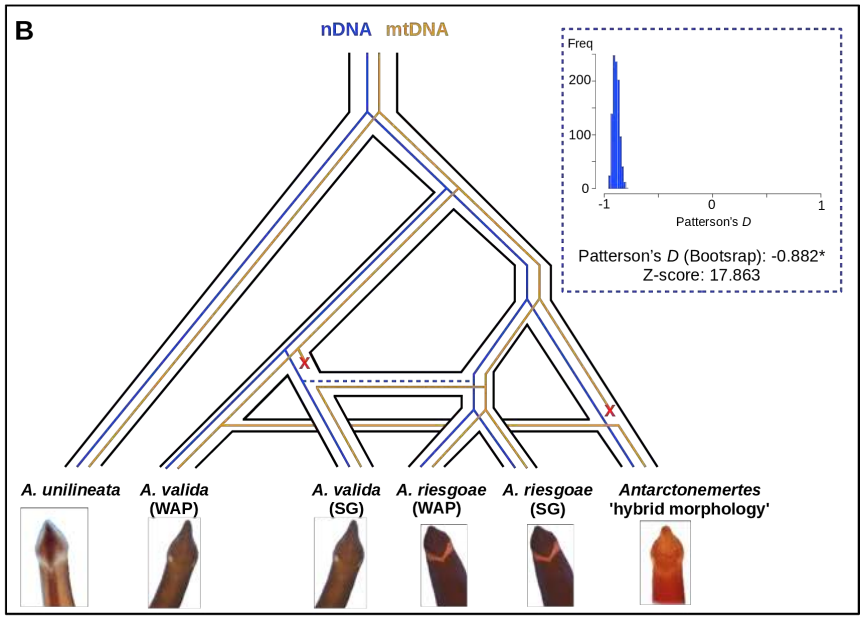
B
nDNA
mtDNA
Freq
Patterson's D
Patterson's D (Bootsrap): -0.882*
Z-score: 17.863
A. unilineata
A. valida (WAP)
A. valida (SG)
A. riesgoae (WAP)
A. riesgoae (SG)
Antarctonemertes 'hybrid morphology'

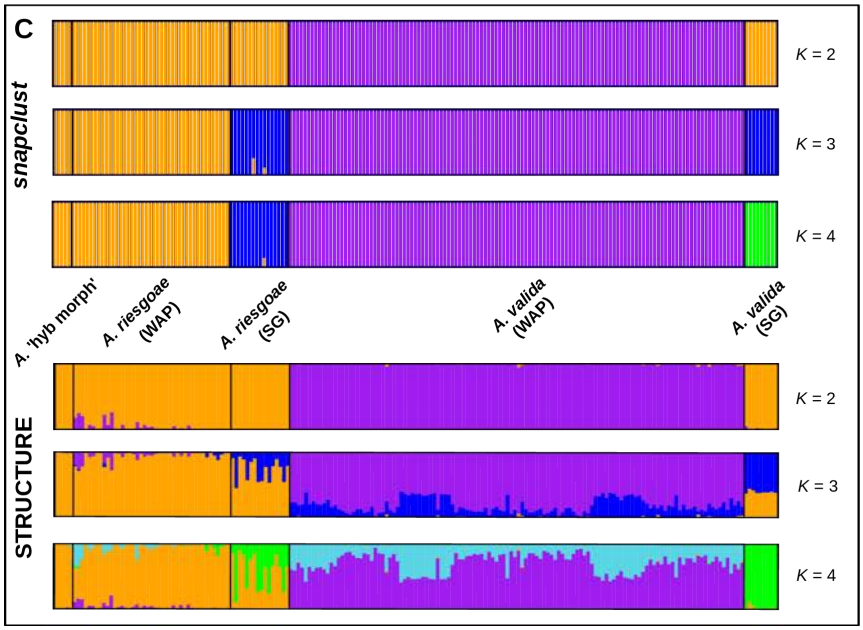
C
snapclust
K = 2
K = 3
K = 4
A. 'hyb morph'
A. riesgoae (WAP)
A. riesgoae (SG)
A. valida (WAP)
A. valida (SG)
STRUCTURE
K = 2
K = 3
K = 4

clusters (*K*) (see Supplementary Material 2A). Two and three clusters were also close to the optimal value, and therefore we represented results with *K* = 2, *K* = 3, and *K* = 4 (Figure 3C). *snapclust* results considering two clusters (*K* = 2) separated *A. valida* from WAP from the rest of individuals. When considering three clusters (*K* = 3), *A. valida* and *A. riesgoae* populations from SG were grouped together, with *Antarctonemertes* 'hybrid morphology' clustering with *A. riesgoae* individuals from WAP. Finally, the structure considering four clusters (*K* = 4) was similar to the structure with three clusters, but the populations of *A. valida* and *A. riesgoae* from SG appeared mostly separated in two different clusters.

The most likely number of clusters inferred from delta *K* using the STRUCTURE results was *K* = 2 (see Supplementary Material 2B). In addition to *K* = 2, we also show the results for three and four clusters (Figure 3C), which are largely consistent with *snapclust* results but with many individuals presenting admixture in their membership probabilities. Remarkably, some *A. riesgoae* individuals from SG presented high membership probabilities of belonging to the cluster that all organisms of *A. valida* from SG belonged to (green cluster in Figure 3C). Also, STRUCTURE results did not completely differentiate between the populations of SG and WAP for *A. riesgoae* as clear as *snapclust* did (Figure 3C).

3.3 | Current hybridisation in SG

Our results of the analyses on the 'SG' dataset are shown in Figure 4. The optimal number of clusters found by *snapclust.choose.k* using the AIC was *K* = 3 (see Supplementary Material 2C). The DAPC plot before hybrid simulation (Figure 4A) showed that most of the samples of each species clustered together in the two most distant clusters, while five individuals of *A. riesgoae* and two of *A. valida* were grouped together in a third cluster located in the middle of the two most distant clusters (Figure 4A). The DAPC plot with the 20 simulated hybrids between the two distant clusters (Figure 4B) showed an overlap between the simulated hybrids and the seven individuals mentioned above, and therefore identified them as hybrids between the two most distant clusters, which were potentially the two parental species. fineRADstructure results supported the hybridisation hypothesis (Figure 4C): organisms belonging to the two parental species (*A. valida* SG and *A. riesgoae* SG) presented high values of shared co-ancestry within clusters (purple to blue and black squares) and low values with the other species (orange to yellow squares); on the other hand, the seven hybrids presented medium values of shared co-ancestry with all the individuals (red to violet squares).

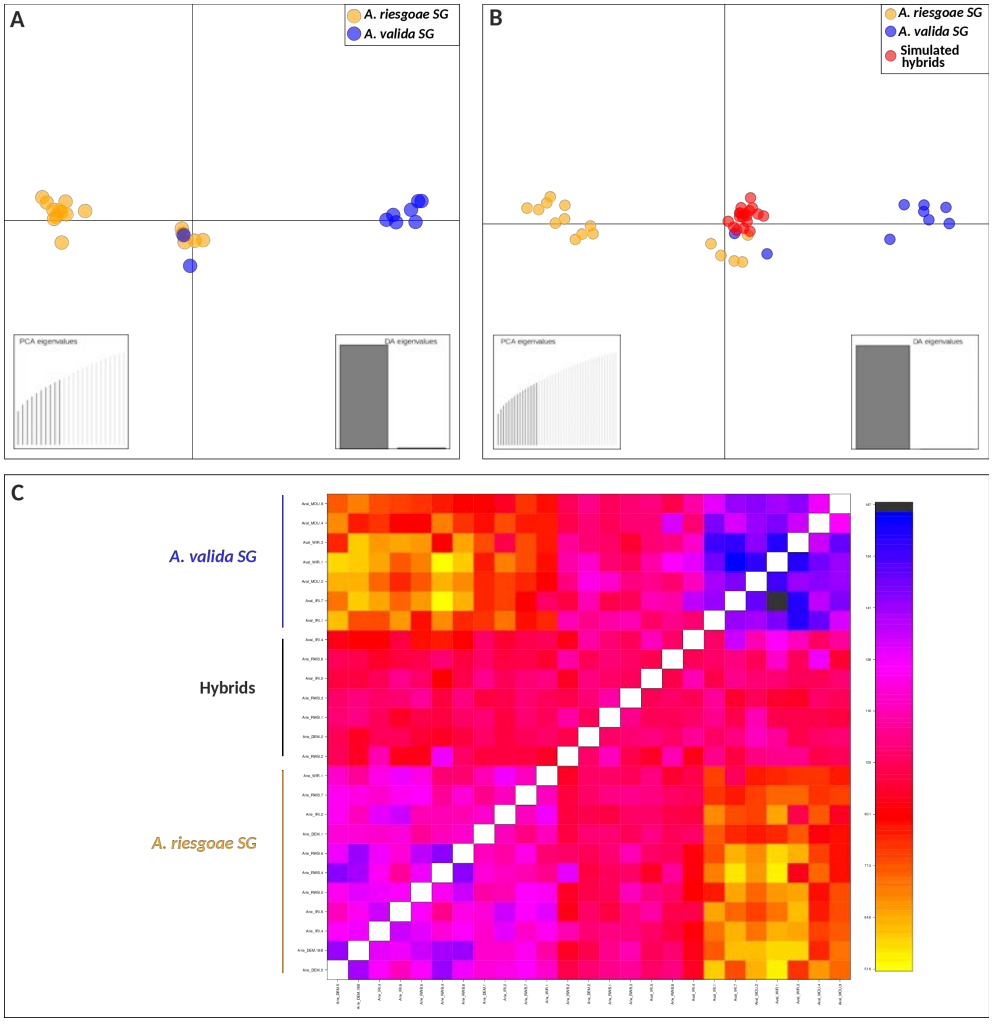

FIGURE 4 Current hybridisation results for the dataset only including organisms from South Georgia Island (25 individuals, 9,396 SNPs). **(A)** DAPC representation of the *snapclust* clustering, showing the morphologically *A. valida* organisms (blue) and the morphologically *A. riesgoae* organisms (orange). **(B)** DAPC representation of the *snapclust* clustering, showing *A. valida* and *A. riesgoae* organisms with the same colours specified in (A), and the simulated hybrids (red). **(C)** Simple co-ancestry matrix obtained from the fineRADstructure analysis, showing two clusters corresponding to *A. valida* and *A. riesgoae* (blue and orange squares, respectively) and the hybrid individuals.

3.4 | *Adaptive ddRAD-loci in* A. valida *from WAP*

A total of 271 SNPs corresponding to 92 RAD-loci were identified by our DAPC-based approach as the most contributing loci to the separation between *A. valida* from WAP and the rest of *Antarctonemertes* lineages (see DAPC plot in Figure 5A). By contrast, BayeScan detected 83 SNPs with signals of positive selection and 27 SNPs with signals of balancing selection (Figures 5B and 5C). The 83 SNPs under positive selection corresponded to 37 RAD-loci, 10 of which were shared with the DAPC-based approach. Hence, we identified a total 119 adaptive RAD-loci, 98 of which matched contigs in our *de novo* assembled reference transcriptome, and 40 with a blast hit against the *nr* NCBI database (Table 2). Among those 40, one matched a bacterial aminotransferase, one a fungal protein, and another one matched a protein of an endosymbiont bacteria associated to the annelid *Escarpia laminata*, a deep-sea sabellid from the Gulf of Mexico's fumarolic cold seeps (Table 2), but the rest matched animal genes. Using the UniProtKB database (https://www.uniprot.org) and its Gene Ontology project - Biological Process section, we assigned the 37 remaining annotated RAD-loci to ten functions (Table 2): (i) immune and stress responses (eight loci); (ii) spermatogenesis and reproduction (six loci); (iii) nervous system, brain and eye development (six loci); (iv) Endoplasmic Reticulum, Golgi apparatus, and vesicle turnover (five loci); (v) digestion (four loci, one locus shared with the nervous system, brain and eye development function); (vi) biosynthetic and catabolic processes (three loci); (vii) RNA processing and splicing (two loci); (viii) cell division fidelity (two locus); (ix) basement membranes (one locus); (x) mitochondrial transcription (one locus); and (xi) muscle development and contraction (one locus, shared with the cell division fidelity function).

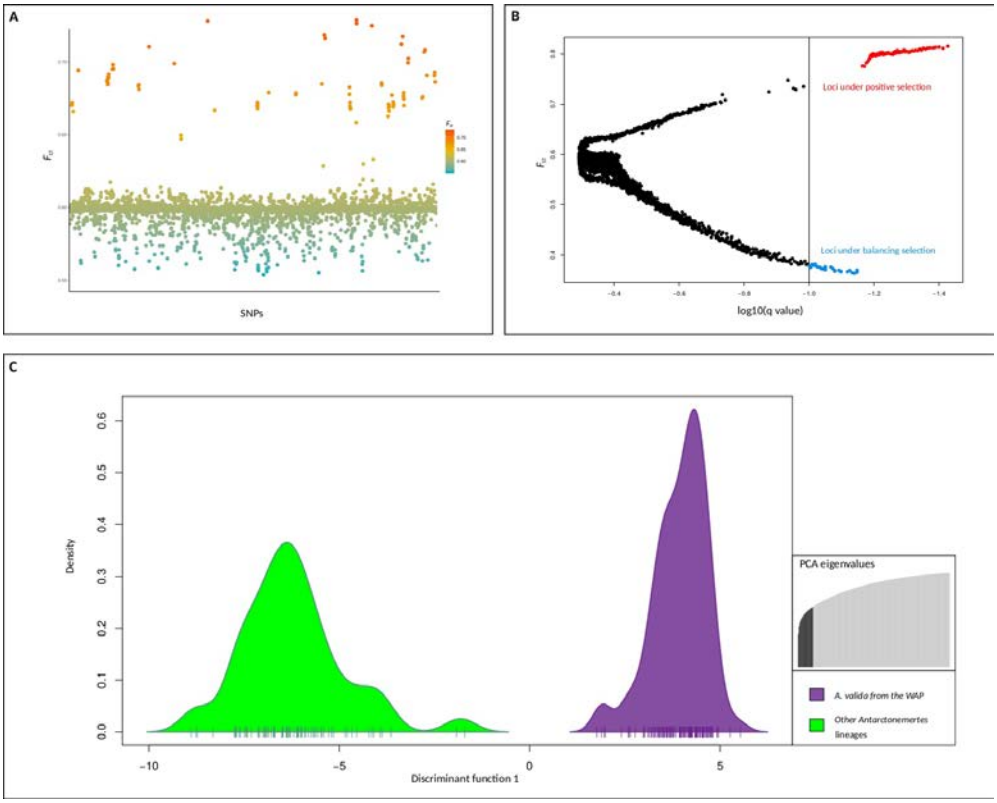

FIGURE 5 **(A)** Plot showing F_{ST} coefficients for all loci. **(B)** BayeScan results showing loci identified as under positive selection and loci under balancing selection with an FDR of 0.10. **(C)** Representation of the DAPC results showing the separation between *A. valida* from WAP and the rest of *Antarctonemertes* lineages. SNPs that contributed most to the Discriminant function 1 were extracted from the DAPC results shown here.

4 | Discussion

4.1 | Mito-nuclear discordances and ancient introgressive hybridisation events

Our results indicate that the evolutionary history of the Antarctic Antarctonemertes is mainly characterised by introgression and hybridisation favoured by the geological changes occurred during the glacial cycles. Our study revealed two mito-nuclear discordances in our Antarctonemertes dataset, with contrasting phylogenetic hypotheses recovered from the mitochondrial COI and the ddRADseq-derived SNPs regarding the position of A. valida from SG and Antarctonemertes 'hybrid morphology'. The former, appeared as the sibling species of the A. riesgoae lineage in the COI phylogeny (Figure 2A), suggesting the presence of two cryptic species or lineages in A. valida, one from the Antarctic Peninsula and the other from South Georgia Island. Although we are aware that their COI differences are greater than the proposed barcode gap for Nemertea (Sundberg, Kvist, & Strand, 2016), we conservatively chose to maintain both lineages within the same species based on the results from the nuclear genome. Indeed, our ddRADseq-derived SNP phylogeny, showed that both A. valida lineages clustered together, in agreement with their external morphological traits (Figure 3A–B). In addition, our admixture and introgression analyses provided a reliable explanation for this mito-nuclear discordance, indicating an introgressive event between A. valida from SG and the A. riesgoae lineage identified with the nuclear dataset (Figure 3A–B). We suggest that this ancient introgressive event that left signals in the nuclear genome may have led to the mito-nuclear discordance in the phylogenetic position of A. valida from SG, allowing the transmission of the mitochondrial genome from the A. riesgoae linage to A. valida from SG, an introgressive scenario that has been already previously reported for other organisms (e.g. Ivanov et al., 2018; Li et al., 2016), but to our knowledge never reported in any marine organism.

Regarding Antarctonemertes 'hybrid morphology', despite they shared COI haplotypes with A. valida from WAP (Figure 2A–B), they were grouped together with A. riesgoae from WAP when using the nuclear ddRADseq-derived SNPs (Figure 3C). In this case, we did not detect any sign of introgression in the nuclear markers, suggesting a shorter hybridisation event followed by backcrosses with the paternal species, a characteristic feature of mitochondrial capture due to the ease with which the mitochondrial genome introgresses (Chan & Levin, 2005; Currat et al., 2008; Wielstra & Arntzen, 2012). Interestingly, the demographic histories recovered from the COI dataset for A. valida from WAP and A. riesgoae indicated that they survived glacial maxima through different strategies (Figure 6A). The former may have survived glacial maxima in

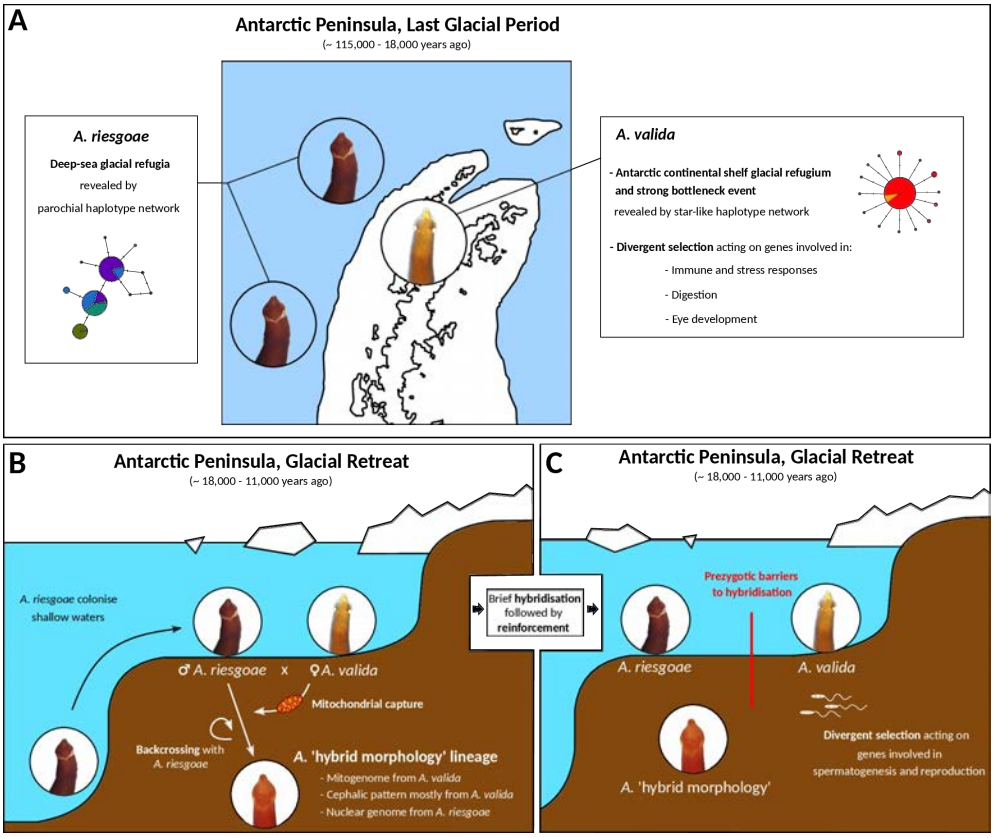

FIGURE 6 Summary figure showing the link between the glacial and hybridising evolutionary history of *Antarctonemertes* in the WAP, and the adaptive loci found in *A. valida*. **(A)** Antarctic Peninsula during the Last Glacial Period, *A. valida* and *A. riesgoae* survived through different glacial-refugium strategies. Then, during the Glacial Retreat, a brief hybridisation event took place after the shallow-water colonisation of *A. riesgoae* **(B)**, followed by a reinforcement event **(C)**.

the Antarctic continental shelf, undergoing severe bottleneck events revealed from its haplotype network with a star-like topology (Figure 2B) and a significantly negative Tajima's D value, which have been described for other Antarctic marine invertebrates (e.g. Díaz et al., 2011; Dietz, Arango, et al., 2015), and correlated to events of Antarctic continental shelf glacial refugia during the last glacial maximum (LGM) (Allcock & Strugnell, 2012; Thatje et al., 2005). In this sense, our EBSP clearly indicated a very recent demographic expansion of the A. valida populations in the Antarctic Peninsula starting at 10,000–15,000 years ago (Figure 2C), which coincides with the time of the glacial retreat in the Antarctic Peninsula after the LGM (Heroy & Anderson, 2007). Contrastingly, our data

RADtag	Contig in reference transcriptome	Annotation	Abbreviation	E-value	Function
11	TRINITY_DN177957_c7_g6	Dynein beta chain, ciliary isoform X6	DNAH6	0	Spermatogenesis and reproduction
115	TRINITY_DN22986_c0_g1	Chymotrypsinogen 2	CTRB1	5.00E-28	Digestion
127	TRINITY_DN6465_c0_g1	Trafficking protein particle complex subunit 8-like isoform X2	TRAPPC8	2.00E-71	Endoplasmic reticulum, Golgi apparatus, and vesicle turnover
167	TRINITY_DN176810_c0_g7	Protein FAM50	FAM50B	6.00E-32	Spermatogenesis and reproduction
336	TRINITY_DN169899_c0_g3	Cholinephosphotransferase 1 isoform X4	CHPT1	5.00E-141	Endoplasmic reticulum, Golgi apparatus, and vesicle turnover
337	TRINITY_DN13418_c0_g2	Ubiquitin carboxyl-terminal hydrolase 30-like	USP30	7.00E-91	Immune and stress responses
617	TRINITY_DN70230_c0_g1	PcSix3/6 Six family protein	SIX3	2.00E-19	Nervous system, brain and eye development
676	TRINITY_DN174290_c5_g1	Centrosomal protein of 70 kDa	CEP70	6.00E-50	Cell division fidelity
679	TRINITY_DN180832_c4_g3	Alpha 1 type IV collagen	COL4A1	8.00E-69	Basement membranes
779	TRINITY_DN29731_c4_g3	Spermine oxidase	SMOX	2.00E-158	Biosynthetic and catabolic processes
894	TRINITY_DN180059_c7_g2	Vacuolar protein sorting-associated protein 13A	VPS13A	2.00E-15	Endoplasmic reticulum, Golgi apparatus, and vesicle turnover
921	TRINITY_DN24523_c0_g1	Maltase-glucoamylase, intestinal-like isoform X2	MGAM	0	Digestion
1043	TRINITY_DN12770_c0_g1	Phosphatidylinositol-glycan biosynthesis class W protein-like isoform X1	PIGW	0.005	Biosynthetic and catabolic processes
1134	TRINITY_DN62340_c0_g1	Serine/threonine-protein kinase 36-like isoform X2	STK36	4.00E-46	Nervous system, brain and eye development
1240	TRINITY_DN12744_c0_g1	N-acetyl-D-glucosamine kinase	NAGK	9.00E-81	Digestion
1465	TRINITY_DN29774_c4_g10	peptide methionine sulfoxide reductase-like	MSRA	2.00E-74	Immune and stress responses
1635	TRINITY_DN81863_c0_g1	tRNA wybutosinesynthesizing protein putative [Fungi]		3.2	
1658	TRINITY_DN26044_c0_g1	RING finger protein 17-like	RNF17	2.00E-20	Spermatogenesis and reproduction
2522	TRINITY_DN167513_c0_g1	Protein PRQFV-amide-like	PRQFVa	1.00E-10	Nervous system, brain and eye development; Digestion
6185	TRINITY_DN11414_c0_g1	L1-like cell adhesion molecule	L1CAM	1.00E-11	Nervous system, brain and eye development
6584	TRINITY_DN154024_c0_g2	Fatty acyl-CoA elongase/Polyunsaturated fatty acid specific elongation	ELOVL6	0.002	Biosynthetic and catabolic processes
6719	TRINITY_DN180630_c4_g1	Titin isoform X12	TTN	6.00E-39	Muscle development and contraction; Cell division fidelity
6809	TRINITY_DN177856_c1_g1	Transmembrane and coiled-coil domains protein 2-like isoform X5	TMCC2	9.00E-115	Endoplasmic reticulum, Golgi apparatus, and vesicle turnover
7571	TRINITY_DN172321_c2_g5	GDP-fucose protein O-fucosyltransferase 1 isoform X2	POFUT1	9.00E-122	Nervous system, brain and eye development
15481	TRINITY_DN14544_c0_g1	Glycerol-3-phosphate dehydrogenase, mitochondrial-like isoform X2	GPD2	1.00E-155	Nervous system, brain and eye development
18027	TRINITY_DN176338_c1_g1	Myeloid differentiation factor 88	MYD88	1.00E-51	Immune and stress responses
19475	TRINITY_DN172366_c0_g2	Zinc finger protein DZIP1 isoform X4	DZIP1	0.68	Spermatogenesis and reproduction
21693	TRINITY_DN180262_c24_g7	Aminotransferase class III-fold pyridoxal phosphate-dependent [Bacteria]		0.66	
22311	TRINITY_DN29807_c1_g1	Dual specificity protein kinase CLK2 isoform X4	CLK2	2.00E-166	RNA processing and splicing
22510	TRINITY_DN27594_c1_g3	peptide methionine sulfoxide reductase-like	MSRA	3.00E-72	Immune and stress responses
24357	TRINITY_DN20670_c0_g1	Speckle targeted PIP5K1A-regulated poly(A) polymerase	TUT1	4.00E-79	RNA processing and splicing
24369	TRINITY_DN173720_c1_g1	Protein lingerer	LIG	5.00E-27	Spermatogenesis and reproduction
25351	TRINITY_DN162646_c0_g4	Transcriptional repressor CTCF-like	CTCF	0.0004	Spermatogenesis and reproduction
25681	TRINITY_DN180285_c1_g1	DJ031_00175 [bacterium endosymbiont of *Escarpia laminata*]		7.00E-173	
26472	TRINITY_DN28452_c0_g1	F-box only protein 16-like	FBXO16	1.00E-87	Immune and stress responses
26965	TRINITY_DN8632_c0_g1	Putative methyltransferase DDB_G0268948-like	DDB1	5.00E-30	Immune and stress responses
26997	TRINITY_DN160354_c0_g1	Glutaredoxin-3	GLRX3	5.00E-27	Immune and stress responses
27043	TRINITY_DN75354_c0_g1	Dimethyladenosine transferase 2, mitochondrial-like isoform X2	TFB2M	2.00E-11	Mitochondrial transcription
27101	TRINITY_DN178646_c5_g6	Conserved oligomeric Golgi complex subunit 7-like	COG7	2.00E-97	Endoplasmic reticulum, Golgi apparatus, and vesicle turnover
29786	TRINITY_DN16781_c0_g2	E3 ubiquitin-protein ligase RNF115-like	RNF115	1.00E-66	Immune and stress responses

TABLE 2 Identified loci with a putative adaptive role for *A. valida* from WAP, and their BLAST annotations and functions.

indicates that A. riesgoae may have survived in deep-sea glacial refugia, presenting a parochial haplotype network, a positive Tajima's D value, and older and more stable populations illustrated by the EBSP (Figure 2C), which have been used as evidences for deep-sea glacial refugia in Antarctica (e.g. Allcock & Strugnell, 2012; Baird et al., 2011). Indeed, although A. riesgoae is very abundant in shallow waters and the intertidal, it is also occasionally found in deeper waters, such as the individual found at 128 m depth off the Antarctic Peninsula (de la Uz, 2005).

Taking into account these contrasting demographic histories, we suggest that the introgressive hybridisation event producing the mitochondrial capture observed in *Antarctonemertes* 'hybrid morphology' occurred after the LGM, during the Antarctic continental shelf colonization of *A. riesgoae* from their deep-sea refugia over the populations of *A. valida* from the WAP (Figure 6B). In these conditions of range expansion of one species over another, mitochondrial captures are frequent (Excoffier et al., 2009; Wielstra & Arntzen, 2012), and hybrids may have been positively selected once because of the higher fitness that may have conferred them the combination of features of both parental species, as has been suggested for other animal hybrids in previous studies (e.g. Cruz, Rolán-Álvarez, & García, 2001; Galindo, Rivas, Saura, & Rolán-Álvarez, 2014; Pfennig, Chunco, & Lackey, 2007). Moreover, the mitochondrial genome commonly introgresses asymmetrically, from the local species to the invading one (Currat et al., 2008; Petit & Excoffier, 2009; Wielstra & Arntzen, 2012), which is the pattern found here: a morphologically hybrid population with the mitochondrial genome from the originally local *A. valida* and a nuclear background of the invading *A. riesgoae* (Figures 2 and 3).

4.2 | Contemporary hybridisation at South Georgia Island

In addition to unveiling two ancient introgressive hybridisation events, our results revealed the presence of hybrid individuals between *A. valida* and *A. riesgoae* at SG (Figure 4). Although previous studies on other nemertean species also suggested hybridisation events in the phylum (e.g. Ament-Velásquez et al., 2016; Maslakova & Norenburg, 2008; Tulchinsky, Norenburg, & Turbeville, 2011), to our knowledge, this is the first time that contemporary natural hybrids are undoubtedly identified using the genome of a representative of the phylum. This contemporary hybridisation is consistent with and possibly facilitated by the historical admixture observed between *A. valida* from SG and the *A. riesgoae* lineage (Figure 3A–B). The hybridisation pattern observed herein indicated that the external morphological traits in the studied species are maternally inherited, because of the coincidence between the cephalic pigmentation and the mitochondrial *COI*

of the hybrids, while the admixture was observed in their nuclear genome-wide markers. This is also consistent with our 'hybrid morphology' individuals, which showed the *COI* haplotype and cephalic colour pattern of mostly *A. valida*, and the nuclear structure of *A. riesgoae*. Another example of hybridisation in Antarctic marine invertebrates is the case of the Southern Ocean giant sea spider *Colossendeis megalonyx*, whose divergent mitochondrial lineages are able to hybridise originating mito-nuclear discordances (Dietz et al., 2015). In contrast to the study regarding *C. megalonyx*, where the authors suggest that the ongoing hybridisation is occurring between linages of the same species (Dietz et al., 2015), we propose here that both *A. valida* and *A. riesgoae* may remain as two different species based on their morphological and genetic differences (Taboada et al., 2013; 2018), despite the high hybridisation potential they present at South Georgia Island.

4.3 | *Linking historical demography with adaptive loci of* Antarctonemertes valida *from the Western Antarctic Peninsula*

Here we suggest that the particular demographic history of *A. valida* from WAP, surviving the LGM in an *in situ* Antarctic continental shelf glacial refugium might have led to adaptive evolution, leaving signals in the nuclear genome. Indeed, although *A. valida* from WAP clustered with *A. valida* from SG in the TreeMix analysis (Figure 3A), both STRUCTURE and *snapclust* analyses clearly indicated a strong divergence in the nuclear genome of *A. valida* from WAP (Figure 3C). Although we cannot discard random genetic drift in the *A. valida* population surviving the LGM in Antarctic shallow waters, our results of 37 annotated adaptive loci seem to rather indicate the importance of adaptation and speciation in the evolutionary history of *A. valida* (Figure 6C).

Six loci were found to be related to spermatogenesis and reproduction (Table 2), fundamental functions that are commonly found under selection or presenting rapid evolutionary rates in studies involving speciation, sexual selection, and reproductive isolation (e.g. Civetta, Rajakumar, Brouwers, & Bacik, 2005; Foote, 2018; Llopart & Comeron, 2006). Mutations in one of the genes in this class, *DNAH6*, have been identified as responsible for azoospermia in humans (Gershoni et al., 2017), highlighting its relevance in spermatogenesis. Likewise, changes in DNA methylation of *FAM50B* are associated to low sperm motility in infertile men (Xu et al., 2016). *RNF17* and *DZIP1* are also crucial for spermatogenesis (VanGompel & Xu, 2011; Wasik et al., 2015), while *LIG* is related to male mating behaviour and control of copulatory organs in *Drosophila* (Kuniyoshi et al., 2002). Selective pressure in these genes may have led to differences in the sperm, copulation, and reproductive behaviour of *A. valida* from the WAP, acting as prezygotic barriers during

a possible reinforcement event (selection against hybrids) after a secondary contact. This is in agreement with the absence of contemporary hybridisation between *A. riesgoae* and *A. valida* in the Antarctic Peninsula and also with the apparently brief hybridisation event that resulted in the mitochondrial capture within the individuals ascribed to the *Antarctonemertes* 'hybrid morphology'. To our knowledge, only two studies have investigated genomic signatures of reinforcement, in the Texas wildflower *Phlox* genus (Hopkins, Levin, & Rausher, 2012) and in the hybrid zone between the mice *Mus musculus musculus* and *M. m. domesticus* (Smadja et al., 2015). In agreement with our results for *Antarctonemertes*, both studies found signals of reinforcement in genes involved in reproductive functions: in the colouration of the *Phlox* flowers and in pheromone signalling and olfactory recognition in *Mus musculus*.

We also identified eight genes directly related to the immune and stress responses (Table 2), prevalent functions appearing in studies concerning local adaptation (e. g. Gleason & Burton, 2016; Leiva et al., 2019; VanWallendael et al., 2019). Among them, *USP30*, *FBXO16*, and *RNF115* are related to ubiquitination, an essential function for removing macromolecular debris generated by different cellular stresses (Kültz, 2003). Moreover, ubiquitination is also involved in the immune system, regulating the pattern-recognition receptor signalling that mediates immune responses (Hu & Sun, 2016). Similarly, adaptive selection found in five genes related to the Endoplasmic Reticulum, Golgi apparatus, and vesicle turnover (Table 2) may also be due to an adaptation of the cellular stress response, because of the pivotal role of the endomembranous compartments in oxidative, hypotonic, and salt stresses (Jiang & Storrie, 2005; Malhotra & Kaufman, 2007; Jiang et al., 2011; Kang et al., 2008). Additionally, we identified six genes with functions related to the nervous system, brain, and eye development (Table 2). Specifically, the transcription factor *SIX3* and its homologous genes, play crucial roles on the development of the entire visual system (Cheyette et al., 1994; Oliver et al., 1995), trigging the genetic pathway leading to lens formation (see Sinn & Wittbrodt, 2010). Also, we identified four loci with digestion functions, for instance, *PRQFVa*, which in *Aplysia* is linked to the neural system modulating the feeding system (Furukawa et al., 2003). An adaptation in the visual and digestive systems and in the immune and cellular stress response is consistent with the *in situ* glacial refugium in Antarctic shallow waters identified for *A. valida*. Indeed, water conditions and planktonic communities and dynamics in polynyas vastly differ from open coastal environments (Arrigo & van Dijken, 2003; 2004; Smith & Gordon, 1997), which may have required these adaptations in *A. valida*. Although RADseq techniques only cover a tiny portion of the entire genome, they

are considered well suited for genome scans for adaptive variation (e.g. Catchen et al., 2017, Gleason & Burton, 2016). Hence, although the genomic adaptation of *A. valida* from WAP must imply other regions not captured by our approach, we lay the foundations here to understand the genetic bases of adaptation and speciation of Antarctic marine organisms.

Conclusions

In this study, we aimed to shed light on the phylogeographic and evolutionary history of the Antarctic *Antarctonemertes* with a special focus on the species boundaries through time and space, contrasting the information from both mitochondrial (*COI*) and nuclear markers (ddRADseq-derived SNPs). We detected two ancient introgressive hybridisation events among the species, as well as current hybridisation between the populations of *A. valida* and *A. riesgoae* in South Georgia Island. Our results, consistent with other genome-wide studies on non-model organisms (see Taylor & Larson, 2019), challenge species concepts that require intrinsic reproductive isolation, highlighting the pervasive occurrence of hybridisation in nature, both in the past and in the present. Moreover, we identified and annotated 37 loci that could have played a role in the adaptation and survival of *A. valida* in its refugium during the last glacial period, and found six loci with reproductive functions that may have been involved in a reinforcement event, rising prezygotic barriers to gene flow. Due to the glacial history of Antarctica and its effects on shallow-water organisms (see Allcock & Strugnell, 2012), we suggest that more studies focusing on their evolutionary histories accounting for introgressive hybridisation events should be addressed, using a combination of mitochondrial and genome-wide nuclear markers when possible.

Acknowledgements

We are indebted to Patricia Álvarez-Campos, Oriol Sacristán, Javier Cristobo, Juan Junoy, Carlos Angulo-Preckler, Blanca Figuerola, Conxita Ávila, 'Pacote', Miguel Ángel Ojeda, Sacha Cleminson, and Frances Alexander for their help collecting samples. We really thank the excellent job of the Spanish Antarctic Base Gabriel de Castilla, BIO Hespérides, and PHAROS SG crews during the rough conditions accompanying expeditions in Antarctic

waters. We thank all members of the Giribet Lab and Riesgo Lab for their help and support during laboratory work, as well as the technical support from the Bauer Core Facilities (Harvard University) and the NHM Sequencing Facilities. Special thanks are given to Elena San Miguel for her computing support and to Thibaut Jombart, Vanina Tonzo, and Eugènia Almacellas for their help analysing data and discussing results. This work was supported by three DIF grants of the Natural History Museum of London (SDF14032 and SDR17012) to A.R., the Heredity Fieldwork Grant from The Genetics Society to C.L., and two grants from the Spanish Ministry of Economy and Competitiveness in which A.R., S.T., G.G., J.M., and C.L. have been involved (ACTIQUIM II: CTM2010-17415/ANT and DISTANTCOM: CTM2013-42667/ANT).

Author Contributions

All authors conceived and designed the study, conducted fieldwork and collected samples, conducted laboratory work, performed statistical analyses, and interpreted the results; C.L. wrote the first version of the manuscript, A.R. and S.T. contributed to the final version of the manuscript.

References

Allcock, A. L., & Strugnell, J. M. (2012). Southern Ocean diversity: new paradigms from molecular ecology. *Trends in Ecology & Evolution*, *27*, 520-528.

Altschul, S. F., Gish, W., Miller, W., Myers, E. W., & Lipman, D. J. (1990). Basic local alignment search tool. *Journal of Molecular Biology*, *215*, 403-410.

Altschul, S. F., Madden, T. L., Schäffer, A. A., Zhang, J., Zhang, Z., Miller, W., & Lipman, D. J. (1997). Gapped BLAST and PSI-BLAST: a new generation of protein database search programs. *Nucleic Acids Research*, *25*, 3389-3402.

Ament-Velásquez, S. L., Figuet, E., Ballenghien, M., Zattara, E. E., Norenburg, J. L., Fernández-Álvarez, F. A., ... & Galtier, N. (2016). Population genomics of sexual and asexual lineages in fissiparous ribbon worms (Lineus, Nemertea): hybridisation, polyploidy and the

Meselson effect. *Molecular Ecology*, *25*, 3356-3369.

Andrews, K. R., Good, J. M., Miller, M. R., Luikart, G., & Hohenlohe, P. A. (2016). Harnessing the power of RADseq for ecological and evolutionary genomics. *Nature Reviews Genetics*, *17*, 81.

Andrews, S. (2010) FastQC: A quality control tool for high throughput sequence data. Available online at: http://www.bioinformatics.babraham.ac.uk/projects/fastqc

Arnold, M. L., & Kunte, K. (2017). Adaptive genetic exchange: a tangled history of admixture and evolutionary innovation. *Trends in Ecology & Evolution*, *32*, 601-611.

Arrigo, K. R., & Van Dijken, G. L. (2003). Phytoplankton dynamics within 37 Antarctic coastal polynya systems. *Journal of Geophysical Research: Oceans*, *108*.

Arrigo, K. R., & van Dijken, G. L. (2004). Annual changes in sea-ice, chlorophyll a, and primary production in the Ross Sea, Antarctica. *Deep Sea Research Part II: Topical Studies in Oceanography*, *51*, 117-138.

Baird, H. P., Miller, K. J., & Stark, J. S. (2011). Evidence of hidden biodiversity, ongoing speciation and diverse patterns of genetic structure in giant Antarctic amphipods. *Molecular Ecology*, *20*, 3439-3454.

Bandelt, H. J., Forster, P., & Röhl, A. (1999). Median-joining networks for inferring intraspecific phylogenies. *Molecular Biology and Evolution*, *16*, 37-48.

Banguera-Hinestroza, E., Sawall, Y., Al-Sofyani, A., Mardulyn, P., Fuertes-Aguilar, J., Cardenas-Henao, H., ... & Flot, J. F. (2018). mtDNA recombination indicative of hybridisation suggest a role of the mitogenome in the adaptation of reef building corals to extreme environments. *bioRxiv*, 462069.

Bernal, M. A., Gaither, M. R., Simison, W. B., & Rocha, L. A. (2017). Introgression and selection shaped the evolutionary history of sympatric sister species of coral reef fishes (genus: Haemulon). *Molecular Ecology*, *26*, 639-652.

Beugin, M. P., Gayet, T., Pontier, D., Devillard, S., & Jombart, T. (2018). A fast likelihood solution to the genetic clustering problem. *Methods in Ecology and Evolution*, *9*, 1006-1016.

Blackmon, H., & Adams, R. A. (2015). EvobiR: tools for comparative analyses and teaching evolutionary biology. https://doi.org/10.5281/zenodo.30938.

Blanco-Bercial, L., & Bucklin, A. (2016). New view of population genetics of zooplankton: RADseq analysis reveals population structure of the North Atlantic planktonic copepod *Centropages typicus*. *Molecular Ecology*, *25*, 1566-1580.

Bolger, A. M., Lohse, M., & Usadel, B. (2014). Trimmomatic: a flexible trimmer for Illumina sequence data. *Bioinformatics*, *30*, 2114-2120.

Bouchemousse, S., Liautard-Haag, C., Bierne, N., & Viard, F. (2016). Distinguishing contemporary hybridisation from past introgression with postgenomic ancestry-informative SNP s in strongly differentiated Ciona species. *Molecular Ecology*, *25*, 5527-5542.

Bouckaert, R., Heled, J., Kühnert, D., Vaughan, T., Wu, C. H., Xie, D., ... & Drummond, A. J. (2014). BEAST 2: a software platform for Bayesian evolutionary analysis. *PLoS Computational Biology*, *10*, e1003537.

Catchen, J. M., Hohenlohe, P. A., Bassham, S., Amores, A., & Cresko, W. A. (2013). Stacks: an analysis tool set for population genomics. *Molecular Ecology*, *22*, 3124-3140.

Catchen, J. M., Hohenlohe, P. A., Bernatchez, L., Funk, W. C., Andrews, K. R., & Allendorf, F. W. (2017). Unbroken: RADseq remains a powerful tool for understanding the genetics of adaptation in natural populations. *Molecular Ecology Resources*, *17*, 362-365.

Chan, K. M., & Levin, S. A. (2005). Leaky prezygotic isolation and porous genomes: rapid introgression of maternally inherited DNA. *Evolution*, *59*, 720-729.

Cheyette, B. N., Green, P. J., Martin, K., Garren, H., Hartenstein, V., & Zipursky, S. L. (1994). The Drosophila sine oculis locus encodes a homeodomain-containing protein required for the development of the entire visual system. *Neuron*, *12*, 977-996.

Civetta, A., Rajakumar, S. A., Brouwers, B., & Bacik, J. P. (2005). Rapid evolution and gene-specific patterns of selection for three genes of spermatogenesis in Drosophila. *Molecular Biology and Evolution*, *23*, 655-662.

Clarke, A., & Johnston, I. A. (1996). Evolution and adaptive radiation of Antarctic fishes. *Trends in Ecology & Evolution*, *11*, 212-218.

Collins, E. E., Galaska, M. P., Halanych, K. M., & Mahon, A. R. (2018). Population genomics of *Nymphon australe* Hodgson, 1902 (Pycnogonida, Nymphonidae) in the Western Antarctic. *The Biological Bulletin*, *234*, 180-191.

Combosch, D. J., & Vollmer, S. V. (2015). Trans-Pacific RAD-Seq population genomics confirms introgressive hybridisation in Eastern Pacific Pocillopora corals. *Molecular Phylogenetics and Evolution*, *88*, 154-162.

Cruz, R., Rolán-Álvarez, E., & García, C. (2001). Sexual selection on phenotypic traits in a hybrid zone of Littorina saxatilis (Olivi). *Journal of Evolutionary Biology*, *14*, 773-785.

Currat, M., Ruedi, M., Petit, R. J., & Excoffier, L. (2008). The hidden side of invasions: massive introgression by local genes. *Evolution: International Journal of Organic Evolution*, *62*, 1908-1920.

de la Uz S (2005) Fauna bentónica de nemertinos (Hoplonemertea) antárticos – BENTART 2003. Seminario de Investigación. Universidad de Oviedo. http://www.bentart.es/articulos/De_la_Uz__Nemertinos_DEA_Univ_Oviedo.pdf. Accessed 5 June 2019.

Deagle, B. E., Faux, C., Kawaguchi, S., Meyer, B., & Jarman, S. N. (2015). Antarctic krill population genomics: apparent panmixia, but genome complexity and large population size muddy the water. *Molecular Ecology*, *24*, 4943-4959.

Díaz, A., Féral, J. P., David, B., Saucède, T., & Poulin, E. (2011). Evolutionary pathways among shallow and deep-sea echinoids of the genus *Sterechinus* in the Southern Ocean. *Deep Sea Research Part II: Topical Studies in Oceanography*, *58*, 205-211.

Dietz, L., Arango, C. P., Dömel, J. S., Halanych, K. M., Harder, A. M., Held, C., ... & Weis, A. (2015). Regional differentiation and extensive hybridisation between mitochondrial clades of the Southern Ocean giant sea spider *Colossendeis megalonyx*. *Royal Society Open Science*, *2*, 140424.

Dray, S., & Dufour, A. B. (2007). The ade4 package: implementing the duality diagram for ecologists. *Journal of Statistical Software*, *22*, 1-20.

Durand, E. Y., Patterson, N., Reich, D., & Slatkin, M. (2011). Testing for ancient admixture between closely related populations. *Molecular Biology and Evolution*, *28*, 2239-2252.

Earl, D. A. (2012). STRUCTURE HARVESTER: a website and program for visualizing STRUCTURE output and implementing the Evanno method. *Conservation Genetics Resources*, *4*, 359-361.

Excoffier, L., Foll, M., & Petit, R. J. (2009). Genetic consequences of range expansions. *Annual Review of Ecology, Evolution, and Systematics*, *40*, 481-501.

Feder, J. L., Egan, S. P., & Nosil, P. (2012). The genomics of speciation-with-gene-flow. *Trends in Genetics*, *28*, 342-350.

Foll, M. & Gaggiotti, O. E. (2008) A genome scan method to identify selected loci appropriate for both dominant and codominant markers: A Bayesian perspective. *Genetics*, *180*, 977-993

Foote, A. D. (2018). Sympatric speciation in the genomic era. Trends in Ecology & Evolution, 33, 85-95.

Furukawa, Y., Nakamaru, K., Sasaki, K., Fujisawa, Y., Minakata, H., Ohta, S., ... & Ellis, T. A. (2003). PRQFVamide, a novel pentapeptide identified from the CNS and gut of Aplysia. Journal of Neurophysiology, 89, 3114-3127.

Galaska, M. P., Sands, C. J., Santos, S. R., Mahon, A. R., & Halanych, K. M. (2017a). Geographic structure in the Southern Ocean circumpolar brittle star Ophionotus victoriae (Ophiuridae) revealed from mtDNA and single-nucleotide polymorphism data. Ecology and Evolution, 7, 475-485.

Galaska, M. P., Sands, C. J., Santos, S. R., Mahon, A. R., & Halanych, K. M. (2017b). Crossing the divide: admixture across the Antarctic polar front revealed by the brittle star Astrotoma agassizii. The Biological Bulletin, 232, 198-211.

Galindo, J., Rivas, M. J., Saura, M., & Rolan-Alvarez, E. (2014). Selection on hybrids of ecologically divergent ecotypes of a marine snail: the relative importance of exogenous and endogenous barriers. Biological journal of the Linnean Society, 111(2), 391-400.

Gershoni, M., Hauser, R., Yogev, L., Lehavi, O., Azem, F., Yavetz, H., ... & Kleiman, S. E. (2017). A familial study of azoospermic men identifies three novel causative mutations in three new human azoospermia genes. Genetics in Medicine, 19, 998.

Gleason, L. U., & Burton, R. S. (2016). Genomic evidence for ecological divergence against a background of population homogeneity in the marine snail Chlorostoma funebralis. Molecular Ecology, 25, 3557-3573.

Gompert, Z., Lucas, L. K., Nice, C. C., Fordyce, J. A., Forister, M. L., & Buerkle, C. A. (2012). Genomic regions with a history of divergent selection affect fitness of hybrids between two butterfly species. Evolution: International Journal of Organic Evolution, 66, 2167-2181.

González-Wevar, C. A., Saucède, T., Morley, S. A., Chown, S. L., & Poulin, E. (2013). Extinction and recolonization of maritime Antarctica in the limpet Nacella concinna (Strebel, 1908) during the last glacial cycle: toward a model of Quaternary biogeography in shallow Antarctic invertebrates. Molecular Ecology, 22, 5221-5236.

Goudet, J. (2005). Hierfstat, a package for R to compute and test hierarchical F-statistics. Molecular Ecology Notes, 5, 184-186.

Grabherr, M. G., Haas, B. J., Yassour, M., Levin, J. Z., Thompson, D. A., Amit, I., ... & Chen, Z. (2011). Trinity: reconstructing a full-length transcriptome without a genome from RNA-Seq data. *Nature Biotechnology*, *29*, 644.

Harper, F. M., Addison, J. A., & Hart, M. W. (2007). Introgression versus immigration in hybridising high dispersal echinoderms. *Evolution: International Journal of Organic Evolution*, *61*, 2410-2418.

Hatta, M., Fukami, H., Wang, W., Omori, M., Shimoike, K., Hayashibara, T., ... & Sugiyama, T. (1999). Reproductive and genetic evidence for a reticulate evolutionary history of mass-spawning corals. *Molecular Biology and Evolution*, *16*, 1607-1613.

Held, C., & Wägele, J. W. (2005). Cryptic speciation in the giant Antarctic isopod *Glyptonotus antarcticus* (Isopoda: Valvifera: Chaetiliidae). *Scientia Marina*, *69*, 175-181.

Heroy, D. C., & Anderson, J. B. (2007). Radiocarbon constraints on Antarctic Peninsula ice sheet retreat following the Last Glacial Maximum (LGM). *Quaternary Science Reviews*, *26*, 3286-3297.

Hopkins, R., Levin, D. A., & Rausher, M. D. (2012). Molecular signatures of selection on reproductive character displacement of flower color in *Phlox drummondii*. *Evolution: International Journal of Organic Evolution*, *66*, 469-485.

Hu, H., & Sun, S. C. (2016). Ubiquitin signaling in immune responses. *Cell Research*, *26*, 457.

Ivanov, V., Lee, K. M., & Mutanen, M. (2018). Mitonuclear discordance in wolf spiders: Genomic evidence for species integrity and introgression. *Molecular Ecology*, *27*, 1681-1695.

Jakobsson, M., & Rosenberg, N. A. (2007). CLUMPP: a cluster matching and permutation program for dealing with label switching and multimodality in analysis of population structure. *Bioinformatics*, *23*, 1801-1806.

Jeffries, D. L., Copp, G. H., Lawson Handley, L., Olsén, K. H., Sayer, C. D., & Hänfling, B. (2016). Comparing RAD seq and microsatellites to infer complex phylogeographic patterns, an empirical perspective in the Crucian carp, *Carassius carassius*, L. *Molecular Ecology*, *25*, 2997-3018.

Jiang, S., & Storrie, B. (2005). Cisternal rab proteins regulate Golgi appparatus redistribution in response to hypotonic stress. *Molecular Biology of the Cell*, *16*, 2586-2596.

Jiang, Z., Hu, Z., Zeng, L., Lu, W., Zhang, H., Li, T., & Xiao, H. (2011). The role of the Golgi apparatus in oxidative stress: is this organelle less significant than mitochondria? *Free Radical Biology and Medicine*, *50*, 907-917.

Jombart, T. (2008). adegenet: a R package for the multivariate analysis of genetic markers. *Bioinformatics*, *24*, 1403-1405.

Jombart, T., & Ahmed, I. (2011). adegenet 1.3-1: new tools for the analysis of genome-wide SNP data. *Bioinformatics*, *27*, 3070-3071.

Jombart, T., & Collins, C. (2015). A tutorial for discriminant analysis of principal

components (DAPC) using adegenet 2.0. 0. *London: Imperial College London, MRC Centre for Outbreak Analysis and Modelling*.

Jombart, T., Devillard, S., & Balloux, F. (2010). Discriminant analysis of principal components: a new method for the analysis of genetically structured populations. *BMC Genetics*, *11*, 94.

Kamvar, Z. N., Tabima, J. F., & Grünwald, N. J. (2014). Poppr: an R package for genetic analysis of populations with clonal, partially clonal, and/or sexual reproduction. *PeerJ*, *2*, e281.

Kang, J. S., Frank, J., Kang, C. H., Kajiura, H., Vikram, M., Ueda, A., ... & Lee, S. Y. (2008). Salt tolerance of Arabidopsis thaliana requires maturation of N-glycosylated proteins in the Golgi apparatus. *Proceedings of the National Academy of Sciences*, *105*, 5933-5938.

Katoh, K., Misawa, K., Kuma, K. I., & Miyata, T. (2002). MAFFT: a novel method for rapid multiple sequence alignment based on fast Fourier transform. *Nucleic Acids Research*, *30*, 3059-3066.

Kearse, M., Moir, R., Wilson, A., Stones-Havas, S., Cheung, M., Sturrock, S., ... & Thierer, T. (2012). Geneious Basic: an integrated and extendable desktop software platform for the organization and analysis of sequence data. *Bioinformatics*, *28*, 1647-1649.

Keenan, K., McGinnity, P., Cross, T. F., Crozier, W. W., & Prodöhl, P. A. (2013). diveRsity: An R package for the estimation and exploration of population genetics parameters and their associated errors. *Methods in Ecology and Evolution*, *4*, 782-788.

Krabbe, K., Leese, F., Mayer, C., Tollrian, R., & Held, C. (2010). Cryptic mitochondrial lineages in the widespread pycnogonid *Colossendeis megalonyx* Hoek, 1881 from Antarctic and Subantarctic waters. *Polar Biology*, *33*, 281-292.

Kültz, D. (2003). Evolution of the cellular stress proteome: from monophyletic origin to ubiquitous function. *Journal of Experimental Biology*, *206*, 3119-3124.

Kuniyoshi, H., Baba, K., Ueda, R., Kondo, S., Awano, W., Juni, N., & Yamamoto, D. (2002). *lingerer*, a Drosophila gene involved in initiation and termination of copulation, encodes a set of novel cytoplasmic proteins. *Genetics*, *162*, 1775-1789.

Lack, J. B., Greene, D. U., Conroy, C. J., Hamilton, M. J., Braun, J. K., Mares, M. A., & Van Den Bussche, R. A. (2012). Invasion facilitates hybridisation with introgression in the *Rattus rattus* species complex. *Molecular Ecology*, *21*, 3545-3561.

Leiva, C., Taboada, S., Kenny, N. J., Combosch, D., Giribet, G., Jombart, T., & Riesgo, A. (2019). Population substructure and signals of divergent adaptive selection despite admixture in the sponge *Dendrilla antarctica* from shallow waters surrounding the

Antarctic Peninsula. *Molecular Ecology*, *28*, 3151-3170.

Li, G., Davis, B. W., Eizirik, E., & Murphy, W. J. (2016). Phylogenomic evidence for ancient hybridisation in the genomes of living cats (Felidae). *Genome Research*, *26*, 1-11.

Llopart, A., & Comeron, J. M. (2008). Recurrent events of positive selection in independent *Drosophila* lineages at the spermatogenesis gene roughex. *Genetics*, *179*, 1009-1020.

Mahon, A. R., Thornhill, D. J., Norenburg, J. L., & Halanych, K. M. (2010). DNA uncovers Antarctic nemertean biodiversity and exposes a decades-old cold case of asymmetric inventory. *Polar Biology*, *33*, 193-202.

Malhotra, J. D., & Kaufman, R. J. (2007). Endoplasmic reticulum stress and oxidative stress: a vicious cycle or a double-edged sword?. *Antioxidants & Redox Signaling*, *9*, 2277-2294.

Malinsky, M., Trucchi, E., Lawson, D. J., & Falush, D. (2018). RADpainter and fineRADstructure: population inference from RADseq data. *Molecular Biology and Evolution*, *35*(5), 1284-1290.

Manni, F., Guerard, E., & Heyer, E. (2004). Geographic patterns of (genetic, morphologic, linguistic) variation: how barriers can be detected by using Monmonier's algorithm. *Human Biology*, *76*, 173-190.

Martin, S. H., Davey, J. W., & Jiggins, C. D. (2014). Evaluating the use of ABBA–BABA statistics to locate introgressed loci. *Molecular Biology and Evolution*, *32*, 244-257.

Maslakova, S. A., & Norenburg, J. L. (2008). Revision of the smiling worms, genus *Prosorhochmus* Keferstein, and description of a new species, *Prosorhochmus belizeanus* sp. nov.(Prosorhochmidae, Hoplonemertea, Nemertea) from Florida and Belize. *Journal of Natural History*, *42*, 1219-1260.

Mayr, E. (1963). Animal Species and Evolution. *Belknap Press*, *Cambridge*, *Massacusetts*.

Mcfadden, C. S., & Hutchinson, M. B. (2004). Molecular evidence for the hybrid origin of species in the soft coral genus *Alcyonium* (Cnidaria: Anthozoa: Octocorallia). *Molecular Ecology*, *13*, 1495-1505.

Nadeau, N. J., Martin, S. H., Kozak, K. M., Salazar, C., Dasmahapatra, K. K., Davey, J. W., ... & Jiggins, C. D. (2013). Genome-wide patterns of divergence and gene flow across a butterfly radiation. *Molecular Ecology*, *22*, 814-826.

Oliver, G., Mailhos, A., Wehr, R., Copeland, N. G., Jenkins, N. A., & Gruss, P. (1995). Six3, a murine homologue of the sine oculis gene, demarcates the most anterior border of the developing neural plate and is expressed during eye development. *Development*, *121*, 4045-4055.

Paradis, E. (2010). pegas: an R package for population genetics with an integrated–modular approach. *Bioinformatics*, *26*, 419-420.

Paradis, E., Claude, J., & Strimmer, K. (2004). APE: analyses of phylogenetics and evolution in R language. *Bioinformatics*, *20*, 289-290.

Paris, J. R., Stevens, J. R., & Catchen, J. M. (2017). Lost in parameter space: a road map for stacks. *Methods in Ecology and Evolution*, *8*, 1360-1373.

Patterson, N., Moorjani, P., Luo, Y., Mallick, S., Rohland, N., Zhan, Y., ... & Reich, D. (2012). Ancient admixture in human history. *Genetics*, *192*, 1065-1093.

Perry, K. D., Baker, G. J., Powis, K. J., Kent, J. K., Ward, C. M., & Baxter, S. W. (2018). Cryptic *Plutella* species show deep divergence despite the capacity to hybridise. *BMC Evolutionary Biology*, *18*, 77.

Petit, R. J., & Excoffier, L. (2009). Gene flow and species delimitation. *Trends in Ecology & Evolution*, *24*, 386-393.

Pfennig, K. S., Chunco, A. J., & Lackey, A. C. (2007). Ecological selection and hybrid fitness: hybrids succeed on parental resources. *Evolutionary Ecology Research*, *9*, 341-354.

Pickrell, J. K., & Pritchard, J. K. (2012). Inference of population splits and mixtures from genome-wide allele frequency data. *PLoS Genetics*, *8*, e1002967.

Posada, D. (2008). jModelTest: phylogenetic model averaging. *Molecular Biology and Evolution*, *25*, 1253-1256.

Pritchard, J. K., Stephens, M., & Donnelly, P. (2000). Inference of population structure using multilocus genotype data. *Genetics*, *155*, 945-959.

R Core Team (2014). A language and environment for statistical computing. http://www.R-project.org.

Rambaut, A., Drummond, A. J., Xie, D., Baele, G., & Suchard, M. A. (2018). Posterior summarization in Bayesian phylogenetics using Tracer 1.7. *Systematic Biology*, *67*, 901-904.

Reich, D., Green, R. E., Kircher, M., Krause, J., Patterson, N., Durand, E. Y., ... & Maricic, T. (2010). Genetic history of an archaic hominin group from Denisova Cave in Siberia. *Nature*, *468*, 1053.

Riesgo, A., Pérez-Portela, R., Pita, L., Blasco, G., Erwin, P. M., & López-Legentil, S. (2016). Population structure and connectivity in the Mediterranean sponge *Ircinia fasciculata* are

affected by mass mortalities and hybridisation. *Heredity*, *117*, 427.

Rogers, A. D. (2007). Evolution and biodiversity of Antarctic organisms: a molecular perspective. *Philosophical Transactions of the Royal Society B: Biological Sciences*, *362*, 2191-2214.

Ronquist, F., & Huelsenbeck, J. P. (2003). MrBayes 3: Bayesian phylogenetic inference under mixed models. *Bioinformatics*, *19*, 1572-1574.

Seehausen, O., Butlin, R. K., Keller, I., Wagner, C. E., Boughman, J. W., Hohenlohe, P. A., ... & Brelsford, A. (2014). Genomics and the origin of species. *Nature Reviews Genetics*, *15*, 176.

Sinn, R., & Wittbrodt, J. (2013). An eye on eye development. *Mechanisms of Development*, *130*, 347-358.

Smadja, C. M., Loire, E., Caminade, P., Thoma, M., Latour, Y., Roux, C., ... & Boursot, P. (2015). Seeking signatures of reinforcement at the genetic level: a hitchhiking mapping and candidate gene approach in the house mouse. *Molecular Ecology*, *24*, 4222-4237.

Smith Jr, W. O., & Gordon, L. I. (1997). Hyperproductivity of the Ross Sea (Antarctica) polynya during austral spring. *Geophysical Research Letters*, *24*, 233-236.

Stamatakis, A. (2014). RAxML version 8: a tool for phylogenetic analysis and post-analysis of large phylogenies. *Bioinformatics*, *30*, 1312-1313.

Sundberg, P., Kvist, S., & Strand, M. (2016). Evaluating the utility of single-locus DNA barcoding for the identification of ribbon worms (phylum Nemertea). *PLoS One*, *11*, e0155541.

Taboada, S., Junoy, J., Andrade, S. C., Giribet, G., Cristobo, J., & Avila, C. (2013). On the identity of two Antarctic brooding nemerteans: redescription of *Antarctonemertes valida* (Bürger, 1893) and description of a new species in the genus *Antarctonemertes* Friedrich, 1955 (Nemertea, Hoplonemertea). *Polar Biology*, *36*, 1415-1430.

Taboada, S., Leiva, C., Junoy, J., Alexander, F., & Riesgo, A. (2018). A new member of the genus *Antarctonemertes* (Hoplonemertea, Nemertea) from Antarctic waters. *Polar Biology*, *41*, 1463-1473.

Tajima, F. (1989). Statistical method for testing the neutral mutation hypothesis by DNA polymorphism. *Genetics*, *123*, 585-595.

Taylor, S. A., & Larson, E. L. (2019). Insights from genomes into the evolutionary importance and prevalence of hybridisation in nature. *Nature Ecology & Evolution*, *3*, 170.

Thatje, S., Hillenbrand, C. D., & Larter, R. (2005). On the origin of Antarctic marine benthic community structure. *Trends in Ecology & Evolution*, *20*, 534-540.

Toews, D. P., & Brelsford, A. (2012). The biogeography of mitochondrial and nuclear discordance in animals. *Molecular Ecology*, *21*, 3907-3930.

Tulchinsky, A. Y., Norenburg, J. L., & Turbeville, J. M. (2012). Phylogeography of the marine interstitial nemertean *Ototyphlonemertes parmula* (Nemertea, Hoplonemertea) reveals cryptic diversity and high dispersal potential. *Marine Biology*, *159*, 661-674.

Van Oppen, M. J., Willis, B. L., Van Rheede, T., & Miller, D. J. (2002). Spawning times, reproductive compatibilities and genetic structuring in the *Acropora aspera* group: evidence for natural hybridisation and semi permeable species boundaries in corals. *Molecular Ecology*, *11*, 1363-1376.

VanGompel, M. J., & Xu, E. Y. (2011). The roles of the DAZ family in spermatogenesis: more than just translation? *Spermatogenesis*, *1*, 36-46.

VanWallendael, A., Soltani, A., Emery, N. C., Peixoto, M. M., Olsen, J., & Lowry, D. B. (2019). A Molecular View of Plant Local Adaptation: Incorporating Stress-Response Networks. *Annual Review of Plant Biology*, *70*.

Wasik, K. A., Tam, O. H., Knott, S. R., Falciatori, I., Hammell, M., Vagin, V. V., & Hannon, G. J. (2015). RNF17 blocks promiscuous activity of PIWI proteins in mouse testes. *Genes & Development*, *29*, 1403-1415.

Weber, A. A. T., Stöhr, S., & Chenuil, A. (2019). Species delimitation in the presence of strong incomplete lineage sorting and hybridisation: lessons from *Ophioderma* (Ophiuroidea: Echinodermata). *Molecular Phylogenetics and Evolution*, *131*, 138-148.

Wickham, H. (2016) *ggplot2*: Elegant Graphics for Data Analysis. Springer-Verlag New York.

Wielstra, B., & Arntzen, J. W. (2012). Postglacial species displacement in *Triturus* newts deduced from asymmetrically introgressed mitochondrial DNA and ecological niche models. *BMC Evolutionary Biology*, *12*, 161.

Wilson, N. G., Hunter, R. L., Lockhart, S. J., & Halanych, K. M. (2007). Multiple lineages and absence of panmixia in the “circumpolar” crinoid Promachocrinus kerguelensis from the Atlantic sector of Antarctica. Marine Biology, 152, 895-904.

Xu, J., Zhang, A., Zhang, Z., Wang, P., Qian, Y., He, L., ... & Du, J. (2016). DNA methylation levels of imprinted and nonimprinted genes DMR s associated with defective human spermatozoa. Andrologia, 48, 1027-1035.

CHAPTER 4

Towards a network of connected Marine Protected Areas in Antarctica: insights from genetic connectivity of benthic invertebrates

[1]Department of Life Sciences, The Natural History Museum of London, London, UK

[2]Department of Genetics, Microbiology and Statistics, Faculty of Biology, University of Barcelona, Barcelona, Spain

[3]Marine Laboratory, University of Guam, Mangilao, Guam

[4]Department of Organismic and Evolutionary Biology, Harvard University, Cambridge, Massachusetts, USA

[5]Australian National University, Canberra, Australia

[6]Department of Biology (Zoology), Faculty of Science, Autonomous University of Madrid, Madrid, Spain

Towards a network of connected Marine Protected Areas in Antarctica: insights from genetic connectivity of benthic invertebrates

Authors:

Carlos Leiva[1,2], David Combosch[3], Gonzalo Giribet[4], Rachel Downey[5], Ana Riesgo[1], Sergi Taboada[1,6]

Abstract

Networks of connected Marine Protected Areas (MPAn) are recognised as the key area-based management tool in order to preserve biodiversity, conduct a rational use of the marine living resources, and increase ecological resilience to climate change. Regardless of the paramount role of larval dispersal and gene flow in metapopulation persistence, genetic connectivity is not generally considered during MPA design. In the Southern Ocean, due to the unique condition of the Antarctic continent lacking national sovereignty, MPAs are implemented by the international Commission for the Conservation of the Antarctic Marine Living Resources (CCAMLR), but their efforts are usually hindered by fishing interests. Here, we assessed the genetic connectivity of five benthic invertebrates with contrasting reproductive strategies between the South Georgia and South Sandwich Islands MPA (SGSSI MPA), the South Orkney Islands, and the Western Antarctic Peninsula region, where an MPA was proposed (Domain 1 MPA, D1MPA) but rejected in the 2018 CCAMLR Meeting. Using mitochondrial and genome-wide markers we obtained a consistent lack of contemporary connectivity between SGSSI MPA and the WAP region for all the studied species. Moreover, a review of the population genetic studies on benthic invertebrates carried out in the study area largely confirmed our results, expanding our conclusions to the community level. Additionally, our results suggested a stepping-stone role of South Orkney Islands between the two genetically differentiated areas (SGSSI MPA and WAP). Altogether, our results indicate the need of implementing an MPA covering the waters off the Antarctic Peninsula and the continental shelf waters adjacent to the South Orkneys, highlighting the valuable information that genetic connectivity of benthic invertebrates can provide to MPAn design.

Keywords: *COI*, ddRADseq-derived SNPs, MPA, Western Antarctic Peninsula, South Georgia Island, South Orkneys Islands, stepping stones, CCAMLR

1 | Introduction

Connectivity and larval dispersal are fundamental pillars in the design of Marine Protected Areas (MPAs) and instrumental to articulate the concept of a network of connected MPAs (MPAn) (Palumbi, 2003). Indeed, population connectivity is a key factor for metapopulation persistence (Cowen & Sponaugle, 2009), determining the potential of a given species/population to colonise new habitats and recover from perturbations, and hence playing a central role in species and ecosystems resilience. Currently, incorporating connectivity into MPAn design presents challenges due to, for instance, the confusion or conflict between scientists and stakeholders regarding the precise definition and function of connectivity (Jenkins & Stevens, 2018) or the different methodologies used to estimate connectivity patterns (Botsford et al., 2009; Burgess et al., 2014; Bryan-Brown et al., 2017; Balbar & Metaxas, 2019). Many population genetic studies provide explicit MPA recommendations based on direct evaluations of connectivity, genetic diversity, and structure (e.g. Buonaccorsi et al., 2005; Duncan et al., 2015; Jackson et al., 2015; Taboada et al., 2018), which could be highly valuable for MPAn planning. However, there is still a gap between science and management, as genetic methods are not generally discussed in the management literature concerning MPA design (Balbar & Metaxas, 2019).

Two strong biases appear in the scientific literature regarding genetic connectivity in the context of MPAn design: a taxonomic bias, with most of the studies focused on ray-finned fishes (Actinopterygii), and a geographic bias towards Australian and North American waters (Balbar & Metaxas, 2019). The taxonomic bias is particularly concerning, since benthic invertebrates are considered better candidates than highly mobile fishes for genetic connectivity assessment between MPAs (Jenkins & Stevens, 2018). This is because their dispersal is usually defined during a pelagic reproductive early-life stage, with adults remaining relatively sedentary (Cowen & Sponaugle, 2009). However, this is an oversimplified generalisation, as some benthic invertebrates present non-planktonic reproductive strategies, such as brooding species or species with crawling larvae, which present *a priori* lower dispersal potential. In any case, connectivity patterns of benthic invertebrates generally reflect local hydrological conditions (Jenkins & Stevens, 2018). Besides the taxonomic bias, it is worth noting that most of the studies investigating genetic connectivity between MPAs only used one “flagship” species, which is usually an emblematic species, economically or environmentally relevant. However, since dispersal and connectivity capabilities can vary between species due to species-specific traits such as their reproductive strategy, it is recommended to consider assessing genetic

connectivity in more than one species with differing biological strategies in order to obtain ecologically relevant results (Jenkins & Stevens, 2018).

With respect to the gap between science and management, Antarctic waters are not an exception. Population genetic studies of Antarctic species provide fundamental information for management (e.g. Hemery et al., 2012; González-Wevar et al., 2013; Galaska et al., 2017), but traditionally, they are not incorporated in the process of MPA design. Due to the peculiar status of the Antarctic continent as the only land in the world that does not belong to any country, all its coastal waters are considered Marine Areas Beyond National Jurisdiction, internationally managed by the Antarctic Treaty System (ATS), and by the Commission for the Conservation of Antarctic Marine Living Resources (CCAMLR) and its treaty (the CAMLR Convention). Area-based management tools of the ATS include 75 Antarctic Specifically Protected Areas (ASPAs) and seven Antarctic Specifically Managed Areas (ASMAs), thirteen of them protecting marine or partially marine environments. In parallel, CCAMLR delimited two Antarctic MPAs: South Orkney Islands Southern Shelf MPA (SOISS MPA) and the Ross Sea Region MPA. Although the SOISS MPA (Figure 1A-B) protects a large continental shelf area, it fails to protect the shallower regions adjacent to the South Orkneys, which are not only biologically rich and present high conservation values, but are also prime fishing grounds (Brooks, 2013). Fishing interests in Antarctica have been influencing CCAMLR resolutions, since CCAMLR decision-making process requires unanimity (Brooks, 2013; Cordonnery & Kriwoken, 2015; Smith et al., 2016). Apart from the SOISS MPA, the South Georgia and the South Sandwich Islands MPA (SGSSI MPA), designated by the United Kingdom, also protects a vast region of the Scotia Sea (Figure 1B). In the present study we focused on three MPAs, two currently implemented (SOISS MPA and SGSSI MPA), and one proposed in the 37th CCAMLR Meeting (2018), the Domain 1 MPA (D1MPA), which included areas along the West Antarctic Peninsula (WAP), its associated islands, and the South Orkney Islands (Figure 1B). However, the D1MPA proposal was not approved by the Commission. From our point of view, in order to establish an effective network of connected Antarctic MPAs, connectivity between the different protected areas should be assessed. However, both MPAs of the Scotia Sea (SOISS and SGSSI MPAs) and the D1MPA proposal contemplated only the protection of specific habitats and key areas for emblematic or economically interesting species such as penguins, humpback whales, birds, krill, and toothfish, but did not consider genetic diversity and connectivity patterns in their MPA designs (https://www.ccamlr.org/en/wg-emm-14/25; http://www.gov.gs/environment/marine-protected-area; https://www.ccamlr.org/en/ccamlr-xxxvii/31).

Apart from the vital knowledge regarding connectivity, genetic studies can also provide valuable information for MPA planning about genetic diversity. These measures of diversity should be taken into account for MPA design due to the direct relationship between genetic diversity and resilience to changing climatic conditions (Luck et al., 2003; Ehlers et al., 2008; Schaberg et al., 2008). This is especially important for MPA planning in our study area, because some regions of the WAP are currently undergoing one of the most rapid warmings recorded on Earth (Vaughan et al., 2003; Schmidtko et al., 2014). For instance, surface water summer temperature off the WAP increased by more than 1°C during the second half of the 20th century (Meredith & King, 2005; Mulvaney et al., 2012),

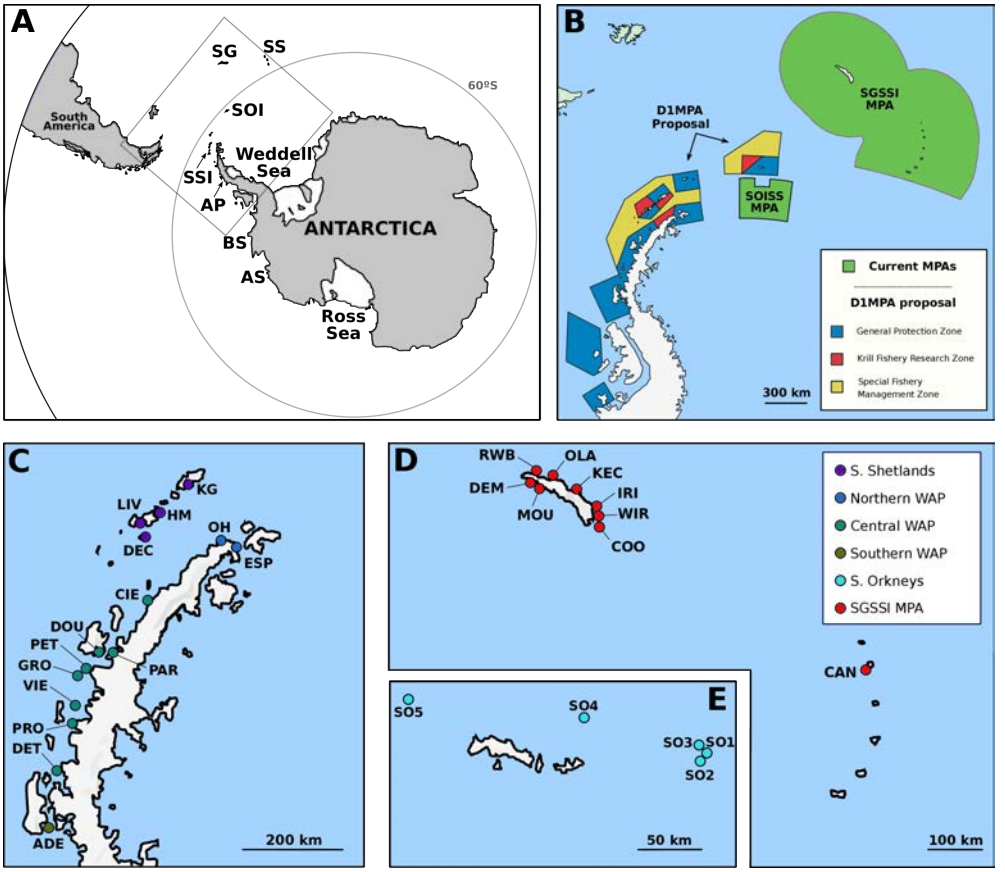

FIGURE 1 **(A)** Map of Antarctica and the Southern Ocean; square indicates our study area, represented on (B). Abbreviations: SG, South Georgia Island; SS, South Sandwich Islands; SOI, South Orkney Islands; SSI, South Shetland Islands; AP, Antarctic Peninsula; BS, Bellingshausen Sea; AS, Amundsen Sea. **(B)** Map of our study area representing current MPAs (SGSSI MPA, South Georgia and South Shetland Islands MPA; SOISS MPA, South Orkney Islands Southern Shelf MPA) and Domain 1 MPA proposal. (C-E) Sampling stations at the West Antarctic Peninsula region **(C)**, SGSSI MPA **(D)**, and South Orkney Islands **(E)**. See Table 1 for sampling sites abbreviations.

with severe consequences for ice sheets and glaciers (Cook et al., 2005; Cook & Vaughan, 2010; Cook et al., 2016). Profound changes in glaciers are also occurring in the Bellingshausen and Amundsen Seas (Mouginot et al., 2014; Rignot et al., 2014). This aspect is particularly problematic for Antarctic shallow-water invertebrates, given that their essential biological functions are exceptionally sensitive to temperature increases and fluctuations (Peck & Conway, 2000; Peck et al., 2004).

Our main aim here is to assess whether the two MPAs at the Scotia Sea (SGSSI MPA and SOISS MPA) and the D1MPA proposal present significant levels of genetic connectivity, in order to make recommendations on MPA design based on gene flow, population structure, and genetic diversity. To achieve it, we used the information from sequences of the mitochondrial *COI* marker of five benthic invertebrate species (a total of 808 individuals) belonging to three different phyla and covering a wide range of reproductive strategies and dispersal capabilities, following recommendations from Jerkins & Stevens (2018). Our species selection comprised: the two brooding nemerteans *Antarctonemertes valida* and *Antarctonemertes riesgoae*, whose connectivity exclusively depends on the passive transportation of adults on drifting algae; the sponge *Mycale acerata*, with non-feeding lecithotrophic larvae; the annelid *Pterocirrus giribeti*, putatively presenting feeding planktotrophic larvae; and the annelid *Neanthes kerguelensis*, with an epitokous life cycle and a planktotrophic larva. Moreover, in order to obtain higher resolution in our connectivity results for the areas SGSSI MPA and D1MPA, we used ddRADseq-derived markers for the two brooding nemerteans *A. valida* and *A. riesgoae*. Finally, we reviewed the previous population genetic studies on benthic invertebrates performed in the study area that presented relevant results on genetic connectivity and structure, allowing us to obtain a thorough understanding of the gene flow patterns in the Scotia Sea and the WAP region at a broad community level.

2 | Materials & Methods

2.1 Sample collection, preservation and DNA extraction

A total of 808 samples of five different species were used in this study, collected during six campaigns from 2012 to 2017 (Table 1). Sampling stations were grouped in six different areas: South Georgia & the South Sandwich Islands MPA (SGSSI MPA), South Orkney Islands, South Shetland Islands, Northern WAP, Central WAP, and Southern WAP. *Antarctonemertes valida*, *A. riesgoae*, *P. giribeti*, and *N. kerguelensis* individuals were collected from WAP and SGSSI MPA shallow waters, in the intertidal or by SCUBA-diving at a maximum depth of 25 m. *Mycale acerata* specimens were collected from WAP shallow waters by SCUBA-diving at 5–25 m depth, and from South Orkneys and SGSSI MPA deep waters using bottom trawls, at 733–2190 m and at 326 m depth, respectively (Table 1).

Complete individuals of *A. valida*, *A. riesgoae*, *P. giribeti*, and *N. kerguelensis* and ~1 cm^3 of tissue samples of *M. acerata* were preserved in 96% ethanol. Ethanol was replaced three times and samples were stored at -20°C until further processing. DNA was extracted from all samples using the DNeasy Blood & Tissue kit (Qiagen) following the manufacturer's protocol, with minor modifications in the cell lysis time (overnight incubation) and the final DNA elution step (performed twice using 50 uL of elution buffer each time).

2.2 Mitochondrial COI *amplification and sequencing, and population structure and connectivity analyses*

A fragment of the mitochondrial cytochrome *c* oxidase subunit I (*COI*) was amplified for 643 individuals using primers and amplification protocols specified in Supplementary Material 1. PCR products were purified and sequenced in both directions at the *Centres Científics i Tecnològics de la Universitat de Barcelona* (CCiT-UB) and the Sequencing Facilities of the Natural History Museum of London (NHM). Overlapping sequences were cleaned and assembled into consensus sequences using the software Geneious v.10.2.6 (Kearse et al., 2012). In addition, we used the 126 *COI* sequences of *P. giribeti* from the WAP and South Shetland Islands from Leiva et al. (2018), obtaining a final *COI* dataset of 769 sequences.

The *COI* dataset of each species was used to calculate genetic structure and connectivity between MPAs. Sequences were aligned in Geneious v.10.2.6 using the Q-INS-I algorithm of MAFFT version 7 (Katoh & Standley, 2013). Alignments were used to construct un-rooted haplotype networks using the median-joining network option (Bandelt

Sampling area	Sampling station	Abbreviation	Coordinates	*A. valida*	*A. riesgoae*	*P. giribeti**	*N. kerguelensis*	*M. acerata*
Antarctic Peninsula								
Northern WAP	Esperanza Bay	ESP	63°23'47"S 56°59'47"W	26	17		1	1
	O'Higgins Bay	OH	63°18'52"S 57°54'27"W	25	29	*9*	19	4
Central WAP	Cierva Cove	CIE	64°09'20"S 60°57'12"W	26	30	*35*	17	4
	Paradise Bay	PAR	64°49'24"S 62°51'24"W	14	1	*2*	4	
	Petermann Is.	PET	65°10'24"S 64°08'36"W	22		*22*	11	
	Doumer Is.	DOU	64°52'32"S 63°34'59"W					1
	Prospect Point	PRO	66°00'29"S 65°20'18"W					1
	Vieugué Is.	VIE	65°40'50"S 65°12'20"W					1
	Detaille Is.	DET	66°52'00"S 66°47'01"W					1
	Grot o Is.	GRO	65°13'59"S 64°14'59"W					1
Southern WAP	Adelaide Is.	ADE	67°34'04"S 68°08'55"W		26		1	
South Shetland Is.	King George Is.	KG	62°11'55"S 58°56'59"W	15	26	*13*	20	
	Half Moon Is.	HM	62°35'41"S 59°54'07"W	22	25	*30*	17	
	Livingston Is.	LIV	62°39'07"S 60°36'28"W	24	10	*15*		
	Decept on Is.	DEC	62°59'25"S 60°37'31"W	30	24		18	5
SGSSI MPA								
South Georgia Is.	Cape Demidov	DEM	54°08'23"S 37°43'21"W	6	18	7		
	Mouse Cove	MOU	54°14'26"S 37°19'51"W	7				
	Right Whale Bay	RWB	54°00'44"S 37°41'27"W	6	14	12		
	Iris Bay	IRI	54°44'10"S 35°52'49"W	13	13	5		
	Wirik Bay	WIR	54°45'10"S 35°50'48"W	6	6	12		
	Cooper Is.	COO	54°48'30"S 35°46'37"W				3	
	King Edward Cove	KEC	54°16'52"S 36°29'49"W				14	
	Prince Olav Harbour	OLA	54°03'34"S 37°08'43"W				8	
South Sandwich Is.	Candlemas Is.	CAN	57°09'51"S 26°47'37"W					3
South Orkney Is.								
South Orkney Is.	JR15005_2471	SO1	60°45'11"S 42°57'47"W					1
	JR15005_2360	SO2	60°45'34"S 42°58'28"W					1
	JR15005_2617	SO3	60°43'38"S 43°00'01"W					1
	JR15005_2100	SO4	60°28'19"S 44°25'09"W					1
	JR15005_1402	SO5	60°19'32"S 46°46'03"W					6
			TOTAL	242	239	162	133	32

TABLE 1 Collection details for all sampling sites indicating sampling areas, abbreviations, coordinates and the number of individuals collected of each species. *We used the *COI* sequences of the individuals from the Antarctic Peninsula of *P. giribeti* (italic numbers) from Leiva et al. (2018).

et al., 1999) with the program POPART 1.7 (www.popart.otago.ac.nz). The software DNAsp 5.10 (Librado & Rozas, 2009) was used to calculate the number of segregation sites (*S*), number of haplotypes (*h*), haplotype diversity (*Hd*), nucleotide diversity (π), and Tajima's *D* values for each species and sampling area. Furthermore, pairwise fixation indices (ϕ_{ST}) were estimated to measure the differentiation between pairs of sampling stations, as implemented in *Arlequin* version 3.5.2.2 (Excoffier & Lischer 2010), evaluating the corresponding *p*-values after 20,000 permutations. Pairwise ϕ_{ST} tables were used by the software Barrier v. 2.2 (Manni et al., 2004) to identify and represent the most robust breaks in each genetic landscape. In addition, hierarchical analyses of molecular variance (AMOVA) were performed using the *poppr.amova* function in the *poppr* R package (Kamvar et al., 2014) in order to calculate the proportion of genetic variation explained by the Barrier's genetic breaks, and whether this proportion represented a significant part of the total genetic variation.

2.3 ddRADseq library preparation and sequencing and locus assembly

ddRADseq library preparation was conducted for the two *Antarctonemertes* species, *A. valida* and *A. riesgoae*, following Leiva et al. (2019). Libraries were prepared at the Museum of Comparative Zoology Labs, Harvard University (Cambridge, MA, USA), and the NHM. ddRADseq Libraries were paired end sequenced (150bp) on two lanes of an Illumina HiSeq 2500 (Illumina): one at the Center for Systems Biology, Harvard University, and another at the facilities of Macrogene Europe (Macrogene).

ddRADseq locus assembly was performed using the Stacks pipeline, version 2.2 (Catchen et al., 2013). RAD-tags were processed and demultiplexed using the Stacks *process_radtags* module, where low quality reads, reads with uncalled bases, and reads without a complete barcode or restriction cut site were removed. According to Jeffries et al. (2016) and Paris et al. (2017), we ran preliminary tests to optimise *ustacks* and *cstacks* parameters, which were finally set to M = 4, m = 5, and n = 4.

In order to optimise the number of loci and their coverage, we ran the Stacks *populations* module twice and hence generated two different datasets, one for each species. Both *populations* runs were run with the "--write_single_SNP" option, in order to retain only the first SNP from each RAD-tag. This option prevents the inclusion of physically linked SNPs in the resulting dataset, which is an assumption of subsequent population genetics analyses. For each dataset, we ran the Stacks *populations* module to retain those SNPs present in at least 30% of the individuals (r = 0.3), and then filtered out individuals with less than 20% of the loci using the *adegenet* R package (Jombart, 2008), resulting in a dataset containing 134 individuals and 959 SNPs, with an average of 44.72% of missing data for *A. valida*, and 70 individuals and 694 SNPs, with an average of 45.97% of missing data for *A. riesgoae*.

Subsequently, in order to differentiate neutral SNPs from putative SNPs under selection, both databases were analysed using default parameters in BayeScan version 2.1 (Foll & Gaggiotti, 2008). All SNPs were neutrals in the *A. valida* dataset, while two SNPs were detected as under selection in the *A. riesgoae* dataset. Hence, the final datasets that were used for subsequent population genetic analyses consisted of 959 neutral SNPs for *A. valida* and 692 neutral SNPs for *A. riesgoae*.

2.4 Population diversity, structure and connectivity analyses using ddRADseq-derived SNPs

Genetic diversity and demographic statistics for *A. valida* and *A. riesgoae* ddRADseq-derived SNPs datasets were calculated using *ape* (Paradis et al., 2004), *pegas* (Paradis,

2010), and *adegenet* R packages. Expected (*He*) and observed (*Ho*) heterozygosities per SNP were extracted and averaged across samples within areas for each species. Inbreeding coefficients (F_{IS}) for each area and for all samples analysed together were estimated from heterozygosity (F_{IS} = 1 – (*Ho*/*He*)).

Population structure was assessed using STRUCTURE version 2.3 (Pritchard et al., 2000), and the *snapclust* function (Beugin et al., 2018) and the discriminant analyses of principal components (DAPC) both implemented in the *adegenet* R package. STRUCTURE was run for 200,000 MCMC iterations using the admixture model, with a burn-in of 100,000 iterations, and setting the putative *K* (number of clusters) from 1 to 8 with 5 replicates for each run. STRUCTURE HARVESTER (Earl, 2012) was used to determine the most likely number of clusters and subsequently we used CLUMPP v.1.1.2 (Jakobsson & Rosenberg, 2007) to average each individual's membership coefficient across the *K* value replicates. The DAPC analyses were performed by grouping samples by areas, and then choosing the optimal number of retained principal components analysis axes using the cross-validation *xvalDapc* function in the *adegenet* R package. For the *snapclust* analysis, we used both Akaike Information Criterion (IC = AIC) and Bayesian Information Criterion (IC = BIC) to identify the optimal number of clusters in the *snapclust.choose.k* function. Then, initial memberships for *snapclust* were chosen using the k-means algorithm (pop.ini = "kmeans"), allowing a maximum *K* of 10 (max = 10), and a number of iterations of 100 (max.iter = 100).

Pairwise F_{ST} values were estimated to measure the differentiation between pairs of sampling areas using the *pairwise.fst* function in the *hierfstat* R package (Goudet, 2005). Their significance was tested with 1,000 permutations using the *ade4* R package (Dray & Dufour, 2007). Barrier version 2.2 was then used to identify and position genetic breaks in the sampling area. Finally, in order to identify current gene flow patterns in the study area, Nei's G_{ST} method was used to estimate the relative contemporary migration between sampling areas, using the *divMigrate* function of the *diveRsity* R package (Keenan et al., 2013).

3 | Results

3.1 Population structure and connectivity from mitochondrial COI datasets

Table 2 summarises genetic diversity indices inferred from *COI* datasets for each species and area, showing an absence of a clear pattern of genetic diversity across species. For instance, when considering haplotype diversity (*Hd*), the most diverse area was SGSSI MPA for *A. valida* and *N. kerguelensis*, the Northern WAP for *A. riesgoae*, the S. Shetlands for *P. giribeti*, and the Central WAP for *M. acerata* (Table 2). Regarding nucleotide diversity (π), the most diverse area was SGSSI MPA for *A. valida*, the Northern WAP for *A. riesgoae* and *N. kerguelensis*, the Central WAP for *P. giribeti*, and the S. Orkneys for *M. acerata* (Table 2).

We found the following number of *COI* haplotypes for each species: *A. valida* = 27; *A. riesgoae* = 13; *P. giribeti* = 43; *N. kerguelensis* = 14; and *M. acerata* = 3 (Table 2; Figure 2). Importantly, no haplotype was shared between the Subantarctic SGSSI MPA and the WAP (including S. Shetlands) in any species (Figure 2). Interestingly, in *M. acerata*, although no haplotype was shared between SGSSI MPA and the WAP (including S. Shetlands), the haplotypes observed in the S. Orkney Islands were shared with both SGSSI MPA and the WAP (including S. Shetlands) (Figure 2E, 2F).

Pairwise ϕ_{ST} tables are shown in Table 3. In contrast with the lack of pattern across species for the genetic diversity results, pairwise fixation indices in all species did follow a similar trend, with the SGSSI MPA populations presenting the highest ϕ_{ST} values, and therefore indicating that SGSSI MPA populations were the most differentiated (Table 3). Barrier identified the same genetic break for all species as the most robust barrier, separating SGSSI MPA populations from the rest of the sampling areas (see summary map in Figure 2F). Genetic barriers identified by Barrier were all verified by AMOVA analyses (Table 4). The percentage of genetic variation explained by the main genetic barrier represented a high and significant (p-values < 0.001) proportion of the total genetic variation in all species: 99.19% in *A. valida*, 77.44% in *A. riesgoae*, 36.95% in *P. giribeti*, 71.10% in *N. kerguelensis*, and 72.75% in *M. acerata* (Table 4).

A. valida

	N	S	h	Hd	π
SGSSI MPA	35	11	12	0.755	0.00214
S. Shetlands	90	7	8	0.19	0.00071
Northern WAP	47	3	4	0.248	0.00049
Central WAP	48	5	6	0.337	0.00071
Total	220	45	27	0.458	0.01541

A. riesgoae

	N	S	h	Hd	π
SGSSI MPA	45	2	3	0.547	0.00135
S. Shetlands	75	5	7	0.397	0.00098
Northern WAP	46	3	4	0.576	0.00148
Central WAP	30	1	2	0.067	0.00015
Southern WAP	26	3	4	0.547	0.00017
Total	222	12	13	0.771	0.00475

P. giribeti

	N	S	h	Hd	π
SGSSI MPA	36	22	12	0.837	0.00514
S. Shetlands	58	33	24	0.918	0.00811
Northern WAP	9	9	4	0.583	0.00413
Central WAP	59	27	17	0.917	0.01054
Total	162	46	43	0.946	0.00993

N. kerguelensis

	N	S	h	Hd	π
SGSSI MPA	25	12	8	0.79	0.00533
S. Shetlands	55	22	3	0.446	0.01714
Northern WAP	20	21	3	0.542	0.01978
Central WAP	32	2	3	0.232	0.00044
Southern WAP	1	-	-	-	-
Total	133	44	14	0.616	0.02418

M. acerata

	N	S	h	Hd	π
SGSSI MPA	3	0	1	0	0
S. Orkney	10	3	3	0.378	0.00124
S. Shetlands	5	0	1	0	0
Northern WAP	5	0	1	0	0
Central WAP	9	1	2	0.389	0.00064
Total	32	3	3	0.589	0.00147

TABLE 2 *COI* genetic diversity estimators for each species and sampling area. *N*, number of individuals; *S*, segregating sites; *h*, number of haplotypes; *Hd*, haplotype diversity; *π*, nucleotide diversity.

A. valida

	SGSSI MPA	S. Shetlands	Northern WAP	Central WAP
SGSSI MPA	0			
S. Shetlands	**0.98418**	0		
Northern WAP	**0.97857**	0.00207	0	
Central WAP	**0.9765**	**0.0295**	**0.03129**	0

A. riesgoae

	SGSSI MPA	S. Shetlands	Northern WAP	Central WAP	Southern WAP
SGSSI MPA	0				
S. Shetlands	**0.86628**	0			
Northern WAP	**0.86628**	**0.34187**	0		
Central WAP	**0.92028**	**0.66522**	**0.1773**	0	
Southern WAP	**0.92914**	**0.81844**	**0.68779**	**0.92324**	0

P. giribeti

	SGSSI MPA	S. Shetlands	Northern WAP	Central WAP
SGSSI MPA	0			
S. Shetlands	**0.41728**	0		
Northern WAP	**0.58254**	0.04615	0	
Central WAP	**0.35229**	0.00975	**0.07431**	0

N. kerguelensis

	SGSSI MPA	S. Shetlands	Northern WAP	Central WAP
SGSSI MPA	0			
S. Shetlands	**0.72247**	0		
Northern WAP	**0.73847**	0	0	
Central WAP	**0.94762**	**0.23457**	**0.42548**	0

M. acerata

	SGSSI MPA	S. Orkneys	S. Shetlands	Northern WAP	Central WAP
SGSSI MPA	0				
S. Orkneys	**0.77473**	0			
S. Shetlands	**1**	**0.49741**	0		
Northern WAP	**1**	**0.52646**	0	0	
Central WAP	**0.91734**	**0.46656**	0	0	0

TABLE 3 Pairwise F_{ST} values for the *COI* dataset of the five studied species. Significant values are shown in bold.

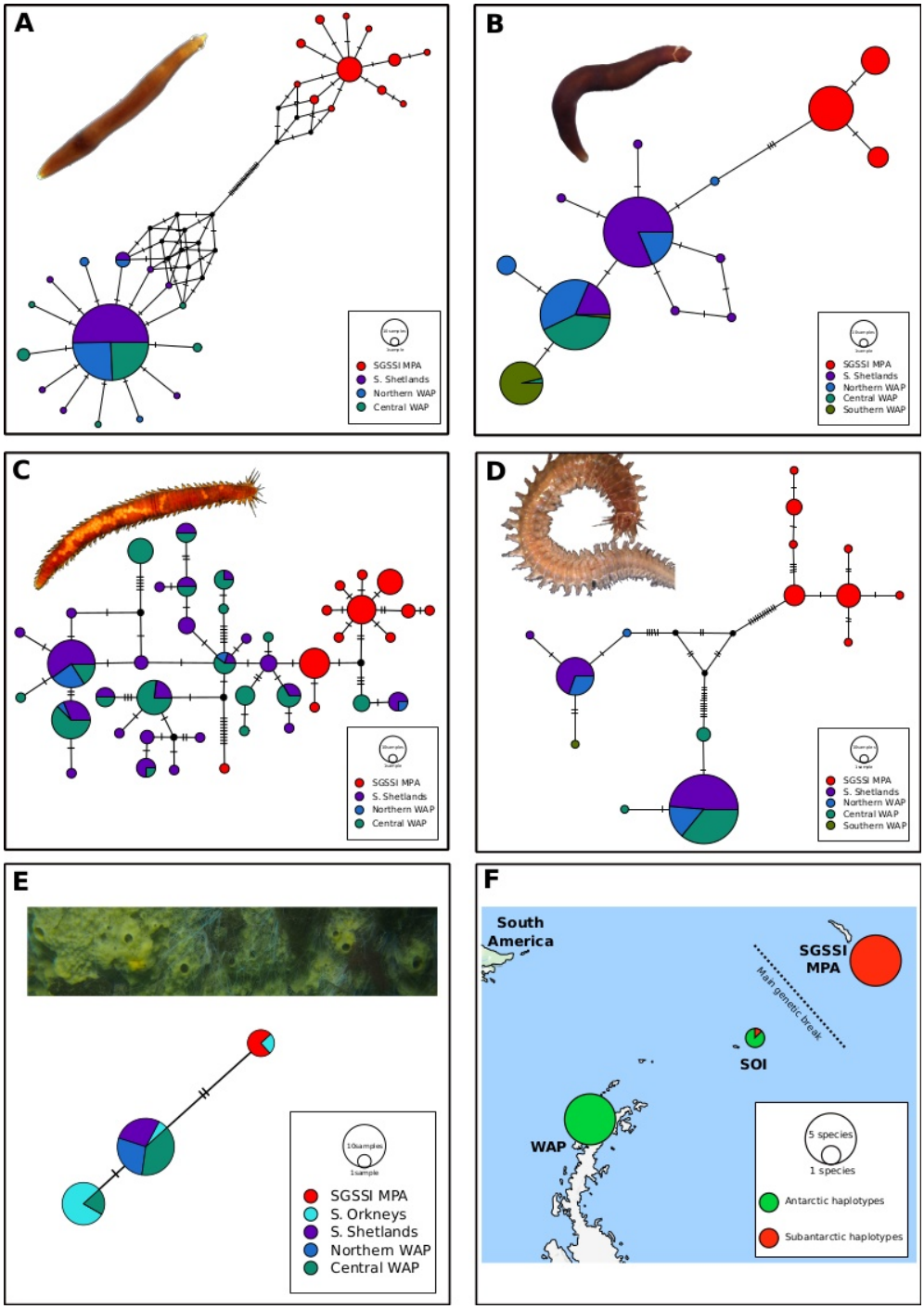
A
SGSSI MPA
S. Shetlands
Northern WAP
Central WAP
B
SGSSI MPA
S. Shetlands
Northern WAP
Central WAP
Southern WAP
C
SGSSI MPA
S. Shetlands
Northern WAP
Central WAP
D
SGSSI MPA
S. Shetlands
Northern WAP
Central WAP
Southern WAP
E
SGSSI MPA
S. Orkneys
S. Shetlands
Northern WAP
Central WAP
F
South America
SGSSI MPA
Main genetic break
SOI
WAP
5 species
1 species
Antarctic haplotypes
Subantarctic haplotypes

	df	Sum Sq	Mean Sq	Percentage of variation	P-value
A. valida					
WAP / SGSSI MPA	1	1629.38	1629.38	99.19	**0.0001**
Between areas	2	0.74	0.37	9.01E-03	**0.02**
Within areas	216	48.32	0.22	8.02E-01	0.25
A. riesgoae					
WAP / SGSSI MPA	1	296.73	296.73	77.44	**0.0001**
Between areas	3	87.1	29.03	14.54	**0.0001**
Within areas	217	82.72	0.38	8.02	**0.0001**
P. giribeti					
WAP / SGSSI MPA	1	158.22	158.22	36.95	**0.0001**
Between areas	2	18.31	9.15	1.87	**0.03**
Within areas	158	693.38	4.39	61.18	0.24
N. kerguelensis					
WAP / SGSSI MPA	1	811.71	811.71	71.1	**0.0001**
Between areas	3	130.1	43.37	6.4	**0.0001**
Within areas	128	756.81	5.91	22.5	0.21
M. acerata					
WAP + SOI / SGSSI MPA	1	10.78	10.78	72.75	**0.0001**
Between areas	3	7.05	2.35	11.86	**0.0001**
Within areas	27	9.91	0.37	15.39	0.18

TABLE 4 AMOVA results for the *COI* datasets. Evaluation of the percentage of variation explained by the genetic differentiation between and within the two groups inferred from the Barrier results for the five studied species.

FIGURE 2 *COI* haplotype networks for *Antarctonemertes valida* **(A)**, *Antarctonemertes riesgoae* **(B)**, *Pterocirrus giribeti* **(C)**, *Neanthes kerguelensis* **(D)**, and *Mycale acerata* **(E)**. Colours represent the different areas considered in our study: Northern WAP ("deepskyblue3" in R), Central WAP ("aquamarine4" in R), Southern WAP ("darkolivegreen" in R), South Shetland Islands ("darkorchid4" in R), South Orkney Islands ("cyan3" in R), SGSSI MPA ("red" in R). Mutational steps between haplotypes are represented by crossed lines and missing inferred haplotypes are depicted in black. **(F)** Summary map of the haplotype networks results (A-E). Green represents haplotypes found in the WAP region, while red represents haplotypes appearing at SGSSI MPA. Circle size is proportional to the number of species genotyped in each area, being all five species at SGSSI MPA and WAP region, and just one species (*M. acerata*) at the South Orkney Islands (SOI). The main genetic break from the Barrier analyses is also shown, represented by a dashed line.

3.2 Population structure and connectivity from ddRADseq-derived SNPs in Antarctonemertes

Averaged (across loci) expected (*He*) and observed (*Ho*) heterozygosity estimations from ddRADseq data for each area in both *Antarctonemertes* species are shown in Table 5. Regarding genetic diversity (*He*), both species showed a similar pattern, with SGSSI MPA populations presenting the highest values of *He* (Table 5). In *A. valida*, *He* ranged from 0.094 in Northern WAP to 0.478 in SGSSI MPA with a value of 0.147 for the whole dataset, while in *A. riesgoae*, *He* ranged from 0.134 in Southern WAP to 0.167 in SGSSI MPA with a value of 0.19 for all samples analysed together. However, regarding inbreeding (F_{IS}), differences arose: for *A. valida*, the area with the highest inbreeding was SGSSI MPA (F_{IS} = 0.837), while for *A. riesgoae*, Northern WAP area presented the highest inbreeding value (F_{IS} = 0.522). Despite these differences, all inbreeding values for both species were positive, resulting from heterozygosity deficit, and global inbreeding coefficient values (i.e., F_{IS} for the entire datasets) were similar, with values of 0.449 in *A. valida* and 0.437 in *A. riesgoae*.

Population structure and connectivity results for *A. valida* are shown in Figure 3. For the STRUCTURE analysis, the most likely number of clusters was *K* = 2 (see Supplementary Material 2A), showing that all samples from WAP areas presented high membership probabilities of belonging to Cluster 1, while all SGSSI MPA samples belonged to Cluster 2 (Figure 3A). Similarly, *snapclust* results indicated an optimal *K* of 2–3 clusters (see Supplementary Material 2B), assigning to Cluster 1 all samples from WAP areas and to Cluster 2 all SGSSI MPA samples when *snapclust* was run setting *K* = 2 (Figure 3B, D). The two dimensional representation of the DAPC results (Figure 3C) again showed the differentiation between WAP areas and SGSSI MPA samples, with the first DAPC axis accounting for almost all the genetic variation of the samples (see DA eigenvalues plot in Figure 3C).

	He	*Ho*	*Fis*
A. riesgoae			
S. Georgia	0.167	0.129	0.228
S. Shetlands	0.144	0.105	0.271
Northern WAP	0.136	0.065	0.522
Central WAP	0.138	0.092	0.333
Southern WAP	0.134	0.101	0.246
Total	0.19	0.107	0.437
A. valida			
S. Georgia	0.478	0.078	0.837
S. Shetlands	0.121	0.091	0.248
Northern WAP	0.094	0.069	0.266
Central WAP	0.119	0.078	0.345
Total	0.147	0.081	0.449

TABLE 5 Expected (*He*) and observed (*Ho*) heterozygosities and inbreeding coefficients (F_{IS}) for the ddRADseq-derived SNP datasets of *A. valida* and *A. riesgoae*.

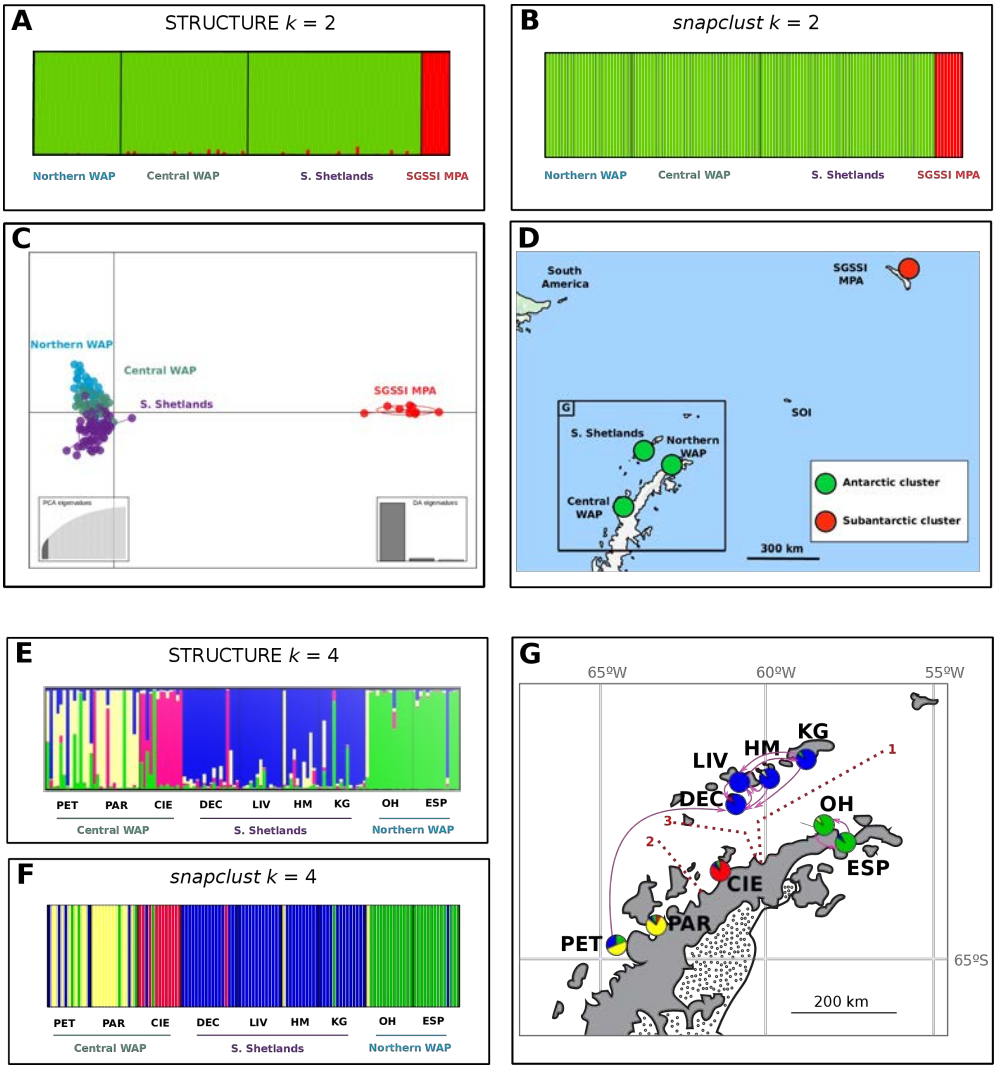

FIGURE 3 Population structure and connectivity analyses for *A. valida* using ddRADseq-derived SNP dataset. **A-D** show results for the entire dataset (individuals collected from SGSSI MPA and WAP region): STRUCTURE **(A)** and *snapclust* **(B)** plot results with *K* = 2. **(C)** DAPC plot results for the two-dimensional representation of the first two PCA eigenvalues. **(D)** Summary map of the STRUCTURE and *snapclust* results. Green represents the cluster appearing at the WAP region, while red represents the cluster found at SGSSI MPA. **E-G** show results for the individuals collected from the WAP region: STRUCTURE **(E)** and *snapclust* **(F)** results with K = 4. **(G)** Map of the WAP region summarising *snapclust*, Barrier, and G_{ST} migration network results. Each sampling site is represented by a circle, where each colour represents the proportion of individuals assigned to each of the four clusters recovered by STRUCTURE and *snapclust*. Genetic barriers are represented by red dashed lines, with a number (1–3) indicating their relevance revealed by the Barrier analysis. Migration values higher than 0.60 in the G_{ST} migration network (see Supplementary Material 4) are illustrated by pink arrows. See Table 1 for sampling sites abbreviations.

Due to the high differentiation between the *A. valida* organisms collected in the WAP area and those collected in SGSSI MPA, we ran hierarchical STRUCTURE and *snapclust* analyses within the WAP. ddRADseq-derived SNPs unveiled a hidden genetic structure for *A. valida* in the WAP region (Figure 3E—3G) that passed unnoticed in the *COI* and in the complete ddRADseq datasets. Both STRUCTURE and *snapclust* agreed in $K = 4$ as the most likely number of clusters (see Supplementary Material 2C and 2D, respectively), suggesting a population genetic structure with four different clusters corresponding to four geographic areas (Figures 3E and 3F, respectively). All sampling sites from S. Shetlands (Deception Island, DEC; Livingston Island, LIV; Half Moon Island, HM; King George Island, KG) showed similar cluster assignment proportions, with Cluster 1 predominating over the others (blue cluster in Figures 3E–G). Most of the organisms from Northern WAP (O'Higgins Bay, OH; Esperanza Bay, ESP) belonged to Cluster 2 (green cluster in Figure 3E–G), while at the Central WAP Cluster 3 prevailed in Cierva Cove (CIE) (red cluster in Figures 3E–G) and Cluster 4 in Paradise Bay (PAR) and Petermann Island (PET) (yellow cluster in Figure 3E–G). The results of our Barrier analysis supported the genetic structure obtained by *snapclust* and STRUCTURE, identifying 3 relevant genetic barriers separating the four areas mentioned above, and the most relevant genetic break coinciding with the Peninsula Front (Figure 3G, red dashed lines; pairwise F_{ST} table used as input for Barrier analysis is shown in Supplementary Material 3). Two additional genetic breaks were detected by Barrier (Figure 3G, red dashed lines), one separating PET and PAR and another separating CIE from the rest of locations. In addition, the AMOVA results (Table 6) indicated that the grouping of the individuals in four geographic areas represented a significant 8.03% of the total genetic variation (p-value = 0.01). From the migration analysis, we obtained the highest migration values (> 0.60) within the S. Shetlands indicating high contemporary migration, and also between the two stations at Northern WAP (Figure 3G; the full migration G_{ST} table is shown in Supplementary Material 4). Moreover, high contemporary migration was also detected from Petermann Island (PET) to Deception Island (DEC) (Figure 3G).

Source of variat on	Df	Sum Sq	Mean Sq	% of variat on	p-value
Between geographical clusters	3	2354.12	784.71	8.03	**0.01**
Between samples within clusters	120	18915.74	157.63	23.27	**0.01**
Within samples	124	11652.41	93.97	68.7	**0.01**

TABLE 6 AMOVA results for the *A. valida* ddRADseq dataset including only the individuals collected from the WAP region. Evaluation of the genetic differentiation between and within the four geographical clusters inferred from our connectivity and structuring analyses (see Figure 3E-G).

Our population structure and connectivity results for *A. riesgoae* (Figure 4) revealed a similar pattern than that observed in the entire *A. valida* dataset (see Figure 3A—3D). The optimal number of clusters for the STRUCTURE analysis was *K* = 2 (see Supplementary Material 2E), and 2–3 clusters for *snapclust* (see Supplementary Material 2F). Both STRUCTURE and *snapclust* analyses showed the differentiation between the samples collected at the WAP and the individuals from the SGSSI MPA (Figure 4A–B). Although all samples were assigned with high membership probabilities by *snapclust* (Figure 4B), STRUCTURE results revealed that some individuals presented admixture in their cluster assignment (Figure 4A), in contrast with the results of *A. valida* (Figure 3A, B). The first axis of the two dimensional representation of the DAPC results for *A. riesgoae* illustrated the separation between Antarctic and Subantarctic organisms (Figure 4C), as in *A. valida* (Figure 3C). However, in *A. riesgoae*, the second axis segregated the different areas of the WAP region, showing a conspicuous geographic structure consisting in the samples from the Northern WAP and S. Shetlands grouping together, separated from

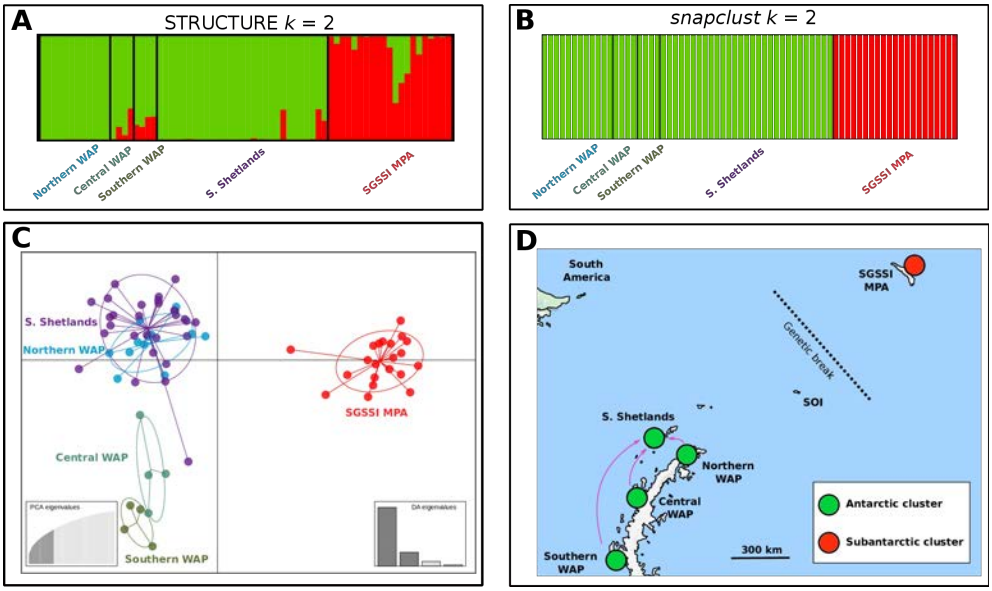

FIGURE 4 Population structure and connectivity analyses for *A. riesgoae* using ddRADseq-derived SNPs. STRUCTURE **(A)** and *snapclust* **(B)** plot results with *K* = 2. **(C)** DAPC plot results for the two-dimensional representation of the first two PCA eigenvalues. **(D)** Summary map of the *snapclust*, Barrier, and GST migration network results. Green represents the cluster appearing at the WAP region, while red represents the cluster found at SGSSI MPA. The main genetic break is represented by a dashed line, and migration values higher than 0.60 in the GST migration network (see Supplementary Material 6) are illustrated by pink arrows.

Central WAP and Southern WAP (Figure 4C). Our Barrier analysis identified the most robust genetic break between the WAP region and the SGSSI MPA (see pairwise F_{ST} table used as input for the Barrier analysis in Supplementary Material 5), in agreement with *COI* Barrier results (Figure 2F) and ddRADseq structuring and connectivity results for *A. riesgoae* (Figure 4A-C). The highest migration values (> 0.60) detected by our G_{ST} migration analysis are represented in Figure 4D, indicating high contemporary migration from Southern, Central, and Northern WAP to the S. Shetlands (full migration G_{ST} table is shown in Supplementary Material 6).

4 | Discussion

Our population genetic analyses unveiled a clear pattern of population structure in our study area, spanning the Western Antarctic Peninsula, South Shetland, South Orkneys, South Georgia, and South Sandwich Islands, essentially consisting in the complete lack of genetic connectivity between the SGSSI MPA and the WAP region.

4.1 Genetic connectivity and population differentiation across regions

Genetic connectivity and structure results from both *COI* and ddRADseq-derived markers revealed a lack of contemporary migration between SGSSI MPA and the WAP region (Figure 2, Figure 3A-D, Figure 4). Particularly, for *A. valida* and *N. kerguelensis*, different allopatric cryptic mitochondrial lineages occurred in the two areas, separated by 26 and 19 *COI* mutational steps, respectively (Figure 2A, 2D), which could be indicating cryptic speciation events. For *A. valida*, the differentiation between the Antarctic and the Subantarctic lineages also appeared in the ddRADseq dataset (Figure 3A-D), masking the genetic structure within the WAP region (Figure 3E-G). Pairwise ϕ_{ST} comparisons (Table 3), Barrier (Figure 2F), and AMOVA results (Table 4) for *COI* datasets of the five species supported this absence of current connectivity, with SGSSI MPA populations significantly appearing as the most differentiated. In line with these results, strong levels of inbreeding were found for both *A. valida* (F_{IS} = 0.449) and *A. riesgoae* (F_{IS} = 0.437) in the ddRADseq datasets, a clear signature of non-random mating between individuals typical of heavily structured populations (see Pérez-Portela & Riesgo, 2016).

Although previous studies did not directly assessed the same question that we addressed here, their results on the genetic diversity and structure also pointed to an absence of current connectivity between the SGSSI MPA (Subantarctic) and the WAP (Antarctic) region (see Table 7). Interestingly, these studies encompassed species with several reproductive strategies, showing that reproductive life history stages appear to have little influence on the genetic structure observed for Antarctic organisms, therefore agreeing with Halanych & Mahon (2018). For instance, Hoffmann et al. (2011) and González-Wevar et al. (2013) found significant levels of genetic differentiation between South Georgia Island and the WAP populations for the Antarctic limpet *Nacella concinna*. Similarly, a noticeable lack of contemporary gene flow between these areas was also found for the crinoid *Promachocrinus kerguelensis* (Wilson et al., 2007; Hemery et al., 2012), the brittle star *Ophionotus victoriae* (Hunter & Halanych, 2010; Galaska et al., 2017), the nematodes of the genera *Sabatieria* and *Desmodora* (Hauquier et al., 2017), the

pycnogonids *Colossendeis megalonyx* (Krabbe et al., 2010) and *Austropallene cornigera* (Dömel et al., 2015), the annelid *Austrolaenilla antarctica* (Neal et al., 2014), and the octopuses *Pareledone turqueti* (Strugnell et al., 2012; Strugnell et al., 2017) and *Adelieledone polymorpha* (Strugnell et al., 2017). Additionally, although less conspicuous and not discussed in the referenced studies below, an accurate review of the results presented for the ribbon worm *Parborlasia corrugatus* (Thornhill et al., 2008), the sea slug *Doris kerguelenensis* (Wilson et al., 2009), the sea stars *Diplasterias* spp. and *Lysasterias* spp. (Moreau et al., 2019), and the bivalve *Lissarca notorcadensis* (Linse et al., 2007), also revealed the same pattern of population differentiation. Interestingly, in contrast to these results, only a handful of studies found genetic homogeneity between SGSSI MPA and the WAP region: in the sea stars *Odontaster validus* (Janosik et al., 2010), *Bathybiaster* sp. and *Notasterias* sp. (Moreau et al., 2019), and the bentho-pelagic shrimp *Nematocarcinus lanceopes* (Raupach et al., 2010).

It is worth discussing in detail the results of the analyses on *Mycale acerata*. The low genetic variability found for in its *COI* dataset is within the levels of the mitochondrial diversity expected for Porifera (see Pérez-Portela & Riesgo, 2016), which is probably related to the presence of mitochondrial repair mechanisms in the phylum (Huang et al., 2008). Similarly, the sponge *Dendrilla antarctica* presented extremely low genetic variability in the full mitochondrial genome all along the WAP and South Shetlands (Leiva et al., 2019). But interestingly, although presenting this low variability, our results for *M. acerata* showed a noteworthy pattern, with haplotypes from both WAP and SGSSI MPA appearing in South Orkney Islands (Figure 2E). This combination of haplotypes suggests a stepping-stone role of the S. Orkneys between the two differentiated regions, a feature considered crucial for MPAn design (Roberts, 1997; Palumbi, 2003).

4.2 Gene flow, structure, and genetic diversity within the D1MPA proposal

Our results regarding the genetic connectivity within the D1MPA proposal suggested high levels of gene flow between the different regions. *Pterocirrus giribeti* presented panmixia within the D1MPA, with a slight genetic substructure produced by the Peninsula Front (see discussion in Leiva et al., 2018). Similarly, our analyses of *COI* sequences for *N. kerguelensis*, *M. acerata*, *A. valida*, and *A. riesgoae* also showed lack of population differentiation within the D1MPA proposal (Figure 2). Although *A. riesgoae* presented some geographic structure (Figure 2B, 4C), its spatial genetic diversity matches a stepping-stone model of genetic connectivity driven by isolation-by-distance (Jenkins & Stevens, 2018). Overall, previous studies also showed general population homogeneity for the WAP

Species	Phylum, Class	Reproductive strategy	Markers	SGSSI MPA – WAP region	Reference
Antarctonemertes valida	Nemertea, Hoplonemertea	Brooding	*COI* & RADseq	Differentiation	This study
Antarctonemertes riesgoae	Nemertea, Hoplonemertea	Brooding	*COI* & RADseq	Differentiation	This study
Neanthes kerguelensis	Annelida, Polychaeta	Epitoky + Planktotrophic larvae	*COI*	Differentiation	This study
Pterocirrus giribeti	Annelida, Polychaeta	Planktotrophic larvae	*COI*	Differentiation	This study
Mycale acerata	Porifera, Demospongiae	Lecithotrophic larvae	*COI*	Differentiation	This study
Austrolaenilla antarctica	Annelida, Polychaeta	Planktotrophic larvae?	*COI*, *16S*, & *H3*	Differentiation	Neal et al. (2014)
Colossendeis megalonyx	Arthropoda, Pycnogonida	Brooding	*COI*	Differentiation	Krabbe et al. (2010)
Austropallene cornigera	Arthropoda, Pycnogonida	Brooding	*COI*, *18S*, & *28S*	Differentiation	Dömel et al. (2015)
Promachocrinus kerguelensis	Echinodermata, Crinoidea	Lecithotrophic larvae	*COI*, *CytB*, *16S*, & *28S*	Differentiation	Wilson et al. (2007); Hemery et al. (2012)
Ophionotus victoriae	Echinodermata, Ophiuroidea	Planktotrophic larvae	*COI*, *16S*, & RADseq	Differentiation	Hunter & Halanych (2010); Galaska et al. (2017)
Pareledone turqueti	Mollusca, Cephalopoda	Benthic paralarvae	Microsatellites	Differentiation	Strugnell et al. (2012); Strugnell et al. (2017)
Adelieledone polymorpha	Mollusca, Cephalopoda	Benthic paralarvae	Microsatellites	Differentiation	Strugnell et al. (2017)
Nacella concinna	Mollusca, Gastropoda	Planktotrophic larvae	*COI*	Differentiation	Hoffmann et al. (2010); González-Wevar et al. (2013)
***Desmodora* sp.**	Nematoda, Chromadorea	Direct development	*COI*, *ITS*, & *18S*	Differentiation	Hauquier et al. (2017)
***Sabatieria* sp.**	Nematoda, Chromadorea	Direct development	*COI*, *ITS*, & *18S*	Differentiation	Hauquier et al. (2017)
***Diplasterias* spp.**	Echinodermata, Asteroidea	Brooding	*COI*	Subtle Differentiation	Moreau et al. (2019)
***Lysasterias* spp.**	Echinodermata, Asteroidea	Brooding	*COI*	Subtle Differentiation	Moreau et al. (2019)
Lissarca notorcadensis	Mollusca, Bivalvia	Brooding	*COI* & *28S*	Subtle Differentiation	Linse et al. (2007)
Doris kerguelenensis	Mollusca, Gastropoda	Direct development	*COI* & *16S*	Subtle Differentiation	Wilson et al. (2009)
Parborlasia corrugatus	Nemertea, Pididiophora	Planktotrophic larvae	*COI* & *16S*	Subtle Differentiation	Thornhill et al. (2008)
Nematocarcinus lanceopes	Arthropoda, Malacostraca	Planktotrophic larvae	*COI*, *16S*, & *28S*	Homogeneity	Raupach et al. (2010)
Odontaster validus	Echinodermata, Asteroidea	Planktotrophic larvae	*COI* & *16S*	Homogeneity	Janosik et al. (2010)
***Bathybiaster* sp.**	Echinodermata, Asteroidea	Lecithotrophic larvae	*COI*	Homogeneity	Moreau et al. (2019)
***Notasterias* sp.**	Echinodermata, Asteroidea	Brooding	*COI*	Homogeneity	Moreau et al. (2019)

TABLE 7 Review of all population genetic studies on benthic invertebrates performed in our study area presenting relevant results on the genetic connectivity and structure between SGSSI MPA and the WAP region. Taxonomic details, reproductive strategy, and markers used are indicated for each species, as well as whether differentiation or homogeneity was found between the two regions.

region, with gene flow and genetic substructure governed by oceanic currents (e.g. Thornhill et al., 2008; González-Wevar et al., 2011; Galaska et al., 2017; Leiva et al., 2019). Interestingly, *N. kerguelensis* presented two cryptic mitochondrial lineages occurring in sympatry in the WAP, separated by 19 *COI* mutational steps (Figure 2D), increasing the genetic diversity of the area conferring the high levels of nucleotide diversity observed in the Northern WAP and South Shetlands for *N. kerguelensis* (Table 2).

Contrasting with the low variability of the mitochondrial *COI* marker in *A. valida* (Figure 2A), our results showed the high-resolution power of ddRADseq-derived SNPs for fine-scale population genomic studies in non-model organisms. In this case, connectivity analyses detected the presence of significant genetic structure in *A. valida*, with four clusters geographically distributed along the studied area (Figure 3E-G). Nonetheless, the genetic structure is in agreement with the oceanic features of the area, with the most relevant genetic break also coinciding with the Peninsula Front (Figure 3G). This pattern was also found in other Antarctic benthic invertebrates studied using genome-wide SNPs obtained through high-throughput sequencing techniques, as in the brittle star *Ophionotus victoriae* (Galaska et al., 2017) and the sponge *Dendrilla antarctica* (Leiva et al., 2019). Also, high migration flow was found between Petermann Island and Deception Island in *A. valida* (Figure 3G) and between Southern and Central WAP and South Shetland Islands in *A. riesgoae* (Figure 4D), which might represent the passive transportation of nemertean adults and/or cocoons with drifting algae, as it has been already suggested for other Antarctic marine invertebrates (e.g. Nikula et al., 2010; Fraser et al., 2017). In this case, this migration may be facilitated by the Antarctic Peninsula Coastal Current and the Antarctic Circumpolar Current, as already proposed for *D. antarctica* (Leiva et al., 2019).

4.3 Implications for conservation and management recommendations

In 2011, CCAMLR adopted a conservation measure for establishing a network of connected MPAs all around Antarctica (Cordonnery & Kriwoken, 2015). MPAn design should take into account gene flow at the community level in order to effectively assess connectivity between and within MPAs (Palumbi, 2003; Jerkins & Stevens, 2018). Our approach using both mitochondrial and genome-wide nuclear markers in a wide range of benthic invertebrates with contrasting reproductive strategies and dispersal capabilities, combined with all the available literature regarding population genetic studies on benthic invertebrates for our study area (Table 7), allowed us to achieve solid conclusions at the community level. All the evidence presented herein points towards the urgency of implementing a new Antarctic MPA following the D1MPA proposal, covering areas of the

WAP region and the waters adjacent to South Orkney Islands, given the lack of genetic connectivity between SGSSI MPA and the D1MPA proposal. Our recommendation is supported by the following arguments:

1- MPAs should be conceived to play ecosystem roles beyond their reserve boundaries (Agardy, 1994). Specifically, in relationship with fishing areas, MPAs should be designed in order to promote exportation of individuals, mainly through larval dispersal, from protected areas to areas where fishing is allowed (DeMartini, 1993). Due to the lack of contemporary genetic connectivity between SGSSI MPA and the WAP region found for most of the benthic invertebrates studied (our results and Table 7), it cannot be assumed that the current MPAs of the Scotia Sea (SGSSI and SOISS MPAs) serve as source populations for the fishing areas in the WAP region.

2- Due to the role of South Orkney Islands as a stepping-stone area, where migration from both Antarctic and Subantarctic origins occur, the continental shelf waters adjacent to the islands should be protected. Although this result was only tested for the *M. acerata* dataset, this characteristic is deemed as essential for an effective connectivity within an MPAn (Roberts, 1997; Palumbi, 2003). Future studies should be addressed to investigate whether other benthic invertebrates also exhibit a similar pattern.

3- Although a spatial pattern of genetic diversity was not observed in our results (Tables 2 and 5), the tip of the Western Antarctic Peninsula (Northern WAP + South Shetlands) is considered a hotspot of genetic diversity for many Antarctic marine organisms (e.g. Wilson et al., 2007; Mahon et al., 2008; Janosik et al., 2010; Galaska et al., 2017). This is due to both the putative role of the area as a glacial refugium (Jażdżewska, 2011; Galaska et al., 2017) and the mixing of waters that occurs in the Bransfield Strait, where waters from the Weddell Sea merge with waters from the Bellingshausen Sea transported by the Antarctic Circumpolar Current (Sangrà et al., 2011). We should examine this genetic diversity pattern under the premise that MPAs should protect areas with high genetic diversity (Green et al., 2007; McLeold et al., 2009) due to the direct relationship between genetic diversity, connectivity, and resilience (Botsford et al., 2009). The Bransfield Strait waters should be thus contemplated as a high priority area for conservation, but it is also the main fishing ground for the krill fishery in Antarctica (Santa Cruz et al., 2018). We consider that D1MPA proposal wisely overcame this trade-off between fishing and conservation interests, designing both fishing and protected zones at the South Shetlands and Northern WAP (see Figure 1). Taking into account that both areas presented high migration values within themselves (Figure 3G), our results fully support the implementation of the D1MPA proposed in the 37th CCAMLR Meeting (2018).

4.4 Future perspectives for conservation of Antarctic marine ecosystems under global warming

Finally, although out of the scope of this study, it is worth mentioning that future management plans of WAP waters should be carefully designed to include all available information on how the Antarctic ecosystem is responding (and is expected to respond) to the rapid warming undergoing in West Antarctica due to global climate change (Brooks et al., 2018). As water temperature increases, krill density and distribution undergo major changes, with populations decreasing (Atkinson et al., 2004; Hill et al., 2019) and moving southwards (Atkinson et al., 2019). Hence, Antarctic krill fishery is expected to move southwards as well, a trend that should be considered in MPA design. Indeed, an evaluation of krill-fishing fleet behaviour has already identified a southward movement from the Drake sector to the Bransfield Strait sector (Santa Cruz et al., 2018).

A recent review from Siegert et al. (2019) examined the alterations that will experience the Antarctic Peninsula under a 1.5°C global warming scenario, anticipating profound impacts on the atmosphere, ocean, land ice, ice shelves, and both marine and terrestrial ecosystems. Furthermore, changes in ocean circulation and currents are also expected in the Southern Ocean (Meijers, 2014), which will undoubtedly affect migration and population connectivity. For instance, changes in the Circumpolar Deep Water have already been documented (Schmidtko et al., 2014), which has become warmer and shallower, as well as an increase in the amount of turbulence in the Southern Ocean (Hogg et al., 2015). Additionally, since larval metabolism depends on water temperature, planktonic larval duration is expected to be shortened by increased water temperatures (Kendall et al., 2013; O'Connor et al., 2007), also affecting connectivity. All in all, apart from being useful for MPA design in the present, our results can serve as a baseline for future assessments of genetic connectivity between Antarctic MPAs under the effects of climate change.

Acknowledgements

We are indebted to Juan Moles, Patricia Álvarez-Campos, Cesar Cárdenas, Claire Goodwin, Oriol Sacristán, Javier Cristobo, Juan Junoy, Carlos Angulo-Preckler, Blanca Figuerola, Conxita Ávila, 'Pacote', Miguel Ángel Ojeda, and Sacha Clemison for their help during sample collection. Also, members of the crew of the *Gabriel de Castilla* Spanish Antarctic Base and the BIO-Hespérides and PHAROS SG research vessels are greatly acknowledge. We thank all members of Giribet and Riesgo Labs for their invaluable help and support during laboratory work. This work was supported by two DIF grants of the Natural History Museum of London (SDF14032 and SDR17012) to A.R., the Heredity Fieldwork Grant from the Genetics Society to C.L., and two grants from the Spanish Ministry of Economy and Competitiveness in which A.R., S.T., and C.L. were involved (ACTIQUIM II: CTM2010-17415/ANT and DISTANTCOM: CTM2013-42667/ANT).

Authors Contributions

C.L., A.R., and S.T., conceived and designed the study; C.L., G.G., R.D., A.R., S.T. conducted fieldwork and collected samples; C.L., D.C., A.R., and S.T. conducted laboratory work; C.L., A.R., and S.T. performed statistical analyses and interpreted the results; C.L. wrote the first version of the manuscript, A.R. and S.T. contributed to the current version of the manuscript.

References

Agardy, M. T. (1994). Advances in marine conservation: the role of marine protected areas. *Trends in Ecology & Evolution*, *9*, 267-270.

Atkinson, A., Siegel, V., Pakhomov, E., & Rothery, P. (2004). Long-term decline in krill stock and increase in salps within the Southern Ocean. *Nature*, *432*, 100.

Atkinson, A., Hill, S. L., Pakhomov, E. A., Siegel, V., Reiss, C. S., Loeb, V. J., ... & Sailley, S. F. (2019). Krill (*Euphausia superba*) distribution contracts southward during rapid regional warming. *Nature Climate Change*, *9*, 142.

Balbar, A. C., & Metaxas, A. (2019). The current application of ecological connectivity in the design of marine protected areas. *Global Ecology and Conservation*, e00569.

Bandelt, H. J., Forster, P., & Röhl, A. (1999). Median-joining networks for inferring intraspecific phylogenies. *Molecular Biology and Evolution*, *16*, 37-48.

Beugin, M. P., Gayet, T., Pontier, D., Devillard, S., & Jombart, T. (2018). A fast likelihood solution to the genetic clustering problem. *Methods in Ecology and Evolution*, *9*, 1006-1016.

Botsford, L. W., White, J. W., Coffroth, M. A., Paris, C. B., Planes, S., Shearer, T. L., ... & Jones, G. P. (2009). Connectivity and resilience of coral reef metapopulations in marine protected areas: matching empirical efforts to predictive needs. *Coral Reefs*, *28*, 327-337.

Brooks, C. M. (2013). Competing values on the Antarctic high seas: CCAMLR and the challenge of marine-protected areas. *The Polar Journal*, *3*, 277-300.

Brooks, C. M., Ainley, D. G., Abrams, P. A., Dayton, P. K., Hofman, R. J., Jacquet, J., & Siniff, D. B. (2018). Watch over Antarctic waters. *Nature*, *558*, 177-180.

Bryan-Brown, D. N., Brown, C. J., Hughes, J. M., & Connolly, R. M. (2017). Patterns and trends in marine population connectivity research. *Marine Ecology Progress Series*, *585*, 243-256.

Buonaccorsi, V. P., Kimbrell, C. A., Lynn, E. A., & Vetter, R. D. (2005). Limited realized dispersal and introgressive hybridization influence genetic structure and conservation strategies for brown rockfish, *Sebastes auriculatus*. *Conservation Genetics*, *6*, 697-713.

Burgess, S. C., Nickols, K. J., Griesemer, C. D., Barnett, L. A., Dedrick, A. G., Satterthwaite, E. V., ... & Botsford, L. W. (2014). Beyond connectivity: how empirical methods can quantify population persistence to improve marine protected-area design. *Ecological Applications*, *24*, 257-270.

Cook, A. J., & Vaughan, D. G. (2010). Overview of areal changes of the ice shelves on the Antarctic Peninsula over the past 50 years. *The Cryosphere.*, *4*, 77-98.

Catchen, J., Hohenlohe, P. A., Bassham, S., Amores, A., & Cresko, W. A. (2013). Stacks: an analysis tool set for population genomics. *Molecular Ecology*, *22*, 3124-3140.

Cook, A. J., Fox, A. J., Vaughan, D. G., & Ferrigno, J. G. (2005). Retreating glacier fronts on the Antarctic Peninsula over the past half-century. *Science*, *308*, 541-544.

Cook, A. J., Holland, P. R., Meredith, M. P., Murray, T., Luckman, A., & Vaughan, D. G. (2016). Ocean forcing of glacier retreat in the western Antarctic Peninsula. *Science*, *353*, 283-286.

Cordonnery, L., & Kriwoken, L. (2015). Advocating a Larger Role for Environmental Nongovernment Organizations in Developing a Network for Marine Protected Areas in the Southern Ocean. *Ocean Development & International Law*, *46*, 188-207.

Cowen, R. K., & Sponaugle, S. (2009). Larval dispersal and marine population connectivity. *Annual Review of Marine Science*, *1*, 443-466.

DeMartini, E. E. (1993). Modeling the potential of fishery reserves for managing Pacific coral reef fishes. *Fisheries Bulletin*, *91*, 414-427.

Dömel, J. S., Convey, P., & Leese, F. (2015). Genetic Data Support Independent Glacial Refugia and Open Ocean Barriers to Dispersal for the Southern Ocean Sea Spider *Austropallene cornigera*. *Journal of Crustacean Biology*, *35*, 480-490.

Dray, S., & Dufour, A. B. (2007). The *ade4* package: implementing the duality diagram for ecologists. *Journal of Statistical Software*, *22*, 1-20.

Duncan, M., James, N., Fennessy, S. T., Mutombene, R. J., & Mwale, M. (2015). Genetic structure and consequences of stock exploitation of *Chrysoblephus puniceus*, a commercially important sparid in the South West Indian Ocean. *Fisheries Research*, *164*, 64-72.

Earl, D. A. (2012). STRUCTURE HARVESTER: a website and program for visualizing STRUCTURE output and implementing the Evanno method. *Conservation Genetics Resources*, *4*, 359-361.

Ehlers, A., Worm, B., & Reusch, T. B. (2008). Importance of genetic diversity in eelgrass *Zostera marina* for its resilience to global warming. *Marine Ecology Progress Series*, *355*, 1-7.

Excoffier, L. & Lischer, H. E. (2010) Arlequin suite ver 3.5: a new series of programs to perform population genetics analyses under Linux and Windows. *Molecular Ecology Resources*, *10*, 564–567.

Foll, M., & Gaggiotti, O. (2008). A genome-scan method to identify selected loci appropriate for both dominant and codominant markers: a Bayesian perspective. *Genetics*, *180*, 977-993.

Galaska, M. P., Sands, C. J., Santos, S. R., Mahon, A. R., & Halanych, K. M. (2017). Geographic structure in the Southern Ocean circumpolar brittle star *Ophionotus victoriae* (Ophiuridae) revealed from mtDNA and single-nucleotide polymorphism data. *Ecology and Evolution*, *7*, 475-485.

Gonzalez-Wevar, C. A., David, B., & Poulin, E. (2011). Phylogeography and demographic inference in *Nacella* (*Patinigera*) *concinna* (Strebel, 1908) in the western Antarctic Peninsula. *Deep Sea Research Part II: Topical Studies in Oceanography*, *58*, 220-229.

González-Wevar, C. A., Saucède, T., Morley, S. A., Chown, S. L., & Poulin, E. (2013). Extinction and recolonization of maritime Antarctica in the limpet *Nacella concinna* (Strebel, 1908) during the last glacial cycle: toward a model of Quaternary biogeography in shallow Antarctic invertebrates. *Molecular Ecology*, *22*, 5221-5236.

Goudet, J. (2005). *Hierfstat*, a package for R to compute and test hierarchical F-statistics. *Molecular Ecology Notes*, *5*, 184-186.

Green, A., Lokani, P., Sheppard, S., Almany, J., Keu, S., Aitsi, J., ... & Lipsett-Moore, G. (2007). Scientific design of a resilient network of marine protected areas, Kimbe Bay, West New Britain, Papua New Guinea. *TNC Pacific Island Countries Report*, *2*.

Hauquier, F., Leliaert, F., Rigaux, A., Derycke, S., & Vanreusel, A. (2017). Distinct genetic differentiation and species diversification within two marine nematodes with different habitat preference in Antarctic sediments. *BMC Evolutionary Biology*, *17*, 120.

Hemery, L. G., Eléaume, M., Roussel, V., Améziane, N., Gallut, C., Steinke, D., ... & Wilson, N. G. (2012). Comprehensive sampling reveals circumpolarity and sympatry in seven mitochondrial lineages of the Southern Ocean crinoid species *Promachocrinus kerguelensis* (Echinodermata). *Molecular Ecology*, *21*, 2502-2518.

Hill, S. L., Atkinson, A., Pakhomov, E. A., & Siegel, V. (2019). Evidence for a decline in the population density of Antarctic krill *Euphausia superba* still stands. A comment on Cox et al. *Journal of Crustacean Biology*, *39*, 316-322.

Hoffman, J. I., Peck, L. S., Linse, K., & Clarke, A. (2010). Strong population genetic structure in a broadcast-spawning Antarctic marine invertebrate. *Journal of Heredity*, *102*, 55-66.

Huang, D., Meier, R., Todd, P. A., & Chou, L. M. (2008). Slow mitochondrial *COI* sequence evolution at the base of the metazoan tree and its implications for DNA barcoding. *Journal of Molecular Evolution*, *66*, 167-174.

Hunter, R. L., & Halanych, K. M. (2010). Phylogeography of the Antarctic planktotrophic brittle star *Ophionotus victoriae* reveals genetic structure inconsistent with early life history. *Marine Biology*, *157*, 1693-1704.

Jackson, A. M., Munguía-Vega, A., Beldade, R., Erisman, B. E., & Bernardi, G. (2015). Incorporating historical and ecological genetic data for leopard grouper (*Mycteroperca rosacea*) into marine reserve design in the Gulf of California. *Conservation Genetics*, *16*,

811-822.

Jakobsson, M., & Rosenberg, N. A. (2007). CLUMPP: a cluster matching and permutation program for dealing with label switching and multimodality in analysis of population structure. *Bioinformatics*, *23*, 1801-1806.

Janosik, A. M., Mahon, A. R., & Halanych, K. M. (2011). Evolutionary history of Southern Ocean *Odontaster* sea star species (Odontasteridae; Asteroidea). *Polar Biology*, *34*, 575-586.

Jażdżewska, A. (2011). Soft bottom sublittoral amphipod fauna of Admiralty Bay, King George Island, Antarctic. *Oceanological and Hydrobiological Studies*, *40*, 1-10.

Jeffries, D. L., Copp, G. H., Lawson Handley, L., Olsén, K. H., Sayer, C. D., & Hänfling, B. (2016). Comparing RADseq and microsatellites to infer complex phylogeographic patterns, an empirical perspective in the Crucian carp, *Carassius carassius*, L. *Molecular Ecology*, *25*, 2997-3018.

Jenkins, T. L., & Stevens, J. R. (2018). Assessing connectivity between MPAs: Selecting taxa and translating genetic data to inform policy. *Marine Policy*, *94*, 165-173.

Jombart, T. (2008). *adegenet*: a R package for the multivariate analysis of genetic markers. *Bioinformatics*, *24*, 1403-1405.

Kamvar, Z. N., Tabima, J. F., & Grünwald, N. J. (2014). *Poppr*: an R package for genetic analysis of populations with clonal, partially clonal, and/or sexual reproduction. *PeerJ*, *2*, e281.

Katoh, K., & Standley, D. M. (2013). MAFFT multiple sequence alignment software version 7: improvements in performance and usability. *Molecular Biology and Evolution*, *30*, 772-780.

Kearse, M., Moir, R., Wilson, A., Stones-Havas, S., Cheung, M., Sturrock, S., ... & Thierer, T. (2012). Geneious Basic: an integrated and extendable desktop software platform for the organization and analysis of sequence data. *Bioinformatics*, *28*, 1647-1649.

Keenan, K., McGinnity, P., Cross, T. F., Crozier, W. W., & Prodöhl, P. A. (2013). *diveRsity*: An R package for the estimation and exploration of population genetics parameters and their associated errors. *Methods in Ecology and Evolution*, *4*, 782-788.

Kendall, M. S., Poti, M., Wynne, T. T., Kinlan, B. P., & Bauer, L. B. (2013). Consequences of the life history traits of pelagic larvae on interisland connectivity during a changing climate. *Marine Ecology Progress Series*, *489*, 43-59.

Krabbe, K., Leese, F., Mayer, C., Tollrian, R., & Held, C. (2010). Cryptic mitochondrial lineages in the widespread pycnogonid *Colossendeis megalonyx* Hoek, 1881 from Antarctic and Subantarctic waters. *Polar Biology*, *33*, 281-292.

Leiva, C., Riesgo, A., Avila, C., Rouse, G. W., & Taboada, S. (2018). Population structure and phylogenetic relationships of a new shallow-water Antarctic phyllodocid annelid. *Zoologica Scripta*, *47*, 714-726.

Leiva, C., Taboada, S., Kenny, N. J., Combosch, D., Giribet, G., Jombart, T., & Riesgo, A. (2019). Population substructure and signals of divergent adaptive selection despite admixture in the sponge Dendrilla antarctica from shallow waters surrounding the Antarctic Peninsula. Molecular ecology, 28(13), 3151-3170.

Librado, P., & Rozas, J. (2009). DnaSP v5: a software for comprehensive analysis of DNA polymorphism data. *Bioinformatics*, *25*, 1451-1452.

Linse, K., Cope, T., Lörz, A. N., & Sands, C. (2007). Is the Scotia Sea a centre of Antarctic marine diversification? Some evidence of cryptic speciation in the circum-Antarctic bivalve *Lissarca notorcadensis* (Arcoidea: Philobryidae). *Polar Biology*, *30*, 1059-1068.

Luck, G. W., Daily, G. C., & Ehrlich, P. R. (2003). Population diversity and ecosystem services. *Trends in Ecology & Evolution*, *18*, 331-336.

Mahon, A. R., Arango, C. P., & Halanych, K. M. (2008). Genetic diversity of *Nymphon* (Arthropoda: Pycnogonida: Nymphonidae) along the Antarctic Peninsula with a focus on *Nymphon australe* Hodgson 1902. *Marine Biology*, *155*, 315-323.

Manni, F., Guerard, E., & Heyer, E. (2004). Geographic patterns of (genetic, morphologic, linguistic) variation: how barriers can be detected by using Monmonier's algorithm. *Human Biology*, *76*, 173-190.

McLeod, E., Salm, R., Green, A., & Almany, J. (2009). Designing marine protected area networks to address the impacts of climate change. *Frontiers in Ecology and the Environment*, *7*, 362-370.

Meredith, M. P., & King, J. C. (2005). Rapid climate change in the ocean west of the Antarctic Peninsula during the second half of the 20th century. *Geophysical Research Letters*, *32*.

Meijers, A. J. S. (2014). The Southern Ocean in the coupled model intercomparison project phase 5. *Philosophical Transactions of the Royal Society A: Mathematical, Physical and Engineering Sciences*, *372*, 20130296.

Moreau, C., Danis, B., Jossart, Q., Eléaume, M., Sands, C., Achaz, G., ... & Saucède, T. (2019). Is reproductive strategy a key factor in understanding the evolutionary history of Southern Ocean Asteroidea (Echinodermata)?. *Ecology and Evolution*, *9*, 8465-8478.

Mouginot, J., Rignot, E., & Scheuchl, B. (2014). Sustained increase in ice discharge from the Amundsen Sea Embayment, West Antarctica, from 1973 to 2013. *Geophysical Research Letters*, *41*, 1576-1584.

Mulvaney, R., Abram, N. J., Hindmarsh, R. C., Arrowsmith, C., Fleet, L., Triest, J., ... & Foord,

S. (2012). Recent Antarctic Peninsula warming relative to Holocene climate and ice-shelf history. *Nature*, *489*, 141.

Neal, L., Wiklund, H., Muir, A. I., Linse, K., & Glover, A. G. (2014). The identity of juvenile Polynoidae (Annelida) in the Southern Ocean revealed by DNA taxonomy, with notes on the status of *Herdmanella gracilis* Ehlers *sensu* Augener. *Memoirs of Museum Victoria*, *71*, 203-216.

O'Connor, M. I., Bruno, J. F., Gaines, S. D., Halpern, B. S., Lester, S. E., Kinlan, B. P., & Weiss, J. M. (2007). Temperature control of larval dispersal and the implications for marine ecology, evolution, and conservation. *Proceedings of the National Academy of Sciences*, *104*, 1266-1271.

Palumbi, S. R. (2003). Population genetics, demographic connectivity, and the design of marine reserves. *Ecological Applications*, *13*, 146-158.

Paradis, E. (2010). *pegas*: an R package for population genetics with an integrated–modular approach. *Bioinformatics*, *26*, 419-420.

Paradis, E., Claude, J., & Strimmer, K. (2004). *APE*: analyses of phylogenetics and evolution in R language. *Bioinformatics*, *20*, 289-290.

Paris, J. R., Stevens, J. R., & Catchen, J. M. (2017). Lost in parameter space: a road map for stacks. *Methods in Ecology and Evolution*, *8*, 1360-1373.

Peck, L. S., & Conway, L. Z. (2000). The myth of metabolic cold adaptation: oxygen consumption in stenothermal Antarctic bivalves. *Geological Society*, *London*, *Special Publications*, *177*, 441-450.

Peck, L. S., Webb, K. E., & Bailey, D. M. (2004). Extreme sensitivity of biological function to temperature in Antarctic marine species. *Functional Ecology*, *18*, 625-630.

Pérez-Portela, R., & Riesgo, A. (2018). Population genomics of early-splitting lineages of metazoans. In Om P. Rajora (Ed.), *Population genomics* (pp. 1–35). Cham, Switzerland: Springer.

Pritchard, J. K., Stephens, M., & Donnelly, P. (2000). Inference of population structure using multilocus genotype data. *Genetics*, *155*, 945-959.

Raupach, M. J., Thatje, S., Dambach, J., Rehm, P., Misof, B., & Leese, F. (2010). Genetic homogeneity and circum-Antarctic distribution of two benthic shrimp species of the Southern Ocean, *Chorismus antarcticus* and *Nematocarcinus lanceopes*. *Marine Biology*, *157*, 1783-1797.

Rignot, E., Mouginot, J., Morlighem, M., Seroussi, H., & Scheuchl, B. (2014). Widespread, rapid grounding line retreat of Pine Island, Thwaites, Smith, and Kohler glaciers, West Antarctica, from 1992 to 2011. *Geophysical Research Letters*, *41*, 3502-3509.

Roberts, C. M. (1997). Connectivity and management of Caribbean coral reefs. *Science*, *278*, 1454-1457.

Schmidtko, S., Heywood, K. J., Thompson, A. F., & Aoki, S. (2014). Multidecadal warming of Antarctic waters. *Science*, *346*, 1227-1231.

Sangrà, P., Gordo, C., Hernández-Arencibia, M., Marrero-Díaz, A., Rodríguez-Santana, A., Stegner, A., ... & Pichon, T. (2011). The Bransfield current system. *Deep Sea Research Part I: Oceanographic Research Papers*, *58*, 390-402.

Santa Cruz, F., Ernst, B., Arata, J. A., & Parada, C. (2018). Spatial and temporal dynamics of the Antarctic krill fishery in fishing hotspots in the Bransfield Strait and South Shetland Islands. *Fisheries Research*, *208*, 157-166.

Schaberg, P. G., DeHayes, D. H., Hawley, G. J., & Nijensohn, S. E. (2008). Anthropogenic alterations of genetic diversity within tree populations: implications for forest ecosystem resilience. *Forest Ecology and Management*, *256*, 855-862.

Siegert, M. J., Rumble, J., Atkinson, A., Rogelj, J., Edwards, T., Davies, B. J., ... & Convey, P. (2019). The Antarctic Peninsula under a 1.5° C global warming scenario. *Frontiers in Environmental Science*, *7*, 102.

Smith, D., McGee, J., & Jabour, J. (2016). Marine protected areas: a spark for contestation over 'rational use' of Antarctic marine living resources in the Southern Ocean?. *Australian Journal of Maritime & Ocean Affairs*, *8*, 180-198.

Strugnell, J. M., Allcock, A. L., & Watts, P. C. (2017). Closely related octopus species show different spatial genetic structures in response to the Antarctic seascape. *Ecology and Evolution*, *7*, 8087-8099.

Strugnell, J. M., Watts, P. C., Smith, P. J., & Allcock, A. L. (2012). Persistent genetic signatures of historic climatic events in an Antarctic octopus. *Molecular Ecology*, *21*, 2775-2787.

Taboada, S., Riesgo, A., Wiklund, H., Paterson, G. L., Koutsouveli, V., Santodomingo, N., ... & Glover, A. G. (2018). Implications of population connectivity studies for the design of marine protected areas in the deep sea: An example of a demosponge from the Clarion-Clipperton Zone. *Molecular Ecology*, *27*, 4657-4679.

Thornhill, D. J., Mahon, A. R., Norenburg, J. L., & Halanych, K. M. (2008). Open-ocean barriers to dispersal: a test case with the Antarctic Polar Front and the ribbon worm *Parborlasia corrugatus* (Nemertea: Lineidae). *Molecular Ecology*, *17*, 5104-5117.

Vaughan, D. G., Marshall, G. J., Connolley, W. M., Parkinson, C., Mulvaney, R., Hodgson, D. A., ... & Turner, J. (2003). Recent rapid regional climate warming on the Antarctic Peninsula. *Climatic Change*, *60*, 243-274.

Wilson, N. G., Schrödl, M., & Halanych, K. M. (2009). Ocean barriers and glaciation:

evidence for explosive radiation of mitochondrial lineages in the Antarctic sea slug *Doris kerguelenensis* (Mollusca, Nudibranchia). *Molecular Ecology*, *18*, 965-984.

Wilson, N. G., Hunter, R. L., Lockhart, S. J., & Halanych, K. M. (2007). Multiple lineages and absence of panmixia in the “circumpolar” crinoid *Promachocrinus kerguelensis* from the Atlantic sector of Antarctica. *Marine Biology*, *152*, 895-904.

General Discussion & Conclusions

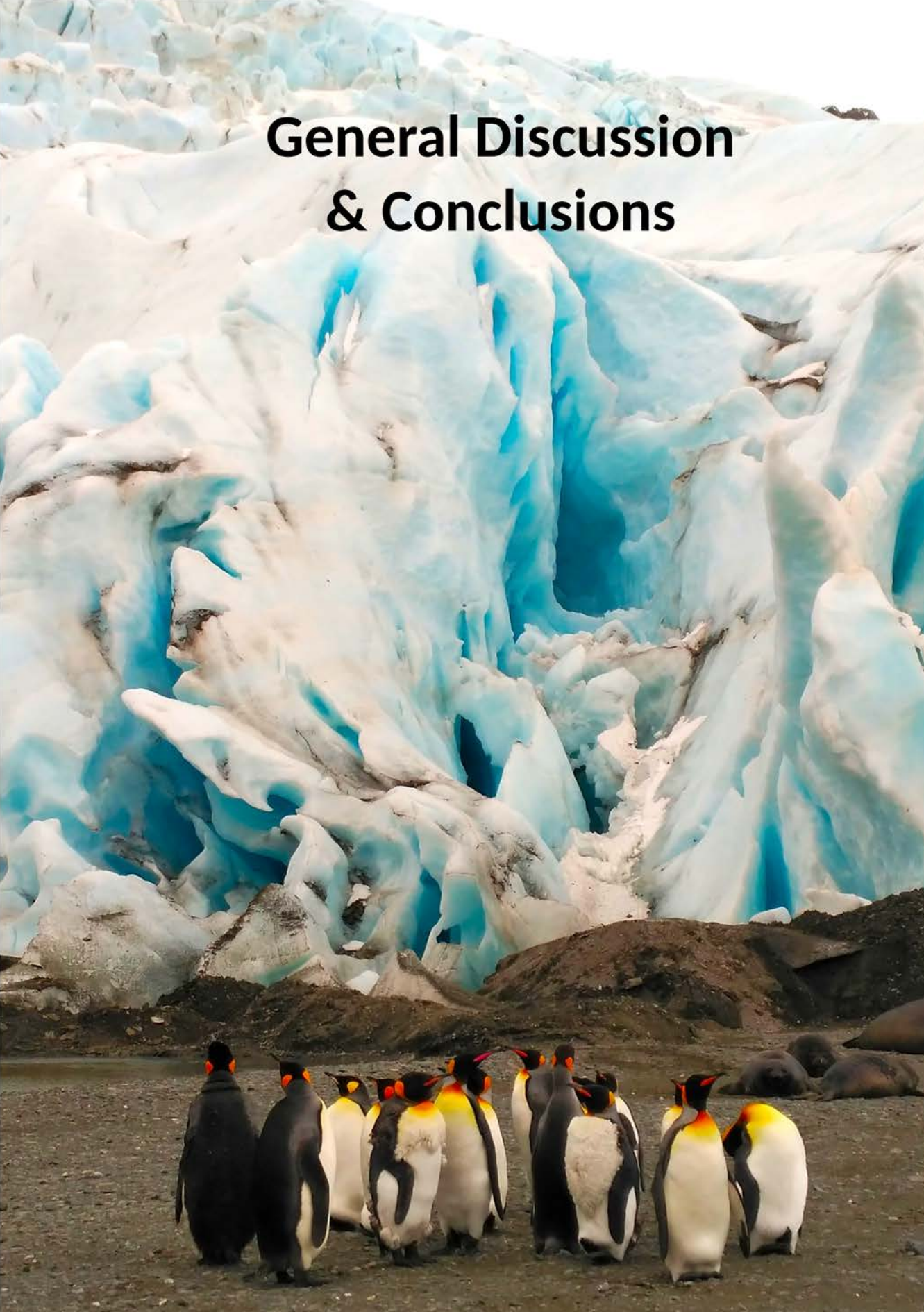

1- Evolutionary history of Antarctic shallow-water benthic invertebrates

Using a combination of different sequencing techniques, genetic markers, and biostatistical analyses, we were able to detect in our target species the genetic signals left by their evolutionary histories, infer connectivity patterns, and identify adaptive loci (see summary Table 1).

In general terms, we identified signals of demographic expansions after bottleneck events in most of the species, revealed by significantly negative neutrality tests (e.g. Tajima's *D*, Fu's F) and haplotype networks with star-like topologies. This pattern was observed for *Pterocirrus giribeti* (Chapter 1), *Dendrilla antarctica* (Chapter 2), *Antarctonemertes valida* (Chapters 3 and 4), and *Neanthes kerguelensis* (Chapter 4). For some of the species these results were more pronounced (*A. valida* and *N. kerguelensis*) than for others (*P. giribeti*), suggesting different evolutionary histories and population dynamics. Indeed, our results for *A. valida* and *N. kerguelensis* matched the expectations for organisms surviving *in situ* the Last Glacial Maximum (LGM) in Antarctic continental shelf refugia (Allcock & Strugnell, 2012). Similar results were obtained for the sea urchin *Sterechinus neumayeri* (Díaz et al., 2011, 2018), the ribbon worm *Parborlasia corrugatus* (Thornhill et al., 2008), and the shrimp *Chorismus antarcticus* (Raupach et al., 2010). In addition, the dating of the demographic expansion of *A. valida* (Chapter 3, Figure 2C) roughly coincided with the time of the glacial retreat in the Antarctic Peninsula after the LGM, between 10,000 and 18,000 years ago (Heroy & Anderson, 2007). Contrastingly, for the congeneric *A. riesgoae* we identified a parochial haplotype network (Chapter 3, Figure 2B), older populations (Chapter 3, Figure 2E), and a positive Tajima's *D* value (Chapter 3), indicating a deep-sea glacial refugium, as suggested for the amphipods *Eusirus* spp. (Baird et al., 2011). Our results for the two species of *Antarctonemertes* studied here clearly indicate the importance of studying closely related species with similar dispersal abilities, since different evolutionary histories might be inferred, as it has been widely documented for other marine invertebrates in the Atlanto-Mediterranean area (see Discussion in Taboada & Perez-Portela 2016).

In the particular case of *N. kerguelensis*, we also detected two cryptic mitochondrial lineages occurring in sympatry in the Western Antarctic Peninsula (WAP), which may indicate multiple glacial refugia in the WAP, followed by demographic expansion (both lineages presented star-like topologies, see Chapter 4, Figure 2D) and secondary contact, similar to what has been revealed for the Antarctic crinoid *Promachocrinus kerguelensis* (Hemery et al., 2012). Although not included in Chapter 4, we

also sequenced the nuclear 18S and 28S rRNA markers for two individuals of each mitochondrial lineage of *N. kerguelensis* from the WAP, obtaining exactly the same sequences for both markers. This mito-nuclear discordance could be the result of incomplete lineage sorting due to the different mutation rates and population effective sizes of the nuclear and the mitochondrial genome (Brown et al., 1979; Funk & Omland, 2003; Zink & Barrowclough, 2008). However, alternatively, it could be an indication of gene flow and nuclear homogeneity between the two mitochondrial lineages (e.g. Dasmahapatra et al., 2010). This hypothesis can be further tested using for instance nuclear markers with higher resolution, such as ddRADseq-derived SNPs. The presence of a third mitochondrial lineage at South Georgia Island (Chapter 4, Figure 2D) suggests another glacial refugium in the Subantarctic Island. The haplotype network of this third lineage did not present a star-like topology (Chapter 4, Figure 2D), indicating a milder bottleneck, and potentially less impact of the last glacial period in the Subantarctic population. This is supported by the additional EBSP analysis (not included in Chapter 4 and included here for clarity) that we ran for each of the three mitochondrial lineages (Figure 1). EBSP results showed that the South Georgia Island population, although also presented a demographic

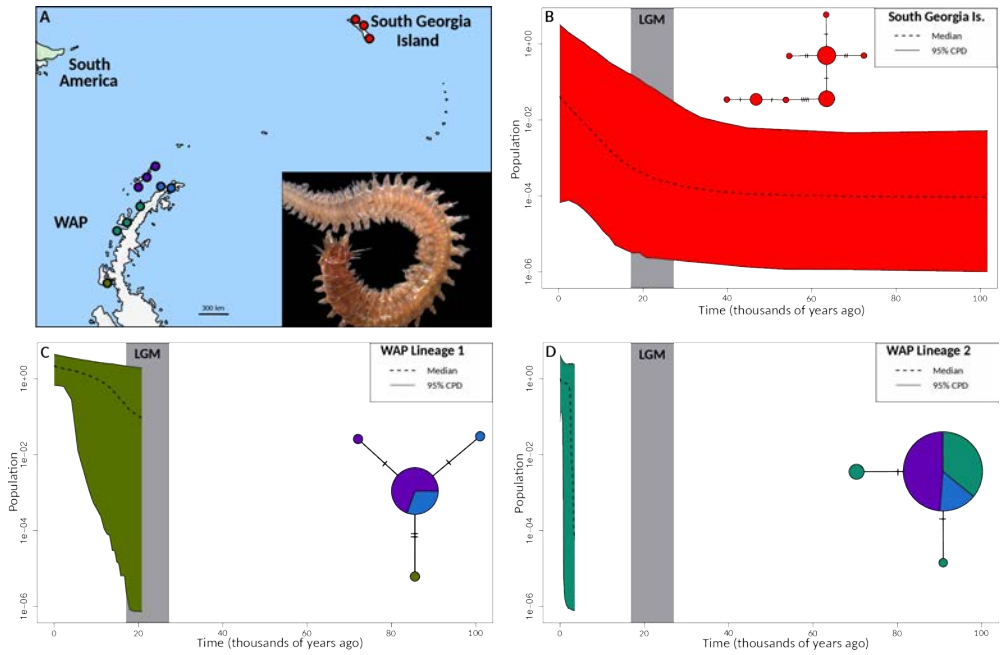

FIGURE 1 Additional EBSP analyses ran for the three lineages of *Neanthes kerguelensis*. **(A)** Sampling sations for *N. kerguelensis*, indicated by coloured circles. **(B-D)** EBSP results for the *N. kerguelensis* lineages from South Georgia Island **(B)**, and the two sympatric lineages from the WAP **(C** and **D)**.

expansion dated after the LGM, is the oldest and the most stable population (Figure 1B), compared to the recent expansions of the mitochondrial lineages inhabiting the WAP (Figures 1C and 1D).

Although in Chapter 1 we suggested that a Subantarctic glacial refugium may have been possible for *P. giribeti* due to the presence of the species at South Georgia Island, our results from Chapter 4, which included additional sequences of individuals from South Georgia Island, were not in agreement with the expected pattern under this glacial-refugium strategy (compare Figure 2C in Chapter 4 with Figure 5C in the Introduction, the latter showing the *COI* haplotype network of *Nacella concinna*, from González-Wevar et al., 2013). Our results for *P. giribeti* seem to rather indicate a deep-sea glacial refugium, with a diffuse *COI* haplotype network typical of species with a high-dispersal planktonic stage (see Allcock & Strugnell, 2012), such as the Antarctic shrimp *Nematocarcinus lanceopes* (Raupach et al., 2010) and the Antarctic brittle star *Astrotoma agassizii* (Hunter & Halanych, 2008), both shown in Figure 5B of the Introduction.

The combined use of mitochondrial and ddRADseq-derived SNPs in *Antarctonemertes* (Chapter 3) allowed us to unveil an extraordinary evolutionary history characterised by the reticulate evolution of the *Antarctonemertes* lineages in the Southern Ocean. We identified two mito-nuclear discordances, one due to an ancient introgressive event that left signals in the nuclear genome (Chapter 3, Figure 3B), and the other due to a mitochondrial capture produced by a short introgression followed by a reinforcement event. Our results regarding the introgressive history in the genus *Antarctonemertes* were in agreement with the evolutionary history of the different species, since the mitochondrial capture detected followed the model proposed when one species expands over another's species range, with the mitochondrial introgressing asymmetrically from the local species to the expanding one (Currat et al., 2008; Excoffier et al., 2009; Petit & Excofier, 2009; Wielstra & Arntzen, 2012). This is the case of the introgressive event that occurred in the WAP after the continental shelf colonization by the expanding populations of *A. riesgoae* from their deep-sea refugium. Indeed, the *Antarctonemertes* 'hybrid morphology' lineage, which is the result of this short hybridisation, presented the mitochondrial genome of the originally local *A. valida* with a nuclear background of the invading *A. riesgoae*. Moreover, the historically blurred species boundaries of the *Antarctonemertes* species were in agreement with the finding of contemporary hybrids between *A. valida* and *A. riesgoae* at South Georgia Island (Chapter 3, Figure 4).

Species	Markers	Inferred glacial refugium	Hybridization	Cryptic lineages	Adaptation addressed
Pterocirrus giribeti	*COI* and *16S*	Deep-sea	No	No	No
Dendrilla antarctica	Mitogenome and ddRADseq-derived SNPs	?	No	No	Yes, intraspecifically
Antarctonemertes valida	*COI* and ddRADseq-derived SNPs	Continental shelf	Yes	Yes, 2	Yes, interspecifically
Antarctonemertes riesgoae	*COI* and ddRADseq-derived SNPs	Deep-sea	Yes	No	Yes, interspecifically
Neanthes kerguelensis	*COI*	Continental shelf and Subantarctica	No	Yes, 3	No
Mycale acerata	*COI*	?	No	No	No

TABLE 1 Summary of table showing studied species, markers used, inferred glacial refugium for each species, and whether we found signals of hybridization, cryptic speciation, and adaptation.

2- Natural selection in action: genomic signals of adaptive selection

Signals of adaptation and natural selection were revealed for *Dendrilla antarctica* (Chapter 2) and *Antarctonemertes* (Chapter 3) in their ddRADseq datasets. For *D. antarctica*, we identified loci under positive selection in different populations that presented high contemporary gene flow, an illustrative example of adaptation with gene flow at the intraspecific level. On the other hand, we detected loci with an adaptive role between different *Antarctonemertes* species, shedding light into the genomics of speciation, reinforcement, and adaptation to particular evolutionary histories.

2.1- Selective pressures at the intraspecific level

Once considered a rare phenomenon in the ocean, local adaptation in marine systems has recently received relatively high attention (Sanford & Kelly, 2011). Although it may seem counter-intuitive, high gene-flow levels between populations of a species are not considered to impede local adaptation, as just a few successful migrants per generation are sufficient to maintain genetic homogeneity in neutral loci, while they are not enough to generate homogeneity across the entire genome (Sanford & Kelly, 2011). Examples of local adaptation in marine invertebrates presenting high levels of population connectivity have been recently found, for instance, in the marine snail *Chlorostoma funebralis* (Gleason & Burton, 2016), and the red abalone *Haliotis rufescens* (De Wit & Palumbi, 2013). Also, some fishes present similar patterns, such as the Atlantic cod *Gadus morhua* (Barth et al., 2017) and the Atlantic herring *Clupea harengus* (Limborg et al., 2012).

For *D. antarctica*, we found signals of divergent selection in 140 loci (Chapter 2), which provided a significant geographic structure suggesting different selective pressures between the Southern WAP (Adelaide Island), Central WAP (Paradise Bay), and the Bransfield Strait area. Using our *de novo* transcriptome as intermediary between the RAD-loci and the *nr* NCBI database, we were able to annotate 14 of these loci with signatures of positive selection. Most of the loci were related to cellular functions involved in the stress and immune responses, such as cytoskeleton reorganization, apoptosis, ubiquitination, and response to environmental stressors (Chapter 2, Figure 4), which is part of the molecular toolkit that sponges use to differentiate between food, pathogens, and symbionts in the seawater that they filter (Pita et al., 2018). Also, two of these loci blasted against genes that are involved in the assembly, function, motility, and power stroke of flagella and cilia, indicating divergent selection in the filter abilities of the sponges inhabiting the Bransfield Strait, Central WAP, and Southern WAP. We suggest that the

vastly different composition and abundance of planktonic communities between these areas may have driven local adaptation of *D. antarctica* populations. In turn, planktonic communities off the WAP vary with sea-ice extent and duration (Ducklow et al., 2013), which spans from below 150 days a year in the Northern WAP to ca. 250 days a year in Adelaide Island (Stammerjohn et al., 2008). This may be the key factor after *D. antarctica* local adaptation, showing this remarkable sea-ice—benthos coupling via planktonic communities.

Future perspectives under global warming anticipate a decline on sea-ice levels at the WAP, mostly at the Bransfield Strait area (Siegert et al., 2019). This trend has already been detected from satellite data since 1979 and climate models, showing that sea-ice extent is declining at a rate of 6–10% per decade (Turner et al., 2015) and the sea-ice duration has been shortened by 4 days per year since 1979 to 2010 (Massom et al., 2018), which means that the sea-ice season duration in the WAP has been reduced by more than three months since 1979 (Stammerjohn et al., 2012). Hence, since the sea ice is a decisive factor governing planktonic communities, which in turn are apparently the main aspect promoting local adaptation of *D. antarctica* populations, we expect considerable changes in the near future for the populations of *D. antarctica* in the WAP. Under the projections of a declining sea-ice extent and duration, we anticipate a remarkable vulnerability of *D. antarctica* to global warming due to its link to the sea ice and planktonic communities, which could be certainly extended to other benthic Antarctic species, due to the high dependence on the sea ice of the coastal marine ecosystems of the WAP (Ducklow et al., 2013). With the sea-ice perspectives being especially concerning for the Northern WAP region, we propose that the Bransfield Strait area should be considered as a high priority region to conservation due to its serious sensitivity to the already ongoing global warming, in agreement with our conclusions from the genetic connectivity and diversity results (Chapter 4, discussed below).

2.2- Genomics of speciation and adaptation to particular glacial-refugium strategies

In Chapter 3, we aimed to identify loci with an adaptive role for *A. valida* to its *in situ* glacial survival of the LGM in Antarctic shallow waters. Using two different approaches, including the F_{ST}-outlier method implemented in BayeScan and a DAPC-based procedure, we detected 119 loci with signals of divergent selection between *A. valida* and the rest of *Antarctonemertes* lineages. The blast search using our *de novo* transcriptomes as intermediaries resulted in 37 annotated loci matching animal genes. Most of them blasted against the molluscan genomes of *Lottia gigantea*, *Pomacea canaliculata*, and *Crassostrea*

gigas, or the brachiopod *Lingula anatina*, thus validating our RAD-loci and transcriptome contigs, as these lophotrochozoan genomes are the most closely related available genomes for *Antarctonemertes* due to the lack of a properly annotated nemertean genome.

Within the 37 annotated loci, 13 of them blasted against genes with functions related to the immune and stress responses, acting directly on the response pathways or through cellular mechanisms that involve endomembranous compartments responsive to cellular stress (endoplasmic reticulum, Golgi apparatus, and vesicle turnover). As already discussed for *D. antarctica* (Chapter 2 and previous discussion section), immune and stress responses are ubiquitous functions appearing in studies concerning local adaptation, due to their role mitigating the cellular stress provoked by the environmental factors that particular populations may be adapting to (e.g. Bay & Palumbi, 2014; Jin et al., 2016; Gleason & Burton, 2016; van Oppen et al., 2018; VanWallendael et al., 2019). Within the immune and stress responses function, ubiquitination appeared as a prevalent function involved in adaptation, represented by different families of ubiquitin-ligases. One of them, the RING finger protein family (RNF), was present in both RADseq datasets analysed in this PhD dissertation: the RNF157 for *D. antarctica*, and the RNF115 for *Antarctonemertes*. These results were not unexpected, as ubiquitination plays a central role both in the immune response regulating the pattern-recognition signalling (Hu & Sun, 2016), and in the stress response as part of the ubiquitin-proteasome system, targeting irreversibly damaged proteins and macromolecular debris generated by cellular stress for their proteolysis (degradation) in the proteasome (Kültz, 2003; Nassif et al., 2014).

Apart from these 13 loci, six loci related to the nervous system, brain and eye development and four loci involved in the digestion were identified as adaptative loci for *A. valida* from the WAP. We suggest that the signals of diversifying selection detected in these loci may be related to the differences between shallow-water and deep-sea glacial refugia. Indeed, coastal polynyas similar to those where *A. valida* may have survived the LGM present several particularities in terms of nutrients, water conditions, light, and planktonic communities and dynamics (Arrigo & van Dijken, 2003, 2004; Smith & Gordon, 1997), which may have required the adaptation of the visual and digestive systems in *A. valida* that we report in Chapter 3.

Finally, in the *Antarctonemertes* dataset (Chapter 3) we also identified six adaptive loci involved in spermatogenesis and reproduction, relevant functions found in studies concerning sexual selection, speciation and reinforcement events, and reproductive isolation (e.g. Civetta et al., 2005; Llopart & Comeron, 2006; Hopkins et al.,

2012; Smadja et al., 2015; Foote, 2018). Selective pressure in these genes is in agreement with the prezygotic barriers expected in speciation and reinforcement events (Garner et al., 2018), such as differences in the sperm, copulation, and reproductive behaviour that differences in the identified genes may imply. This hypothesis agrees with our results regarding the evolutionary history of *Antarctonemertes* in the WAP: a short introgressive event between *A. riesgoae* and *A. valida*, involving a mitochondrial capture and producing the *Antarctonemertes* 'hybrid morphology' lineage that exists nowadays. This hybridisation was then followed by a reinforcement event characterised by the selective pressure that we identified in genes with spermatogenesis and reproductive functions, which is also consistent with the absence of current hybrids between *A. valida* and *A. riesgoae* in the WAP, while the Subantarctic lineages are still able to hybridise at South Georgia Island.

3- Genetic connectivity patterns of Antarctic benthic invertebrates: management and conservation implications

Genetic connectivity is an omnipresent topic throughout this PhD dissertation, being one of the few subjects appearing in all Chapters. In Chapters 1 and 2 it is discussed as one of the main aspects studied for our target species. In Chapter 3, although it is not directly addressed, our results also revealed certain connectivity patterns, which are thoroughly discussed later in Chapter 4. This last Chapter is completely dedicated to the genetic connectivity patterns of Antarctic benthic invertebrates, summarising and reviewing results from previous Chapters and published studies, and discussing them from a management and conservation perspective. In this sense, we aimed to test whether the current state of Marine Protected Areas (MPAs) in our study area (Scotia Sea and WAP) is enough to maintain appropriate connectivity levels between the different regions, and hence whether it is promoting and ensuring ecosystem resilience and persistence.

3.1- Genetic connectivity patterns within the Western Antarctic Peninsula

In Chapters 1, 2, and 4, we discussed gene-flow levels between the different sampling stations and areas of the WAP. In general, high levels of genetic connectivity were detected for all the studied species regardless of their reproductive strategy, from the brooding nemerteans to the planktotrophic larvae of *P. giribeti*. Long-distance connectivity was already detected in other shallow-water benthic invertebrates along the WAP, such as the brittle stars *Ophionotus victoriae* (Galaska et al., 2017a) and *Astrotoma agassizii* (Galaska et al., 20017b), the Antarctic limpet *Nacella concinna* (González-Wevar et al., 2013), and the nemertean *Parborlasia corrugatus* (Thornhill et al., 2008). Although this long-distance connectivity is common within Antarctic marine invertebrates, the high gene flow detected for *D. antarctica* (Chapter 2) is exceptional for sponges, which usually display strong genetic structure even at local scales (Pérez-Portela & Riesgo, 2016). Remarkably, our results for the genetic substructures across the different species agreed with the oceanic current system of the WAP, being the Peninsula Front the main genetic break for *P. giribeti* (Chapter 1, Figure 4), *D. antarctica* (Chapter 2, Figure 2), and *A. valida* (Chapter 4, Figure 3). This genetic barrier is interpreted as a semi-permeable barrier in these three cases, as our results suggested that it is frequently crossed by dispersal propagules (larvae or adults/cocoons in drifting algae). Indeed, dispersal propagules may be crossing this barrier assisted by the inter-frontal anticyclonic eddy system located between the Peninsula Front and the Bransfield Current (Sangrà et al., 2011), taking

advantage of the intra-annual seasonal weakening of the Peninsula Front (Zhou et al., 2006; Sangrà et al., 2011; Huneke et al., 2016), or due to its inter-annual variation depending on the Southern Annual Mode (SAM) and El Niño Southern Oscillation (ENSO) (Dotto et al., 2016; Barlett et al., 2018).

In addition, contemporary migration analyses also revealed the overlapping between genetic connectivity patterns and the ocean circulation. For instance, high gene flow between the Southern WAP and the South Shetland Islands was detected for *D. antarctica* (Chapter 2, Figure 3), probably as a consequence of the Antarctic Peninsula Coastal Current (APCC) running southwards off the WAP (Moffat et al., 2008) and the ACC running northwards. This connection between the South Shetlands and Southern WAP areas was also revealed for *A. valida*, for which high migration was detected between Petermann Island and Deception Island (Chapter 4, Figure 3G).

Regarding the genetic diversity patterns, the Bransfield Strait waters are considered a hotspot of genetic diversity for many Antarctic marine organisms (e.g. Wilson et al., 2007; Mahon et al., 2008; Janosik et al., 2010; Galaska et al., 2017a). Although our results from Chapter 1 (Chapter 1, Table 2), Chapter 2 (Chapter 2, Table 2), and Chapter 4 (Chapter 4, Tables 2 and 5) did not entirely match these expectations, we still believe that the Bransfield Strait area should be considered as a high priority area for conservation in Antarctica given its role as a hotspot of genetic diversity. Besides, as discussed above in section 2, the Bransfield Strait area will certainly undergo major changes in the near future due to global warming and, additionally, it is currently the main fishing ground for the krill fishery in Antarctica (Santa Cruz et al., 2018). On the whole, we consider that this region urgently requires a special management similar to the planned within the Domain 1 MPA (D1MPA) proposal, with both fishing and protected zones designed at the South Shetlands and Northern WAP (see Chapter 4, Figure 1B).

3.2- Genetic connectivity across the Scotia Sea and the Western Antarctic Peninsula

Our results for the genetic connectivity and structure presented in Chapter 4 evidenced the lack of contemporary migration between the South Georgia and South Sandwich Islands MPA (SGSSI MPA) and the WAP region. This result was revealed from *COI* data consistently throughout the five studied species (Chapter 4, Figure 2), which presented different reproductive strategies and dispersal abilities (see Introduction, Box 3). Additionally, our results from ddRADseq-derived SNPs for *A. valida* and *A. riesgoae* also confirmed this genetic break between Antarctic and Subantarctic populations (Chapter 4, Figures 3 and 4). Interestingly, most studies of marine benthic organisms distributed across

these areas present genetic differentiation between their SGSSI MPA and WAP populations (see Chapter 4, Table 7). Hence, we corroborated that population connectivity of benthic invertebrates in the Southern Ocean is not linked to the reproductive strategy, as already suggested by Halanych and Mahon (2018). Remarkably, our results for *M. acerata* suggested a stepping-stone role of the South Orkney Islands between the two disconnected areas, which is considered a key feature of MPAs within an MPA network in order to achieve the beneficial outcome of a connected MPA network (Roberts, 1997; Palumbi, 2003).

Our community-level results presented in Chapter 4 provide relevant genetic connectivity information in order to establish a connected network of MPAs in the Southern Ocean. We recommend the urgent implementation of an MPA in the WAP region, expanding northwards to the shallow waters adjacent to the South Orkney Islands, following the Domain 1 MPA (D1MPA) that was proposed in the 37th CCAMLR Meeting in 2018, but was not approved by the Commission. Chapter 4 was conceived to fill the existing gap between the scientific knowledge on the connectivity of Antarctic benthic invertebrates and the current plans for implementing an MPA network in the Southern Ocean, presenting our data and discussing the results following the recommendations from Jenkins and Stevens (2018).

Conclusions

This PhD dissertation was conceived to answer questions regarding evolutionary history, phylogeographic and connectivity patterns of Antarctic shallow-water benthic invertebrates. A broad range of target species was selected, and studied using both mitochondrial and genome-wide nuclear markers. In the light of the results exposed throughout my PhD dissertation, I reached several general conclusions, which are succinctly presented below:

- Regarding evolutionary history, we found different glacial-survival strategies for our selected species, revealing (i) the independence between glacial-survival strategy and reproductive mode, and (ii) that almost all species presented signals of recent bottleneck events, highlighting the influence of glacial cycles on the evolutionary history of Antarctic shallow-water benthic invertebrates. We also demonstrated that particular evolutionary histories and glacial-refugium strategies leave adaptive signals across the genome.

- Our phylogeographic results for *Antarctonemertes* evidenced the blurred species boundaries that closely related lineages may present. We suggest that glacial cycles played a central role in hybridisation of Antarctic shallow-water benthic organisms, due to the repeated rounds of isolation during glacial periods and secondary contacts during interglacials that marine life experienced in the Southern Ocean. In addition, we illustrated how the detection of adaptive genes can inform about the prezygotic barriers that emerged during speciation and reinforcement events.

- Our genetic connectivity results showed high gene-flow levels within the Western Antarctic Peninsula (WAP) for all the studied species, indicating that connectivity in the WAP is not determined by *a priori* dispersal abilities resulting from different reproductive strategies, which is the general rule in warmer seas. Genetic substructure was governed by oceanic currents and fronts in our target species, and again, regardless of their dispersal potential. The strong currents flowing around the austral continent may have originated these peculiarities in the connectivity patterns of Southern Ocean organisms.

- Our results also showed that local adaptation can concur with long-distance connectivity. We suggest that the sea ice can be a relevant factor driving local adaptation of benthic invertebrates in the WAP, since the entire coastal marine ecosystem is ice-dependent and

many organisms rely on sea-ice extent, duration, and seasonality for feeding. These results exhibit the vulnerability of the WAP benthic ecosystems due to the decline on the sea ice predicted for the near future.

- Our gene-flow results showed that long-distance connectivity does not surpass the regional WAP scale. Thus, our genetic diversity and connectivity results supported the implementation of a Marine Protected Area (MPA) covering the WAP and the shelf waters adjacent to the South Orkney Islands, due to (i) the lack of migration between the South Georgia and South Sandwich Islands MPA (SGSSI MPA) and the WAP, and (ii) the remarkable stepping-stone role detected for the South Orkney Islands.

Overall, the results presented herein challenge the classic idea of Antarctic benthic communities being stable and unaltered through time. Indeed, this PhD dissertation demonstrated the adaptability with which Antarctic shallow-water benthic invertebrates have responded to the natural fluctuations of the Southern Ocean. However, it is a matter of concern whether these communities will resist the consequences of the already ongoing rapid global warming, combined with local pressures such as fishing and tourism, and threatened by profound changes in sea-ice extent and duration. Area-based management tools such as MPAs will be of paramount relevance if they are designed under an MPA network approach, providing enough ecosystem resilience in order to ensure conservation and persistence of the unique Antarctic ecosystems.

References

Allcock, A. L., & Strugnell, J. M. (2012). Southern Ocean diversity: new paradigms from molecular ecology. *Trends in Ecology & Evolution*, *27*, 520-528.

Allcock, A. L., Strugnell, J. M., Prodöhl, P., Piatkowski, U., & Vecchione, M. (2007). A new species of Pareledone (Cephalopoda: Octopodidae) from Antarctic Peninsula waters. *Polar Biology*, *30*, 883-893.

Allcock, A. L., Barratt, I., Eleaume, M., Linse, K., Norman, M. D., Smith, P. J., ... & Strugnell, J. M. (2011). Cryptic speciation and the circumpolarity debate: a case study on endemic Southern Ocean octopuses using the *COI* barcode of life. *Deep Sea Research Part II: Topical Studies in Oceanography*, *58*, 242-249.

Anderson, J. B., Shipp, S. S., Lowe, A. L., Wellner, J. S., & Mosola, A. B. (2002). The Antarctic Ice Sheet during the Last Glacial Maximum and its subsequent retreat history: a review. *Quaternary Science Reviews*, *21*, 49-70.

Andrássy, I. (1998). Nematodes in the sixth continent. *Journal of Nematode Morphology and Systematics*, *1*, 107-186.

Andrews, K. R., Good, J. M., Miller, M. R., Luikart, G., & Hohenlohe, P. A. (2016). Harnessing the power of RADseq for ecological and evolutionary genomics. *Nature Reviews Genetics*, *17*, 81.

Arango, C. P., Soler-Membrives, A., & Miller, K. J. (2011). Genetic differentiation in the circum—Antarctic sea spider *Nymphon australe* (Pycnogonida; Nymphonidae). *Deep Sea Research Part II: Topical Studies in Oceanography*, *58*, 212-219.

Arntz, W. E., Gutt, J., & Klages, M. (1997). Antarctic marine biodiversity: an overview. Antarctic communities: species, structure and survival. Cambridge University Press, Cambridge, 3-14.

Arrigo, K. R., & Van Dijken, G. L. (2003). Phytoplankton dynamics within 37 Antarctic coastal polynya systems. *Journal of Geophysical Research: Oceans*, *108*.

Arrigo, K. R., & van Dijken, G. L. (2004). Annual changes in sea-ice, chlorophyll a, and primary production in the Ross Sea, Antarctica. *Deep Sea Research Part II: Topical Studies in Oceanography*, *51*, 117-138.

Ayre, D. J., Minchinton, T. E., & Perrin, C. (2009). Does life history predict past and current connectivity for rocky intertidal invertebrates across a marine biogeographic barrier?. *Molecular Ecology*, *18*, 1887-1903.

Baco, A. R., Etter, R. J., Ribeiro, P. A., Von der Heyden, S., Beerli, P., & Kinlan, B. P. (2016). A synthesis of genetic connectivity in deep-sea fauna and implications for marine reserve design. *Molecular Ecology*, *25*, 3276-3298.

Baird, H. P., Miller, K. J., & Stark, J. S. (2011). Evidence of hidden biodiversity, ongoing speciation and diverse patterns of genetic structure in giant Antarctic amphipods. *Molecular Ecology*, *20*, 3439-3454.

Barlett, E. M. R., Tosonotto, G. V., Piola, A. R., Sierra, M. E., & Mata, M. M. (2018). On the temporal variability of intermediate and deep waters in the Western Basin of the Bransfield Strait. *Deep Sea Research Part II: Topical Studies in Oceanography*, *149*, 31-46.

Barnes, D. K., Hodgson, D. A., Convey, P., Allen, C. S., & Clarke, A. (2006). Incursion and excursion of Antarctic biota: past, present and future. *Global Ecology and Biogeography*, *15*, 121-142.

Barth, J. M., Berg, P. R., Jonsson, P. R., Bonanomi, S., Corell, H., Hemmer-Hansen, J., ... & Moksnes, P. O. (2017). Genome architecture enables local adaptation of Atlantic cod despite high connectivity. *Molecular Ecology*, *26*, 4452-4466.

Bay, R. A., & Palumbi, S. R. (2014). Multilocus adaptation associated with heat resistance in reef-building corals. *Current Biology*, *24*, 2952-2956.

Bernal, M. A., Gaither, M. R., Simison, W. B., & Rocha, L. A. (2017). Introgression and selection shaped the evolutionary history of sympatric sister species of coral reef fishes (genus: Haemulon). *Molecular Ecology*, *26*, 639-652.

Brooks, C. M. (2013). Competing values on the Antarctic high seas: CCAMLR and the challenge of marine-protected areas. *The Polar Journal*, *3*, 277-300.

Brown, W. M., George, M., & Wilson, A. C. (1979). Rapid evolution of animal mitochondrial DNA. *Proceedings of the National Academy of Sciences*, *76*, 1967-1971.

Catchen, J. M., Hohenlohe, P. A., Bernatchez, L., Funk, W. C., Andrews, K. R., & Allendorf, F. W. (2017). Unbroken: RADseq remains a powerful tool for understanding the genetics of adaptation in natural populations. *Molecular Ecology Resources*, *17*, 362-365.

Chwedorzewska, K., & Korczak, M. (2010). Human impact upon the environment in the vicinity of Arctowski Station, King George Island, Antarctica. *Polish Polar Research*, *31*, 45-60.

Civetta, A., Rajakumar, S. A., Brouwers, B., & Bacik, J. P. (2005). Rapid evolution and gene-specific patterns of selection for three genes of spermatogenesis in *Drosophila*. *Molecular Biology and Evolution*, *23*, 655-662.

Clancy, R., Manning, J., & Brolsma, H. (2013). Mapping Antarctica: a five hundred year record of discovery. Springer Science & Business Media.

Clarke, A., & Johnston, I. A. (1996). Evolution and adaptive radiation of Antarctic fishes. *Trends in Ecology & Evolution*, *11*, 212-218.

Clarke, A., & Johnston, N. M. (2003). Antarctic marine benthic diversity. In Oceanography and Marine Biology, An Annual Review, Volume 41 (pp. 55-57). CRC Press.

Collins, E. E., Galaska, M. P., Halanych, K. M., & Mahon, A. R. (2018). Population genomics of *Nymphon australe* Hodgson, 1902 (Pycnogonida, Nymphonidae) in the Western Antarctic. *The Biological Bulletin*, *234*, 180-191.

Cook, A. J., Fox, A. J., Vaughan, D. G., & Ferrigno, J. G. (2005). Retreating glacier fronts on the Antarctic Peninsula over the past half-century. *Science*, *308*, 541-544.

Cordonnery, L., & Kriwoken, L. (2015). Advocating a Larger Role for Environmental Nongovernment Organizations in Developing a Network for Marine Protected Areas in the Southern Ocean. *Ocean Development & International Law*, *46*, 188-207.

Corrigan, S., Delser, P. M., Eddy, C., Duffy, C., Yang, L., Li, C., ... & Naylor, G. J. (2017). Historical introgression drives pervasive mitochondrial admixture between two species of pelagic sharks. *Molecular Phylogenetics and Evolution*, *110*, 122-126.

Cowen, R. K., & Sponaugle, S. (2009). Larval dispersal and marine population connectivity. *Annual Review of Marine Science*, *1*, 443-466.

Crame, J. A. (1999). An evolutionary perspective on marine faunal connections between southernmost South America and Antarctica. *Scientia Marina*, *63*, 1-14.

Culik BM, Wilson RP (1991) Penguins crowded out? *Nature* 351:340

Currat, M., Ruedi, M., Petit, R. J., & Excoffier, L. (2008). The hidden side of invasions: massive introgression by local genes. *Evolution: International Journal of Organic Evolution*, *62*, 1908-1920.

Dasmahapatra, K. K., Elias, M., Hill, R. I., Hoffman, J. I., & Mallet, J. (2010). Mitochondrial DNA barcoding detects some species that are real, and some that are not. *Molecular Ecology Resources*, *10*, 264-273.

Deagle, B. E., Faux, C., Kawaguchi, S., Meyer, B., & Jarman, S. N. (2015). Antarctic krill population genomics: apparent panmixia, but genome complexity and large population size muddy the water. *Molecular Ecology*, *24*, 4943-4959.

DeConto, R. M., & Pollard, D. (2003). Rapid Cenozoic glaciation of Antarctica induced by declining atmospheric CO_2. *Nature*, *421*, 245.

De Wit, P., & Palumbi, S. R. (2013). Transcriptome-wide polymorphisms of red abalone (*Haliotis rufescens*) reveal patterns of gene flow and local adaptation. *Molecular Ecology*, *22*, 2884-2897.

Díaz, A., Féral, J. P., David, B., Saucède, T., & Poulin, E. (2011). Evolutionary pathways among shallow and deep-sea echinoids of the genus Sterechinus in the Southern Ocean. *Deep Sea Research Part II: Topical Studies in Oceanography*, *58*, 205-211.

Díaz, A., Gerard, K., González-Wevar, C., Maturana, C., Féral, J. P., David, B., ... & Poulin, E. (2018). Genetic structure and demographic inference of the regular sea urchin *Sterechinus neumayeri* (Meissner, 1900) in the Southern Ocean: The role of the last glaciation. *PloS One*, *13*, e0197611.

Diester-Haass, L., & Zahn, R. (2001). Paleoproductivity increase at the Eocene–Oligocene climatic transition: ODP/DSDP Sites 763 and 592. *Palaeogeography, Palaeoclimatology, Palaeoecology*, *172*, 153-170.

Dotto, T. S., Kerr, R., Mata, M. M., & Garcia, C. A. (2016). Multidecadal freshening and lightening in the deep waters of the Bransfield Strait, Antarctica. *Journal of Geophysical Research: Oceans*, *121*, 3741-3756.

Ducklow, H. W., Fraser, W. R., Meredith, M. P., Stammerjohn, S. E., Doney, S. C., Martinson, D. G., ... & Amsler, C. D. (2013). West Antarctic Peninsula: an ice-dependent coastal marine ecosystem in transition. *Oceanography*, *26*, 190-203.

Egan, K. E., Rickaby, R. E., Hendry, K. R., & Halliday, A. N. (2013). Opening the gateways for diatoms primes Earth for Antarctic glaciation. *Earth and Planetary Science Letters*, *375*, 34-43.

Ehlers, E. H. (1897). Polychaeten: Hamburger Magalhaensische Sammelreise. Friederichsen.

Eijgelaar, E., Thaper, C., & Peeters, P. (2010). Antarctic cruise tourism: the paradoxes of ambassadorship, “last chance tourism” and greenhouse gas emissions. *Journal of Sustainable Tourism*, *18*, 337-354.

Excoffier, L., Foll, M., & Petit, R. J. (2009). Genetic consequences of range expansions. *Annual Review of Ecology, Evolution, and Systematics*, *40*, 481-501.

Foote, A. D. (2018). Sympatric speciation in the genomic era. *Trends in Ecology & Evolution*, *33*, 85-95.

Fraser, C. I., Terauds, A., Smellie, J., Convey, P., & Chown, S. L. (2014). Geothermal activity helps life survive glacial cycles. *Proceedings of the National Academy of Sciences*, *111*, 5634-5639.

Fretwell, P., Pritchard, H. D., Vaughan, D. G., Bamber, J. L., Barrand, N. E., Bell, R., ... & Catania, G. (2012). Bedmap2: improved ice bed, surface and thickness datasets for Antarctica. *The Cryosphere Discussions*, *6*, 4305-4361.

Friedlaender, A., Modest, M., & Johnson, C. (2018) Whales of the Antarctic Peninsula – Science and Conservation for the 21st Century. A report for policymakers from the University of California, Santa Cruz and WWF Antarctic Conservation Programme. DOI: 10.13140/RG.2.2.29921.76640

Funk, D. J., & Omland, K. E. (2003). Species-level paraphyly and polyphyly: frequency, causes, and consequences, with insights from animal mitochondrial DNA. *Annual Review of Ecology, Evolution, and Systematics*, *34*, 397-423.

Fyke, J. G., D'Orgeville, M., & Weaver, A. J. (2015). Drake Passage and Central American Seaway controls on the distribution of the oceanic carbon reservoir. *Global and Planetary Change*, *128*, 72-82.

Galaska, M. P., Sands, C. J., Santos, S. R., Mahon, A. R., & Halanych, K. M. (2017a). Geographic structure in the Southern Ocean circumpolar brittle star *Ophionotus victoriae* (Ophiuridae) revealed from mtDNA and single-nucleotide polymorphism data. *Ecology and Evolution*, *7* 475-485.

Galaska, M. P., Sands, C. J., Santos, S. R., Mahon, A. R., & Halanych, K. M. (2017b). Crossing the divide: admixture across the Antarctic polar front revealed by the brittle star *Astrotoma agassizii*. *The Biological Bulletin*, *232*, 198-211.

Garner, A., Goulet, B., Farnitano, M., Molina-Henao, Y., & Hopkins, R. (2018). Genomic signatures of reinforcement. *Genes*, *9*, 191.

Gleason, L. U., & Burton, R. S. (2016). Genomic evidence for ecological divergence against a background of population homogeneity in the marine snail *Chlorostoma funebralis*. *Molecular Ecology*, *25*, 3557-3573.

Goldner, A., Herold, N., & Huber, M. (2014). Antarctic glaciation caused ocean circulation changes at the Eocene–Oligocene transition. *Nature*, *511*, 574.

Gompert, Z., Lucas, L. K., Nice, C. C., Fordyce, J. A., Forister, M. L., & Buerkle, C. A. (2012). Genomic regions with a history of divergent selection affect fitness of hybrids between two butterfly species. *Evolution: International Journal of Organic Evolution*, *66*, 2167-2181.

González-Wevar, C. A., Saucède, T., Morley, S. A., Chown, S. L., & Poulin, E. (2013). Extinction and recolonization of maritime A ntarctica in the limpet N acella concinna (Strebel, 1908) during the last glacial cycle: toward a model of Quaternary biogeography in shallow A ntarctic invertebrates. *Molecular Ecology*, *22*, 5221-5236.

Gordon, A. L., & Nowlin Jr, W. D. (1978). The basin waters of the Bransfield Strait. *Journal of Physical Oceanography*, *8*, 258-264.

Halanych, K. M., & Mahon, A. R. (2018). Challenging dogma concerning biogeographic patterns of Antarctica and the Southern Ocean. *Annual Review of Ecology, Evolution, and Systematics*, *49*, 355-378.

Havermans, C., Nagy, Z. T., Sonet, G., De Broyer, C., & Martin, P. (2011). DNA barcoding reveals new insights into the diversity of Antarctic species of *Orchomene* sensu lato (Crustacea: Amphipoda: Lysianassoidea). *Deep Sea Research Part II: Topical Studies in Oceanography*, *58*, 230-241.

Haye, P. A., Segovia, N. I., Muñoz-Herrera, N. C., Gálvez, F. E., Martínez, A., Meynard, A., ... & Faugeron, S. (2014). Phylogeographic structure in benthic marine invertebrates of the southeast Pacific coast of Chile with differing dispersal potential. *PLoS One*, *9*, e88613.

Hemery, L. G., Eléaume, M., Roussel, V., Améziane, N., Gallut, C., Steinke, D., ... & Wilson, N. G. (2012). Comprehensive sampling reveals circumpolarity and sympatry in seven mitochondrial lineages of the Southern Ocean crinoid species *Promachocrinus kerguelensis* (Echinodermata). *Molecular Ecology*, *21*, 2502-2518.

Heroy, D. C., & Anderson, J. B. (2007). Radiocarbon constraints on Antarctic Peninsula ice sheet retreat following the Last Glacial Maximum (LGM). *Quaternary Science Reviews*, *26*, 3286-3297.

Hopkins, R., Levin, D. A., & Rausher, M. D. (2012). Molecular signatures of selection on reproductive character displacement of flower color in *Phlox drummondii*. *Evolution: International Journal of Organic Evolution*, *66*, 469-485.

Hu, H., & Sun, S. C. (2016). Ubiquitin signaling in immune responses. *Cell Research*, *26*, 457.

Huneke, W. G. C., Huhn, O., & Schröeder, M. (2016). Water masses in the Bransfield Strait and adjacent seas, austral summer 2013. *Polar Biology*, *39*, 789-798.

Hunter, R. L., & Halanych, K. M. (2008). Evaluating connectivity in the brooding brittle star *Astrotoma agassizii* across the Drake Passage in the Southern Ocean. *Journal of Heredity*, *99*, 137-148.

Irisarri, I., Singh, P., Koblmüller, S., Torres-Dowdall, J., Henning, F., Franchini, P., ... & Sturmbauer, C. (2018). Phylogenomics uncovers early hybridization and adaptive loci shaping the radiation of Lake Tanganyika cichlid fishes. *Nature Communications*, *9*, 3159.

Ivany, L. C., Patterson, W. P., & Lohmann, K. C. (2000). Cooler winters as a possible cause of mass extinctions at the Eocene/Oligocene boundary. *Nature*, *407*, 887.

Janosik, A. M., Mahon, A. R., & Halanych, K. M. (2011). Evolutionary history of Southern Ocean *Odontaster* sea star species (Odontasteridae; Asteroidea). *Polar Biology*, *34*, 575-586.

Jenkins, T. L., & Stevens, J. R. (2018). Assessing connectivity between MPAs: Selecting taxa and translating genetic data to inform policy. *Marine Policy*, *94*, 165-173.

Jin, Y. K., Lundgren, P., Lutz, A., Raina, J. B., Howells, E. J., Paley, A. S., ... & van Oppen, M. J. (2016). Genetic markers for antioxidant capacity in a reef-building coral. *Science Advances*, *2*, e1500842.

Kennett, J. P. (1977). Cenozoic evolution of Antarctic glaciation, the circum-Antarctic Ocean, and their impact on global paleoceanography. *Journal of Geophysical Research*, *82*, 3843-3860.

Kinberg, J. G. H. (1866). Annulata nova. *Öfversigt Af Kongliga Vetenskaps akademiens Förhandlingar*, *22*, 167–179.

Koutsouveli, V., Taboada, S., Moles, J., Cristobo, J., Ríos, P., Bertran, A., ... & Riesgo, A. (2018). Insights into the reproduction of some Antarctic dendroceratid, poecilosclerid, and haplosclerid demosponges. *PloS One*, *13*, e0192267.

Krabbe, K., Leese, F., Mayer, C., Tollrian, R., & Held, C. (2010). Cryptic mitochondrial lineages in the widespread pycnogonid *Colossendeis megalonyx* Hoek, 1881 from Antarctic and Subantarctic waters. *Polar Biology*, *33*, 281-292.

Krueck, N. C., Ahmadia, G. N., Green, A., Jones, G. P., Possingham, H. P., Riginos, C., ... & Mumby, P. J. (2017). Incorporating larval dispersal into MPA design for both conservation and fisheries. *Ecological Applications*, *27*, 925-941.

Kültz, D. (2003). Evolution of the cellular stress proteome: from monophyletic origin to ubiquitous function. *Journal of Experimental Biology*, *206*, 3119-3124.

Lack, J. B., Greene, D. U., Conroy, C. J., Hamilton, M. J., Braun, J. K., Mares, M. A., & Van Den Bussche, R. A. (2012). Invasion facilitates hybridization with introgression in the *Rattus rattus* species complex. *Molecular Ecology*, *21*, 3545-3561.

Lawver, L. A., & Gahagan, L. M. (2003). Evolution of Cenozoic seaways in the circum-Antarctic region. *Palaeogeography*, *Palaeoclimatology*, *Palaeoecology*, *198*, 11-37.

Lear, C. H., & Lunt, D. J. (2016). How Antarctica got its ice. *Science*, *352*, 34-35.

Li, G., Davis, B. W., Eizirik, E., & Murphy, W. J. (2016). Phylogenomic evidence for ancient hybridization in the genomes of living cats (Felidae). *Genome Research*, *26*, 1-11.

Liebrand, D., de Bakker, A. T., Beddow, H. M., Wilson, P. A., Bohaty, S. M., Ruessink, G., ... & Huck, C. E. (2017). Evolution of the early Antarctic ice ages. *Proceedings of the National Academy of Sciences*, *114*, 3867-3872.

Limborg, M. T., Helyar, S. J., De Bruyn, M., Taylor, M. I., Nielsen, E. E., Ogden, R. O. B., ... & Bekkevold, D. (2012). Environmental selection on transcriptome-derived SNPs in a high gene flow marine fish, the Atlantic herring (*Clupea harengus*). *Molecular Ecology*, *21*, 3686-3703.

Llopart, A., & Comeron, J. M. (2008). Recurrent events of positive selection in independent *Drosophila* lineages at the spermatogenesis gene roughex. *Genetics*, *179*, 1009-1020.

Mahon, A. R., Arango, C. P., & Halanych, K. M. (2008). Genetic diversity of Nymphon (Arthropoda: Pycnogonida: Nymphonidae) along the Antarctic Peninsula with a focus on *Nymphon australe* Hodgson 1902. *Marine Biology*, *155*, 315-323.

Martín, J., De Neve, L., Fargallo, J. A., Polo, V., & Soler, M. (2004). Factors affecting the escape behaviour of juvenile chinstrap penguins, *Pygoscelis antarctica*, in response to human disturbance. *Polar Biology*, *27*, 775-781.

Massom, R. A., Scambos, T. A., Bennetts, L. G., Reid, P., Squire, V. A., & Stammerjohn, S. E. (2018). Antarctic ice shelf disintegration triggered by sea ice loss and ocean swell. *Nature*, *558*, 383.

McIntosh, W. C. (1876). Descriptions of some new species of Annelida from Kerguelen's Island. *Journal of Natural History*, *17*, 318-323.

McIntosh, W. C. (1885). Report on the Annelida Polychaeta collected by HMS "Challenger" during the years 1873-76. Reports on the Scientific Results of the Voyage of HMS "Challenger". *Zoology*, *12*, 1-554.

Meredith, M. P., & King, J. C. (2005). Rapid climate change in the ocean west of the Antarctic Peninsula during the second half of the 20th century. *Geophysical Research Letters*, *32*.

Mokhtar-Jamaï, K., Pascual, M., Ledoux, J. B., Coma, R., Féral, J. P., Garrabou, J., & Aurelle, D. (2011). From global to local genetic structuring in the red gorgonian *Paramuricea clavata*: the interplay between oceanographic conditions and limited larval dispersal. *Molecular Ecology*, *20*, 3291-3305.

Moles, J., Wägele, H., Ballesteros, M., Pujals, Á., Uhl, G., & Avila, C. (2016). The end of the cold loneliness: 3D comparison between *Doto antarctica* and a new sympatric species of *Doto* (Heterobranchia: Nudibranchia). *PloS One*, *11*, e0157941.

Mouginot, J., Rignot, E., & Scheuchl, B. (2014). Sustained increase in ice discharge from the Amundsen Sea Embayment, West Antarctica, from 1973 to 2013. *Geophysical Research Letters*, *41*, 1576-1584.

Mulvaney, R., Abram, N. J., Hindmarsh, R. C., Arrowsmith, C., Fleet, L., Triest, J., ... & Foord, S. (2012). Recent Antarctic Peninsula warming relative to Holocene climate and ice-shelf history. *Nature*, *489*, 141.

Nagel, M. M., Sewell, M. A., & Lavery, S. D. (2015). Differences in population connectivity of a benthic marine invertebrate *Evechinus chloroticus* (Echinodermata: Echinoidea) across large and small spatial scales. *Conservation Genetics*, *16*, 965-978.

Naish, T., Powell, R., Levy, R., Wilson, G., Scherer, R., Talarico, F., ... & Carter, L. (2009). Obliquity-paced Pliocene West Antarctic ice sheet oscillations. *Nature*, *458*, 322.

Nassif, N. D., Cambray, S. E., & Kraut, D. A. (2014). Slipping up: Partial substrate degradation by ATP-dependent proteases. *IUBMB life*, *66*, 309-317.

Nicol, S., Foster, J., & Kawaguchi, S. (2012). The fishery for Antarctic krill–recent developments. Fish and Fisheries, 13(1), 30-40.

O'Donnell, J. L., Beldade, R., Mills, S. C., Williams, H. E., & Bernardi, G. (2017). Life history, larval dispersal, and connectivity in coral reef fish among the Scattered Islands of the Mozambique Channel. *Coral Reefs*, *36*, 223-232.

O'Leary, M. J., Hearty, P. J., Thompson, W. G., Raymo, M. E., Mitrovica, J. X., & Webster, J. M. (2013). Ice sheet collapse following a prolonged period of stable sea level during the last interglacial. *Nature Geoscience*, *6*, 796.

Ottenburghs, J., van Hooft, P., van Wieren, S. E., Ydenberg, R. C., & Prins, H. H. (2016). Hybridization in geese: a review. *Frontiers in Zoology*, *13*, 20.

Palumbi, S. R. (2003). Population genetics, demographic connectivity, and the design of marine reserves. *Ecological Applications*, *13*, 146-158.

Pascual, M., Rives, B., Schunter, C., & Macpherson, E. (2017). Impact of life history traits on gene flow: A multispecies systematic review across oceanographic barriers in the Mediterranean Sea. *PLoS One*, *12*, e0176419.

Peck, L. S., & Conway, L. Z. (2000). The myth of metabolic cold adaptation: oxygen consumption in stenothermal Antarctic bivalves. *Geological Society, London, Special Publications*, *177*, 441-450.

Peck, L. S., Webb, K. E., & Bailey, D. M. (2004). Extreme sensitivity of biological function to temperature in Antarctic marine species. *Functional Ecology*, *18*, 625-630.

Pérez-Portela, R., & Riesgo, A. (2018). Population genomics of early-splitting lineages of metazoans. In Om P. Rajora (Ed.), *Population genomics* (pp. 1-35). Cham, Switzerlands: Springer

Perry, K. D., Baker, G. J., Powis, K. J., Kent, J. K., Ward, C. M., & Baxter, S. W. (2018). Cryptic Plutella species show deep divergence despite the capacity to hybridize. *BMC Evolutionary Biology*, *18*, 77.

Petit, R. J., & Excoffier, L. (2009). Gene flow and species delimitation. *Trends in Ecology & Evolution*, *24*, 386-393.

Piggott, M. P., Banks, S. C., Tung, P., & Beheregaray, L. B. (2008). Genetic evidence for different scales of connectivity in a marine mollusc. *Marine Ecology Progress Series*, *365*, 127-136.

Pita, L., Hoeppner, M. P., Ribes, M., & Hentschel, U. (2018). Differential expression of immune receptors in two marine sponges upon exposure to microbial-associated molecular patterns. *Scientific Reports*, *8*, 16081.

Pollard, D., & DeConto, R. M. (2009). Modelling West Antarctic ice sheet growth and collapse through the past five million years. *Nature*, *458*(7236), 329.

Prothero, D. R. (1994). The late eocene-oligocene extinctions. *Annual Review of Earth and Planetary Sciences*, *22*, 145-165.

Raupach, M. J., Thatje, S., Dambach, J., Rehm, P., Misof, B., & Leese, F. (2010). Genetic homogeneity and circum-Antarctic distribution of two benthic shrimp species of the Southern Ocean, Chorismus antarcticus and Nematocarcinus lanceopes. *Marine Biology*, *157*, 1783-1797.

Raymo, M. E., & Mitrovica, J. X. (2012). Collapse of polar ice sheets during the stage 11 interglacial. *Nature*, *483*, 453.

Richards, V. P., Thomas, J. D., Stanhope, M. J., & Shivji, M. S. (2007). Genetic connectivity in the Florida reef system: comparative phylogeography of commensal invertebrates with contrasting reproductive strategies. *Molecular Ecology*, *16*, 139-157.

Riesgo, A., Taboada, S., & Avila, C. (2015). Evolutionary patterns in Antarctic marine invertebrates: An update on molecular studies. *Marine Genomics*, *23*, 1-13.

Riesgo, A., Pérez-Portela, R., Pita, L., Blasco, G., Erwin, P. M., & López-Legentil, S. (2016). Population structure and connectivity in the Mediterranean sponge *Ircinia fasciculata* are affected by mass mortalities and hybridization. *Heredity*, *117*, 427.

Riesgo, A., Taboada, S., Pérez-Portela, R., Melis, P., Xavier, J. R., Blasco, G., & López-Legentil, S. (2019). Genetic diversity, connectivity and gene flow along the distribution of the emblematic Atlanto-Mediterranean sponge *Petrosia ficiformis* (Haplosclerida, Demospongiae). *BMC Evolutionary Biology*, *19*, 24.

Rignot, E., Mouginot, J., Morlighem, M., Seroussi, H., & Scheuchl, B. (2014). Widespread, rapid grounding line retreat of Pine Island, Thwaites, Smith, and Kohler glaciers, West Antarctica, from 1992 to 2011. *Geophysical Research Letters*, *41*, 3502-3509.

Roberts, C. M. (1997). Connectivity and management of Caribbean coral reefs. *Science*, *278*, 1454-1457.

Rogers, A. D. (2007). Evolution and biodiversity of Antarctic organisms: a molecular perspective. *Philosophical Transactions of the Royal Society B: Biological Sciences*, *362*, 2191-2214.

Sanford, E., & Kelly, M. W. (2011). Local adaptation in marine invertebrates. *Annual Review of Marine Science*, *3*, 509-535.

Sangrà, P., Gordo, C., Hernández-Arencibia, M., Marrero-Díaz, A., Rodríguez-Santana, A., Stegner, A., ... & Pichon, T. (2011). The Bransfield current system. *Deep Sea Research Part I: Oceanographic Research Papers*, *58*, 390-402.

Santa Cruz, F., Ernst, B., Arata, J. A., & Parada, C. (2018). Spatial and temporal dynamics of the Antarctic krill fishery in fishing hotspots in the Bransfield Strait and South Shetland Islands. *Fisheries Research*, *208*, 157-166.

Schmidtko, S., Heywood, K. J., Thompson, A. F., & Aoki, S. (2014). Multidecadal warming of Antarctic waters. *Science*, *346*, 1227-1231.

Schüller, M. (2011). Evidence for a role of bathymetry and emergence in speciation in the genus *Glycera* (Glyceridae, Polychaeta) from the deep Eastern Weddell Sea. *Polar Biology*, *34*, 549-564.

Selkoe, K. A., & Toonen, R. J. (2011). Marine connectivity: a new look at pelagic larval duration and genetic metrics of dispersal. *Marine Ecology Progress Series*, *436*, 291-305.

Siegert, M. J., Rumble, J., Atkinson, A., Rogelj, J., Edwards, T., Davies, B. J., ... & Convey, P. (2019). The Antarctic Peninsula under a 1.5° C global warming scenario. *Frontiers in Environmental Science*, *7*, 102.

Smadja, C. M., Loire, E., Caminade, P., Thoma, M., Latour, Y., Roux, C., ... & Boursot, P. (2015). Seeking signatures of reinforcement at the genetic level: a hitchhiking mapping and candidate gene approach in the house mouse. *Molecular Ecology*, *24*, 4222-4237.

Smith, J. A., Hillenbrand, C. D., Pudsey, C. J., Allen, C. S., & Graham, A. G. (2010). The presence of polynyas in the Weddell Sea during the Last Glacial Period with implications for the reconstruction of sea-ice limits and ice sheet history. *Earth and Planetary Science Letters*, *296*, 287-298.

Smith Jr, W. O., & Gordon, L. I. (1997). Hyperproductivity of the Ross Sea (Antarctica) polynya during austral spring. *Geophysical Research Letters*, *24*, 233-236.

Spiegel, D. S., Raymond, S. N., Dressing, C. D., Scharf, C. A., & Mitchell, J. L. (2010). Generalized Milankovitch cycles and long-term climatic habitability. *The Astrophysical Journal*, *721*, 1308.

Stammerjohn, S. E., Martinson, D. G., Smith, R. C., & Iannuzzi, R. A. (2008). Sea ice in the western Antarctic Peninsula region: Spatio-temporal variability from ecological and climate change perspectives. *Deep Sea Research Part II: Topical Studies in Oceanography*, *55*, 2041-2058.

Sutter, J., Gierz, P., Grosfeld, K., Thoma, M., & Lohmann, G. (2016). Ocean temperature thresholds for Last Interglacial West Antarctic Ice Sheet collapse. *Geophysical Research Letters*, *43*, 2675-2682.

Taboada, S., & Pérez-Portela, R. (2016). Contrasted phylogeographic patterns on mitochondrial DNA of shallow and deep brittle stars across the Atlantic-Mediterranean area. *Scientific reports*, *6*, 32425.

Taboada, S., Junoy, J., Andrade, S. C., Giribet, G., Cristobo, J., & Avila, C. (2013). On the identity of two Antarctic brooding nemerteans: redescription of *Antarctonemertes valida* (Bürger, 1893) and description of a new species in the genus *Antarctonemertes* Friedrich, 1955 (Nemertea, Hoplonemertea). *Polar Biology*, *36*, 1415-1430.

Thatje, S., Hillenbrand, C. D., & Larter, R. (2005). On the origin of Antarctic marine benthic community structure. *Trends in Ecology & Evolution*, *20*, 534-540.

Thornhill, D. J., Mahon, A. R., Norenburg, J. L., & Halanych, K. M. (2008). Open-ocean barriers to dispersal: a test case with the Antarctic Polar Front and the ribbon worm *Parborlasia corrugatus* (Nemertea: Lineidae). *Molecular Ecology*, *17*(23), 5104-5117.

Turner, J., Hosking, J. S., Bracegirdle, T. J., Marshall, G. J., & Phillips, T. (2015). Recent changes in Antarctic sea ice. *Philosophical Transactions of the Royal Society A: Mathematical, Physical and Engineering Sciences*, *373*, 20140163.

van Oppen, M. J., Bongaerts, P., Frade, P., Peplow, L. M., Boyd, S. E., Nim, H. T., & Bay, L. K. (2018). Adaptation to reef habitats through selection on the coral animal and its associated microbiome. *Molecular Ecology*, *27*, 2956-2971.

VanWallendael, A., Soltani, A., Emery, N. C., Peixoto, M. M., Olsen, J., & Lowry, D. B. (2019). A molecular view of plant local adaptation: incorporating stress-response networks. *Annual Review of Plant Biology*, *70*, 559-583.

Vaughan, D. G., Marshall, G. J., Connolley, W. M., Parkinson, C., Mulvaney, R., Hodgson, D. A., ... & Turner, J. (2003). Recent rapid regional climate warming on the Antarctic Peninsula. *Climatic Change*, *60*, 243-274.

Vecchi, M., Cesari, M., Bertolani, R., Jönsson, K. I., Rebecchi, L., & Guidetti, R. (2016). Integrative systematic studies on tardigrades from Antarctica identify new genera and new species within Macrobiotoidea and Echiniscoidea. *Invertebrate Systematics*, *30*, 303-322.

Wielstra, B., & Arntzen, J. W. (2012). Postglacial species displacement in *Triturus* newts deduced from asymmetrically introgressed mitochondrial DNA and ecological niche models. *BMC Evolutionary Biology*, *12*, 161.

Wilson, N. G., Hunter, R. L., Lockhart, S. J., & Halanych, K. M. (2007). Multiple lineages and absence of panmixia in the “circumpolar” crinoid *Promachocrinus kerguelensis* from the Atlantic sector of Antarctica. *Marine Biology*, *152*, 895-904.

Wilson, N. G., Schrödl, M., & Halanych, K. M. (2009). Ocean barriers and glaciation: evidence for explosive radiation of mitochondrial lineages in the Antarctic sea slug *Doris kerguelenensis* (Mollusca, Nudibranchia). *Molecular Ecology*, *18*, 965-984.

Wilson, N. G., Maschek, J. A., & Baker, B. J. (2013). A species flock driven by predation? Secondary metabolites support diversification of slugs in Antarctica. *PLoS One*, *8*, e80277.

Zachos, J. C., Quinn, T. M., & Salamy, K. A. (1996). High-resolution (104 years) deep-sea foraminiferal stable isotope records of the Eocene-Oligocene climate transition. *Paleoceanography*, *11*, 251-266.

Zhou, M., Niiler, P. P., & Hu, J. H. (2002). Surface currents in the Bransfield and Gerlache straits, Antarctica. *Deep Sea Research Part I: Oceanographic Research Papers*, *49*, 267-280.

Zhou, M., Niiler, P. P., Zhu, Y., & Dorland, R. D. (2006). The western boundary current in the Bransfield Strait, Antarctica. *Deep Sea Research Part I: Oceanographic Research Papers*, *53*, 1244-1252.

Zink, R. M., & Barrowclough, G. F. (2008). Mitochondrial DNA under siege in avian phylogeography. *Molecular Ecology*, *17*, 2107-2121.

Supplementary Material

CHAPTER 1
Supplementary Material 1

Primers	Sequence 5'-3'	Reference	PCR programme
COI			95ºC – 15 min
jgLCO	TITCIACIAAYCAYAARGAYATTGG	Geller *et al.* (2013)	94ºC – 30 s 44ºC – 70 s 72ºC – 90 s x 40 cycles
jgHCO	TAIACYTCIGGRTGICCRAARAAYCA	Geller *et al.* (2013)	
polyLCO	GAYTATWTTCAACAAATCATAAAGATATTGG	Carr *et al.* (2011)	
polyHCO	TAMACTTCWGGGTGACCAAARAATCA	Carr *et al.* (2011)	72ºC – 10 min
16S rRNA			95ºC – 5 min
16S arL	CGCCTGTTTATCAAAAACAT	Palumbi *et al.* (1991)	95ºC – 30 s 55ºC (-0.5/cyc) – 30 s x 10 cycles
16S brH	CCGGTCTGAACTCAGATCACGT	Palumbi *et al.* (1991)	
			68ºC – 60 s 95ºC – 30 s 50ºC – 30 s 68ºC – 60 s x 10 cycles
			95ºC – 30 s 45ºC – 30 s 68ºC – 60 s x 15 cycles
			68ºC – 10 min
18S rRNA			
18S 1F	AYCTGGTTGATCCTGCCAGT	Medlin *et al.* (1988)	95ºC – 2 min
18S 5R	ACCTTGTTACGACTTTTACTTCCTC	Medlin *et al.* (1988)	95ºC – 30 s 48ºC – 60 s 72ºC – 3 min x 35 cycles
18S 4F	GCCTGCGGCTTAATTTGACTCAACAC	Medlin *et al.* (1988)	
18S 7R	GCATCACAGACCTGTTATTGC	Giribet *et al.* (1996)	
18S a2.0	ATGGTTGCAAAGCTGAAAC	Whiting *et al.* (1997)	72ºC – 5 min
18S 9R	GATCCTTCCGCAGGTTCACCTAC	Whiting *et al.* (1997)	
28S rRNA			95ºC – 2 min
28S rd1a	CCCSCGTAAYTTAGGCATAT	Edgecombe & Giribet (2006)	94ºC – 30 s 45ºC – 40 s 72ºC – 60 s x 30 cycles
28S rd5b	CCACAGCGCCAGTTCTGCTTAC	Whiting (2002)	72ºC – 7 min

CHAPTER 1
Supplementary Material 2

Species	Voucher	Locality	16S	18S	28S	COI	Reference
Chaetoparia nilssoni	SMNH90970	Sweden	AY996069	AY996090	AY996108	AY996125	Eklöf et al. (2007)
Eteone picta	SMNH90971	France	AY996068	AY996089	AY996107	AY996124	Eklöf et al. (2007)
Eulalia bilineata	SMNH90972	Norway	AY996067	AY996088	AY996106	-	Eklöf et al. (2007)
Eulalia expusilla	SMNH90973	Norway	AY996066	AY996087	-	-	Eklöf et al. (2007)
Eulalia mustela	SMNH90974	Sweden	AY996065	AY996086	AY996105	AY996123	Eklöf et al. (2007)
Eulalia levicornuta	BAMPOL0411	Canada				HM473376	Unpublished
Eulalia viridis	SMNH90975	Sweden	AY996064	AY996085	AY996104	AY996122	Eklöf et al. (2007)
Eulalia viridis	HUNTSPOL0218	Canada				HQ024018	Carr et al. (2011)
Eulalia viridis	WS0104	Russia				GU672585	Hardy et al. (2011)
Eulalia viridis	IDJ143	Norway				KT709564	Schimmenti et al. (2016)
Eulalia viridis	IDJ152	Sweden				KT709563	Schimmenti et al. (2016)
Eulalia viridis	IDJ39	Sweden				KT709562	Schimmenti et al. (2016)
Eulalia viridis	IDI859	Sweden				KT709561	Schimmenti et al. (2016)
Eulalia viridis	IDI858	Sweden				KT709560	Schimmenti et al. (2016)
Eulalia viridis	SMNH 81641	Sweden	AY340455	AY340428	AY340392		Rousset et al. (2007)
Eulalia viridis	LMBP19-004	Portugal				KR916829	Lobo et al. (2015)
Eulalia viridis	LMBP19-003	Portugal				KR916828	Lobo et al. (2015)
Eulalia viridis	LMBLP7-001	Portugal				KR916827	Lobo et al. (2015)
Eulalia viridis	LMBP19-001	Portugal				KR916826	Lobo et al. (2015)
Eulalia viridis	BIOUG<CAN>:WS0229	Russia				GU672477	Hardy et al. (2011)
Eulalia viridis	BIOUG<CAN>:WS0274	Russia				GU672434	Hardy et al. (2011)
Eulalia viridis	BIOUG<CAN>:WS0274	Russia				GU672436	Hardy et al. (2011)
Eumida arctica	SMNH90976	Spitsbergen	AY996063	AY996084	AY996103	-	Eklöf et al. (2007)
Eumida bahusiensis			GU199008	GU199014	GU199019	GU199025	Unpublished
Eumida ockelmanni			-	GU199013	GU199018	GU199024	Unpublished
Eumida sanguinea	SMNH90977	Sweden	AY996062	AY996083	-	AY996121	Eklöf et al. (2007)
Mystides caeca	SMNH90978	Norway	AY996060	AY996081	-	AY996119	Eklöf et al. (2007)
Nereiphylla lutea	SMNH90979	Norway	AY996059	AY996080	AY996101	AY996118	Eklöf et al. (2007)
Notophyllum foliosum	SMNH90980	Norway	-	AY996079	AY996100	AY996117	Eklöf et al. (2007)
Paranaitis kosteriensis	SMNH90083	Norway	-	AY996078	AY996099	AY996116	Eklöf et al. (2007)
Paranaitis wahlbergi	SMNH90981	Norway	AY996058	AY996077	AY996098	AY996115	Eklöf et al. (2007)
Phyllodoce groenlandica	SMNH90982	Norway	AY996057	AY996076	AY996097	AY996114	Eklöf et al. (2007)
Phyllodoce longipes	SMNH90983	Sweden	AY996056	AY996075	AY996096	AY996113	Eklöf et al. (2007)
Protomystides exigua	SMNH90084	Norway	AY996055	AY996074	AY996095	-	Eklöf et al. (2007)
Pseudomystides limbata	SMNH90984	Sweden	AY996054	AY996073	AY996094	AY996112	Eklöf et al.

							(2007)
Pterocirrus burtoni	**SIO-BIC-A2624**	**California, USA**	**MH567599**	**MH567604**	**MH567608**	**MH567613**	**This study**
***Pterocirrus giribeti* sp. nov.**	**NHMUK ANEA.2018-25412**	**Cierva Cove, Antarctica**	**MH567602**	**MH567603**	**MH567611**	**MH567616**	**This study**
Pterocirrus macroceros	SMNH90985	France	AY996053	AY996072	**AY996093**	AY996111	Eklöf et al. (2007)
Pterocirrus nidarosiensis	**SIO-BIC-A6056**	**Norway**	**MH567601**	**MH567606**	**MH567610**	**MH567615**	**This study**
Pterocirrus montereyensis	**SIO-BIC-A2631**	**California, USA**	**MH567600**	**MH567605**	**MH567609**	**MH567614**	**This study**
***Pterocirrus* sp.**	**SIO-BIC-A4755**	**Belize**		**MH567607**	**MH567612**	**MH567617**	**This study**
Sige fusigera	SMNH90986	Sweden	**AY996052**	AY996071	AY996092	AY996110	Eklöf et al. (2007)
Aglaophamus malmgreni	SMNH90988	Spitsbergen	AY996070	AY996091	**AY996109**	AY996126	Eklöf et al. (2007)
Glycera capitata	**FS11**		**KT989320**	**KT989344**	**KT989344**	**KT989320**	**Richter et al. (2015)**
Aphrodita aculeata	**SMNH118956**	**Sweden**	**JN852882**	**AY176281**	**JN852846**	**AY839578**	**Norlinder et al. (2012)**
Rhynchonereella gracilis			**GU199007**	**GU199012**	**GU199017**	GU199023	Unpublished
Lacydonia eliasoni	SMNH90987	Norway	AY996061	AY996082	AY996102	AY996120	Eklöf et al. (2007)
Alciopina sp. 1	**JE-2010**		GU199009			GU199026	Unpublished
Alciopina sp.*2*	**THS-2006**			DQ790073	DQ790021		Struck et al. (2007)
Torrea sp. *1*	**JE-2010**		GU199006			GU199022	Unpublished
Torrea sp. *2*	**THS-2006**			DQ790096	DQ790068		Struck et al. (2007)

CHAPTER 1
Supplementary Material 3

Genus *Pterocirrus* Claparède, 1868

Pterocirrus giribeti sp. n. Leiva & Taboada (Suppl. Mat. 4, 5B)

Holotype. The Holotype consists of 1 specimen (NHMUK ANEA.2018-25412) preserved in 95 % EtOH, which was collected by Sergi Taboada in the intertidal of Cierva Cove (64º09'20"S 60º57'12"W), on January 5th, 2013.

Paratypes Series. The Paratypes Series consists of 1 specimen (NHMUK ANEA.2018-25516) preserved in 10% buffered formalin in seawater and later transferred to 70 % ethanol, and 141 specimens preserved in 95 % EtOH. One specimen (NHMUK ANEA.2018-25516) was collected by Sergi Taboada in the intertidal of Deception Island (62º59'25"S 60º37'31"W), on January 13th, 2010. 15 specimens (NHMUK ANEA.2018-25501 to NHMUK ANEA.2018-25515) were collected by Sergi Taboada in the intertidal of Livingston Island (62º39'05"S 60º35'50"W), on December 28th, 2012. 32 specimens (NHMUK ANEA.2018-25469 to NHMUK ANEA.2018-25500) were collected by Sergi Taboada in the intertidal of Half Moon Island (62º35'41"S 59º54'07"W), on January 2nd, 2013. 21 specimens (NHMUK ANEA.2018-25442 to NHMUK ANEA.2018-25462) were collected by Sergi Taboada in the intertidal of King George Island (62º11'55"S 58º56'59"W), on December 30th, 2012. 35 specimens (NHMUK ANEA.2018-25412 to NHMUK ANEA.2018-25441 and NHMUK ANEA.2018-25463 to NHMUK ANEA.2018-25468) were collected by Sergi Taboada in the intertidal of Cierva Cove (64º09'20"S 60º57'12"W), on January 5th, 2013. 22 specimens (NHMUK ANEA.2018-25390 to NHMUK ANEA.2018-25411) were collected by Carlos Leiva in the intertidal of Petermann Island (65º10'24"S 64º08'36"W), on February 14th, 2016. Two specimens (NHMUK ANEA.2018-25388 and NHMUK ANEA.2018-25389) were collected by Carlos Leiva in Paradise Bay (64º49'24"S 62º51'24"W), at 8 m depth, on February 16th, 2016. 13 specimens (NHMUK ANEA.2018-25375 to NHMUK ANEA.2018-25387) were collected by Carlos Leiva in the intertidal of O'Higgins Bay (63º18'52"S 57º54'27"W), on February 19th, 2016. One specimen (NHMUK ANEA.2018-25374) was collected by Carlos Leiva in the intertidal of Esperanza Bay (63º23'45"S 56º59'45"W), on February 22nd, 2016.

Other material examined. *Eulalia subulifera* NHMUK1930.10.8.1002-1003 from South Georgia Island, East Cumberland Bay, 20–30 meters depth, collected by Monro on February 11th, 1925 during the Discovery Expedition.

Etymology: *Pterocirrus giribeti* sp. n. is named after Professor Gonzalo Giribet, to acknowledge him for all the support we received during the DISTANCOM-1 Antarctic cruise where some of the samples were collected, and also for his unlimited predisposition for help in the lab and the invaluable advice we have always received from him.

Diagnosis. *Pterocirrus giribeti* sp. n. is an unusual species in *Pterocirrus* because it does not share some of the defining characters of the genus (see Description and Remarks sections below). It is characterised by its singular colouration in life (see Suppl. Mat. 4A and 4G). Moreover, it is also surprising that the nuchal organs are not observable.

Description

Measurements. Length 5–13 mm; maximum width 0.6–1.7 mm. Segment number between 38 and 47 for adult individuals.

Colour. In life, colour of body orange-brown; dorsal cirri brown, darker terminally (Suppl. Mat. 4A and 4G). Tentacular cirri brown proximally, darker in the middle, and white at the distal end (Suppl. Mat. 4A and 4G). Paired antennae, palps, and median antenna light brown proximally and white at the distal end (Suppl. Mat. 4A and 4G). Overall, these colours are retained after preservation.

Morphology. Prostomium pentagonal to rounded, slightly wider than long, without a clear delineated protuberance at insertion of paired antennae in the living organisms (Suppl. Mat. 4A and 4G), which is, nonetheless, subtle in some fixed individuals (Suppl. Mat. 4B). Eyes rounded, medium-sized, located on the posterior part of the prostomium (Suppl. Mat. 4A and 4G), also observed in preserved material. In some individuals, eyes partially covered by the first segment. Median antenna centrally inserted, as long as paired ones, approximately as long as the prostomium width (Suppl. Mat. 4A, 4B, 4D, 4G). Everted proboscis densely covered with diffusely distributed elongated papillae, terminal ring with 15 papillae (seen on the paratype NHMUK ANEA.2018-25505) (Suppl. Mat. 4C). Nuchal organs not observed.

Segment 1 dorsally visible and well developed (Suppl. Mat. 4A, 4B, 4G), ventrally fused with segment 2 (Suppl. Mat. 4D) and laterally fused with the prostomium. Segmental bands of cilia absent. Four pairs of tentacular cirri, 0.5–1 mm long, cylindrical and similar in shape except for ventral ones, which are slightly flattened (Suppl. Mat. 4A, 4B, 4D, 4G). Tentacular cirri of segment 1 reaching segment 6; dorsal tentacular cirri of segments 2 and 3 reaching segment 10; ventral tentacular cirri of segment 2 reaching segment 7 (Suppl. Mat. 4B). Composite spinigerous chaetae present from segment 2 (Suppl. Mat. 4B, 4G); segment 2 with small neuropodial lobes with 8–11 chaetae. Medium-sized neuropodial lobes in segment 3 with 9–12 chaetae. From segment 4, neuropodial chaetigerous lobes slightly asymmetrical, with supra-acicular lobes slightly longer than sub-acicular lobes, bearing 16–28 compound chaetae. Uniramous parapodia with dorsal cordiform cirri, oblong and symmetrical (Suppl. Mat. 4B, and 4E). Rostrum of chaetal shaft with a high number of teeth, decreasing in size proximally; appendages with numerous spines (Suppl. Mat. 4F). Ventral cirri slightly asymmetrical with rounded tips, longer than chaetigerous lobes (Suppl. Mat. 4D and 4E). Pygidial cirri with rounded to pointed ends, about 1.5 times as long as broad and median pygidial papilla absent.

Remarks. Due to the current taxonomical uncertainties about the reliability of the defining characters for genera of Eteoninae with five antennae (e.g., *Eumida*, *Eulalia*, *Pterocirrus*, *Pirakia*, and *Sige*; see Eklöf *et al.*, 2007), the assignment of the new species to a specific genus was initially difficult. These five genera have an interesting and confusing history full of descriptions and re-descriptions, reconsiderations from subgenus to genus and vice versa, synonymies, and transfer of species –including type species– among the different genera (e.g., Savigny, 1818; Grube, 1860; Claparède, 1868; Malmgren, 1865; Levinsen, 1883; Gravier, 1896; Bergström, 1914; Hartmann-Schröder, 1971; Perkins, 1984; Pleijel, 1990; 1991; Eibye-Jacobsen, 1991; Eklöf et al., 2007). Although *Pterocirrus giribeti* sp. n. lacks some the defining morphological characters of the genus, it shares (i) the absence of the delineated protuberance at the insertion of the paired antennae, and (ii) the development of the first segment, which is dorsally visible and partially fused with the prostomium. Moreover, the parapodial morphology also broadly agrees with the parapodia of other *Pterocirrus* taxa. In

addition, our phylogenetic analyses placed *P. giribeti* sp. n. unequivocally in a monophyletic clade including all the *Pterocirrus* species whose sequences are currently available.

One of the main characters that clearly distinguishes *Pterocirrus giribeti* sp. n. is its colour in life, especially the terminal darker area of each dorsal cirrus. This colour pattern was identified as a distinctive character by Ehlers (1897) in material collected in the Magellan Strait and South Georgia that he described as *Eulalia subulifera* Ehlers, 1897. However, Ehlers (1897) probably collected two different species and described them under the same specific name, mixing their characters in the description, but only deposited material for the species collected in the Magellan Strait. The revision of the type material of *E. subulifera* collected in the Magellan Strait clearly revealed that the organism collected by Ehlers and deposited at the Hamburg Zoological Museum (V4717) does not present all the characters that Ehlers specified in its original description. Moreover, its morphological characters do not even correspond with the typical morphology of *Eulalia*: the presence of a nuchal papilla instead of a median antenna, the proboscis and papillae shape, the degree of fusion of the anterior segments, and the tentacular and dorsal cirri shape (Suppl. Mat. 5A). Thus, we suggest that this species needs a thorough review to clarify its status as a species of *Eulalia* or to transfer it to another genus, which in our opinion could be the genus *Nereiphylla*. We thus believe that the species collected by Ehlers (1897) in South Georgia probably corresponded to *P. giribeti* sp. n. Later on, during the Discovery Expedition in 1925–1927, Monro (1930) collected *P. giribeti* sp. n. in South Georgia, which was however erroneously identified as *E. subulifera* probably due to the confusion in the original description of the species provided by Ehlers (1897).

To our knowledge, *P. giribeti* sp. n. is the first species of the genus *Pterocirrus* described in the Southern Ocean.

Habitat: *Pterocirrus giribeti* sp. n. occurs in the intertidal and subtidal (0–30 m) under rocks and among algae and bryozoans.

Distribution: *Pterocirrus giribeti* sp. n. is distributed along the Western Antarctic Peninsula and the South Shetland Islands and also occurs at the Subantarctic South

Georgia Island (material collected by Monro during the Discovery Expedition 1925–1927; Suppl. Mat. 5B).

CHAPTER 1
Supplementary Material 4

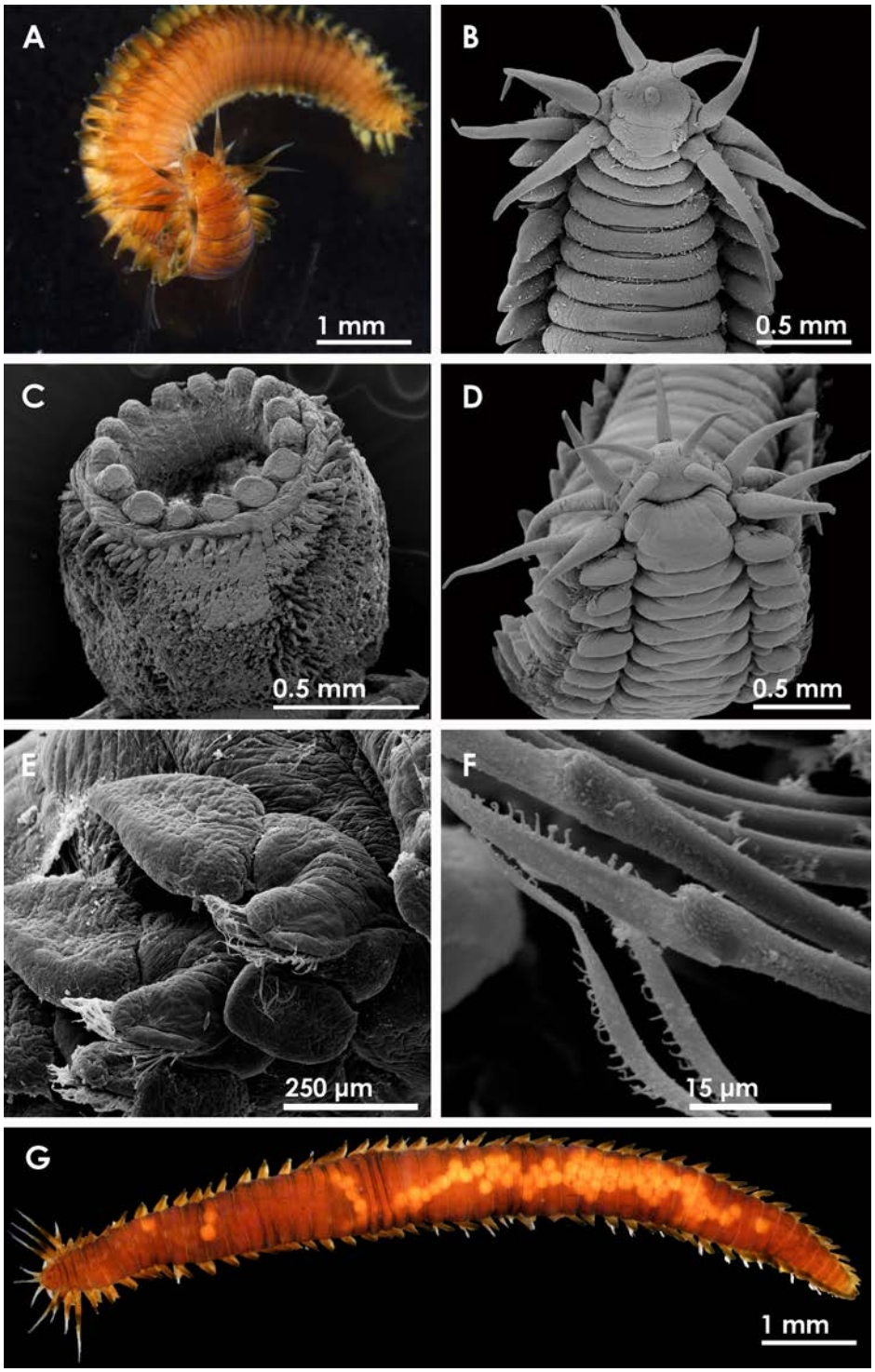

CHAPTER 2
Supplementary Material 4

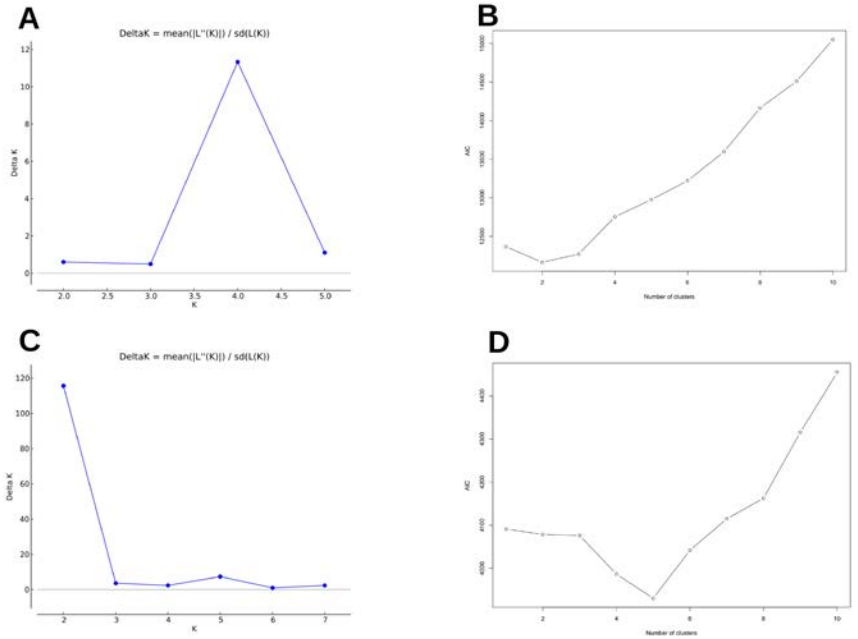

SUPPLEMENTARY MATERIAL 4: Delta K and AIC plots for STRUCTURE and snapclust analyses, respectively, showing the most probable number of clusters for the 389 neutral SNPs dataset (A and B) and for the 140 under positive selection SNPs dataset (C and D).

CHAPTER 2
Supplementary Material 5

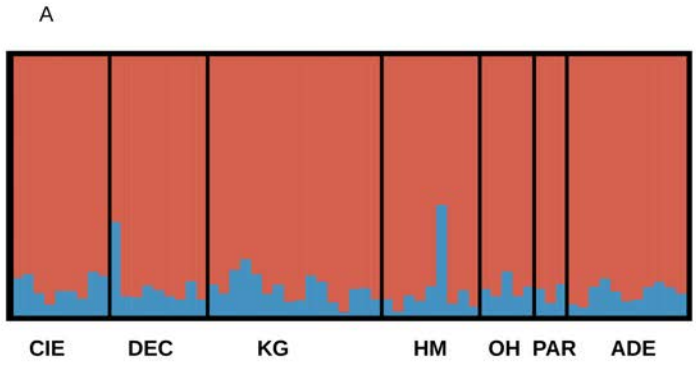

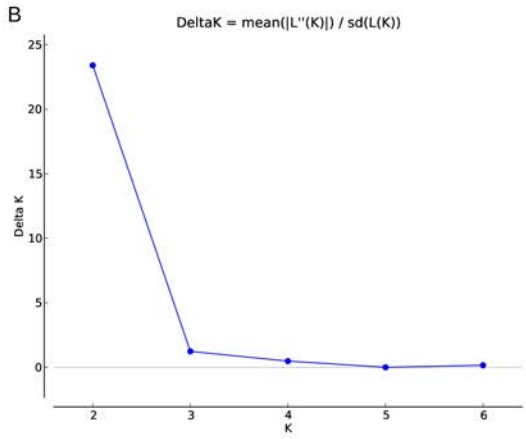

SUPPLEMENTARY MATERIAL 5: (A) STRUCTURE results for the dataset just including the 210 neutral SNPs in Hardy-Weinberg equilibrium. (B) Delta *K* plot showing 2 clusters as the most likely number of clusters.

CHAPTER 2
Supplementary Material 6

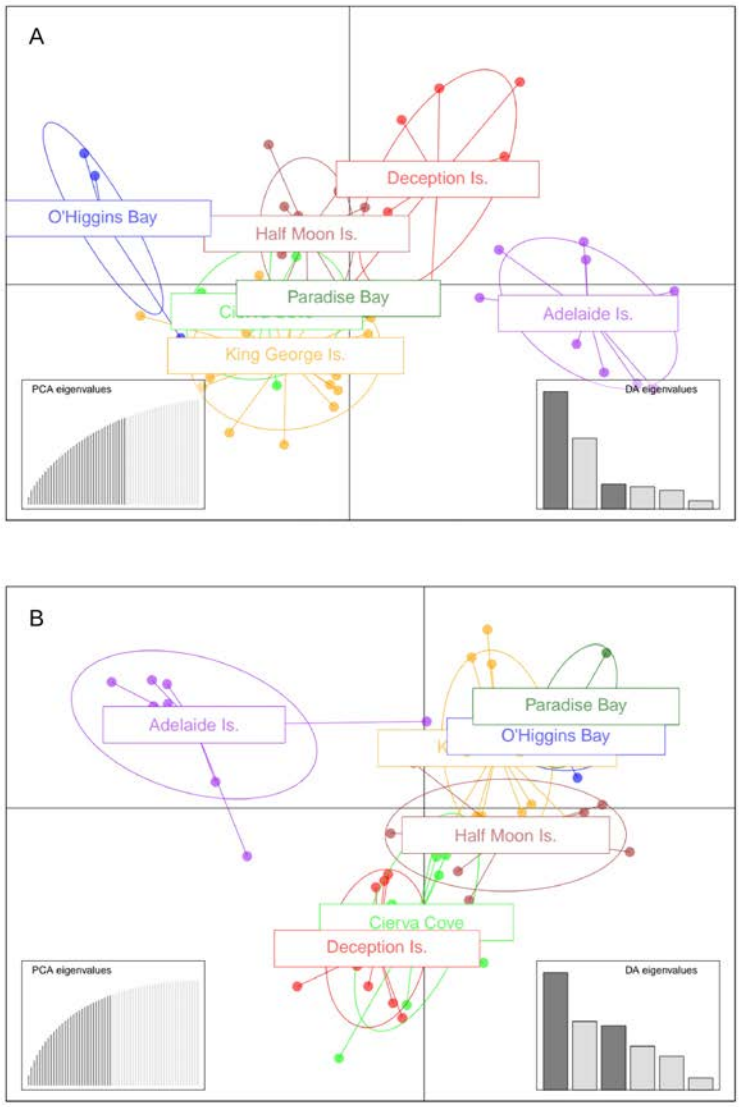

SUPPLEMENTARY MATERIAL 6: Two-dimensional representation of the DAPC results taking the first and third DAPC axes for the (A) neutral dataset and the (B) 140 SNPs under positive selection

CHAPTER 2
Supplementary Material 6

	Cierva Cove	Deception Is.	King George Is.	Half Moon Is.	O'Higgins Bay	Paradise Bay	Adelaide Is.
Cierva Cove		0.564	0.650	0.613	0.351	0.174	0.587
Deception Is.	0.461		0.820	0.615	0.386	0.174	0.993
King George Is.	0.512	0.762		0.808	0.603	0.224	1.000
Half Moon Is.	0.505	0.644	0.926		0.410	0.171	0.850
O'Higgins Bay	0.429	0.459	0.820	0.690		0.189	0.694
Paradise Bay	0.252	0.218	0.278	0.228	0.254		0.380
Adelaide Is.	0.377	0.651	0.911	0.895	0.476	0.201	

CHAPTER 3
Supplementary Material 2

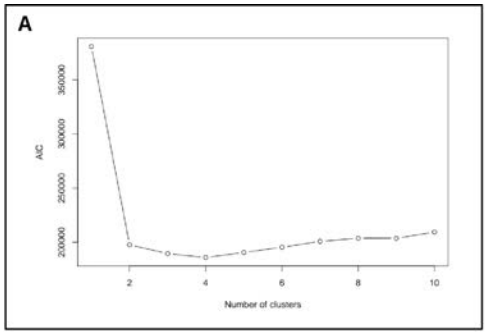

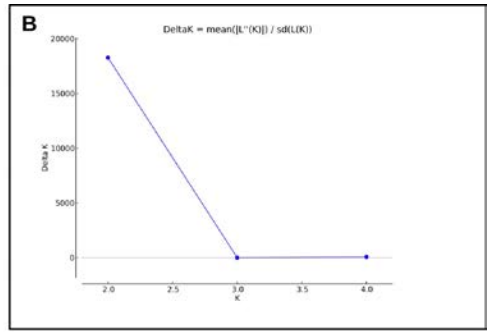

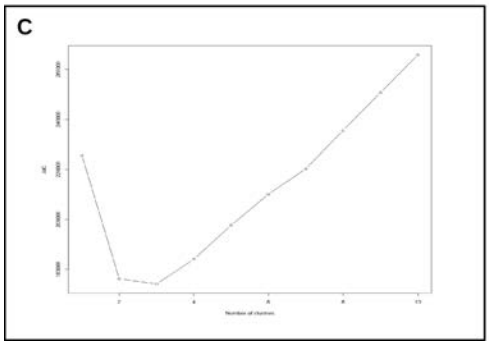

Supplementary Material 2
Graphics for the selection of the optimal number of clusters in the structuring analyses. snapclust AIC (A) and STRUCTURE delta K (B) plots for the 'WAP-SG' dataset. (C) snapclust AIC plot for the 'SG' dataset.

CHAPTER 4
Supplementary Material 1

Supplementary Material S1. Information about PCR primers and PCR programs used to amplify *COI* for the five species included in the present study

PCR primer	Species	Sequence	PCR program	Reference
COI_MycF	*Mycale acerata*	AGGAGGCTTTGGAAATTGGT	95°C/5 min; (95 °C/1 min; 55 °C/1min; 72 °C/1 min) x 30 cycles; 72 °C/5 min	This study
COI_MycF		CCAGTTGGCACCGCTATTAT		This study
ANT_COI-F	*Antarctonemertes valida*,	GGCACTGCTCTTAGATTAC	94°C/1.5 min; (94°C/45s; 40°C/1 min; 72°C/1 min) x 33 cycles; 72°C/5 min	Taboada et al. (2018)
ANT_COI-R	*Antarctonemertes riesgoae*	ACAGTAAGAAGTATTGT		Taboada et al. (2018)
LCO_1490	*Pterocirrus giribeti*	GGTCAACAAATCATAAAGATATTGG	95°C/5 min; (95 °C/30s; 45–48°C/30 s; 72°C/1 min) x 35 cycles; 72°C/10 min	Folmer et al. (1994)
HCO_2198	*Neanthes kerguelensis*	TAAACTTCAGGGTGACCAAAAAATCA	95°C/15 min; (95°C/30s; 45°C/30 s; 72°C/1 min) x 5 cycles; (95°C/30s; 50°C/30 s; 72°C/1 min) x 32 cycles; 72°C/10 min	Folmer et al. (1994)

CHAPTER 4
Supplementary Material 2

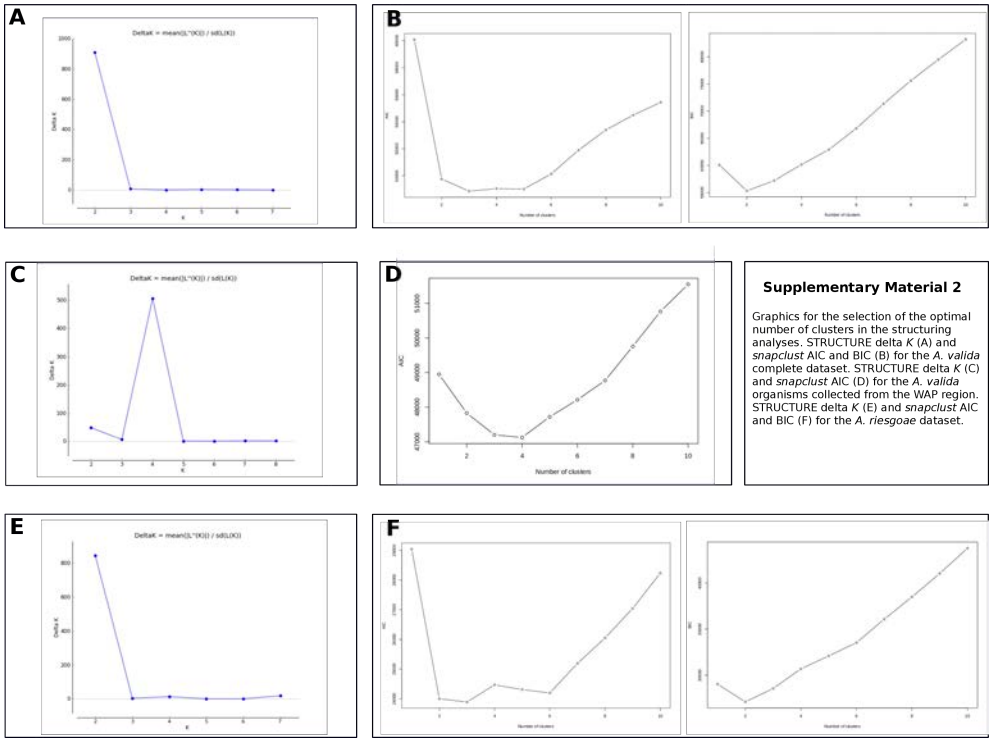

Supplementary Material 2

Graphics for the selection of the optimal number of clusters in the structuring analyses. STRUCTURE delta *K* (A) and *snapclust* AIC and BIC (B) for the *A. valida* complete dataset. STRUCTURE delta *K* (C) and *snapclust* AIC (D) for the *A. valida* organisms collected from the WAP region. STRUCTURE delta *K* (E) and *snapclust* AIC and BIC (F) for the *A. riesgoae* dataset.

CHAPTER 4
Supplementary Material 3

	Deception Is.	Half Moon Is.	King George Is.	Livingston Is.	Esperanza Bay	O'Higgins Bay	Cierva Cove	Paradise Bay	Petermann Is.
Deception Is.									
Half Moon Is.	0.05910497								
King George Is.	0.06036932	0.0603143							
Livingston Is.	0.05653356	0.06445335	0.05424716						
Esperanza Bay	**0.11253972**	**0.08780833**	**0.11361491**	**0.12839316**					
O'Higgins Bay	**0.10713227**	**0.07867335**	**0.09869903**	**0.11788296**	0.06215078				
Cierva Cove	**0.08409543**	**0.09104811**	**0.09963602**	**0.10696438**	**0.12030282**	**0.09851824**			
Paradise Bay	**0.09182616**	**0.07414251**	**0.0911498**	**0.0940299**	**0.11340136**	**0.10106566**	**0.09581511**		
Petermann Is.	**0.09765444**	**0.07658061**	**0.10199396**	**0.10899717**	**0.10279246**	**0.08583979**	**0.10975504**	**0.08541199**	

Supplementary Material 3: Pairwise Fst table for *A. valida* from the WAP region. Significant values (p-value < 0.05) are shown in bold

CHAPTER 4
Supplementary Material 4

	Deception Is.	Half Moon Is.	King George Is.	Livingston Is.	Esperanza Bay	O'Higgins Bay	Cierva Cove	Paradise Bay	Petermann Is.
Deception Is.	NA	0.4228442	0.4996907	0.8326773	0.2491215	0.2862287	0.4630704	0.4209433	0.3728002
Half Moon Is.	0.8368480	NA	0.5895335	0.7598951	0.3238951	0.2894129	0.4167958	0.4552746	0.4662325
King George Is.	0.8579650	0.4694529	NA	1.0000000	0.2612964	0.2481123	0.3804240	0.3495158	0.3704314
Livingston Is.	0.8866254	0.4977186	0.7260699	NA	0.2236093	0.2296152	0.3639567	0.3367794	0.3362835
Esperanza Bay	0.5628116	0.4022039	0.4007882	0.5386577	NA	0.7613199	0.4540872	0.4521709	0.4339101
O'Higgins Bay	0.4376925	0.3205027	0.3682808	0.4307217	0.6664567	NA	0.4244914	0.3200003	0.3947297
Cierva Cove	0.5136068	0.2797003	0.3056885	0.3327434	0.2315393	0.2599769	NA	0.3012864	0.3074164
Paradise Bay	0.5473288	0.4398524	0.4113679	0.4468567	0.2643544	0.2972344	0.4731584	NA	0.5687307
Petermann Is.	0.6157973	0.4744155	0.4542331	0.5473307	0.3427884	0.3516284	0.3946034	0.5104666	NA

Supplementary Material 4: Full Gst table indicating relative migration between sampling stations of *A. valida* from the WAP region.

CHAPTER 4
Supplementary Material 5

	Northern WAP	Central WAP	S. Shetlands	Southern WAP	S. Georgia
Northern WAP					
Central WAP	0.022				
S. Shetlands	0.036	0.03			
Southern WAP	0	0	0.027		
S. Georgia	0.177	0.092	0.203	0.087	

Supplementary Material 5: Pairwise Fst table for *A. riesgoae*. Significant values (p-value < 0.05) are shown in bold.

CHAPTER 4
Supplementary Material 6

	Northern WAP	Central WAP	S. Shetlands	Southern WAP	S. Georgia
Northern WAP	NA	0.229	1.000	0.268	0.253
Central WAP	0.291	NA	0.833	0.409	0.348
S. Shetlands	0.425	0.220	NA	0.205	0.215
Southern WAP	0.257	0.384	0.674	NA	0.303
S. Georgia	0.117	0.143	0.224	0.132	NA

Supplementary Material 6: Full Gst table for *A. riesgoae* indicating relative migration between regions.

Appendix: Participation in other papers not included in this PhD dissertation

1- Taboada S., Ríos P., Tonzo V., Cárdenas P., Mitchell A., Cranston A., **Leiva C.**, Busch K., Koutsouveli V., Cristobo J., Xavier J., Henschel U., Rapp H. T., Riesgo A. (in prep for *Molecular Ecology*) Connecting organisms with conservation strategies: genetic diversity and gene flow in fan-shaped sponges in the North-East Atlantic Deep Sea.

2- Riesgo A., Taboada S., Kenny N., Santodomingo N., Moles J., **Leiva C.**, Cox E., Avila C., Cardona L., & Maldonado M. (submitted to the *Biological Journal of the Linnean Society*) Recycling recourse: silica of diatom frustules as a source for spicule building in Antarctic siliceous demosponges.

3- Taboada S., **Leiva C.**, Junoy J., Alexander F., Riesgo A. (2018) A new member of the genus *Antarctonemertes* (Hoplonemertea, Nemertea) from Antarctic waters. *Polar Biology*. DOI: https://doi.org/10.1007/s00300-018-2298-1.

4- Álvarez-Campos P., Taboada S., San Martín G., **Leiva C.**, Riesgo A. (2018) Phylogenetic relationships and evolution of reproductive modes within flattened syllids (Annelida, Syllidae) with the description of a new genus and five new species. *Invertebrate Systematics*. DOI: https://doi.org/10.1071/IS17011.

5- Angulo-Preckler C., **Leiva C.**, Avila C., Taboada S. (2017) Macroinvertebrate communities from the shallow soft-bottoms of Deception Island (Southern Ocean): A paradise for opportunists. *Marine Environmental Research*.
DOI: https://doi.org/10.1016/j.marenvres.2017.03.008.

6- Taboada S., **Leiva C.**, Bas M., Schult N., McHugh D. (2017) Cryptic species and colonization processes in *Ophryotrocha* (Annelida, Dorvilleidae) inhabiting vertebrate remains in shallow-water Mediterranean habitats. *Zoologica Scripta*.
DOI: https://doi.org/10.1111/zsc.12239.

7- Taboada S., Bas M., **Leiva C.**, Garriga M., Sardà R., Avila C. (2016) Life after death: shallow-water Mediterranean invertebrate communities associated with mammal bones. *Marine Ecology*. DOI: https://doi.org/10.1111/maec.12257.